Using Petroleum Hydrocarbons (PHCs) to Characterize Contamination in the Cold Lake Oil Sands Region, Alberta

Kirsten Smythe

Thesis submitted to the University of Ottawa in partial fulfillment of the requirements for the Master of Science

In
Earth and Environmental Sciences
Specializing in Chemical and Environmental Toxicology

Department of Earth and Environmental Sciences
Faculty of Science
University of Ottawa

Supervisors:
Dr. Jules Blais (University of Ottawa)
Dr. Robert Jack Cornett (University of Ottawa)

Thesis Advisory Committee:

Dr. Jesse Vermaire (Carleton University)
Dr. Ian Clarke (University of Ottawa)
Dr. Clément Bataille (University of Ottawa)

University of Ottawa
Ottawa, Canada

Abstract

In-situ oil sands operations have been the dominant method of bitumen extraction in Canada since 2012; however, research on contaminants attributed to this method is limited in the peer-reviewed scientific literature, compared to that of open-pit mining. The Cold Lake oil sands region operates using exclusively thermal *in-situ* extraction techniques, raising the issue of whether oil sands activity is resulting in petroleum hydrocarbon (PHC) contamination in the absence of open-pit mines, upgraders, refineries, tailings ponds, and other bitumen processing operations. The lack of baseline contamination levels prior to oil sands development hampers debate on contamination from the oil sands industry. We address this shortcoming by using regional lake sediment cores to characterize petroleum hydrocarbons and trace their origin within the Cold Lake oil sands deposit. Petroleum hydrocarbons are hydrophobic compounds that bind to sediments, therefore persisting and accumulating in aquatic environments.

This thesis examines historical levels of polycyclic aromatic hydrocarbons (PACs), petroleum biomarkers, and *n*-alkanes in radiometrically dated sediment cores collected from the depocenter of lakes within the Cold Lake heavy oil field. We used alkylated PACs and a suite of petroleum biomarkers to evaluate *in-situ* operations as potential petroleum-derived contamination sources. We predicted that similarly to open-pit mining, concentrations of PHCs in lake sediments would increase with industrial activity corresponding to proximity from *in-situ* operations. Like open-pit regions, alkylated PACs in Cold Lake sediments were elevated when compared to unsubstituted parent PACs and were significantly enriched in lake sediments deposited after the onset of oil sands operations. These findings imply that *in-situ* oil sands activity is driving the enrichment; however, diagnostic ratios and pyrogenic indices confirm a strongly pyrogenic origin in both pre-industrial and more recent sediments. When compared to a Cold Lake bitumen sample, the principal components driving PHC enrichment do not resemble bitumen. Likewise, diagnostic ratios of petroleum biomarkers and *n*-alkanes do not support bitumen as a significant source of hydrocarbons. PHC inputs in lake sediments are instead from terrestrial vegetation and plant waxes. These findings suggest that bitumen is not significantly contributing to petroleum hydrocarbon enrichment to lakes within the Cold Lake oil field; however, emissions from *in-situ* activity (natural gas burning, diesel trucks, seismic line cutting etc.) is increasingly abundant in more recent sediment.

With >80 % of Canadian bitumen reserves requiring *in-situ* techniques for extraction, this thesis provides the first assessment of the spatial and temporal relationship between contaminant loading and proximity to *in-situ* oil sands operations. Additionally, this study allows for the environmental implications of open-pit mining operations to now be compared to that of *in-situ* techniques.

Acknowledgments

This project has grown and transitioned drastically since it began in 2016. I have received guidance, assistance, and support from so many people, without which this thesis would not have been possible. Firstly, I would like to thank my thesis supervisors Dr. Jules M. Blais and the late Dr. Jack Cornett. Jack, your reminders to enjoy the sunshine and to think of the question when I am stuck, were words of wisdom that helped me even when you were gone. You were greatly missed, and I hope this work would have made you proud. Jules, thank you for your guidance, passion for science, and financial support. Thank you for fishing me out of my diagnostic ratio wormholes, and for always steering me in the right direction. My thesis has been a rollercoaster, and I appreciate your support through all the twists and turns. This experience has taught me so much more than I ever could have imagined.

I much appreciate the valuable insight provided by Colin Cooke and Alberta Environment and Parks. Thank you for your edits, funding, and for letting me sit in the front seat of the helicopter when we were in Fort McMurray. Thank you, Josh Thienpont and Paul Drevnick, for helping me in the field and for hauling the zodiac to each of our lakes.

Thank you to Terry Kutt and Findlay MacDermid of the Cold Lake First Nations for your assistance in the field and the use of your Argos. Without your aid, there is no way that we would have been able to conduct our fieldwork successfully. Your continued enthusiasm in the project and willingness to help were inspiring.

Linda Kimpe and Dave Eickmeyer, thank you for your guidance in the lab, for answering all my incessant questions, and for running all 550 of my samples on the GC-MS. I understand how large a task that was, and I genuinely appreciate it.

To all the Blais and Cornett lab members, thank you for your network of support, assistance with all things R, and for being a sounding board for all of my ideas, thoughts, and worries. My masters would have been so dull and lonely without you all. To my friends both in Ontario and in BC, thank you for your positivity and distractions, you guys believed in me way more than I believed in myself. Without you, I would not have been able to finish this thesis with my sanity.

Most importantly, thank you to my family for always encouraging me and supporting me from across the country. Angie, Joelle, and Mia, thank you for humouring me when I start talking about lake sediments or my machine child (the ARC Gamma counter), for sending me dog videos when I needed a pick-me-up, and for all making the trip out from the west coast to visit me. Thank you to my parents Mona and Bill, for reminding me to “Bear Down” and letting me take over the kitchen any time I came home and needed to interpret chromatograms. The values and work ethic that you raised me with provided me with the skills and perseverance push through this degree. Your unwavering faith in my abilities motivated me to succeed.

Table of Contents

List of Figures

Chapter 1:

Chapter 2:

Chapter 2 – Supplementary Information:

Chapter 3:

Chapter 3 – Supplementary Information:

List of Tables

Chapter 2:

Chapter 2- Supplementary Information:

Chapter 3:

Chapter 3 – Supplementary Information:

Glossary

List of Abbreviations:

ABMI	Alberta Biodiversity Monitoring Institute
AEP	Alberta Environment and Parks
AER	Alberta Energy Regulator
AHC	Agglomerative Hierarchical Clustering
ANOVA	Analysis of Variance
ANCOVA	Analysis of Covariance
AOSR	Athabasca Oil Sands Region
API	American Petroleum Institute Gravity Index
ASE	Accelerated Solvent Extraction
bb	Barrels of Bitumen
Bitumen	Extra-Heavy oil
CAPP	Canadian Association of Petroleum Producers
CCME	Canadian Council of Ministers of the Environment
CEQGs	Canadian Environmental Quality Guidelines
CER	Canadian Energy Regulator
CERI	Canadian Energy Research Institute
CL	Cold Lake, Alberta
CLAWR	Cold Lake Air Weapons Range
CLFN	Cold Lake First Nations
CNRL	Canadian Natural Resource Limited
CNS	Carbon, Nitrogen, Sulfur
COSIA	Canadian's Oil Sands Innovation Alliance
CPI	Carbon Preference Index
CRS	Constant Rate of Supply
CSS	Cyclic Steam Stimulation drilling
Dilbit	Diluted Bitumen
DW	Dry Weight
ECCC	Environment and Climate Change Canada
FTS	Flow to Surface
GC-MS	Gas Chromatography coupled to a Mass Spectrometer
GHG	Greenhouse Gas
H:C	Hydrogen – Carbon Ratio
HMW	High Molecular Weight
HPLC	High-Performance Liquid Chromatography
IAEA	International Atomic Energy Agency
In-Situ	Thermal extraction of oil sands using steam to liquefy bitumen at depth
IPCC	International Panel on Climate Change
IS	Internal Standard
ISQG	Interim Sediment Quality Guidelines

JOSM	Joint Oil Sands Monitoring
LARP	Lower Athabasca Regional Plan
LMW	Low Molecular Weight
LRT	Long-Range Transport
MJ	Mega Joule
MDL	Method Detection Limit
n-Alkanes	Natural Alkanes
NA	Naphthenic Acid
NEBA	National Energy Board Act
NIST	National Institute of Standards and Technology
Open-Pit	Extraction of oil sands using mines exposed to the surface
OSPW	Oil Sands Process Affected Water
PACs	Polycyclic Aromatic Compounds
PCA	Principal Component Analysis
PHC	Petroleum Hydrocarbons
PI	Pyrogenic Index
RPM	Rotations Per Minute
SA-SAGD	Solvent Assisted – Steam Assisted Gravity Drainage drilling
SAGD	Steam Assisted Gravity Drainage drilling
SCO	Synthetic Crude Oil
SMA	Surface Mineable Area
STDEV	Standard Deviation
TOC	Total Organic Carbon
UCM	Unresolved Complex Mixtures
US EPA	United States Environmental Protection Agency
WBEA	Wood Buffalo Environmental Association

Chemical Glossary:

Parent PACs:

ACE	Acenaphthene
ACY	Acenaphthylene
ANT	Anthracene
BaA	Benzo[a]anthracene
BaP	Benzo[a]pyrene
BeP	Benzo[e]pyrene
BbF	Benzo[b]fluoranthene
BghiP	Benzo[g,h,i]perylene
BkF	Benzo[k]fluoranthene
BNT	Benzonaphthothiophene
CHR	Chrysene
DahA	Dibenzo[a,h]anthracene
DBT	Dibenzothiophene
FL	Fluorene
FLA	Fluoranthene
IcdP	Indeno[1,2,3-c,d]pyrene
NAP	Naphthalene
PHE	Phenanthrene
PYR	Pyrene
RET	Retene

Alkylated PACs:

C1-Parent	The specified parent PAC with 1 alkyl group
C2-Parent	The specified parent PAC with 2 alkyl groups
C3-Parent	The specified parent PAC with 3 alkyl groups
C4-Parent	The specified parent PAC with 4 alkyl groups

Petroleum Biomarkers:

GAM	Gammacerane
H	Hopanes
S	Steranes
T	Terpanes

Chemicals:

CO_2	Carbon Dioxide
DCM	Dichloromethane
TMP	Trimethylpentane
WO_3	Tungsten Trioxide

Preface

The following thesis is written as a collection of 2 manuscripts per the guidelines provided by the University of Ottawa's Faculty of Graduate and Postdoctoral Studies. Chapter 1 introduces the necessary background concepts and information relevant to this thesis and elaborates on the available literature regarding the two manuscripts that follow. Chapter 1 also introduces the research objectives, aims, and hypotheses of the thesis. Chapters 2 and 3 each provide brief introductory materials as not to be redundant with Chapter 1. The methodologies, results, and discussions are covered in-depth for both Chapter 2 and Chapter 3 as per the formatting guidelines provided by Elsevier for the journal of Environmental Pollution of each manuscript. Chapter 4 summarizes the findings of each manuscript and provides concluding remarks and future applications of this research.

Statement of Contributions

Chapter 2:

Authors: Kirsten K. Smythe[1]; Colin A. Cooke[2,3]; Paul E. Drevnick[2]; Robert J. Cornett[1,5]; Jules M. Blais[1,4]

Affiliations:
[1] Department of Earth & Environmental Sciences, University of Ottawa, Ottawa, Ontario

[2] Environment & Parks, Government of Alberta, Edmonton, Alberta

[3] Department of Earth and Atmospheric Science, University of Alberta Edmonton, Alberta

[4] Department of Biology, University of Ottawa, Ottawa, Ontario

[5] Deceased

Study Design ……...Kirsten K. Smythe
Colin A. Cooke
Jules M. Blais
Robert J. Cornett

Sample Collection…..……..Kirsten K. Smythe
Joshua R. Thienpont
Paul E. Drevnick
Colin A. Cooke

Alkylated & Parent PAC Extractions……...Kirsten K. Smythe
David C. Eickmeyer
Linda E. Kimpe

Data Analysis & Interpretation…….....Kirsten K.Smythe
David C. Eickmeyer

Manuscript Preparation……....Kirsten K. Smythe

Peer Reviewers…….....Jules M. Blais
Colin A. Cooke

Chapter 3:

Authors: Kirsten K. Smythe[1]; Colin A. Cooke[2,3]; Paul E. Drevnick[2]; Robert J. Cornett[1,5]; Jules M. Blais[1,4]

Affiliations:
[1] Department of Earth & Environmental Sciences, University of Ottawa, Ottawa, Ontario

[2] Environment & Parks, Government of Alberta, Edmonton, Alberta

[3] Department of Earth and Atmospheric Science, University of Alberta Edmonton, Alberta

[4] Department of Biology, University of Ottawa, Ottawa, Ontario

[5] Deceased

Study Design ……...Kirsten K. Smythe
Colin A. Cooke
Jules M. Blais
Robert J. Cornett

Sample Collection…..……..Kirsten K. Smythe
Joshua R. Thienpont
Paul E. Drevnick
Colin A. Cooke

n-Alkane & Petroleum Biomarker Extractions…….Kirsten K. Smythe
David C. Eickmeyer
Linda E. Kimpe

Data Analysis & Interpretation……....Kirsten K. Smythe
David C. Eickmeyer

Manuscript Preparation……....Kirsten K. Smythe

Peer Reviewers……....Jules M. Blais
Colin A. Cooke

Chapter 1. General Introduction

1.1 Alberta Oil Sands Operations

The Canadian oil sands of northern Alberta span an approximate area of 142,200 km^2 and host a proven crude oil reserve of 170 billion barrels, making it the third-largest crude oil reserve in the world (CAPP, 2019). Situated in three primary deposits within Alberta, the Athabasca, Peace River, and Cold Lake reserves comprise the Alberta oil sands (Figure 1-1). The largest of these reserves is the Athabasca Oil Sands region, spanning an area of ~40 000 km^2 within north-eastern Alberta. To the west of the Athabasca oil sands region is the Peace-River oil sands deposit, and to the south is the Cold Lake oil sands deposit. Oil sands operations commenced in the mid-1900s and have been expanding rapidly in both extent and innovation ever since (AER, 2018a; CAPP, 2019). Despite recent constraints on Canadian oil production, projections suggest a 3% increase in total annual output until 2021 and an increase in production of 1.27 million barrels of bitumen per day (bb d^{-1}) by 2034 (CAPP, 2019). Due to their environmental implications, economic significance, and vast geographic extent, the need for proper research and monitoring associated with oil sands production is of the utmost importance (Kelly et al., 2009; Timoney and Lee, 2009).

Dozens of studies have investigated the environmental implications of oil sands activities and their effects on the surrounding region. These studies have assessed the wide-range transport of contaminants such as metals, petcoke (a by-product of upgrading bitumen), naphthenic acids (NAs), and polycyclic aromatic compounds (PACs) to downstream and down-wind environments and have concluded that oil sands operations are releasing contaminants to the Athabasca oil sands region in concentrations concerning to human, ecosystem, and organism health (Ahad et al., 2013; Crump et al., 2017; Guéguen et al., 2016; Jautzy et al., 2015a; Kelly et al., 2009; Kirk et al., 2014; Kurek et al., 2013a; Manzano et al., 2017; Ross et al., 2012; Skierszkan et al., 2013; Thienpont et al., 2017; Timoney and Lee, 2014; Zhang et al., 2016). Kelly et al. (2009) were the first to establish a concentration gradient between PAC loading and proximity to oil sands operations. They found that oil sands operations within the Athabasca area were the epicentre of contamination, as evidenced by an exponential decrease in contaminant loading in snowpack samples as the distance from the mines increased. This study detected

PACs in snowpack samples as far as 50 km downwind from oil sands regions with 391 kg of PAC loading over 4 months. Other studies have investigated the implications that these contaminants, and their distribution as a result of oil sands operations, had on aquatic and terrestrial organisms as well as ecosystem and human health (Arens et al., 2017; Beck et al., 2015; Clair and Percy, 2015; Crump et al., 2017; Evans and Talbot, 2012; Hebert et al., 2011; Hrudey and Xu, 2010; Irvine et al., 2014; Korosi et al., 2017; Ohiozebau et al., 2016; Schuster et al., 2015; Timoney and Lee, 2009; Young et al., 2011)

1.1.1 Oil Sands Monitoring

Oil sands deposits sometimes form exposed outcrops, typically along the banks of large rivers such as the Athabasca River (Hein, 2017). These outcrops can introduce petroleum-derived contaminants, such as the petrogenic polycyclic aromatic compounds (PACs) and trace metals into the surrounding environment (Debenest et al., 2012; Headley et al., 2001; Kelly et al., 2009; Thienpont et al., 2017). These natural sources of contamination have prompted debate on how Alberta oil sands operations may contribute to environmental pollution.

Only limited information is available on environmental contaminants reaching back to before the start of oil sands operations half a century ago. In 1997, the Regional Aquatics Monitoring Program (RAMP) began to monitor the potential cumulative effects of oil sands activities on ecosystems, both upstream and downstream of oil sands developments. RAMP was established as an industry-funded, multi-stakeholder environmental monitoring program to track environmental pollutants from the oil sands. Several experts in the field criticized the RAMP program for its lack of transparency, and sampling designs too inadequate to capture the true extent of oil sands contamination (Ayles et al., 2004). Despite RAMP's good intentions, the program failed to reproduce baseline environmental conditions and was not available for all three of the Alberta oil sands deposits (Ayles et al., 2004; Kurek et al., 2013a; Schindler, 2013).

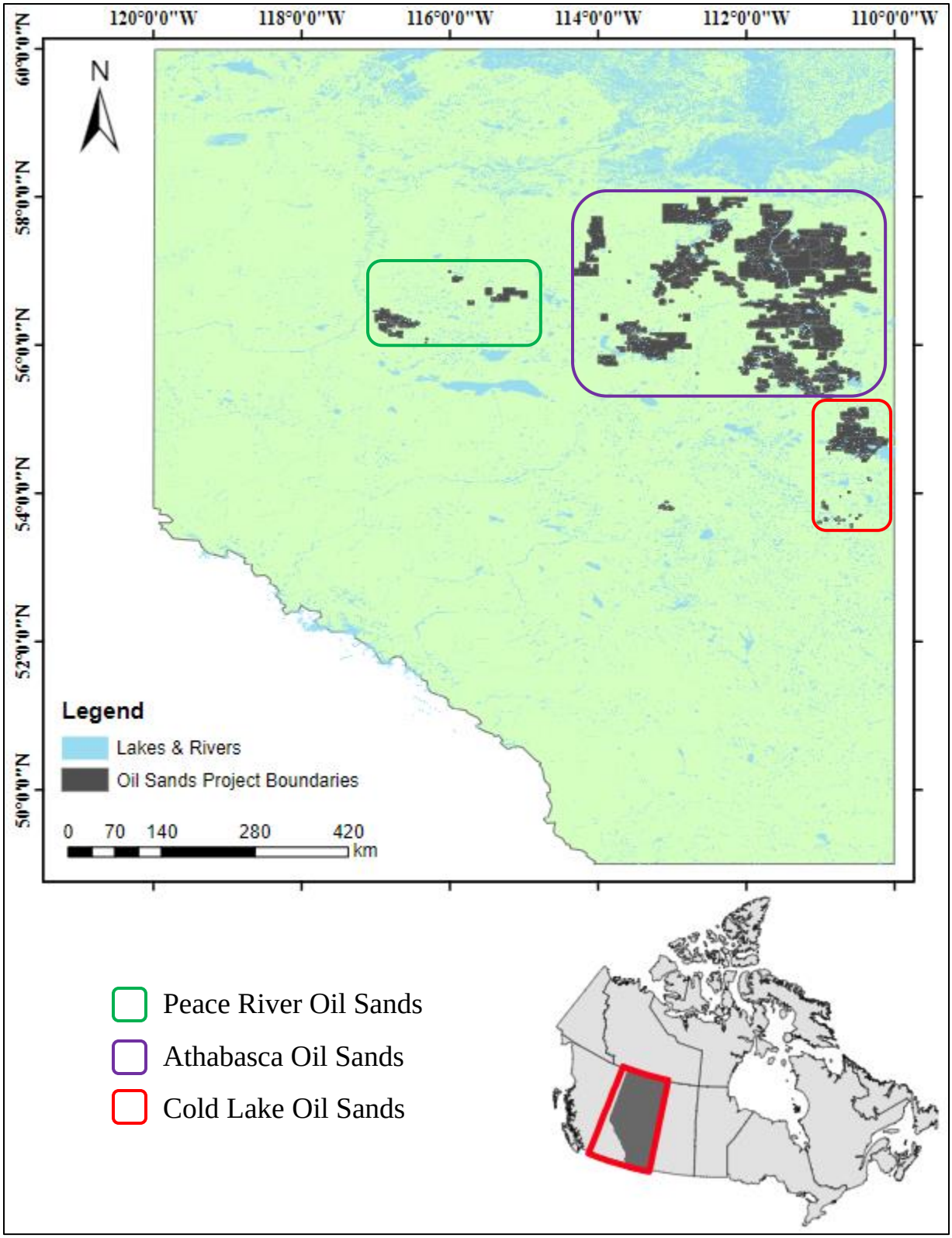

Figure 1- 1: Map of the three Alberta oil sands deposits.

In 2011, the RAMP was replaced by the Joint Oil Sands Monitoring Program (JOSM), also referred to as the Oil Sands Monitoring Program (OSMP), to implement an integrated oil sands environmental monitoring plan. The OSMP aims to track impacts from oil sands development and conduct comprehensive and inclusive monitoring to inform management and regulatory action (OSMP, 2019). The OSMP data is publicly available and requires that all work plans be approved prior to monitoring. Presently, oil sands assessment through the OSMP occurs throughout all three of the oil sands regions in Canada.

1.1.2 Bitumen and the Geologic History of the Canadian Oil Sands

What distinguishes Alberta's reserves from other conventional oil deposits is the form in which the extra-heavy oil occurs, and the methods to extract it from the ground. The oil sands are a viscous mixture of sand, heavy crude bitumen, water, and clay that formed within the Clearwater and McMurray Formation during the Late Devonian to Early Cretaceous periods (Droppo et al., 2019). The bitumen content within the amalgamation ranges from 1-20 % depending on geology, although it is typically around 10 % bitumen, with the remainder being ~83 % silica sand, ~4 % water, and ~3 % fluvial clays (AER, 2018a; CAPP, 2019; Hein and Cotterill, 2006). At the time of formation, an ancient sea covered Alberta forming the Western Canada Sedimentary Basin. Accumulation of marine plant and animal remains compacted over hundreds of millions of years and exerted high pressure and temperature conditions that transformed the deposited biomass into light oil (Broughton, 2013; Hein and Marsh, 2008). Uplifting of the Rocky Mountains, followed by a significant drop in sea level during the Laramide Orogeny, forced the organic reserves to migrate north, bringing with them oxygenated water and forcing large-scale erosion of the overlying mineralogy (Zhou et al., 2008). Collapse-subsidence from salt bed dissolution 200 m below the oil deposits caused McMurray fluvial sands to fill in the trough and become capped by impermeable Clearwater shales (Broughton, 2013; Conly et al., 2002). Over time, the petroleum mixed with the sand, and lighter hydrocarbons were biodegraded by microbes or evaporated (Head et al., 2003; Hein and Cotterill, 2006). This process resulted in the bitumen having lost most of the low molecular weight compounds such as paraffins and naphthalenes, leaving dominantly heavy molecules such as asphaltenes and maltenes (saturates, aromatics, and resins) (Shahimin et al., 2016). Alberta bitumen contains ~18% asphaltenes, giving it a thick viscosity (like honey or molasses) under

atmospheric conditions (Broughton, 2013; Head et al., 2003; Zhou et al., 2008). These extra-heavy crude oil reserves are abundant in large complex molecules containing carbon, oxygen, sulfur, and nitrogen, as well as heavy and base metals (Head et al., 2003; Hein, 2017; Meyer and Freeman, 2006). The Alberta oil sands deposits are also characteristically enriched in rare earth elements (REE), and metals such as vanadium, nickel, titanium, selenium, and tellurium providing challenges during the refining and upgrading processes and introducing contaminants of concern into the environment (Bata et al., 2016; Hein, 2017; Hein and Cotterill, 2006).

1.1.3 Oil Sands Processing

The American Petroleum Institute (API) gravity is a common metric used to quantify the gravity or density of liquid petroleum products with respect to their specific gravity in water. The API gravity is calculated, as seen in equation 1, where SG is the specific gravity of the oil at 60 ^{o}F. An API greater than 35 ^{o} is reflective of a light hydrocarbon product that will float on the surface of the water. Heavy crude oils, such as bitumen, have an API gravity of 8–10 ^{o,} exemplifying their extremely viscous and thick nature. Any bitumen products with an API below 15^{o} are considered as an extra-heavy crude oil (Attanasi et al., 2007; Hein, 2017; Jiang et al., 2010; Mukhametshina and Hascakir, 2014).

$$\text{API} = (141.5 / \text{SG}) - 131.5 \quad (1)$$

Upon separation from the sands, bitumen often requires upgrading and refining to produce the final synthetic crude oil (SCO) for commercial distribution and to increase the API. Regularly, bitumen extracted through *in-situ* thermal techniques is diluted with condensate, paraffinic solvent, or naphthenic solvent to decrease the viscosity to an API of 20–22 ^{o}, allowing it to flow through pipelines at low temperatures without the risk of erosion or corrosion (Charry-Sanchez et al., 2014; Wilson and Kriz, 1984). This diluted bitumen (dilbit) product is sold and transported directly to high-conversion refineries equipped to handle the heavy/sour product. The remaining 35 % of bitumen that requires upgrading is usually a result of a water and solids concentration > 2 %. Sour bitumen, with a sulfur and asphaltene concentration above the refining threshold of 10 %, also requires upgrading to produce a lighter, sweeter intermediate crude oil product before refining. Upgraded SCO is of a higher quality and purity due to the removal of sulfur and metals from the product. As a result, SCO sells at a premium (Charry-Sanchez et al., 2014).

Upgrading consists of 5 main steps, transforming the dilbit into SCO through fractionation and chemical treatment. Dilbit flows through pipelines from *in-situ* wells and crushing facilities to the upgraders where the diluent is recovered from the bitumen and recycled (API 60–80^{o}). The Hydrogen-Carbon (H:C) ratio of the bitumen is then improved by reducing the carbon content (coking) and increasing the hydrogen content (hydroconversion) (Charry-Sanchez et al., 2014; Wilson and Kriz, 1984). The bitumen then undergoes hydrocracking to fractionate the heavy oil into light oil by breaking up complex molecules into shorter hydrocarbon chains. Bitumen can also be converted to lighter hydrocarbons through the distillation of the crude oils, depending on their boiling points (Charry-Sanchez et al., 2014). Sequentially, impurities such as sulfur, nitrogen, and heavy metals are removed, stabilizing the final product through catalytic hydrotreating. Finally, the different recovered fractions of the oil are blended to produce the specific SCO products sold to downstream refineries for ultimate conversion into consumer products (diesel, gasoline, jet fuel, propane, and other petroleum-based crude oils) (Masliyah et al., 2004; Wilson and Kriz, 1984). The final SCO product produced by upgraders typically has an API of ~30–35 ^{o} (Charry-Sanchez et al., 2014). Canada is responsible for ~30 % of refining; however, most of the upgrading occurs in the United States (CAPP, 2019, 2018a).

Bitumen upgrading and refining are areas of oil sands production that are drawing increasing interest within the scientific community with regards to their environmental impacts. Depending on the method of upgrading used, Canadian oil sands processing is estimated to release 240.3-433.4 kg of CO_2 equivalent greenhouse gasses (GHGs) per m^3 of processed bitumen, and 7.9-15.7 g of CO_2 equivalent per MJ of refined SCO (Nimana et al., 2015). In addition to abundant land use and GHG release, thermal conversion of bitumen results in the production of petroleum coke (petcoke), a solid carbonaceous residue subject to widespread atmospheric and aquatic transport of up to 150 km (Jautzy et al., 2015a; Yeh et al., 2010). Research has determined that petcoke is a significant and dominant source of PACs to the surrounding environment in addition to metals such as vanadium, nickel, and molybdenum (Ahad et al., 2014; Jautzy et al., 2015a; Parajulee and Wania, 2014; Xu, 2018; Zhang et al., 2016). The 7.3 million metric tons of petcoke produced annually yield fugitive dust and petcoke piles. Inhaling petcoke dust may lead to respiratory inflammation and transcriptomic effects in animal studies (Camus et al., 2003; Timoney and Lee, 2009; Zhang et al., 2016) and increased

occurrences of cardiovascular disease and lung cancer in humans (Crump et al., 2017; Timoney and Lee, 2009).

1.1.4 Oil Sands Extraction

Across the three Canadian bitumen deposits, the method of oil sand extraction is not uniform. The Athabasca Oil Sands region access the bitumen deposits using open-pit mining techniques as well as *in-situ* thermal extraction; however, the Peace River and the Cold Lake deposits access their reserves via thermal *in-situ* techniques. The use of each method is dependent on the regional geology and the proximity of the oil sands deposit to the surface (CAPP, 2019). A summary of the bitumen production methods and how they have changed over time is observed in Figure 1-2.

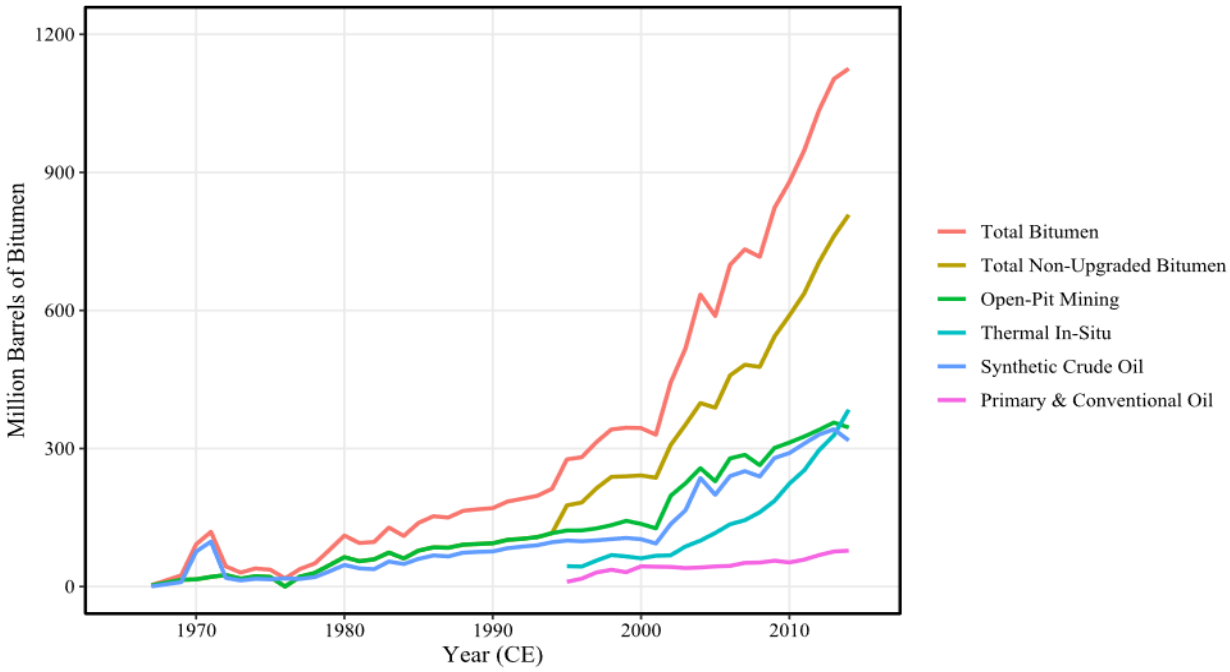

Figure 1- 2:Scatterplot tracking the change in bitumen production throughout the Alberta oil sands, measured in million barrels of bitumen, as a function of time.

1.1.4.1 Open-pit Mining

Open-pit mining is the technique most associated with oil sands extraction in Canada due to the magnitude and extent of the operations. Recovery of bitumen deposits within 70 meters (200 feet) of the surface requires large-scale excavation, creating large open pits. Currently, the

footprint of active open-pit mining spans 900 km^2, a 133 km^2 expansion since 2012, yet encompasses less than 5 % of the total 4800 km^2 surface mineable area (CAPP, 2019). Open-pit mining requires all vegetation, wildlife, and overburden material to be removed from the surface of the bitumen deposit so that large trucks, cranes, and digging machines can extract the bituminous sands and transport them to crushing and oil processing facilities. The excavated material is crushed and mixed into a slurry with naphthenic acids (NAs) and large quantities of hot water are used to separate the bitumen from the sand matrix. The slurry flows through pipelines to extraction facilities where the bitumen is gravity separated from the solids and water, producing an intermediate bitumen froth product (Masliyah et al., 2004). Froth treatment uses flocculation and gravity separation of bitumen followed by secondary froth treatment using solvent or diluent addition to reduce the bitumen viscosity and eliminate adsorbed water and fine solids.

The remaining mixture of water, sand, clay, inorganic ions, NAs, and organic contaminants (also known as oil sands process affected water (OSPW)) from the extraction process are discharged into sizeable tailing storage ponds located adjacent to the processing facilities. The inorganic solids of the OSPW settle to the bottom of the tailing ponds, and the clarified surface water is eligible for recycling. Light-weight silt and clay particles have an affinity for remaining in the water column making it difficult to recycle tailing pond water as it can take these particles up to 30 years to fall out of suspension (AER, 2018a). In 2018, 75% of clarified OSPW was successfully recycled (CAPP, 2019).

Open-pit mining produces 1.14 million barrels of crude oil per day, as reported by the Canadian Association of Petroleum Producers (CAPP, 2018b). Many environmental consequences are associated with the sheer extent and magnitude of these operations. Adjacent surface water systems, such as lakes and rivers, supply much of the water required for the separation process and are in close proximity to these oil sands processing facilities; 65 % of the 253 000 000 m^3 of freshwater used to process oil sands is sourced explicitly from the Athabasca River (AER, 2018a). As a result, the Athabasca oil sands region and the Athabasca River tributaries have been the focus of many scientific studies that assess the implications of this industry. Areas of scientific research include destruction of terrestrial and aquatic habitats, leaching and run-off from tailing ponds, dust and petcoke emissions from mining and oil

processing, the loading of trace metals and chemicals into surrounding environments, and the implications of all these factors on aquatic and terrestrial biota, to name a few (Cheng et al., 2018; Colavecchia et al., 2004; Debenest et al., 2012; Headley et al., 2001; Hsu et al., 2015; Kelly et al., 2009; Manzano et al., 2017, 2016; Parrott et al., 2019; Schiffer and Liber, 2017; Timoney and Lee, 2011; Van Wilgenburg et al., 2013; Xu, 2018; Zhang et al., 2016). Kelly et al. (2010) recorded heavy metal concentrations within the Athabasca River and its tributaries that exceeded the Canadian Water Quality Guidelines (CWQGs) for the Protection of Aquatic Life for metals, including cadmium, copper, lead, mercury, nickel, silver, and zinc. Roy et al. (2016) assessed the risks that tailings ponds pose to shallow riparian groundwater quality and recorded levels of salts, many trace metals, and fluorescence profiles of NAs that exceeded the CWQGs for aquatic health. Although "near-pond" sites were not statistically distinct from "non-pond" sites, this study corroborated results obtained by Frank et al. (2014), establishing that OSPW reached the Athabasca River and tributaries in concentrations detrimental to aquatic health (Frank et al., 2014; Roy et al., 2016).

In addition to the impacts of OSPW and tailing ponds, the oil extraction, refining, and upgrading processes associated with open-pit mining activity are responsible for the release of 10 % of all Canadian GHG emissions and 0.15 % of the global GHG emissions (CAPP, 2018c; IEA, 2017; WRI, 2018). The Alberta Energy Regulator (AER), the Government of Alberta, and industry groups (the Canadian Association of Petroleum Producers (CAPP) and Canada's Oil Sands Innovation Alliance (COSIA)), have identified GHG emissions, air emissions, tailings, water, land use, biodiversity, reclamation, and monitoring to be priority areas for assessing environmental impacts of open-pit mining (OSMP, 2018).

1.1.4.2 In-situ Thermal Extraction

In-situ extraction techniques are less studied within the scientific community despite being the dominant method of oil sands extraction in Canada. In 2012, *in-situ* thermal extraction techniques surpassed open-pit mining as the predominant method of oil sands extraction in Canada (AER, 2015). *In-situ* wells access all bitumen reserves situated deeper than 70 m below the surface, which accounts for ~80 % of all Canadian bitumen deposits (CAPP, 2019). *In-situ* thermal extraction operates using two dominant methods, Cyclic Steam Stimulation drilling

(CSS) and Steam Assisted Gravity Drainage Drilling (SAGD). Both techniques rely heavily on the use of high-temperature steam and solvents (such as propane) to be injected into the McMurray formation to decrease the viscosity of bitumen, separating it from the sands and allowing it to flow to the surface. Once extracted, large storage tanks collect the bitumen, and diluents are used to facilitate transport to upgrading and refining facilities via pipelines. Both methods rely on the use of large volumes of water and the combustion of natural gas to generate steam for injection (Jiang et al., 2009).

The original method of thermal *in-situ* extraction, CSS, relies on one single well drilled vertically and horizontally into the McMurray Formation. Superheated steam and solvents are injected into the well and left for a soaking period of up to two months. Once the viscosity of the bitumen has sufficiently decreased, the injection well is transitioned into a production well and pumps the bitumen into collection tanks at the surface (CAPP, 2019). The soaking of the steam and solvent into the oil sands below increases the pressure within the geologic formation. CSS drilling has resulted in vertical land deformation at a rate of 450 cm $year^{-1}$. Extreme cases of CSS over-pressurization have produced 30 cm of vertical land deformation within a 24-day injection cycle (Samsonov and Czarnogorska, 2014; Shen et al., 2015).

Surface subsidence occurs upon CSS transition into production mode; however, in some instances, over-pressurization of the containment rocks results in bedrock fracturing (Samsonov and Czarnogorska, 2014; Wong et al., 1992). Fractures within the containment rock provide a low-pressure pathway for bitumen to follow, resulting in the release of the bitumen to the surface in non-targeted flow-to-surface events (AER, 2018b; Samsonov and Czarnogorska, 2014). In January of 2009, a flow-to-surface incident occurred within the Primrose Lake oil field, 20 km north of the City of Cold Lake in the Cold Lake oil sands deposit. This flow-to-surface event was the first of five to occur within the Primrose region, the following four occurring between May 20th, 2013, and June 24th, 2013 (AER, 2016). As a result of these non-targeted seeps of bitumen releasing at the surface, a water body informally referred to as Lake 9-21 (Korosi et al., 2016a), was drained and dredged as a cleanup measure, and steaming operations within 1000 m of the seep were suspended (AER, 2016). It is estimated that more than 800 000 m^3 of bitumen was released into the environment as a product of these five flow-to-surface events within the Primrose region of the Cold Lake oil field (AER, 2016).

SAGD methods, developed in 1978 by pioneer Roger Butler, consist of an injection well and production well that work simultaneously. These two wells run in parallel underground within the McMurray formation. The injection well pumps steam and solvent into the sands to decrease the viscosity of the bitumen, the same as CSS; however, the recovery well then pumps the liquid bitumen to the surface (CAPP, 2019). This method does not require a soaking phase, making it the preferred method for *in-situ* thermal extraction. Although there are no recorded incidents of flow-to-surface events attributed to SAGD operations, vertical land deformation does still occur at an uplift rate of 2 cm $year^{-1}$ (Samsonov and Czarnogorska, 2014). SAGD allows for simultaneous injection and recovery; however, it involves the use of more steam and solvent than CSS methods.

Contrary to open-pit mining activity, *in-situ* methods do not require large scale excavation of the landscape above the bitumen deposits nor large volumes of surface water to separate the bitumen from the host rock. *In-situ* methods have been successful in using non-potable groundwater to generate steam and can recycle 85 % of process water, compared to 75 % water recycling for open-pit mining (AER, 2018c). Overall, thermal *in-situ* recovery requires about one-tenth of the equivalent land area as that of open-pit mining, does not produce tailings ponds, and has a limited need for upgrading. As such, the release of contaminants and the effects of *in-situ* mining on the surrounding environment, however, remain widely unstudied. Areas of environmental concern associated with *in-situ* activity include fossil fuel emissions from gas flares, well operation, and steam generation, as well as groundwater contamination, chemical loading to the surrounding environment, aquatic and terrestrial organism health, and non-targeted releases of bitumen to the surface (AER, 2018c; Korosi et al., 2013, 2016a).

To date, there have been four scientific studies regarding the influence of *in-situ* thermal oil sands operations and their release of contaminants. Of these four studies, one focused on localized enrichment of PACs in lake sediments and spruce needles (Korosi et al., 2013), one assessed widespread metal contamination (Skierszkan et al., 2013), one analyzed the cancer risk posed to First Nations people through inhalation and ingestion of PACs (Irvine et al., 2014), and the final study was in response to the flow-to-surface events that took place in 2013 (Korosi et al. 2016). These four studies assessed PACs and metals in soils, lake sediments, spruce needles, and air samples. Korosi et al. (2013) observed an increase in alkylated PACs in Hilda Lake, one of

two lake sediment cores analyzed for their study, suggesting localized enrichment of petroleum-derived contaminants attributed to *in-situ* activity with no evidence of widespread contamination. Skierszkan et al. (2013) observed no significant enrichment in metal concentrations that would suggest bitumen-derived contamination within soils and lake sediments since the onset of *in-situ* oil sands activities in 1985. Irvine et al. (2014) observed negligible cancer risks within the Cold Lake First Nations as a result of inhalation and ingestion of PACs (maximum excess lifetime risk of 0.1 and 0.02 new cases per 100 000). Korosi et al. (2016a) analyzed a lake sediment core from Lake 12-26, which is situated less than 1 km from the Lake 9-21 CNRL flow-to-surface location. Lake 12-26, similar to Hilda Lake from Korosi et al. (2013), showed a historical increase in alkylated PACs since the onset of oil sands operations. The compositional PAC changes within this study differed, suggesting different or multiple sources of PAC pathways into the aquatic systems that were not exclusively a result of *in-situ* operations (Korosi et al., 2016a).

The work conducted previously within the Cold Lake region has suggested that the absence of bitumen processing facilities and open-pit mining activity can account for the lack of metal enrichment within the Cold Lake oil field; however, the enrichment of petrogenic PACs within Lake 12-26 and Hilda Lake implicate *in-situ* activity as a source of PACs. The characterization of the origins and the pathways for PAC deposition within the region remain unknown. Further research within the Cold Lake area, and specifically on the impacts of *in-situ* operations, is required to facilitate mitigation strategies and supplement monitoring efforts (Irvine et al., 2014; Korosi et al., 2013, 2016a). Additionally, it is important to assess the distribution of PAC contaminants that are associated with *in-situ* operations as well as characterize their sources so that PAC distribution may be compared to open-pit mining operations.

In 1988, there were only 4 *in-situ* operations in the Cold Lake deposit with 23 experimental projects in progress. Presently, there are over 210 *in-situ* recovery projects operating within Alberta with 16 experimental *in-situ* projects (Brooks et al., 1988; CAPP, 2019). These operations are responsible for generating 1.51 million barrels of crude bitumen per day. In August 2018, the Alberta Energy Regulator approved a 2-billion-dollar Imperial Oil Cold Lake expansion project. When the project is complete, it is estimated to increase bitumen production of the Cold Lake oil sands by an additional 75 000 bb d^{-1}. This project will include

solvent-assisted (SA-SAGD) as well as steam-assisted gravity drainage recovery. The magnitude of these operations and the rate of growth within Alberta emphasizes the importance of understanding the adverse effects of *in-situ* activity as well as addresses the current knowledge gaps as production continues to grow (AER, 2018c; CAPP, 2018a; Timoney and Lee, 2009).

1.2 The Cold Lake Oil Sands

1920 marked the discovery of the Cold Lake oil sands deposit; however, it was not until 1962 that Imperial Oil drilled the first 10 exploration wells to determine the potential for commercial operations within the area. The first pilot plant was built in Cold Lake in 1964, and primary *in-situ* operations began regular service in 1985 at the Maskwa processing plant. Presently, extraction projects in Cold Lake are operated by Imperial Oil, Devon Canada, Cenovus Energy, Husky Energy, Canadian Natural Resources Limited, and Osum Oil Sands. Figure 1-3 depicts the expansion of active oil sands operations within the Cold Lake oil sands region since the 1980s.

The Cold Lake oil sands, located south-east of the Athabasca oil sands region, are unique in that they operate exclusively through *in-situ* thermal extraction techniques and are isolated from all upgraders, refineries, tailings ponds, and open-pit mining activities by ~300 km. The bitumen deposits within the Cold Lake oil field are situated 300–600 m below the surface and do not encounter the open environment, eliminating the potential of the natural introduction of bituminous derived contaminants to the landscape or surrounding water bodies (CAPP, 2019; Korosi et al., 2013). This region is, therefore, optimal for monitoring the effects of *in-situ* oil sands extraction as any contaminants of bituminous origin would theoretically be introduced as a result of anthropogenic activity.

1.2.1 The Cold Lake Air Weapons Range

The Cold Lake region also hosts the City of Cold Lake and the Cold Lake Air Weapons Range (CLAWR). Developed during the height of the Cold War in the early 1950s, the CLAWR was chosen by the Royal Canadian Air Force to train pilots and test air weapons. The designated military area of 11 700 km^2 across the Alberta-Saskatchewan border is the largest and busiest fighter base in Canada and conducts routine fighter pilot training and live ammunition testing

within their perimeter. Due to the nature of the CLAWR, civilian access is strictly limited, which also limits oil sands development in that region. Oil sands operations off of the CLAWR began in the 1980's, however development did not reach onto the range until the early 2000's. Presetly there are significant oil sands operations both on and off of the CLAWR allowing for the regions to be compared. Development of oil sands activity on the CLAWR and the recent approval of *in-situ* expansion projects are accelerating an expansion of the City of Cold Lake.

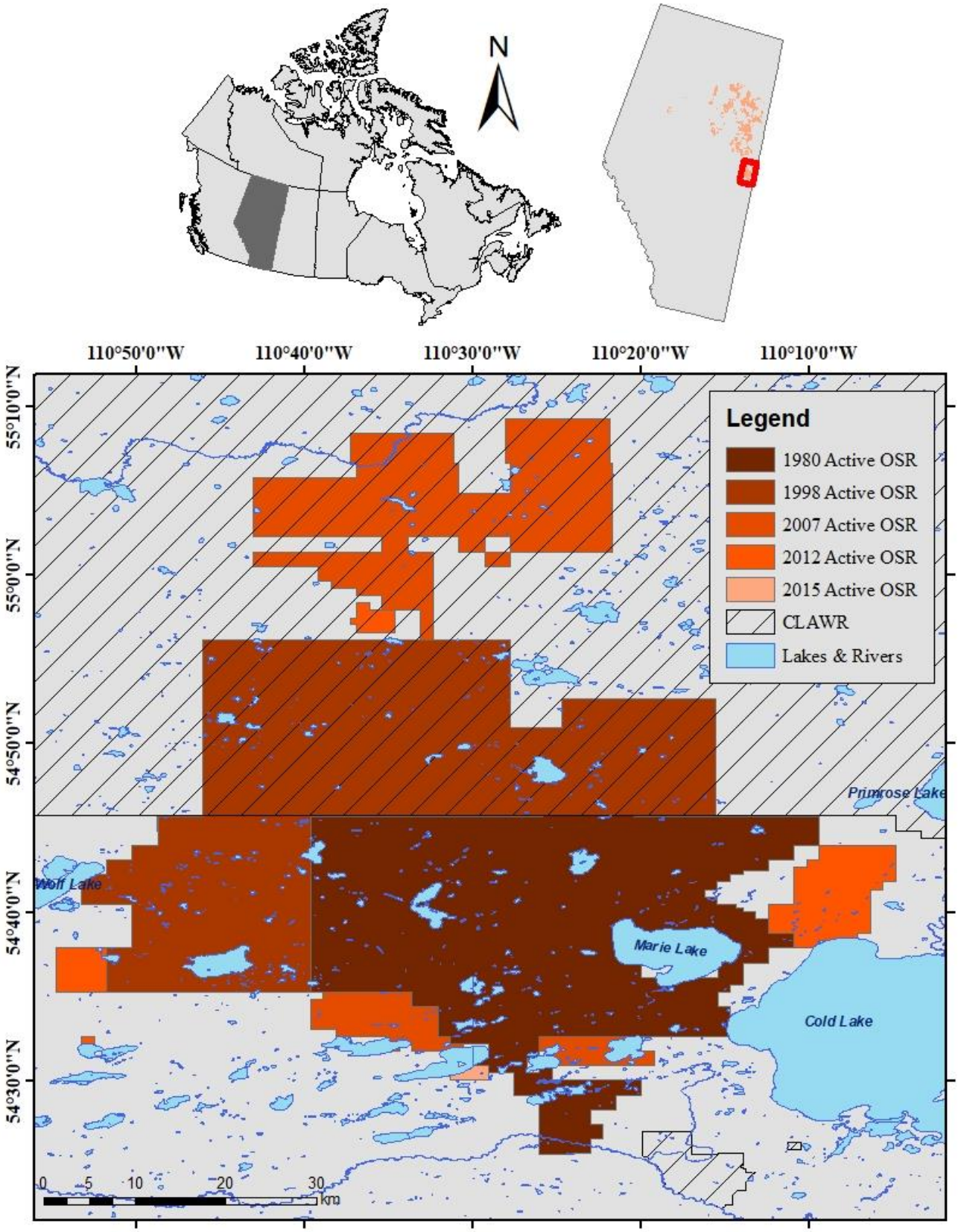

Figure 1- 3: Map of the Cold Lake Oil Field. Map identifying the growth of the active oil sands region (OSR) within the Cold Lake oil field since the onset of industrial activity in the 1980s. Growth of the region is cumulative. The Cold Lake Air Weapons Range (CLAWR), marked by the black hatched line, encompasses the entire northern region of the map, and the airport region to the west of Cold Lake (AEP 2019).

1.3 Characterizing Oil Sands Contaminants

Depending on the conditions of petroleum formation, oil deposits will exhibit unique distribution patterns of *n-a*lkanes, biomarkers, and alkylated PAC homologs. As such, these unique signatures can be used as tools for chemical fingerprinting the source of petroleum (Wang et al., 2016).

1.3.1 Polycyclic Aromatic Compounds (PACs)

PACs are a large group of organic chemical contaminants formed through the incomplete combustion of organic matter. These compounds, comprised of two or more covalently bonded aromatic rings, have known mutagenic, carcinogenic, and toxic properties, the degree of which is dependent on the molecular weight, the mode of accumulation, and degree of alkylation (Barfknecht et al., 1982; Brookes, 1977; Jariyasopit et al., 2016; Lemieux et al., 2015, 2014; Lin et al., 2015). Alkylated compounds have different chemical and physical properties that can influence exposure pathways and fate within an organism (Thorsen et al., 2004). Heavily alkylated compounds are overall more toxic than their unsubstituted parent compounds; however, the United States Environmental Protection Agency (US EPA) has identified 16 non-substituted PACs as priority pollutants as they are found ubiquitously in all environmental compartments (Keith, 2014).

PACs are non-polar, hydrophobic compounds with low ionization potential and therefore are only slightly water-soluble. Low molecular weight (LMW) PACs (e.g., 2 to 3 ring groups of PACs such as naphthalenes, fluorenes, phenanthrenes, and anthracenes) have significant acute toxicity as they are more readily soluble in water, making them less persistent (Evans et al., 2016). High molecular weight (HMW) PACs, (4 to 7 ring groups of PACs from chrysenes to coronenes), are less readily soluble in water and are therefore more persistent and carcinogenic. Although these aromatic compounds have high chemical stability, varying conditions can result in alkyl substitutions and the inclusion of other elements into their structure. Organosulfur compounds, such as dibenzothiophenes (DBTs) and benzonaphthothiophenes (BNTs), constitute an expanded list of PAC compounds contrasted to those purely comprised of hydrogen and carbon (Andersson and Achten, 2015).

Classifications of PACs fall into three categories (biogenic, petrogenic, or pyrogenic) based on their origin and temperature of formation. Biogenic PACs are naturally produced in plants, bacteria, and fungi during diagenesis by microorganisms from biological precursors. This family of PACs does not contribute significantly to PAC concentrations within the Alberta oil sands (Hsu et al., 2015). Pyrogenic PACs are formed in high-temperature, low oxygen combustion environments such, as forest fires, volcanos, and the upgrading and combustion of fossil fuels. When combustion begins, the organic matter fragments into unstable free radicals through a process called cracking. These free radicals then react with each other to create aromatic rings which sequentially react with other small hydrocarbon molecules (Andersson and Achten, 2015). This series of reactions transform the single aromatic ring compound into a chain of multiple aromatic rings that is more chemically stable. These HMW compounds are typically unsubstituted and referred to as parent PACs. Their alkylated homologs, also referred to as petrogenic PACs, are generally emitted from point sources, such as through oil spills, pipeline breaches, or FTS events (Korosi et al., 2013). Petrogenic PACs form under geothermal conditions over a geological time scale. These compounds are frequently alkylated as their slow formation under low-temperature petrogenesis conditions favor substitution and alkylation of the parent molecules (Andersson and Achten, 2015). Petrogenic PACs are typically LMW compounds and are common derivatives of petrochemicals. Their origin, health concerns, and emission source makes petrogenic PAC contaminants of high importance in oil sands research as they are abundantly present in bitumen (Ahad et al., 2015; Evans et al., 2016; Hsu et al., 2015; Korosi et al., 2017; Thienpont et al., 2017).

PACs are mobilized in the environment by adsorbing onto atmospheric particles and aerosols. The deposition of these compounds, through wet and dry fallout, follows a density gradient concerning their originating source (Kelly et al., 2009). HMW compounds preferentially deposit to the ground more readily than LMW compounds and therefore settle closer to their originating source. Once deposited onto the landscape, PACs are subject to degradation through various chemical and biological processes. Some of these degradation pathways include biodegradation, biotransformation, and photooxidation (Andersson and Achten, 2015). The half-life of PACs undergoing these different processes is largely dependent on the number of rings in the compound, the degree of alkylation, and the structural linearity of the molecule (Andersson and Achten, 2015; Thorsen et al., 2004).

1.3.2 Petroleum Biomarkers

Petroleum biomarkers are recalcitrant compounds consisting of terpanes, hopanes, and steranes. These compounds play a crucial role in identifying sources of petroleum products, as they are complex molecules derived from living organisms that synthesized during petroleum formation (Brooks et al., 1988; Wang et al., 2016). The process of chemical fingerprinting uses petroleum biomarkers as a tool to identify genesis, oil biodegradation, and the maturation of petroleum products by comparing their chemical signature to that of their biological precursors. Terpanes, hopanes, and steranes are generated and preserved exclusively within petroleum deposits and have little or no structural change from their parent biochemicals, as they retain most of their original carbon skeleton (Wang et al., 2016). Historically, petroleum biomarkers have been used by geochemists to characterize oil in terms of their host rocks and many geochemical factors of the oil reservoir (Asif et al., 2009; Jia et al., 2013; Wang et al., 2013, 2014; Yim et al., 2011).

Petroleum biomarkers are chemically distinct from their biological precursor and are resistant to degradation, making them highly specific for source identification. Biodegradation of compound classes generally transitions from *n-a*lkanes > acyclic isoprenoids > steranes > hopanes > terpanes, making biomarkers superior compounds for chemical fingerprinting than PACs or *n-a*lkanes which have many sources in the environment (Brooks et al., 1988). Many crude oils exhibit a characteristic biomarker abundance of C_{29} & C_{30} αβ Hopanes and C_{23} & C_{24} terpanes with a sterane dominance of C_{27}, C_{28}, C_{29} S & R homologs. Biomarker concentrations typically decrease with greater thermal maturity of the host reserve; therefore, biomarker concentrations in light oils and condensates are deficient when compared to heavy oils such as bitumen (Stout and Wang, 2016; Wang et al., 2016).

n-Alkanes and PACs are subject to specific compositional and physical property changes and thus become unreliable tools for chemical fingerprinting as petroleum products weather. Conversely, biomarker patterns remain unaffected despite the evaporation and emulsification, dispersion, dissolution, biodegradation, and photooxidation of petroleum products (Jia et al., 2013; Stout and Wang, 2016). As a result, biomarkers are compounds of increasing interest in oil forensics and have been used to determine origins of oil spills, types of source rocks, thermal maturity of petroleum reserves, depositional conditions of environmental contaminants, and

patterns of contaminant deposition (Bieger et al., 1996; Jia et al., 2013; Liao et al., 2012; Wang et al., 2016, 2006; Yang et al., 2012; Yu et al., 2012; Yunker and Macdonald, 2003).

1.3.3 n-Alkanes

n-Alkanes are chemical compounds consisting of homologous long-chain alcohols, aldehydes, esters, and hydrocarbons. Similar to PACs, *n-a*lkanes originate from natural sources such as plant waxes and soils as well as anthropogenic sources such as fossil fuel combustion (Olajire et al., 2008). During bitumen formation, natural alkanes and light hydrocarbons are almost entirely depleted by evaporation, microbial degradation through porous media, or weathering, resulting in a distribution of *n-a*lkanes that is both biological and non-biological in origin (Andreou and Rapsomanikis, 2009; Grice et al., 1968). Similar to petroleum biomarkers, and petrogenic PACs, *n-a*lkanes can be used to help distinguish different petroleum sources based on their proportion of odd-to-even numbered *n-a*lkanes. Plant-derived *n*-alkanes frequently have a distinct odd carbon number preference, whereas petroleum-derived *n*-alkanes tend to exhibit a carbon indifference (Grice et al., 1968; Yang et al., 2011). Studies have found that *n*-alkanes are usually the predominant compounds of an oil derived product that has not been exposed to environmental degradation (Grice et al., 1968; Hostettler et al., 2013).

Unresolved complex mixtures of n-C_{10} to n-C_{40} are indicative of the significant biodegradation of the original crude oils, whereas typically, more refined oils will contain a more substantial fraction of small chained *n-a*lkanes ranging from n-C_9 to n-C_{36} (Yang et al., 2011). Higher viscosity crude oils, such as bitumen, contain less overall *n-a*lkanes, ranging from n-C_{16} to n-C_{36} (Yang et al., 2011). As many *n-a*lkanes are biogenic in origin, the use of a carbon preference index (CPI) can facilitate the differentiation amongst biogenic and petrogenic *n-a*lkane origins. This CPI is calculated by establishing the ratio of odd to even-numbered *n-a*lkanes over a fixed range. Petrogenic hydrocarbons sources have a CPI index approaching 1, whereas biogenic hydrocarbon sources have higher CPI values ranging from 2–12 (Andreou and Rapsomanikis, 2009; Grice et al., 1968; Simoneit, 2005; Zhen Wang et al., 2009). In general, carbon numbers greater than n-C_{27} reflect a carbon signature derived from higher plant waxes and fungi, whereas lower carbon numbers (C_{16} & C_{17}) infer inputs from algae and bacteria. C_{20} & C_{21} *n-a*lkanes are typical of petroleum origins, including diesel exhaust (Miyake et al., 2005; Olajire et al., 2008).

1.4 Paleolimnology

Petroleum hydrocarbons (PHCs) such as PACs, *n-a*lkanes, and biomarkers are present in many environmental compartments including, air, water, soils, sediments, and vegetation. As a result of their hydrophobicity, most PHCs are adsorbed to solids (Carls, 2006; Hall et al., 2012; Hsu et al., 2015). Transportation via surface water, erosion, and run-off, in addition to aerial deposition to watersheds, ultimately results in these compounds accumulating in basins at the bottom of lakes and rivers (Conly et al., 2002; Korosi et al., 2017). Using accumulated deposits within these river and lake basins, we can assess the change in PAC, biomarker, and *n-a*lkane loading within environmental systems and can track contaminant changes over time as a result of developmental changes within the surrounding area. The study of lake sediment cores as historical archives of lake deposits is a concept known as paleolimnology. These changes in contaminant quantity and quality can also be related to biological responses (e.g., changes in diatom community assemblages); a concept known as paleoecotoxicology (Bell and Blais, 2019; Cheney et al., 2020; Kurek et al., 2013a; Rose et al., 2018).

Lake sediment cores have recorded historical changes in contaminants throughout the Canadian oil sands and Northern Canada, including the Cold Lake oil sands, (Korosi et al., 2013, 2016a; Skierszkan et al., 2013), the Athabasca Oil Sands (Jautzy et al., 2013; Kurek et al., 2013a), the Peace-Athabasca Delta (Hall et al., 2012; Jautzy et al., 2015b) ,Yellowknife (Cheney et al., 2020), the Mackenzie Delta Uplands (Thienpont et al., 2013), Cameron Hills (Korosi et al., 2016b) and the Arctic (Bell et al., 2020). By providing a natural archive of environmental conditions, paleolimnology provides insight into spatial and temporal baseline conditions that are otherwise unknown. Lake sediment cores, collected from depositional locations within lake basins, have been used to infer historical depositional trends in environmental contaminants such as persistent organic pollutants and metals as well as fossilized paleobiological indicator species such as daphnia and diatoms (Boyle et al., 2015; Korosi et al., 2017, 2015). As these compounds of interest are deposited within the environment, they are transported through watersheds until they come to settle within lake basins. Over time these sediments accumulate and are compacted, creating layers of deposition. These lake sediments are cored and used as paleolimnological proxies of regional deposition, providing a historical record of the flux of contaminants to the area over time. Targeting a suite of environmentally relevant and chemically stable compounds

within these lake sediments (PACs, *n-a*lkanes, and petroleum biomarkers) therefore offers an opportunity to characterize temporal patterns in contaminant deposition within the Cold Lake oil sands. The use of these paleolimnological profiles can establish pre-industrial conditions and quantify (and attribute) increases in contaminant levels associated with oil sands activity.

1.5 Thesis Aims, Objectives, and Hypotheses

Alberta Oil Sands research has focused strongly on open-pit mining activities within the Athabasca Oil Sands Region, determining the contaminant burden associated with thermal *in-situ* oil sands operations has received less attention. With *in-situ* techniques being the dominant method of oil sands extraction in Canada, it is vital to better characterize the contaminant footprint associated with this method. This research aims to address the current knowledge gaps attributed to PHC production and distribution from *in-situ* oil sands operations.

PHCs such as PACs, *n-a*lkanes, and petroleum biomarkers are useful tools for assessing the source of environmental contaminants within the Cold Lake region as they are source-specific compounds originating from petroleum themselves. This study uses lake sediment cores to reconstruct historical contaminant profiles of PACs, *n-a*lkanes, and petroleum biomarkers to assess petrogenic contamination within the Cold Lake region as it relates to *in-situ* operations. Pinpointing the origin of petrogenic contaminants within the Cold Lake oil sands region will allow for the regional impact of oil sands mining to be determined, for the contaminant contribution of *in-situ* thermal extraction operations to be assessed, and for the Cold Lake oil sands region to be compared to that of the Athabasca oil sands region.

This thesis evaluates whether anthropogenically produced PHCs (1) can be detected and characterized to distinguish their originating source within the Cold Lake region and (2) are produced and distributed significantly because of *in-situ* oil sands operations. Petroleum hydrocarbon sources of primary interest include *in-situ* oil sand extraction operations (well pads), jet fuel from military planes as a result of the Cold Lake Air Weapons Range, local emissions from the city of Cold Lake, and vehicular exhaust.

This thesis aimed to address the following hypothesis: emissions attributed to thermal *in-situ* oil sands operations are significantly altering petroleum hydrocarbon concentrations and deposition rates in regional lakes. The predictions for this thesis are three-fold. (1) I predict that PHCs detected in modern lake sediments will be elevated when compared to those of pre-oil sands lake sediments. Sediments with a radiometric date prior to the onset of oil sands activity in Cold Lake (< ~1980) are indicative of pre-industrial background levels and, as such, are deemed to represent baseline or reference conditions. (2) I predict that PHC contaminant enrichment will increase with proximity to each well pad, like observations in open-pit mining regions regarding proximity to upgraders, petcoke piles and open-pit mines. (3) I predict that the PHC contaminant profile of Cold Lake bitumen can be used to identify and quantify *in-situ* PHCs in regional lakes by comparing the bitumen PHC fingerprint with pre-industrial and industrially influenced sediments.

The following chapters of this thesis provide a robust analysis of the history of PACs, *n-a*lkanes, and petroleum biomarkers within the Cold Lake region. Chapter 2 of this thesis assesses historical changes in PAC deposition rates within 11 lakes surrounding *in-situ* oil sands operations of Cold Lake, Alberta. Chapter 3 looks at petroleum biomarkers and *n-a*lkanes as potential proxies of historical changes in petroleum-derived contaminants. Chapter 4 summarizes the findings of this thesis and provides general conclusions, suggestions, and future directions, as well as outlines the significance of this work.

Chapter 2. Tracking Sources of Polycyclic Aromatic Compounds (PACs) near *In-Situ* Bitumen Operations of Cold Lake, Alberta

Kirsten K. Smythe[1]; Colin A. Cooke[2,3]; Paul E. Drevnick[2]; Robert J. Cornett[1,5]; Jules M. Blais[1,4]

[1] Department of Earth & Environmental Sciences, University of Ottawa, Ottawa, Ontario

[2] Environment & Parks, Government of Alberta, Edmonton, Alberta

[3] Department of Earth and Atmospheric Science, University of Alberta Edmonton, Alberta

[4] Department of Biology, University of Ottawa, Ottawa, Ontario

[5] Deceased

Abstract:

Most of the published environmental research on Canadian oil sands focuses on open-pit mining and bitumen processing operations. The environmental impacts attributable to *in-situ* oil sands are less well known; however, in 2012, *in-situ* methods surpassed open-pit mining as the dominant technique used for oil sands extraction in Canada. The Cold Lake oil sands deposit in Central-Eastern Alberta uses thermal *in-situ* steam injection to extract bitumen as reserves are situated deep below the surface, making them inaccessible to open-pit mining.

Polycyclic aromatic compounds (PACs) are ubiquitous, toxic contaminants of increasing interest in oil sands research because they are produced naturally and from oil sands operations. The lack of baseline monitoring prior to industrial development is catalyzing the debate amongst researchers and scientists as to whether oil sands operations are significant sources of PACs. Within the Cold Lake region, the presence of flow-to-surface events in the absence of exposed bitumen outcrops draws the question of whether *in-situ* activity is leading to regional PAC enrichment.

This thesis chapter examines historical changes in PAC profiles from radiometrically dated ^{210}Pb sediment cores to track spatial and temporal variations in PAC deposition since oil sands activity began in the Cold Lake region. We used alkylated PACs, predominantly petrogenic contaminants, to evaluate *in-situ* operations as potential petroleum contamination sources to surrounding lakes. Like open-pit regions, alkylated PACs in Cold Lake sediments were elevated compared to unsubstituted parent PACs and increased coeval with Cold Lake oil sands activity. Diagnostic ratios and pyrogenic indices provided evidence that PAC sources are strongly pyrogenic, however they shifted towards higher petrogenic contributions coeval with expanding oil sands extraction at Cold Lake. Both alkylated and unsubstituted PACs exhibit statistically significant increases in lake sediments following the development of oil sands operations in Cold Lake compared to pre-development PAC levels. PACs in sediment from regional lakes are weakly correlated to their proximity to *in-situ* oil wells, once corrected for lake area. These results suggest that *in-situ* operations are a likely source of PAC contamination to lakes surrounded by *in-situ* activity; however, emissions are more likely originating from natural gas combustion for steam generation, and exhaust from vehicles contribute more PACs than Cold Lake bitumen itself based on findings from diagnostic ratios.

2.1 Introduction

The Canadian Energy Research Institute (CERI) projected that oil sands production would contribute 1 trillion dollars to the Canadian economy between 2019 and 2029 (Romaniuk et al., 2019). Located 300 km south of the Fort McMurray open-pit mining operations, the Cold Lake oil field is responsible for producing 1.51 million barrels of crude bitumen per day using thermal *in-situ* methods (CAPP, 2019). In 2012, thermal *in-situ* bitumen extraction surpassed open-pit mining as the dominant method of oil sands extraction in Canada. Despite this, its environmental impact is less often reported in the peer-reviewed literature than open-pit mining (Korosi et al., 2013).

Contrary to open-pit mining, *in-situ* extraction does not require large-scale excavation of all vegetation and overburden material above the bitumen deposit. *In-situ* thermal techniques access bitumen reserves situated deeper than 75 m below the surface, approximately 80 % of all bitumen deposits in Canada (AER, 2018b). Briefly, *in-situ* extraction requires the use of vertical and horizontal wells drilled deep into the bitumen formation. Superheated steam and solvent are injected into the bitumen sands to decrease the molasses-like viscosity, at which point the bitumen separates from the sand matrix and flows to the surface through production wells (CAPP, 2017; Moorhouse et al., 2010). Collection tanks at the surface receive sixty-five percent (65%) of the bitumen, where it is mixed with a light hydrocarbon diluent to facilitate its flow through pipelines to refineries. Upgrading facilities process the remaining 35 % of the extracted bitumen, where pipelines then transport it to refineries.

Thermal *in-situ* oil sands extraction has distinct advantages over open-pit mining. For example, *in-situ* extraction requires $1/10^{th}$ of the land area compared to an open-pit mine that produces the same bitumen equivalent (AER, 2018c). *In-situ* extraction requires no crushing and separating facilities, and it produces no tailings ponds (AER, 2018c). *In-situ* extraction requires only 0.2 barrels of freshwater for every barrel of bitumen equivalent produced compared to 2.6 barrels of water per barrel of bitumen equivalent produced by open-pit mining (AER, 2018b). Also, *in-situ* techniques can use non-potable, saline water from groundwater, or oil sands process affected water (OSPW) to generate steam for injection (Moorhouse et al., 2010). Moreover, *in-situ* extraction recycled 86% of the water used for steam generation in 2018 (AER, 2018c).

Despite its advantages, *in-situ* oil sands extraction also has its costs. It consumes large quantities of natural gas for steam generation (AER, 2018c), it contaminates aquifers (CAPP, 2017), and it can result in vertical land deformation at a rate of 450 cm $year^{-1}$ by pressurizing the bedrock (Samsonov and Czarnogorska, 2014). Shen et al. (2015), recorded 30 cm of vertical land deformation after a 24-day injection cycle of Cyclic Steam Stimulation (CSS) drilling. In extreme cases, vertical land deformation can fracture the shale containment rock above the bitumen deposits, allowing non-targeted bitumen seeps to produce flow-to-surface (FTS) events (AER, 2018c). In January of 2009, a flow-to-surface incident occurred within the Primrose Lake oil field, 20 km north of the City of Cold Lake in the Cold Lake oil sands deposit. This flow-to-surface event was the first of five to occur within the Primrose region as a result of the Canada Natural Resource Limited (CNRL) *in-situ* CSS operations (AER, 2016). One such flow-to-surface event contaminated an unnamed water body (9-21, (Korosi et al., 2016a)), which was subsequently drained and dredged as a cleanup measure. Steaming operations within 1000 m of the seep were suspended following this incident (AER, 2016). A conservative estimate of 800 000 m^3 of bitumen flowed to the ground surface as a result of these five flow-to-surface events (AER, 2016).

Bitumen contains several pollutants, including rare earth elements, heavy metals, and organic contaminants that may affect human and ecosystem health. In the case of Cold Lake, however, Skierszkan et al. (2013) concluded that *in-situ* bitumen extraction was not a significant source of arsenic, cadmium, copper, mercury, nickel, lead, or vanadium to nearby lakes. They also observed only minor enrichment of cadmium, arsenic, nickel, and vanadium in soils near *in-situ* operations. All metal concentrations in soil and sediment in the Cold Lake region were well below Canadian regulatory guidelines for the protection of aquatic life (Skierszkan et al., 2013). In contrast, sediment cores from lakes near open-pit mining operations in the Athabasca oil sands region had metal concentrations that exceeded Canadian regulatory guidelines for the protection of aquatic life (Cooke et al., 2017; Klemt et al., 2020).

In addition to metals, organic contaminants such as polycyclic aromatic compounds (PACs) are a contaminant of concern associated with Alberta oil sands because they are naturally present in bitumen at high concentrations. PACs are of particular interest as they are mutagenic, carcinogenic, and toxic. PACs are highly lipophilic with low water solubility, which makes them

persistent in aquatic environments and tissues (Neff et al., 2005). Their toxicity depends on their chemical structure, molecular weight, and degree of alkylation. PACs are studied broadly within the open-pit mining regions of the Alberta oil sands because they are both petrogenic and pyrogenic in origin (Timoney and Lee, 2011). Pyrogenic PACs are unsubstituted parent compounds formed in high-temperature combustion environments such as that of forest fires. Petrogenic PACs form over millions of years under high-pressure and high-temperature petrogenesis conditions. The conditions under which they are formed result in petrogenic PACs having high degrees of alkylation (Thienpont et al., 2017; Tobiszewski and Namieśnik, 2012). Petrogenic and Pyrogenic PACs are traceable to their sources using a range of petroleum fingerprinting techniques (De La Torre-Roche et al., 2009; Yunker et al., 2002). As PACs are emitted during bitumen extraction and processing, several studies have analyzed alkylated PACs in snowpack samples, water, lake sediments, lichen, and moss to trace their presence throughout the Athabasca oil sands region. (Galarneau et al., 2014; Kelly et al., 2009; Kurek et al., 2013b; Landis et al., 2019; Timoney and Lee, 2009; Zhang et al., 2016).

In the Cold Lake region, Korosi et al. (2013) cored two lakes east of the City of Cold Lake: Ethel and Hilda Lake and recorded an increase in alkylated PACs since the onset of commercial *in-situ* bitumen in Hilda Lake, but not in Ethel Lake. In a follow-up study, Korosi et al. (2016a) assessed whether a series of bitumen FTS events had contaminated a nearby lake (Lake 12-26). This study recorded increased alkylated PACs in sediments from Lake 12-26 when oil sands extraction began in 1985, suggesting a petrogenic origin (Korosi et al., 2016a). These two studies show that PAC accumulation differs throughout *in-situ* regions, suggesting multiple different PAC sources are present.

This study aims to determine whether *in-situ* oil sands extraction contributes to PAC contamination in the environment. We quantified PACs in radiometrically-dated lake sediment cores to examine whether or not they increased following *in-situ* bitumen extraction. Statistical interpretations of principal components and regression analyses using parametric and non-parametric tests, allow us to determine how PAC composition in lake sediments relates to petrogenic and pyrogenic PAC sources. If *in-situ* oil sands operations are not contributing to significant environmental contamination, we aim to determine what is driving contaminant loading within the Cold Lake area. Potential emission sources can be distinguished using

diagnostic ratios, pyrogenic indices, and chemical fingerprinting based on chemical composition. Sources of interest include local emissions from the city of Cold Lake, forest fires, traffic emissions, jet-fuel, activity associated with the Cold Lake Air Weapons Range (CLAWR).

2.2 Methodology

2.2.1. Study Area

Our study area was the boreal forest of Central/North-Eastern Alberta in the Cold Lake oil field. The Cold Lake oil sands are unique in that they are the sole oil sands region in Canada to operate exclusively through thermal *in-situ* techniques in the absence of all oil sands processing facilities, upgraders, tailings ponds, and open-pit mining. The dominant wind patterns in Cold Lake are from the west-northwest and move towards the east-southeast, making the Cold Lake oil sands region directly downwind from the open-pit mining of the Athabasca oil sands deposit (Imperial Oil Resources Limited, 2016). The isolation of this region by 300 km from the influence of other bitumen extraction operations makes the Cold Lake oil field idyllic for quantifying petroleum-derived contaminants produced by the *in-situ* activity.

2.2.2 Study Sites and Core Collection

We selected eleven lakes throughout the Cold Lake oil sands region based on their size and proximity to oil sands well pads (Figure 2-1, Table 2-1). We collected sediment cores from the depocenter of each lake with a Uwitec gravity corer (Mondsee, Austria). Cores were sectioned on-site into 0.5-cm intervals using a modified Glew vertical extruder (Glew, 1988). Extruded samples were stored in pre-labelled Whirl-Pak® bags, frozen, and shipped to the University of Ottawa, where they were weighed and stored at -18^{o}C until laboratory analyses began. Homogenized subsamples of selected lake sediment intervals were freeze-dried for percent water determination, radiometric dating, and elemental analysis.

Table 2- 1: Summary of lake parameters and coring locations. Lakes located within the CLAWR are marked with a Y, lakes outside of the CLAWR are marked with an N. Depth refers to the deepest estimated point of the lake basin where the core was collected. Distance refers to the mean distance of each lake from *in-situ* oil wells to the southwest. Well density refers to the number of wells situated within a 7 km radius from the coring location. Unnamed waterbodies have no formal Lake Name.

Coordinates	Lake ID	Lake Name	CLAWR	Depth (m)	Area (m^2)	Distance (m)	Well Density (#)
55.0805, -110.5597	RL02		Y	1.00	147.4	1487	23
55.0673, -110.5645	RL04		Y	1.00	794.3	1299	31
54.9111, -110.6014	RL06		Y	3.90	44.86	4345	13
54.8619, -110.5837	RL08		Y	1.10	144.7	2361	35
54.8028, -110.3778	RL10		Y	1.20	43.10	2809	21
54.7227, -110.6595	L13	Sinclair Lake	N	9.50	1888	3321	43
54.7114, -110.3942	L14	May Lake	N	3.40	3117	4688	15
54.6648, -110.5437	L15	Bourque Lake	N	30.0	9944	1625	>100
54.6081, -110.4601	L16		N	1.20	252.0	916.5	>100
54.5895, -110.4753	L17	McDougall Lake	N	3.90	505.6	1009	88
54.6306, -110.2775	L18	Marie Lake	N	19.0	34 600	6584	5

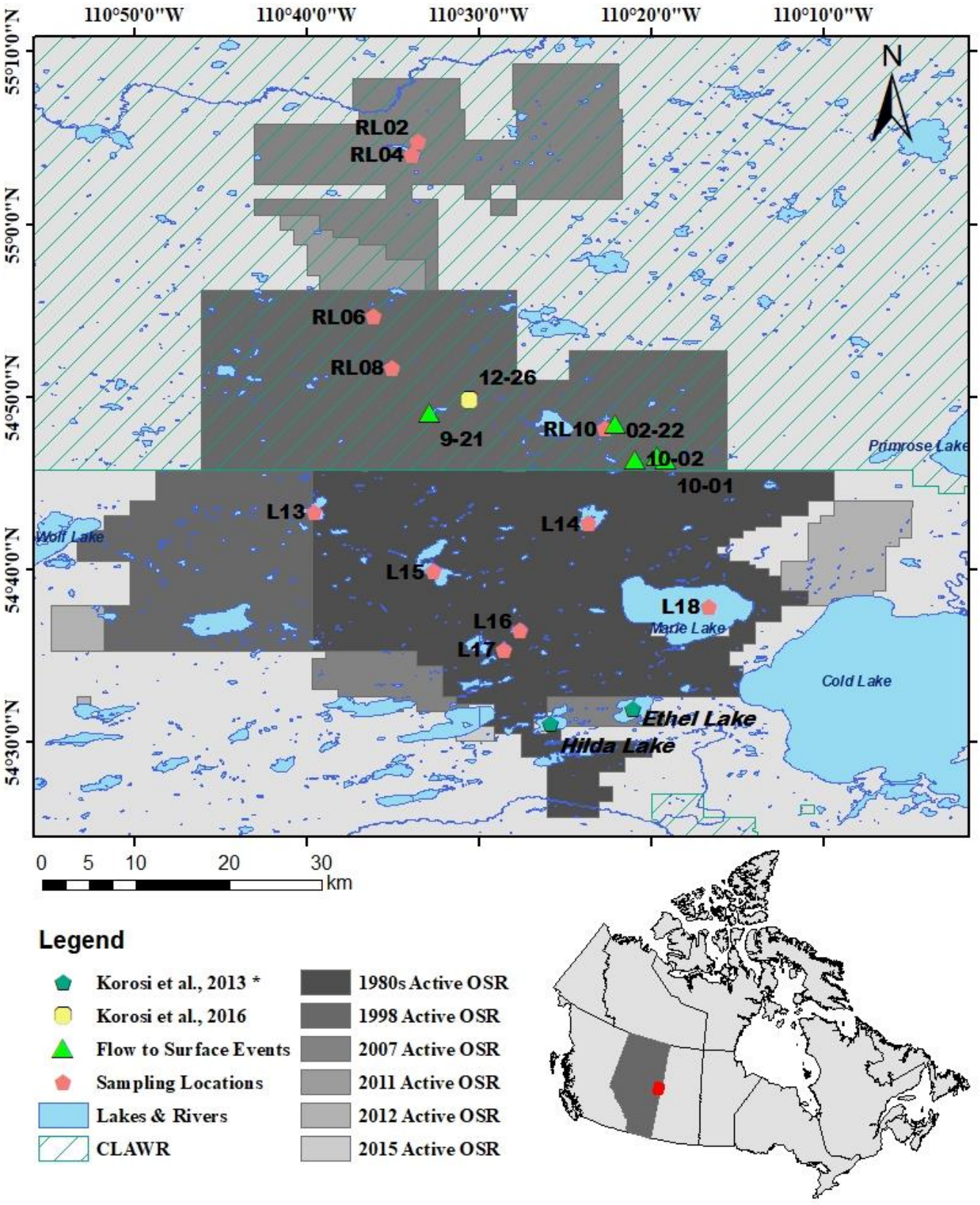

Figure 2- 1: Map of the Cold Lake Oil Sands Region, the timing of development, and our 11 study lakes. Also shown are the study lakes of Korosi et al. (2013;2016), and the location of five historical flow-to-surface events in the region. The change in the active oil sands region is cumulative throughout time since initial development in the 1980s. Ethel and Hilda Lakes analyzed in Korosi et al. (2013) were the same lakes studied by Skierskan et al. (2013) and Thienpont et al. (2017).

2.2.3 Radiometric Dating

We calculated age-depth profiles for each sediment core based on ^{210}Pb gamma spectroscopy at the University of Ottawa. Freeze-dried sediments were counted for 23 hours (82800s) on an Ortec High Purity Germanium Gamma Spectrometer and analyzed using MAESTRO version 6.08 software (Advanced Measurement Technology Inc. Oak Ridge, TN, USA). Certified Reference Materials (IAEA-312 & IAEA-385) from the International Atomic Energy Association (Vienna, Austria) established efficiency calibrations for the gamma spectrometer. ScienTissimMe software (Barry's Bay, ON, Canada) used unsupported ^{210}Pb activity, described by Appleby (2001), to model a constant rate of supply (CRS) dating model and sedimentation rates (Appleby and Oldfield, 1978) for each lake sediment core. We corroborated CRS dates with the 1963 ^{137}Cs peak from atmospheric nuclear weapons testing (Omelchenko et al., 2005; Taylor et al., 1988). Radiometric dating profiles and sedimentation rates are given in the supplementary information (Figure S2-1).

2.2.4 Elemental Analyses

Sediment subsamples were freeze-dried and then acidified in an H_2O: HCl acid desiccator to remove all carbonate content as per Skierszkan et al. (2013). After 48 hours, acidified sediments were rinsed three times with de-ionized water and re-lyophilized. A VarioEL cube elemental analyzer (Elementar Americas Inc., New York) determined the % carbon, nitrogen, and sulphur (%CNS) in 5–10 mg subsamples of the acidified sediment, combined with 10–15 mg of tungsten trioxide (WO_3) in a tin capsule. Calibration standards of sulfanilamide and sulfanilic acid were analyzed alongside the sediment samples to ensure machine detection efficiency. The Ján Veizer Stable Isotope Laboratory (University of Ottawa) performed these analyses.

We measured Mercury concentrations in 4 of the 11 lake sediment cores (RL04, L16, L13 and L15) at the University of Ottawa LANSET laboratories. Approximately 0.05 g of freeze-dried sediments, weighed into an Sp-3D automatic mercury analyzer (Nippon Instrument Corp), ran alongside Marine Sediment Certified Reference Material (MESS-3) and NIST-2704 Buffalo River Sediments from the National Research Council of Canada for instrument efficiency corrections. Every 10th sample was analyzed in duplicate with an average relative standard deviation of 1.05 ng Hg/g recorded. The method uncertainty was determined to be

7.43%. Summaries of all elemental analyses are located in the supplementary information (Figure S2-2).

2.2.5 PAC Extraction and Analysis

Accelerated Solvent Extraction (ASE) extracted PACs from fresh lake sediments using US EPA extraction procedure #3540C. We extracted sediment samples under low light because some PACs are susceptible to photodegradation. Briefly, we homogenized sediment samples to obtain ~0.5 g of total organic carbon (TOC). Samples were centrifuged in falcon tubes for 30 minutes at 3000 rpm using an Eppendorf Centrifuge 5810, decanted, and blended with Hydromatrix ™ diatomaceous earth (Varian Inc. Palo Alto, CA, USA) to eliminate excess water. Samples, including a standard reference material of organics in marine sediments from the National Institute of Standards and Technology (NIST SRM 1941b), were assembled into Dionex ASE-350 cells and spiked with 100 µL of a recovery standard before extraction by ASE in 1:1 acetone: hexanes (Thermo Scientific, Dionex Corporation, Sunnyvale, CA, USA). The recovery standard contained a deuterated mixture of naphthalene (D8, 99.5 %), acenaphthene (D10, 99 %), phenanthrene (D10, 98 %), benz[a]anthracene (D12, 98 %), perylene (D12, 98 %), and n-tetracosane (D50, 98 %), (Cambridge Isotope Laboratories Inc. Tewksbury, MA, USA). We applied recovery groups to the remaining PACs analyzed. Acenaphylene and fluorene were corrected to acenaphthene (D10, 99 %), dibenzothiophene, anthracene, and retene were corrected to phenanthrene (D10, 98 %), fluoranthene, pyrene, and chrysene were corrected to benz[a]anthracene (D12, 98 %), and benzo[b]fluoranthene, benzo[k]fluoranthene, benzo[e]pyrene, benzo[a]pyrene, indeno[1,2,3-c,d]pyrene, dibenz[a,h]anthracene, and benzo[g,h,i]perylene were recovery corrected to perylene (D12, 98 %).

Liquid-liquid extractions of PACs in hexanes eliminated residual water and co-extracts. We collected the non-polar, hexane phase in 2 mL of 2,2,4-Trimethylpentane (TMP) and evaporated to 2 mL with a gentle 0.4 bar nitrogen stream at 23^{o}C in a Zymark ® TurboVap® II (Biotage Charlotte, NC, USA). Samples were centrifuged at 6000 rpm for 10 minutes using a fixed rotor and decanted to eliminate residual surficial emulsions. Using a Pasteur pipette, the sample was transferred to a glass centrifuge tube and evaporated to precisely 1 mL using a Pierce Reacti-Vap™ (Model 18780) gentle nitrogen stream.

We used silica gel column chromatography to collect the F1 (*n*-alkanes & biomarkers) and F2 (aromatics) fractions. Column cleanup required 50 mL solvent-rinsed columns packed with 6 g of grade 644 silica gel (Fisher S7441) to be conditioned with 20 mL of dichloromethane (DCM) and hexanes. Air bubbles were removed from the top inch of the column using a Pasteur pipette, and 1 g of sodium sulphate was added to the top of the column to ensure the elimination of any residual water. The *n*-alkanes and biomarker (F1) fraction was eluted through the column using 22 mL of hexanes, followed by the F2 fraction with 40 mL of 1:1 DCM: hexanes. For this chapter, F1 *n*-alkanes and biomarkers will not be discussed and can be found in Chapter 3. The F2 fraction was collected in 2 mL of TMP and evaporated to 1 mL using a 0.4 bar nitrogen stream. The sample was filtered into a glass and preparative liquid chromatography (Prep-LC) collection vial using a 0.2 µm polytetrafluoroethylene (PTFE) membrane filter (ThermoFisher Scientific Inc #721-1320). Following two 1 mL rinses with DCM, the F2 fraction was analyzed using Prep-LC to remove large complex molecules and pigments. Each sample was evaporated to a final volume of 1 mL in TMP, spiked with 10 µL of p-terphenyl (D_{14}, 98 %) internal standard, and analyzed using gas chromatography coupled with mass spectrometry (GC-MS).

The PAC compounds targeted for analysis included the 16 unsubstituted US-EPA priority PACs and their alkylated homologues as well as benzo[e]perylene, pyrene, retene, benzo[a]pyrene, benzo[b]napthothiophenes, and dibenzothiophene (Table S2-1). We quantified GC-MS chromatographic peaks using MSD ChemStation Data Analysis F.01.03 Software (Agilent Technologies, Santa Clara, CA, USA). Mean recoveries for surrogate target compounds ($\pm$ 1 standard deviation (STDEV)) were 30.9 $\pm$ 11.7 % for *d8*-naphthalene, 45.9 $\pm$15.4 % for *d8*-acenaphthene, 58.0 $\pm$ 15.0 % for *d10*-phenanthrene, 113.6 $\pm$ 17.1 % for *d12*-benzo[a]anthracene, and 98.3 $\pm$ 18.8 % for *d12*-perylene.

2.2.7 Statistical Analyses

We used the RStudio statistical computing environment, version 3.6.1 (R Core Team, 2018) to code all statistics, data visualizations, and analyses for this study. Spatial analyses, mapping and map generation, was completed using ESRI's ArcGIS 10.6.1 (ESRI ArcGIS Desktop, 2018). All graphical plots were generated using the *ggplot2* package and the *ggpubr* package. Historical trends within the data were established by conducting downcore analyses with respect to the CRS dating model.

To ascertain the sources of PACs within our study lakes, we use diagnostic ratios and pyrogenic indices. Diagnostic ratios are commonly applied in oil sands research as they rely on comparisons of PACs with similar molecular weights and physicochemical properties to distinguish petrogenic and pyrogenic PAC origins (Lima et al., 2003; Tobiszewski and Namieśnik, 2012; Yunker et al., 2002). The diagnostic ratios selected for these analyses were used to track historical changes in petrogenic vs. pyrogenic emission sources, to assess fuel emission sources, to determine the contribution of wood burning, and to compare traffic and non-traffic emissions; amongst others. The diagnostic ratios calculated in this chapter include:

1) Fluoranthene / Pyrene ratio = FLA / (FLA+PYR),
2) Indeno[1,2,3-cd]pyrene /Benzo[g,h,i]perylene ratio = IcdP / (IcdP + BghiP),
3) Fluorene / Pyrene ratio = FL / (FL+PYR),
4) Anthracene / Phenanthrene ratio = ANT / (ANT+PHE),
5) Benzo[a]anthracene / Chrysene ratio = BaA / (BaA + CHR)
6) Benzo[b]fluoranthene / Benzo[k]fluoranthene ratio = BbF / BkF
7) Benzo[a]pyrene / Benzo[g,h,i]perylene ratio = BaP/BghiP
8) Retene / Chrysene ratio = RET / (RET+CHR)
9) Benzo[a]pyrene / Benzo[e]pyrene = BaP / (BaP + BeP)
10) ΣLMW/ΣHMW = Σ(2-3ring PACs) / Σ(4-5ring PACs)
11) ΣCOMB/ΣPACs $= \frac{\Sigma(\text{FLA, PYR, BaA, CHR, BkF, BbF, IcdP, BghiP})}{\Sigma(\text{Unsubstituted PACs})}$

The pyrogenic index, as determined by Wang et al. (1999), was calculated using equation 1. This index relies on the comparison of the sum of 3–6 ring EPA PACs to the sum of the five alkylated PAC homologs to assess the change in PAC origin over time. A pyrogenic index $\geq$ 0.05 suggests a pyrogenic influence, 0.02–0.05 suggests a heavy oil/fuel origin, and a pyrogenic index $\leq$ 0.01 implies a light petroleum product source origin (Wang et al., 1999).

$$PI = \Sigma(\text{“other” 3–6 ring EPA PACs})^{*} / \Sigma(\text{5 alkylated PAC homologues})^{**} \quad (1)$$

We categorized each core into pre-development and post-development timeframes, based on the CRS dating model, to quantify the regional change in deposition since oil sands activity began in the southern Cold Lake region. Relative abundances of the means for each compound

[*] 3–6 ring EPA PACs include: ACY, ACE, ANT, FLU, PYR, BaA, BbF, BkF, BaP, IghiP, DahA, BghiP
[**] 5 alkylated PAC homologues include: C0-C4 NAP, C0-C4 PHE, C0-C3 DBT, C0-C3 FL, C0-C3 CHR

facilitated chemical fingerprinting to compare the data to that of a Cold Lake bitumen sample. Petroleum fingerprinting is a useful tool to classify petroleum source origins and therefore is applied in this study to determine whether we can find evidence that Cold Lake bitumen is entering regional lakes (Chen et al., 2012; Wang et al., 2014; Yang et al., 2011). Relative abundance calculations were also applied to perform principal component analyses (PCAs) to assess the variations in the downcore PAC composition in each lake. We created PCA biplots using the fviz_pca_biplot() function within the R package *factoextra.* A Cold Lake bitumen sample was scaled and plotted passively onto the PCA biplot using the *ggbiplot* and *devtools* packages. The US-EPA 16 priority PACs, dibenzothiophene, benzo[e]pyrene, retene, benzo[B]naptho(2,3-1,2d)thiophene, and benzo[B]naphtho(2,1d)thiophene are included in the unsubstituted PAC, PCA analysis.

We conducted regression analyses to assess the spatial and temporal relationship between PAC flux and proximity to oil sands operations following procedures in Cheney et al. (2020). An analysis of variance (ANOVA) assessed the mean PAC flux in pre and post-oil sands development sediment groups (as determined by the CRS dating mode). Log transformations of the PAC sediment flux and the distance downwind from oil wells were necessary to meet the assumptions of parametric tests. Before executing the ANOVA, a Bartlett Test compared the variance between pre and post-development groups to assess for homogeneity of variance (bartlett.test()). When the normality assumption was not met, we used a Levene Test in place of the Bartlett Test to assess the homogeneity of variance amongst the groups (leveneTest()). An ANOVA (using the R packages *Car* and *lmtest)* followed by a Tukey post-hoc test assessed the variation in PAC fluxes amongst groups with homogeneous variance within the datasets. Rejection of the null hypothesis from the Levene and Bartlett tests resulted in a non-parametric Kruskal-Wallis test and Dunn post-hoc test to be used instead of the ANOVA.

We used the Breusch-Pagan studentized test for fitted values (bptest()) to verify that the residuals of our linear model met the assumptions of homoscedasticity. The assumption of serial autocorrelation in residuals was checked using the Durbin-Watson test (dwtest()). The RESET test tested the assumption of linearity in the residuals (resettest()), and the Shapiro Wilk normality test verified the assumption of normality within the residuals (shapiro.test()). The *gvlma* package confirmed that the assumptions were met and that further transformations were

not necessary. The gvlma() function performed a global test on 4 degrees of freedom, a level of significance of 0.05, and assessed Global Stat, Skewness, Kurtosis, Link Function, and Heteroscedasticity.

An analysis of covariance (ANCOVA) further assessed the influence that lake area and proximity to *in-situ* oil wells have on PAC flux in each of the development groups (pre vs. post) that were deemed statistically significantly significant by the ANOVA. As per the ANOVA methods, we tested the residuals of the ANCOVA model to ensure they met the assumptions of parametric tests (using the R packages *Car, gvlma,* and *lmtest)*. If an assumption failed to reject the null hypothesis, a non-parametric permutation test from the *lmperm* package was applied to test the validity of the model.

2.3 Results and Discussion

2.3.1 Historical Changes in PAC Deposition

Total unsubstituted and alkyl PAC concentrations in lake sediment profiles (ng/g dry weight) appeared unaffected by *in-situ* bitumen extraction (Figure 2-2). Most of the lakes exhibited variable sedimentation rates (Figure S2-1). Therefore, we calculated PAC accumulation rates (fluxes) and found that alkylated PAC fluxes increased coeval with *in-situ* bitumen extraction in lakes L18, L17, L16, L15, L14, and L13, suggesting recent increases of petrogenic PACs in those lakes. Additionally, alkylated PAC accumulation rates were greater than unsubstituted PAC accumulation rates, suggesting petrogenic origins. PAC accumulation rates, based on CRS model sedimentation rates (Figure S2-1), increased as early as 1960 when oil sands pilot projects began in L17, L16, and L15.

Lakes located south of the CLAWR, in the densest area of *in-situ* oil sands activity, are significantly higher in alkylated (*p*-value <2e-16) and unsubstituted PAC (*p*-value <2e-16) fluxes than lakes on the CLAWR (Table 2-1). For example, Lake L15 (located south of the CLAWR) reached maximum PAC concentration and flux values of 370 ng g^{-1} and 35 µg m^{-2} yr^{-1}, over 3x higher than the maximum PAC concentrations and fluxes of 95 ng g^{-1} and 12 µg m^{-2} yr^{-1} in Lake RL04 located on the CLAWR (Table 2-2).

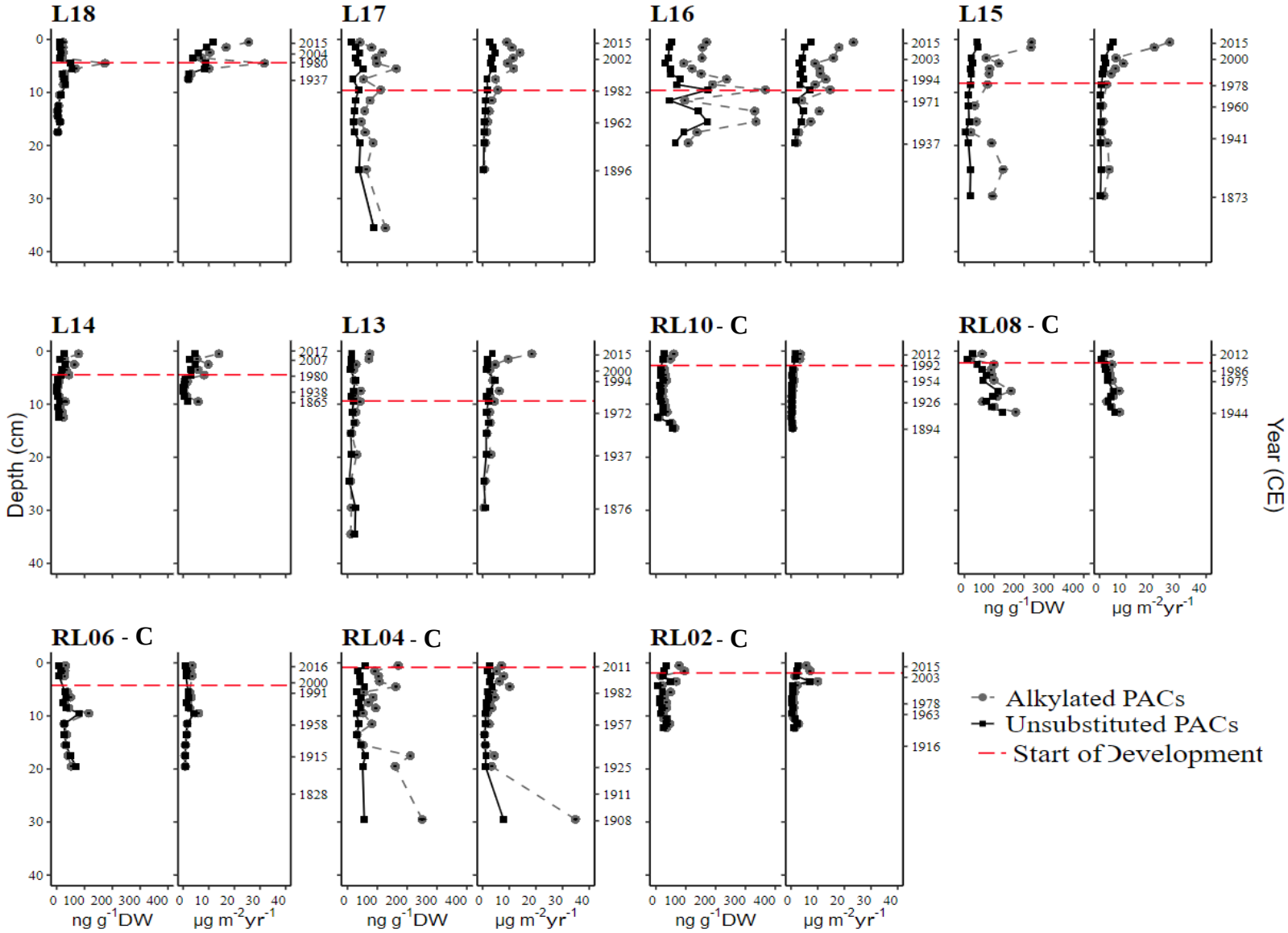

Figure 2- 2: Total alkylated and unsubstituted PAC profiles as a function of depth. Scatter plots of the total concentration (ng g^{-1} DW) of the 16 priority PACs (Unsubstituted) and their alkylated homologues (Alkylated) with respect to PAC accumulation rate (ug m^2 yr^{-1}) down core. All plots have the same Y axis, representing depth downcore in centimeters. Left plots depict the total concentration of PACs corrected for dry weight. Plots to the right depict the rate of total PAC flux. Dates were established using the CRS dating model. PAC flux was not calculated below the horizon of unsupported ^{210}Pb activity as it exceeds the limitations of the CRS dating model. The dashed red line corresponds to the year when oil sands operations began near each lake. "C" indicates lakes located on the CLAWR

Table 2- 2: Summary statistics from an ANOVA comparing the total PAC accumulation rates in lakes located on and off of the Cold Lake Air Weapons Range, measured in µg m^{-2} yr^{-1}. On CLAWR *n* = 5 lakes. Off CLAWR *n* = 6 lakes.

	Min	Max	Mean	Std. Dev	*P*-Value
Unsubstituted PACs					
Off CLAWR	0.0907	11.6	2.73	2.34	< 2e-16
On CLAWR	0.0652	7.84	1.80	1.58	
Alkylated PACs					
Off CLAWR	0.2430	31.7	7.37	6.77	< 2e-16
On CLAWR	0.0872	34.8	3.44	4.56	

Activity from the Cold Lake Air Weapons Range began in the 1950s. Since the CLAWR has strict regulations limiting industrial development, oil sands activity off the CLAWR has expanded more rapidly and extensively than those regions located on the CLAWR (Figure 2-1). Unsubstituted PACs increased as early as the late 1940s in RL06, RL04 and RL02, predating *in-situ* bitumen extraction to that region by 60 years. However, the increased PACs may be attributable to ammunition testing and fighter jet training that began in the 1950s (Figure 2-2). In contrast, alkylated PAC fluxes increased more substantially in the early 2000s in RL10, RL06, RL04 and RL02, coeval with the start of *in-situ* extraction in that part of the CLAWR. RL10, RL04, RL06, and RL02 are all located close to *in-situ* facilities, equipment, and roads (around 200 m or less). These are busy areas (e.g., traffic), which may be significant PAC sources to these lakes.

Lake 12-26, located near the 2013 FTS site 9-21, recorded an increase in PACs since 1985, reaching a maximum alkylated PAC flux and concentration of 50 µg m^{-2} yr^{-1} and 800 ng g^{-1} (Korosi et al., 2016a). Lake RL08, situated 3 km away from the FTS site, exhibited decreases in alkylated and parent PAC fluxes occurring steadily since the 1960s. The lack of increasing PAC deposition in RL08 suggests there is considerable spatial heterogeneity in PAC deposition in this region. These findings indicate that lake 12-26 is a hot-spot of PAC contamination, likely attributed to the FTS event as nearby lakes would have recorded the same atmospheric inputs (AER, 2016; Korosi et al., 2016a).

2.3.2 PAC Composition and Characterization

We examined two diagnostic ratios commonly applied in oil forensics to track the transition between petrogenic and pyrogenic PAC origins (Figure 2-3) (De La Torre-Roche et al., 2009). We typically define petrogenic PACs as having fluoranthene (FLA) and pyrene (PYR) ratios (FLA/(FLA+PYR)) $\geq$ 0.4, whereas ratios between 0.4-0.5 suggest contributions from fossil fuels. FLA/(FLA+PYR) ratios $\geq$ 0.5 suggest pyrogenic sources (wood, coal, grass, etc.) (Thienpont et al., 2017; Tobiszewski and Namieśnik, 2012). Likewise, an IcdP/(IcdP+BghiP) ratio $\leq$ 0.2 denotes petrogenic origin, 0.2-0.5 represents a petroleum combustion source, and $\geq$ 0.5 suggests biomass burning (Thienpont et al., 2017; Yunker et al., 2002).

We observe a distinct shift—from a strongly pyrogenic origin to that more closely reflecting a petrogenic source—in all 11 lakes. In L18 and L15, this transition occurs in the 1980s. Thienpont et al. (2017) measured stable FLA/(FLA+PYR) ratios of 0.7 throughout the Ethyl Lake core, with the IcdP/(IcdP+BghiP) ratio driving the transition to a pyrogenic source. Contrarily, the transition towards petrogenic inputs in our study lakes were driven by the change in FLA/(FLA+PYR) ratios, confirming that there is spatial heterogeneity in the region (Figure 2-3). IcdP/(IcdP+BghiP) ratios remained consistently around 0.5 in Lakes L18, L17, L16, L15, L14, L13, and RL04. An IcdP/(IcdP+BghiP) ratio of 0.5 in Lakes L18, L17, L16, L15, L14, L13, and RL04 suggests PACs from biomass burning or petroleum combustion (Figure S2-4). FLA/(FLA+PYR) ratio > 0.5 in these same lakes (Figure S2-5), also suggested forest fires or biomass burning (Schuster et al., 2015; Yunker et al., 2002).

Diagnostic ratios comparing low molecular weight (LMW) to higher molecular weight (HMW) PACs (ΣLMW/ ΣHMW)(Figure S2-6)(Zhang et al., 2008), and anthracene (ANT) to phenanthrene (PHE) (ANT /(ANT+PHE)) (Figure S2-7) (Pies et al., 2008) provided supporting lines of evidence confirming that pyrogenic PACs originating from forest fires are dominant in lake sediments. We observed petrogenic PACs becoming increasingly abundant as lakes transition towards a petrogenic PAC origin closely resembling a petroleum combustion source.

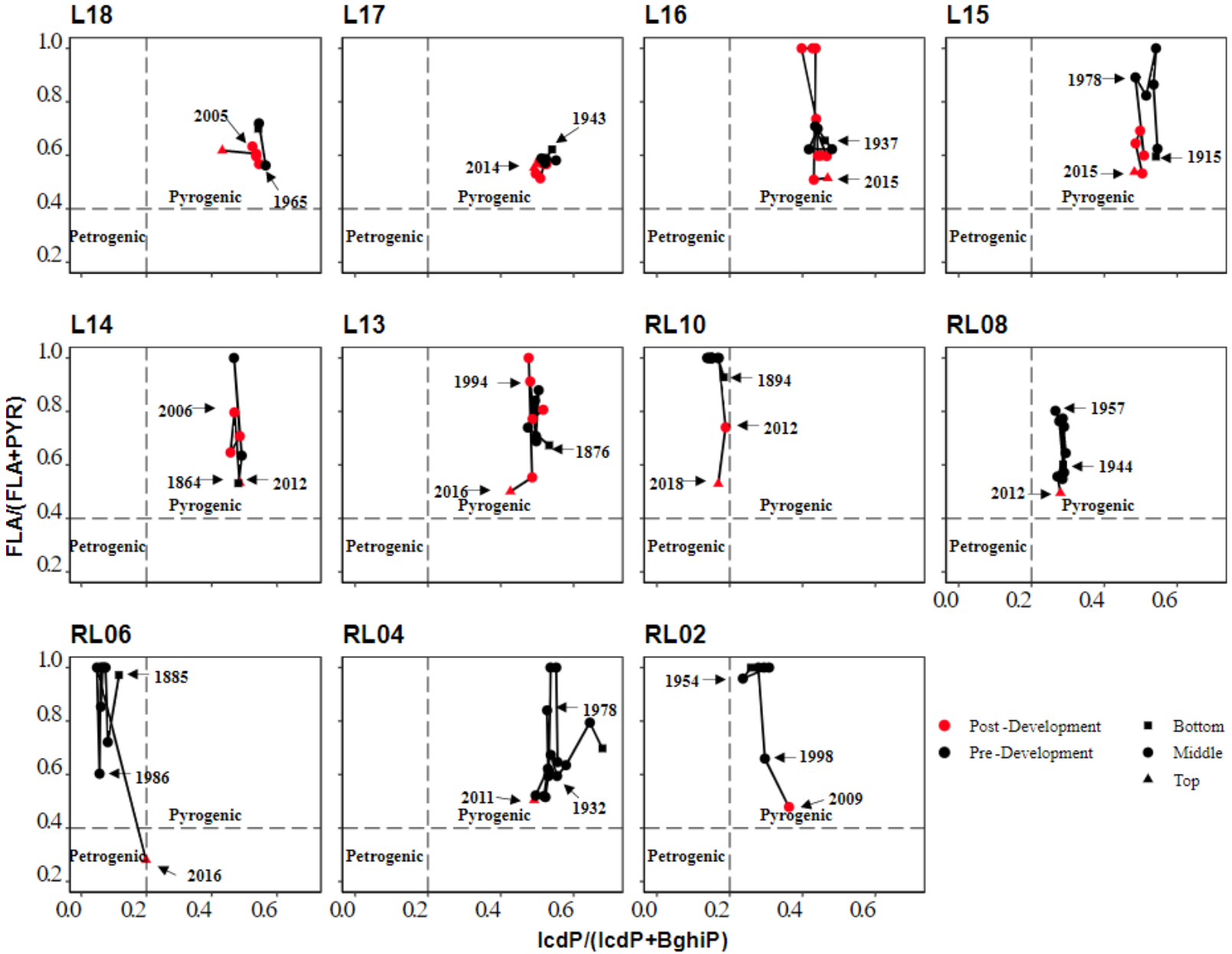

Figure 2- 3: Two-dimensional diagnostic ratio plots depicting the shift in PAC composition throughout time. All plots maintain consistent X and Y axes. Data points are connected to show the deposition history of PACs and are categorized regarding their position within the core, top interval, bottom interval, and middle intervals. The hatched lines show the separations between petrogenic and pyrogenic PAC ratios (Thienpont et al.,2017; Yunker et al.,2002). The red datapoints indicate modern sediments deposited after oil sands operations began near each lake, black datapoints are those deposited prior to developments. Diagnostic ratios of 1 indicate pyrene was below the method of detection limit within the sediment interval.

Katsoyiannis et al. (2007) found benzo[a]pyrene (BaP) / benzo[g,h,i]perylene (BghiP) ratio > 0.6 derived from vehicular emissions. All lakes exhibited an increasing traffic emission influence; however, these inputs are less significant in more isolated lakes, L14, RL10, RL08, and RL06 (Figure S2-8). The input from traffic emissions surpasses 0.6 in Lakes L13, L15, L16, RL04, and RL02 with the onset of oil sands operations. Fossil fuel combustion associated with growing oil sands operations and the traffic associated with the implementation of infrastructure is likely driving this shift.

To distinguish local traffic emissions from those of *in-situ* oil sands activity, we analyzed fluorene (FL), pyrene (PYR) diagnostic ratios, FL/(FL+PYR) (Figure S2-9) (Ravindra et al., 2008). FL/(FL+PYR) values $\leq$ 0.5 indicate a petrol emission source (more likely resulting from city traffic and natural gas combustion), whereas FL/(FL+PYR) values $\geq$ 0.5 denote diesel emission sources (more likely from large vehicles operating within oil sands regions) (Ravindra et al., 2008). FL/(FL+PYR) ratios > 0.5 in Lakes L16, L15, L13, and RL04 indicate a consistent diesel emission source. Throughout time, these lakes transitioned towards FL/(FL+PYR) ratios < 0.5, especially since the onset of oil sands activity in the late 1980s likely from the increased combustion of natural gas by oil sands industries to generate steam for *in-situ* thermal operations. Lakes L18, L17, L14, and RL02 consistently yield FL/(FL+PYR) ratios $\leq$ 0.5; therefore, one traffic emission type is not outweighing the other.

The pyrogenic index (PI), modified from Wang et al. (1999) to incorporate pyrene in place of perylene, relies on the comparison of the sum of 3-6 ring, unsubstituted PACs to that of the 5 alkylated PAC homologues. A pyrogenic index < 0.01 indicates light petroleum product origins, PI's from 0.02-0.05 represent heavy oils and fuels and values > 0.05 denote pyrogenic influences. All 11 lakes transition towards a PI resembling petrogenic origin commencing around the start of oil sands development (Figure 2-4). Range lakes RL10, RL08, and RL06 exhibit a gradual progression to petrogenic origins throughout the entire core. The PI in lakes L15, RL04 and RL02 increase in the early-mid 1900s; however, all reach a maximum PI value of approximately 0.5 and transition back towards petrogenic origins. This peak occurs in the 1980s for L15, in the 1950s for RL04, and in the 1960s for RL02. Lake RL02 then increases to a PI of 1.5 in 2003 before decreasing again towards a petrogenically derived source, coinciding with the development of oil sands operations in the northern region of the CLAWR.

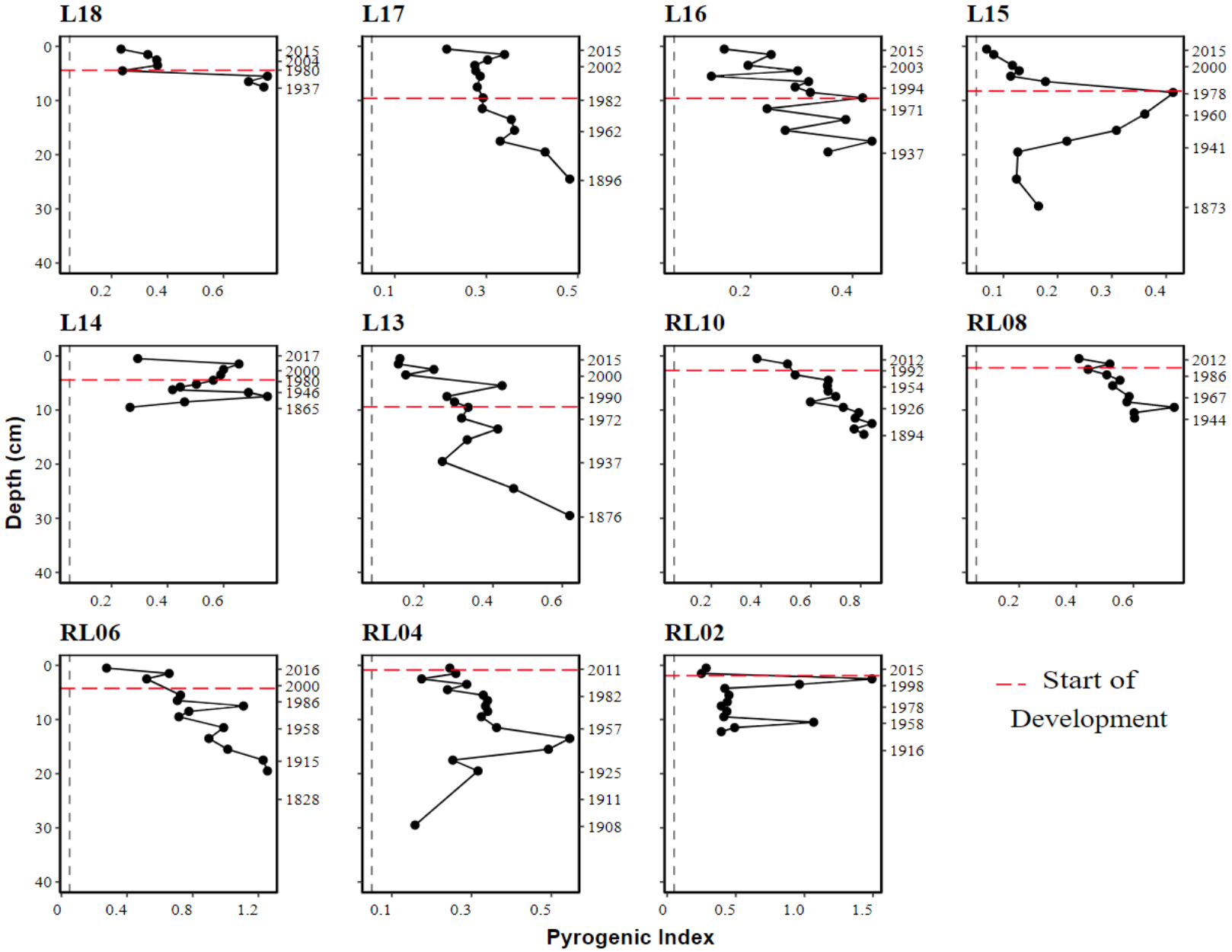

Figure 2- 4: Scatter plots of the PAC Pyrogenic Index (PI) as a function of core depth. Pyrogenic Indices modified from Wang et al. (1999) to represent the transition of petrogenic and pyrogenic inputs throughout time. PI values < 0.01 indicate light petroleum product origins, 0.02-0.05 indicate heavy oil and fuel origins, and > 0.05 represents pyrogenic influences. The vertical dashed line provides a visual representation of the 0.05 pyrogenic index point. The horizontal, red line corresponds to the year when oil sands operations began near each lake.

2.3.3 PAC Chemical Fingerprinting for Source Determination

PACs can enter lakes in the Cold Lake region from a variety of different sources: road and air traffic emissions, fossil fuel combustion for steam generation, wildfires or point-sources (e.g., FTS events). We created bar plots of the five petroleum-characteristic alkylated PACs for each of the 11 lakes and a Cold Lake Bitumen (CLB) sample to compare the PAC distribution in pre and post-oil sands lake sediments (Figure 2-5).

When compared to a Cold Lake Bitumen sample (CLB), we observe that the lakes in this study do not exhibit the marked increase in mean C1-C4 alkylated PAC fluxes indicative of a strong petroleum influence; C0≤C1≤C2≤C3≤C4 (Wang et al., 2014). The stepwise increase in C0-C4 naphthalenes of the CLB sample is weakly reflected in post-development sediments from L15, L16, L17, and L18 with no coincident increases in C0-C3 fluorenes. All of the study lakes are abundant in C1-C4 phenanthrene/anthracene and C0-C3 chrysene/benzo[a]anthracenes in the decreasing order of C0≥C1≥C2≥C3≥C4; strongly indicative of forest fire origins (Vila-Escalé et al., 2007; Yang et al., 2011). The CLB sample is rich in C0-C3 dibenzothiophenes and C0-C3 fluorenes; yet, these compounds are nearly depleted in the study lakes. These findings provide no evidence to support Cold Lake bitumen as a significant source of PACs to these lakes regardless of timeframe before or after oil sands activity began in Cold Lake. Therefore, the transition towards petrogenic PAC inputs observed in Figures 2-3 and 2-4 are not driven by bitumen, and more likely are a result of fossil fuel combustion. Sediments deposited following the onset of oil sands development are abundant in alkylated naphthalenes in a bell-shape distribution from C0-C4 (better visualized in Figure S2-3). Studies have shown that a bell-shaped distribution of these low molecular weight alkylated naphthalenes suggests that there are inputs from lighter hydrocarbon products to these lakes, such as natural gas (Stout and Wang, 2016; Wang et al., 2014). These findings indicate that the combustion of natural gas to generate steam for *in-situ* extraction could drive the naphthalene enrichment observed in our study lakes. Lake sediment cores in the Athabasca oil sands region exhibit increasing PAC concentrations and accumulation rates that match closely with the composition of Athabasca bitumen (Kurek et al., 2013b), however, we can confirm that this is not the case for sediments within the Cold Lake oil field at present.

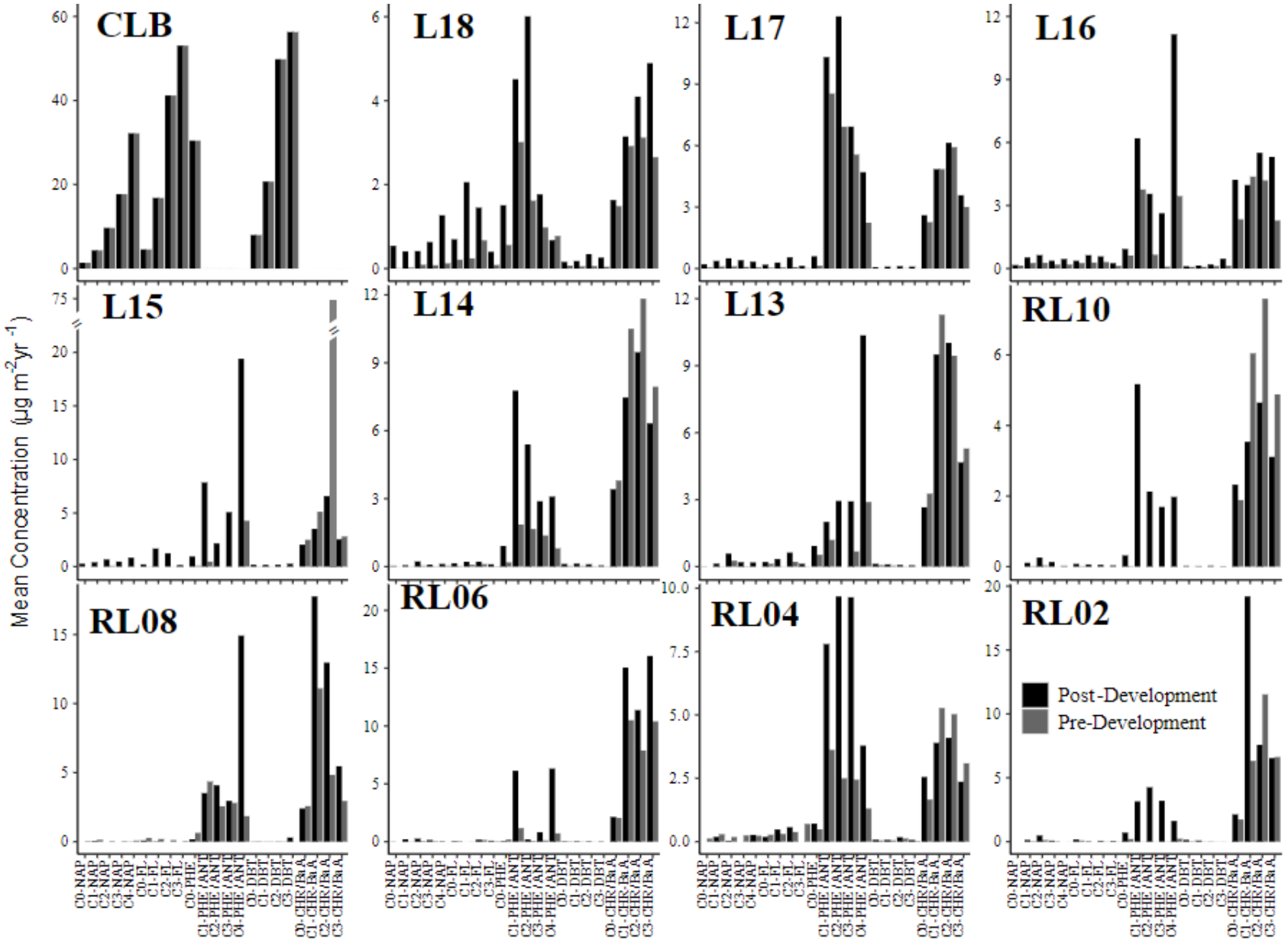

Figure 2- 5: Bar graphs comparing the mean concentration flux of the five petroleum-characteristic alkylated PACs before and after oil sands developments began. Pre-development concentrations represent historical conditions whereas Post-development concentrations are indicative of PAC deposition since the onset of oil sands operations near each lake. A cold lake bitumen (CLB) sample, obtained from Environment and Climate Change Canada (Ottawa, Ontario, Canada), is used for comparative fingerprinting and is measured in µg g^{-1} total weight of oil extracted. The CLB sample is irrespective of pre/post oil sands operations.

Downcore principal component analyses of alkylated PACs recorded the shift in the composition of the top 5 contributing compounds compared to a CLB sample (Figure 2-6). PCA axes 1 and 2 explain ~62.3 % of the variance in the data. L18 composition in modern sediments varied drastically from the oldest recorded sediments, with C4-C3-naphthalenes explaining the highest proportion of variation. The composition of L18 began to resemble a Cold Lake bitumen sample at the time of oil sands activity in 1984. C1-naphthalenes explained most of the variance in RL08, with the directionality shifting away from modern sediments. Samples from ~1996 closely resembled that of a Cold Lake bitumen sample, coinciding with active oil extraction operations that began in 1998 on the CLAWR. Although C4-benzonaphthothiophenes, C1-naphthalenes and C3-chrysenes explain the most variance towards the bottom of the cores, modern sediments are like the Cold Lake bitumen sample and shift in the direction of C2-phenanthrenes and C3-dibenzothiophenes in ordination space. C2-C3-phenanthrenes and benzonaphthothiophenes are among the most abundant PACs recorded Alberta oil sands deposits, yet RL08 exhibited a steady decrease in PACs throughout time (Yang et al. 2011). Lakes L17, L16, L14, L13, and RL04 approached the Cold Lake bitumen sample in the late 1980s with C0-C4 benzonaphthothiophenes explaining the most variance. In lakes where C0-C4 BNTs were dominant, the directionality of the BNTs shifted towards the Cold Lake bitumen sample, indicating that the composition of PACs within the lakes became more similar to that of bitumen. Modern sediments in L16 and L15 shifted in the opposite direction of the C0-C4 BNTs, showing that recent deposits transitioned further away from the Cold Lake bitumen sample. High proportions of variance explained by BNTs, DBTs and NAPs imply petroleum-derived inputs of alkylated PACs as sediments became more similar to the Cold Lake bitumen sample. Light diesel fuels or diluents may also be contributing to the variance explained by alkyl naphthalenes (Korosi et al., 2016a; Wang et al., 2014).

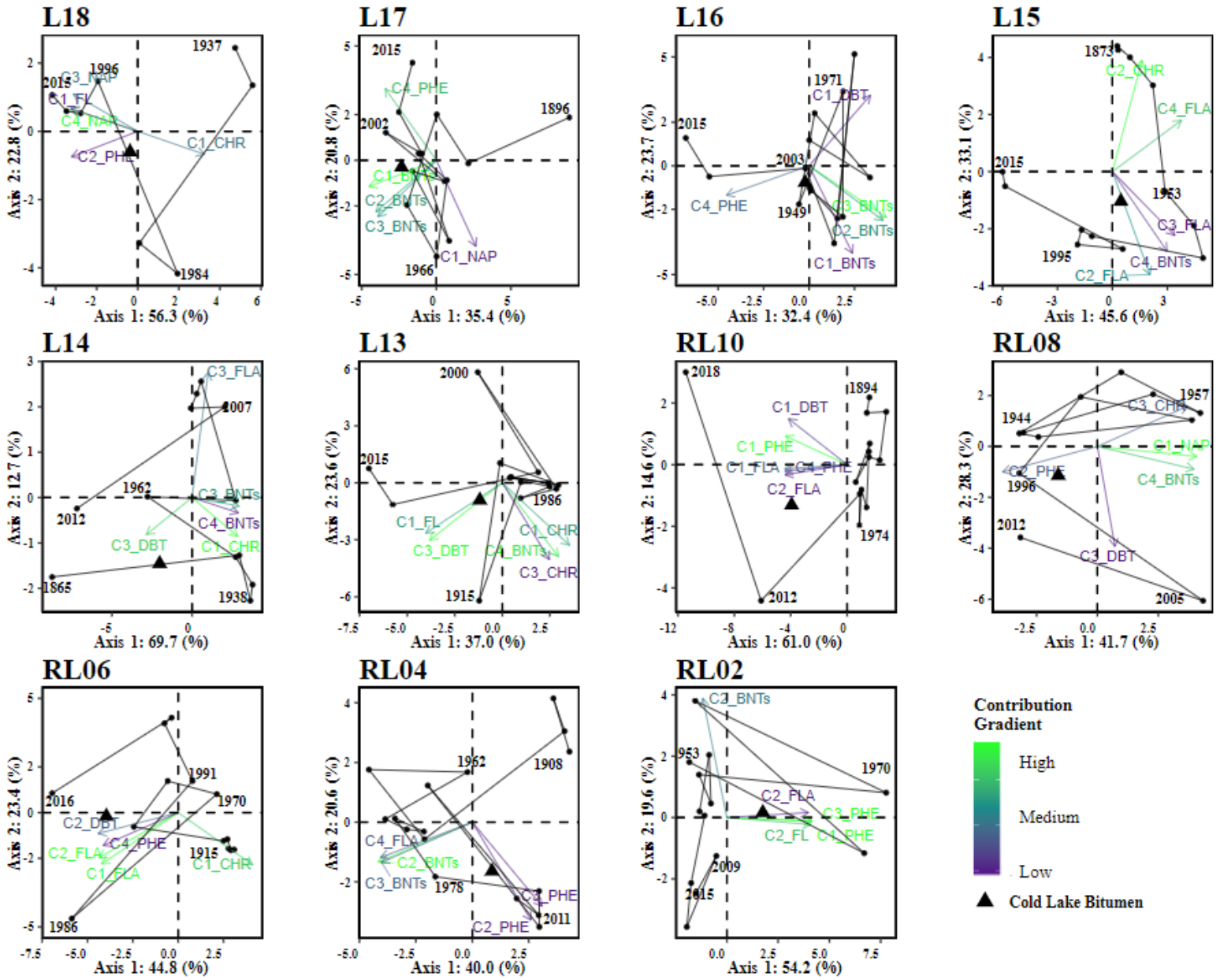

Figure 2- 6: Ordination biplots showing the changes in principal components along axes 1 & 2 scores throughout time for the relative abundance of alkylated PACs in lake sediment cores. Each lake profile depicts sample scores and the top 5 contributing alkylated PACs as the explanatory variables. Sediment intervals are connected in order of downcore chronologies (black sold line) with a Cold Lake bitumen sample (black triangle) plotted passively. The contribution gradient indicates the order of individual contribution to Axes 1:2 for each of the top 5 alkylated compounds.

PCAs of unsubstituted PACs have 73.7% of the variance explained by axes 1 and 2 (Figure 2-7). Benzo[g, h, i]perylene, dibenzo[a,h]anthracene, indeno[1,2,3-c,d]pyrene, and benzo[a]pyrene explain the most variance in the PCAs with low molecular weight compounds not significantly contributing. These compositions suggest PACs originated from forest fire sources (Bytnerowicz et al., 2016). In all study lakes, PACs approached the passively plotted Cold Lake bitumen sample around the start of oil sands operations. The directionality of the significant contributing compounds pointed away from the Cold Lake bitumen sample, suggesting Cold Lake bitumen is not driving the changes in PAC enrichment in modern sediments.

Korosi et al. (2016a) observed similar PCA trends in Lake 12-26; the composition of PACs in the Lake 12-26 exhibited a transition towards a Primrose Lake bitumen sample since oil sands activity began. Despite the similarity to a bitumen sample, Korosi reported that bitumen is unlikely to be the dominant PAC source to Lake 12-26 since there was no coincident increase in vanadium nor was the lake dominated by a petrogenic PI (Korosi et al., 2016a). Additionally, Ethyl nor Hilda Lakes from Korosi et al. (2013) nor in 12-26 from Korosi et al. (2016a) exhibited metal enrichment. Metal analyses of the 11 lakes sampled in this study could be useful to determine whether the shift towards a Cold Lake bitumen sample in the alkylated and unsubstituted PCA analyses are resulting from bituminous inputs.

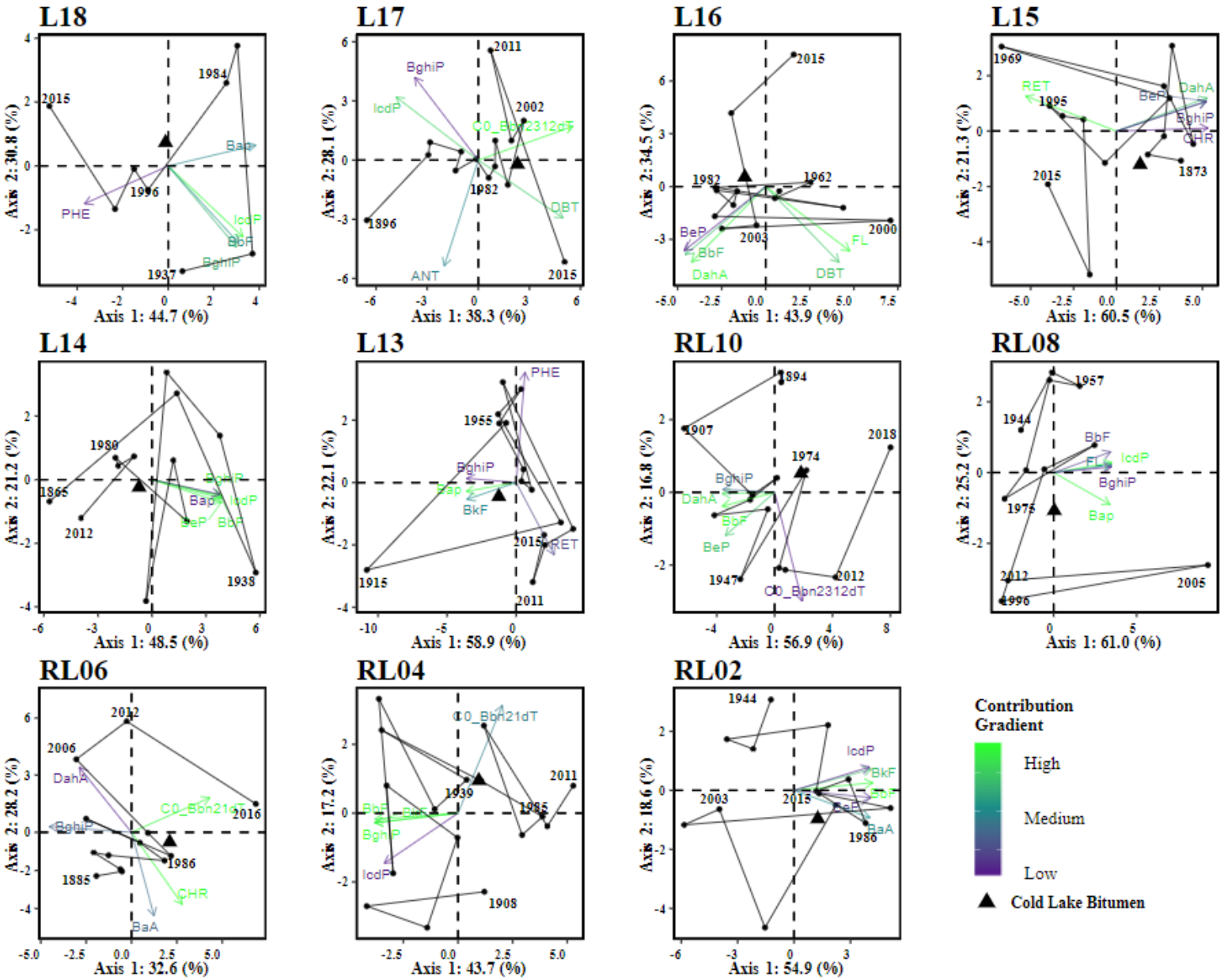

Figure 2- 7: Ordination biplots showing the changes in principal components along axes 1 & 2 scores throughout time for the relative abundance of unsubstituted PACs in lake sediment cores. Each lake profile depicts sample scores and the top 5 contributing alkylated PACs as the explanatory variables. Sediment intervals are connected in order of downcore chronologies (black sold line) with a Cold Lake bitumen sample (black triangle) plotted passively. The contribution gradient indicates the order of individual contribution to Axes 1:2 for each of the top 5 alkylated compounds.

2.3.4 Spatial-Temporal Analyses

Multiple lines of evidence indicate that fuel burning associated with oil sands activity, and not bitumen itself, contributed to PAC enrichment in the Cold Lake region. As petrogenic PAC inputs increased in more recent sediments, pyrogenic indices in regional lakes decreased. We observed increases in alkylated PAC fluxes that coincided with the beginning of oil sands operations in lakes densely surrounded by oil sands infrastructure. Moreover, in all but RL06 and RL08, PAC fluxes in post-development lake sediments were significantly higher than in pre-oil sands sediments (p-value < 0.05) (Figure 2-8). An ANCOVA tested whether there was a statistically significant spatial-temporal relationships between the PAC flux, lake area and distance downwind from *in-situ* wells after accounting for the timing of oil sands development (Figure 2-9A). The ANCOVA first evaluated the regression of the covariates (lake area and distance) on the dependent variable (PAC flux) (Tables S2-2 and S2-3). The ANCOVA yielded a statistically significant association (α=0.05) between alkylated PAC flux and distance downwind from *in-situ* oil wells ($F_{3,138}$ = 17.89, p-Value =4.24×10^{-05}). The influence of the lake area was also significant ($F_{3,138}$ =23.82, p-Value =2.89×10^{-06}). We observed no statistically significant interactions amongst the covariates (lake area and distance) and the grouping variables (pre / post-oil sands activity) which is to be expected as these parameters did not change. Although the alkylated PAC model deems the relationships between flux and distance, and flux and lake area to be statistically significant, the proportion of variance explained by the model is only 43 % (Table S2-2). Classification of the data into pre and post-oil sands development groups explained the most variation in the alkylated PAC data (R^2 = 0.320), with lake area explaining the second most variance (R^2=0.147) and distance explaining the least variance (R^2=0.115).

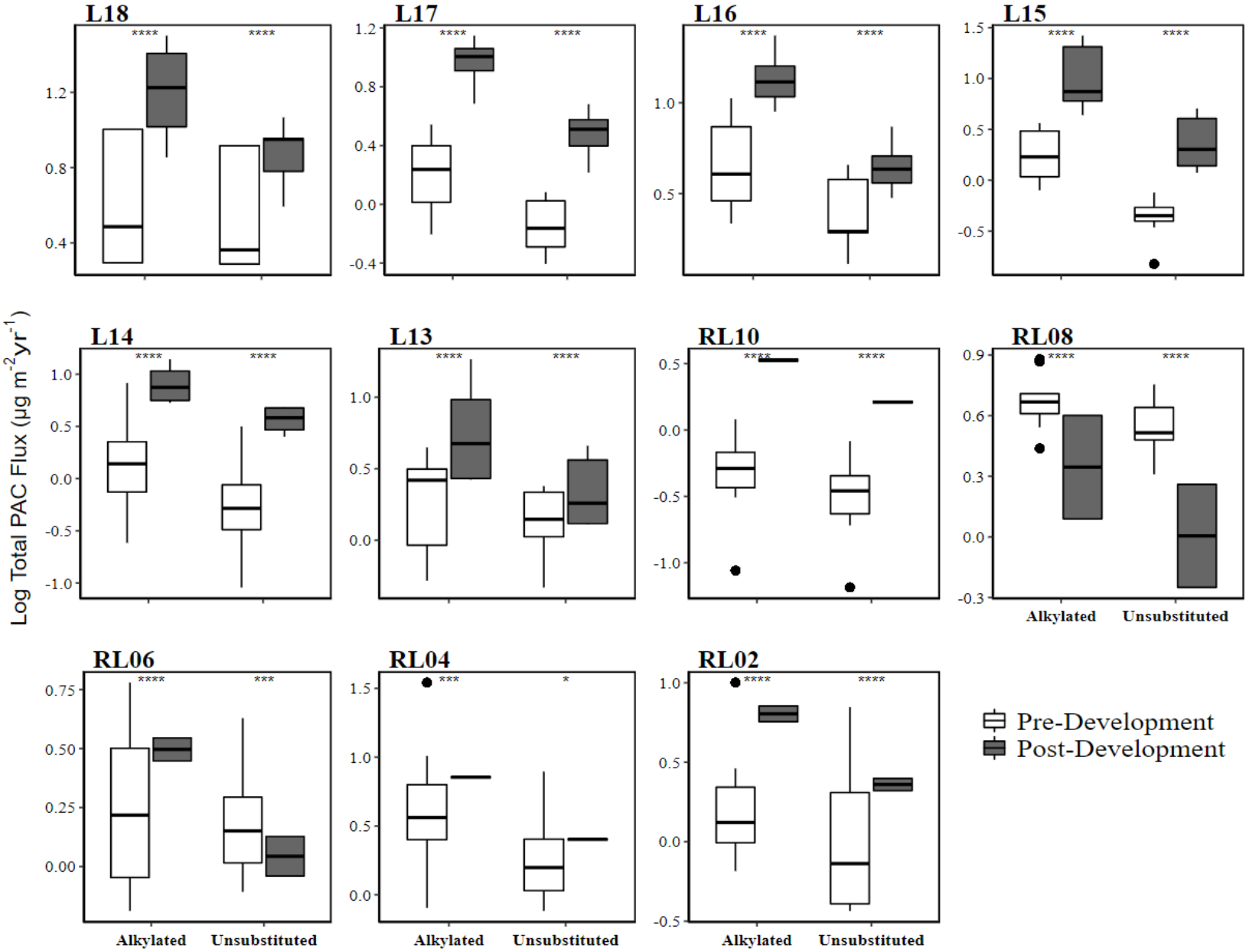

Figure 2- 8: ANOVA and Kruskal-Wallis boxplots comparing the log_{10} total PAC flux in pre- and post-oil sands development time groups. Boxplots represent the flux (ug m^2 yr^{-1}) of the US-EPA 16 priority PACs and their alkylated homologues (Alkylated) within each of the study lakes. Pre-development PAC levels represent historical levels of PACs prior to the onset of oil sands developments near each lake, whereas post-development PAC levels represent the log flux of PACs since oil sands activity began. Outliers are identified by the solid black circles. *P*-values less than an alpha of 0.05 indicate statistically significant changes in pre- and post-development fluxes. Statistically significant relationships are depicted by **** = $p < 0.0001$, *** = $p < 0.001$, and * = $p < 0.05$.

The unsubstituted PAC flux in lake sediments is weakly related to the distance from oil sands infrastructure ($F_{7,135}$ =5.078, *p*-Value =0.026) (Figure 2-9 B). Similar to alkylated PACs, there is also a relationship between the lake area and the unsubstituted PAC flux ($F_{7,135}$ =15.86, *p*-Value =1.11x10^{-04}), with a significant interaction between distance and lake area ($F_{7,135}$ =16.65, *p*-Value =7.65x10^{-05}). There was no interaction between the covariates (lake area and distance) and the grouping variables (pre- or post-oil sands development) (Table S2-3). The ANCOVA regression model for unsubstituted PACs explained 38 % of the model variance, with the most significant proportion of variance explained by the period in which the sediments were deposited (R^2 =0.23) (Figure 2-9B). Of the two covariates, distance downwind from oil wells explained 2.7 % of the variability (R^2 =0.027) , whereas lake area explained 8.8 % (R^2 = 0.088). The interaction between distance and lake area explained 10 % of the variance in the model (R^2 = 0.10).

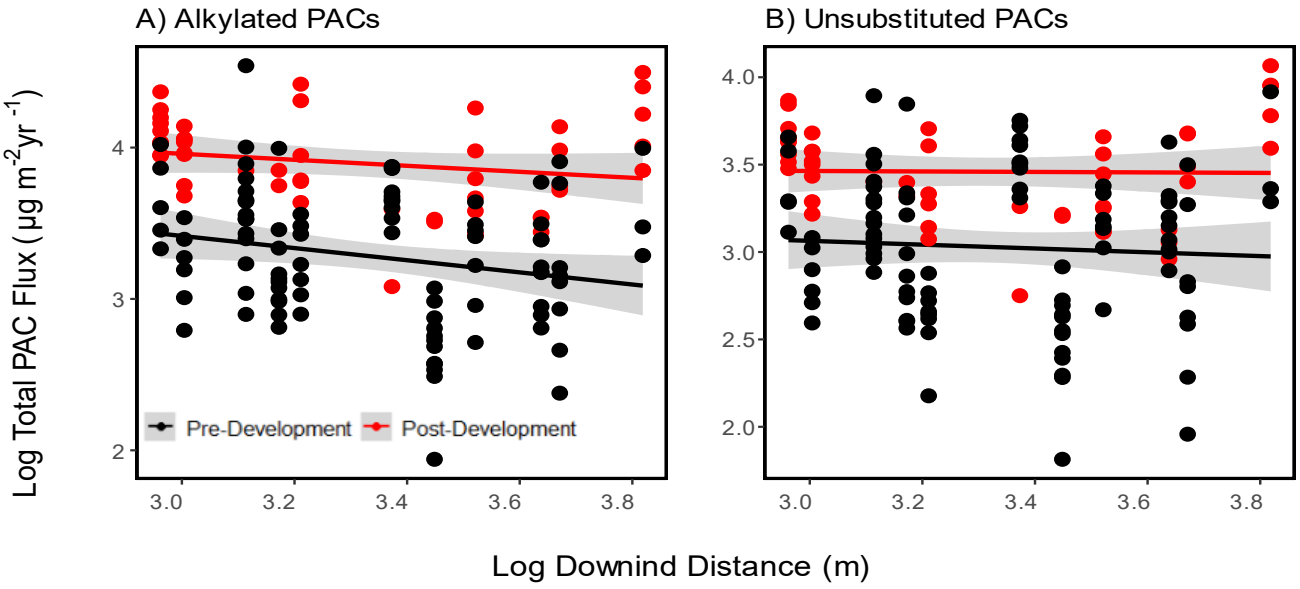

Figure 2- 9: Linear regression model of the alkylated (A) and unsubstituted (B) log_{10} total PAC fluxes as a function of log_{10} distance downwind from *in-situ* oil pads. Red regression lines and datapoints represent sediments deposited post-oil sands development whereas black regression lines and datapoints are indicative of pre-development sediments.

2.4 Conclusion

Our results suggest *in-situ* oil sands activities have raised the concentration and deposition of PACs across the Cold Lake region. Multiple lines of evidence from diagnostic ratios, pyrogenic indices, and principle component analyses indicate that a transition from

strongly pyrogenic PACs towards petrogenic PACs occurred following the regional onset of oil sands activity (~>1980s). This change was driven by increasing alkylated PAC abundances. PAC fluxes significantly increased from pre-industrial levels following the development of oil sands in the 1980s-2000s. Diagnostic ratios and pyrogenic indices demonstrated that PACs in modern sediments closely reflect a petroleum combustion source, most likely from diesel-fueled vehicular emissions and the combustion of natural gas used to generate steam for *in-situ* oil extraction. Expanded oil sands operations within the Cold Lake oil field will likely increase the burden of petrogenic PACs in regional lakes to a point where alkylated species dominate over unsubstituted PACs. Increases in alkylated PAC abundances would have significant environmental and human health implications as these PACs are carcinogenic, mutagenic, and toxic.

Linear modelling demonstrated a statistically significant relationship between the distance from oil sands wells and PAC flux in surrounding lakes. This model can be used to prioritize sampling locations and target regions at risk of being enriched in PACs within *in-situ* oil sands. Kelly et al. (2009) established a gradient of PAC enrichment dependent on the proximity to open-pit mining regions. The characteristic bullseye pattern has influenced monitoring protocols and environmental remediation efforts throughout the Athabasca oil sands region. Our study is the first in the Cold Lake region to apply a statistical model to establish a relationship between oil wells and PAC flux.

Chapter 2: Supplementary Information

Table S2- 1: List of alkylated and unsubstituted PACs analyzed in this study, including the abbreviations used in the text, the target ion for GC-MS and the number of benzene rings in each chemical structure.

Compound	Abbreviation	Target Ion	# of Rings
Alkylated PACs			
Naphthalene	C_0 – NAP	128.00	2
C_1 – Naphthalenes	C_1 – NAP	142.00	2
C_2 – Naphthalenes	C_2 – NAP	156.05	2
C_3 – Naphthalenes	C_3 – NAP	170.10	2
C_4 – Naphthalenes	C_4 – NAP	184.10	2
Fluorene	C_0 – FL	166.05	3
C_1 – Fluorenes	C_1 – FL	180.05	3
C_2 – Fluorenes	C_2 – FL	194.15	3
C_3 – Fluorenes	C_3 – FL	208.15	3
Dibenzothiophene	C_0 – DBT	183.95	3
C_1 – Dibenzothiophenes	C_1 – DBT	198.05	3
C_2 – Dibenzothiophenes	C_2 – DBT	221.10	3
C_3 – Dibenzothiophenes	C_3 – DBT	226.00	3
Phenanthrene	C_0 – PHE	178.05	3
C_1 - Phenanthrenes	C_1 – PHE	192.10	3
C_2 - Phenanthrenes	C_2 – PHE	206.15	3
C_3 – Phenanthrenes	C_3 – PHE	220.15	3
Fluoranthene	C_0 – FLA	234.15	4
C_1 – Fluoranthenes	C_1 – FLA	202.05	4
C_2 – Fluoranthenes	C_2 – FLA	216.15	4
C_3 – Fluoranthenes	C_3 – FLA	230.15	4
C_4 – Fluoranthenes	C_4 – FLA	244.15	4
Benzo[B]naptho(2,3-1,2d)thiophene	BbN2312dT	258.20	4
Benzo[B]naphtho(2,1d)thiophene	BbN21dT	234.20	4
C_1 – Benzo[B]napthothiophenes	C_1 – BNT	234.00	4
C_2 – Benzo[B]napthothiophenes	C_2 – BNT	248.10	4
C_3 – Benzo[B]napthothiophenes	C_3 – BNT	262.10	4
C_4 – Benzo[B]napthothiophenes	C_4 – BNT	276.20	4
Chrysene	C_0 - CHR	290.20	4
C_1 - Chrysenes	C_1 – CHR	228.00	4
C_2 - Chrysenes	C_2 – CHR	242.20	4
C_3 – Chrysenes	C_3 – CHR	256.15	4
USA EPA Priority PACs			
Naphthalene	NAP	128.00	2
Acenaphthylene	ACT	152.05	3
Acenaphthene	ACE	153.05	3
Fluorene	FL	166.05	3
Phenanthrene	PHE	178.05	3

Anthracene	ANT	178.05	3
Fluoranthene	FLA	202.05	4
Pyrene	PYR	202.05	4
Benz[a]anthracene	BaA	228.05	4
Chrysene	CHR	228.00	4
Benzo[b]fluoranthene	BbF	252.10	5
Benzo[k]fluoranthene	BkF	252.10	5
Benzo[a]pyrene	BaP	252.00	5
Indeno[1,2,3-c,d]pyrene	IcdP	276.15	6
Dibenzo[a,h]anthracene	DahA	278.20	5
Benzo[g,h,i]perylene	BghiP	276.15	6
Additional PACs			
Dibenzothiophene	DBT	183.95	3
Retene	RET	234.15	3
Benzo[e]pyrene	BeP	252.00	5

Table S2- 2: Summary of the intercept estimate, standard error (Std.Error), and *p*-Value for the Alkylated PAC ANCOVA regression analysis. The final model *p*-Value, degrees of freedom (DoF) and the Adjusted R^2 (Adj.R^2) are also present.

	Intercept Estimate	**Std.Error**	***P*-Value**
Pre-Development (Intercept)	5.05	0.44	<2.2e-16
Post Development	0.51	0.06	3.13e-13
Log_{10}(Distance)	-0.56	0.13	4.24e-05
Lake Area	0.02	0.00	2.89e-06
p-Value	<2.2e-16		
DoF	138		
Adj.R^2	0.43		

Table S2- 3: Summary of the intercept estimate, standard error (Std.Error), and *p*-Value for the unsubstituted PAC ANCOVA regression analysis. The final model *p*-Value, degrees of freedom (DoF) and the Adjusted R^2 (Adj.R^2) are also present.

	Intercept Estimate	**Std.Error**	***P*-Value**
Pre-Development (Intercept)	4.04	0.62	5.61e-11
Post Development	0.33	0.87	0.7044
Log_{10}(Distance)	-0.41	0.18	0.0258
Lake Area	-0.38	0.095	1.11e-04
p-Value	6.57e-12		
DoF	135		
Adj.R^2	0.35		

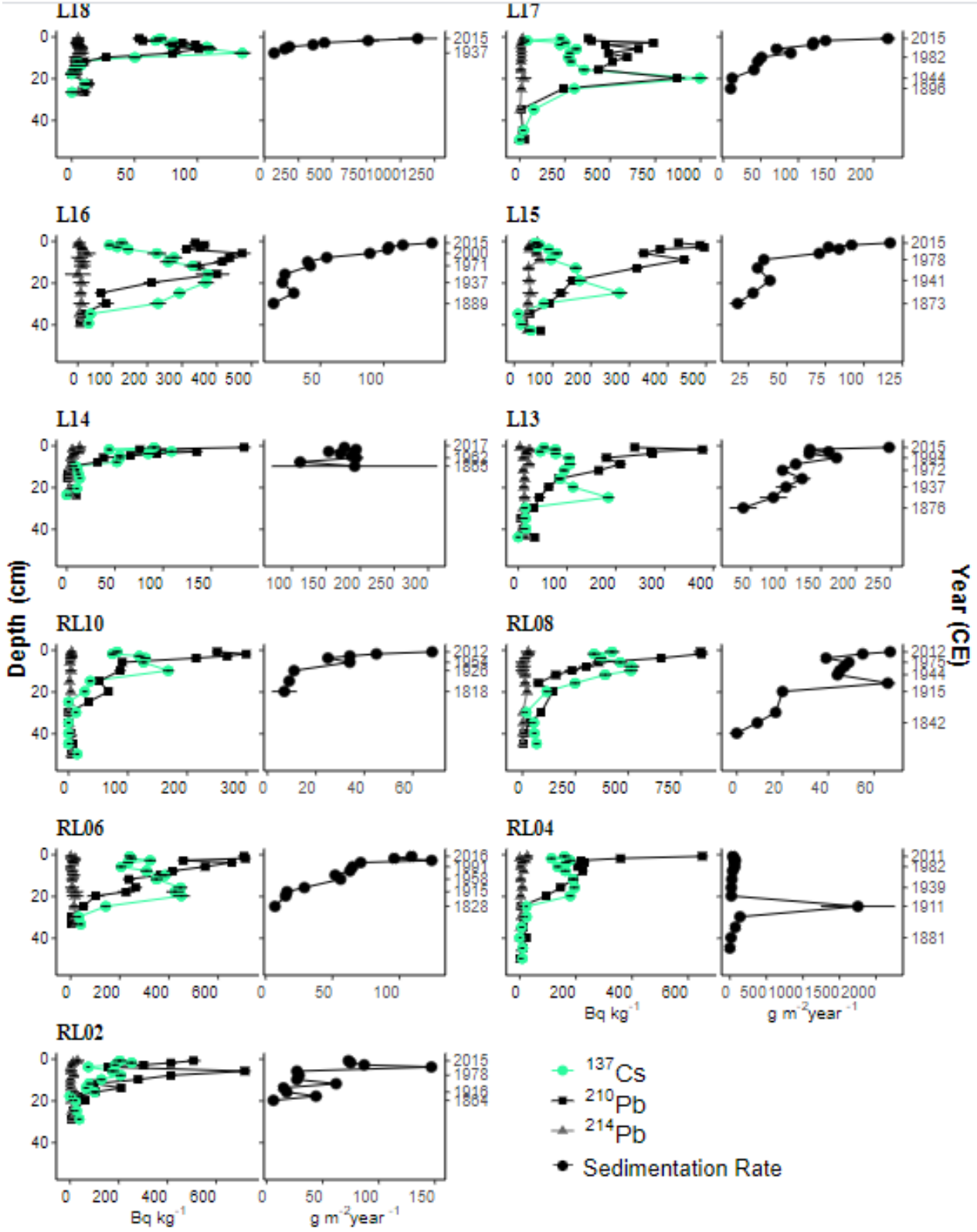

Figure S2- 1: Scatter plots showing radiometric dating profiles, and the sedimentation rate profiles for all 11 study lakes. All sedimentation rates and dates are modeled as per the CRS dating models with the applied Binford rule. The plot on the left represents the activity in Becquerels per kilogram of dried sediment versus depth for ^{210}Pb, ^{214}Pb and ^{137}Cs. The plot on the right depicts the sedimentation rate in grams per m^2 yr^{-1} as a function of depth and the associated CRS model error. Sedimentation rates were not calculated below the horizon of unsupported ^{210}Pb activity indicated as per the CRS model.

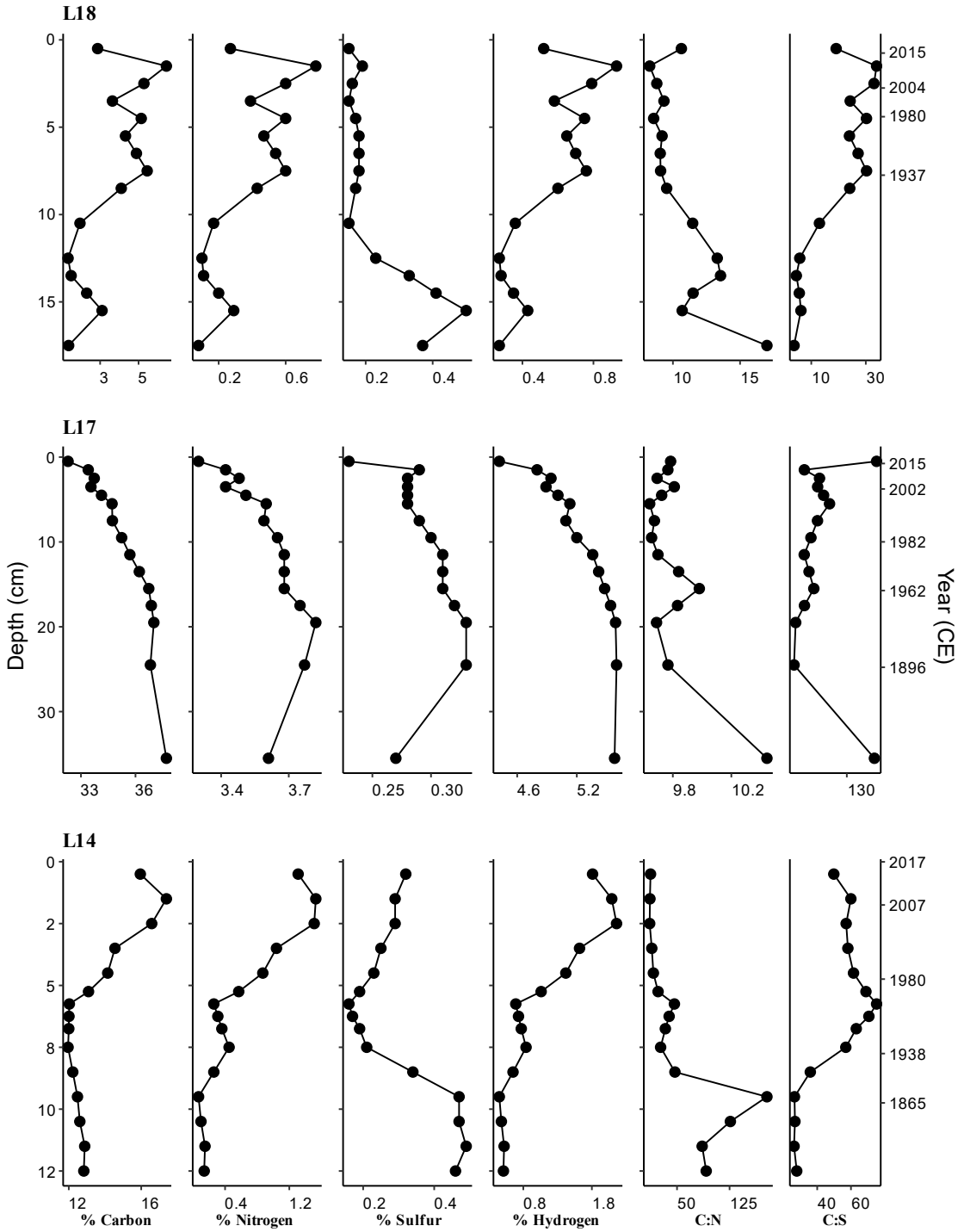

Figure S2- 2A: Scatter plots of stable isotope data as a function of core depth for Lakes L18, L17, and L14. All elemental data, obtained through stable isotope analyses, and plotted downcore as per the CRS dating models. All lakes include %C, %N, %S, %H, Carbon: Nitrogen ratios, and Carbon: Sulfur ratios.

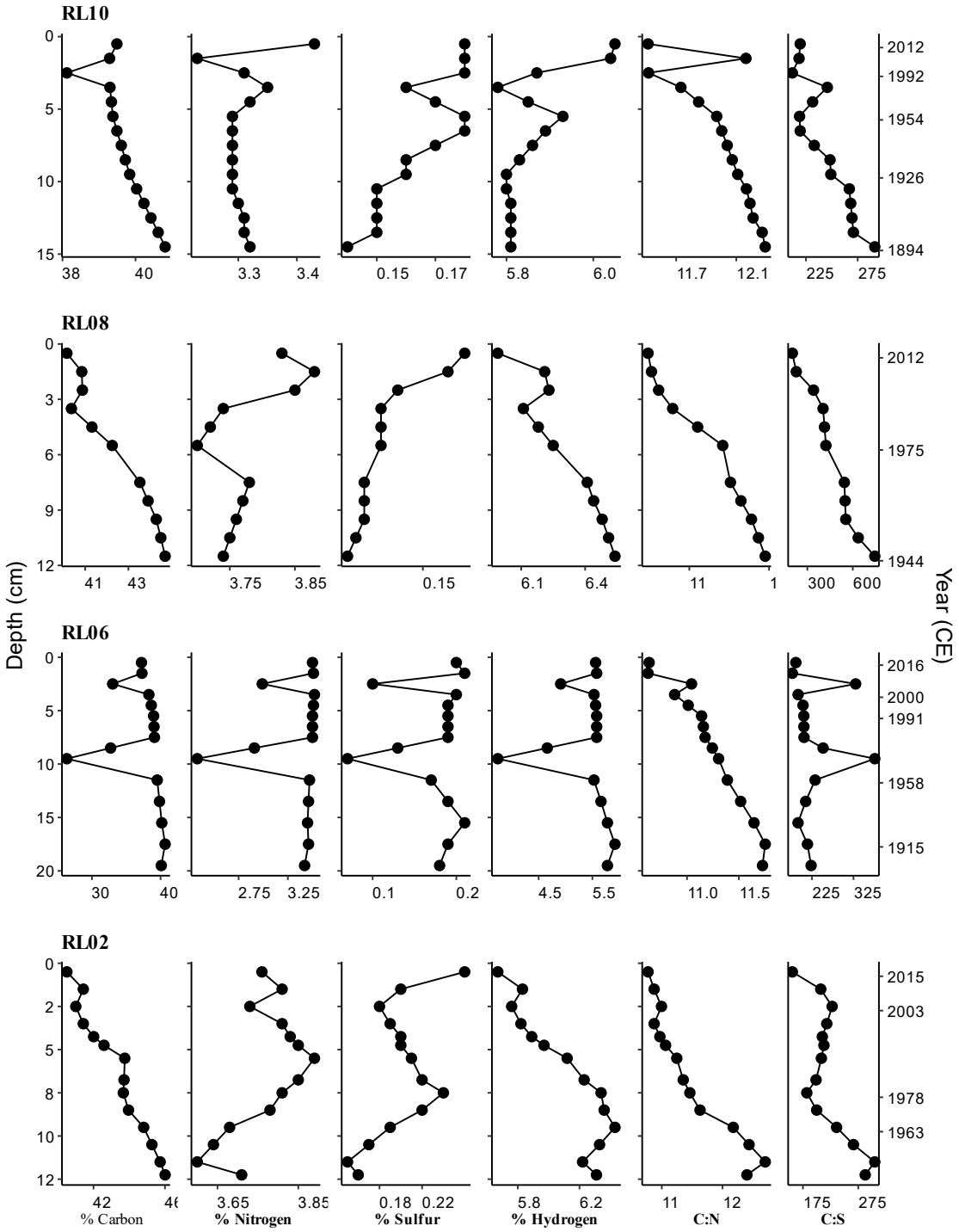

Figure S2-2B: Scatter plots of stable isotope data as a function of core depth for Lakes RL10, RL08, RL06 and RL02. All elemental data, obtained through stable isotope analyses and plotted downcore as per the CRS dating models. All lakes include %C, %N, %S, %H, Carbon: Nitrogen ratios, and Carbon: Sulfur ratios.

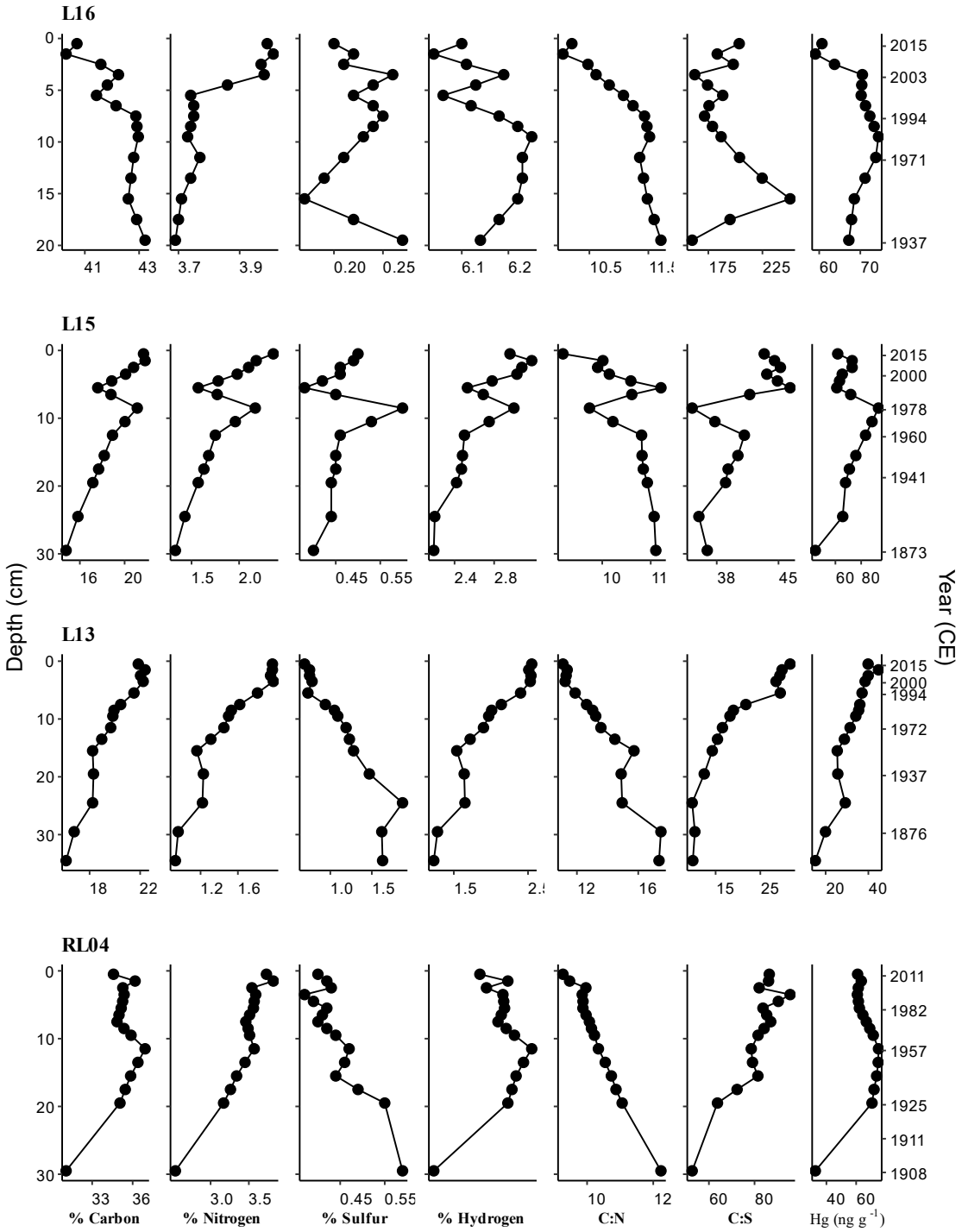

Figure S2-2C: Scatter plots of stable isotope data as a function of core depth for Lakes L16, L15, L13, and RL04. All elemental data, obtained through stable isotope analyses and plotted downcore as per the CRS dating models. All lakes include %C, %N, %S, %H, Carbon: Nitrogen ratios, Carbon: Sulfur ratios, and total mercury (ng g^{-1}).

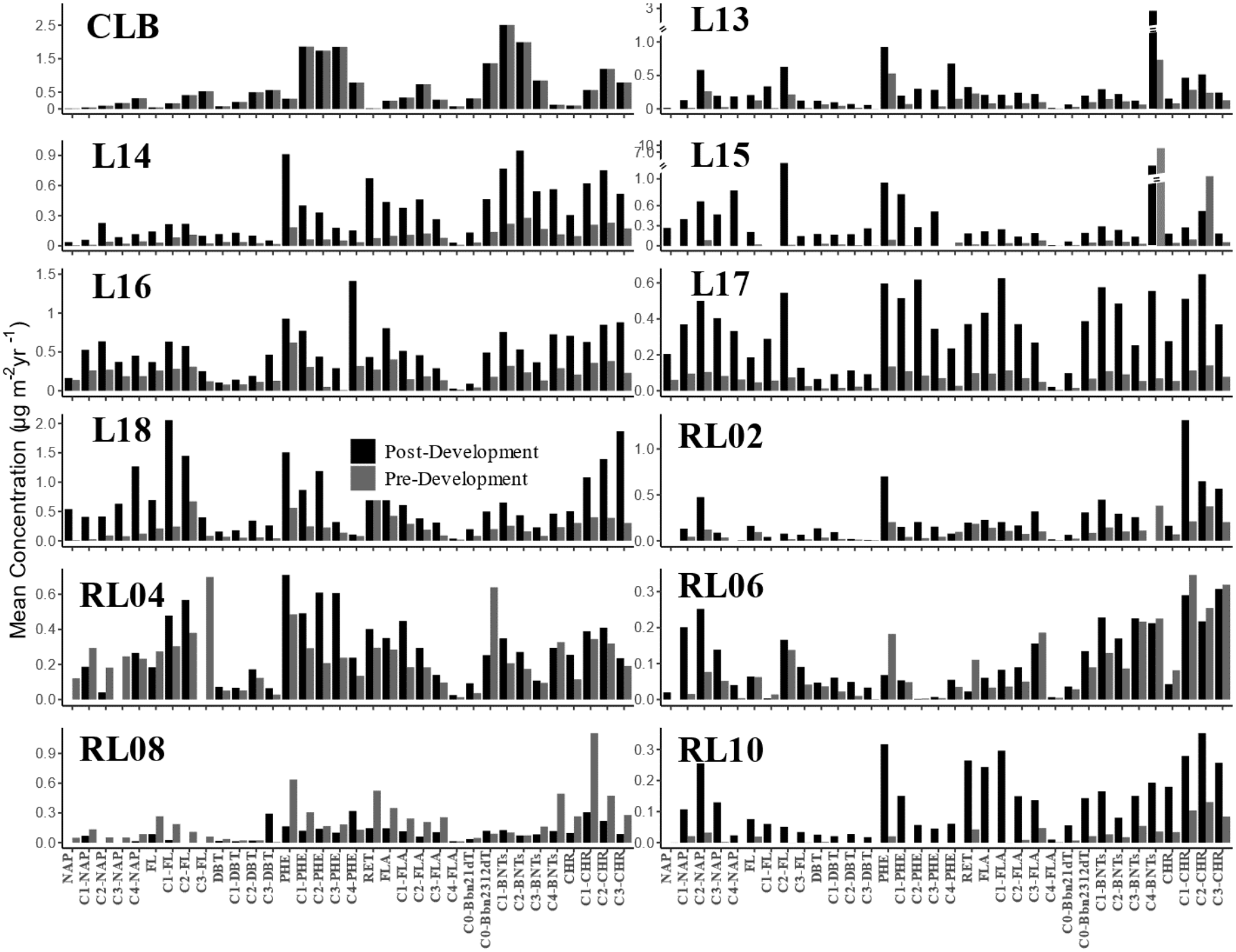

Figure S2- 3: Bar graph distribution of the mean flux concentrations of all Alkylated PACs when compared to a Cold Lake bitumen sample (CLB). All mean alkylated PAC concentrations are categorized based on the time in which they were deposited Pre (Grey) and Post (Black) -oil sands development. The CLB sample is measured in µg g^{-1} of the total weight of bitumen extracted whereas the remainder of the plots are recorded as mean concentration of alkylated PACs per m^2 of sediment deposited per year within each lake. CLB sample is irrespective of pre/post conditions.

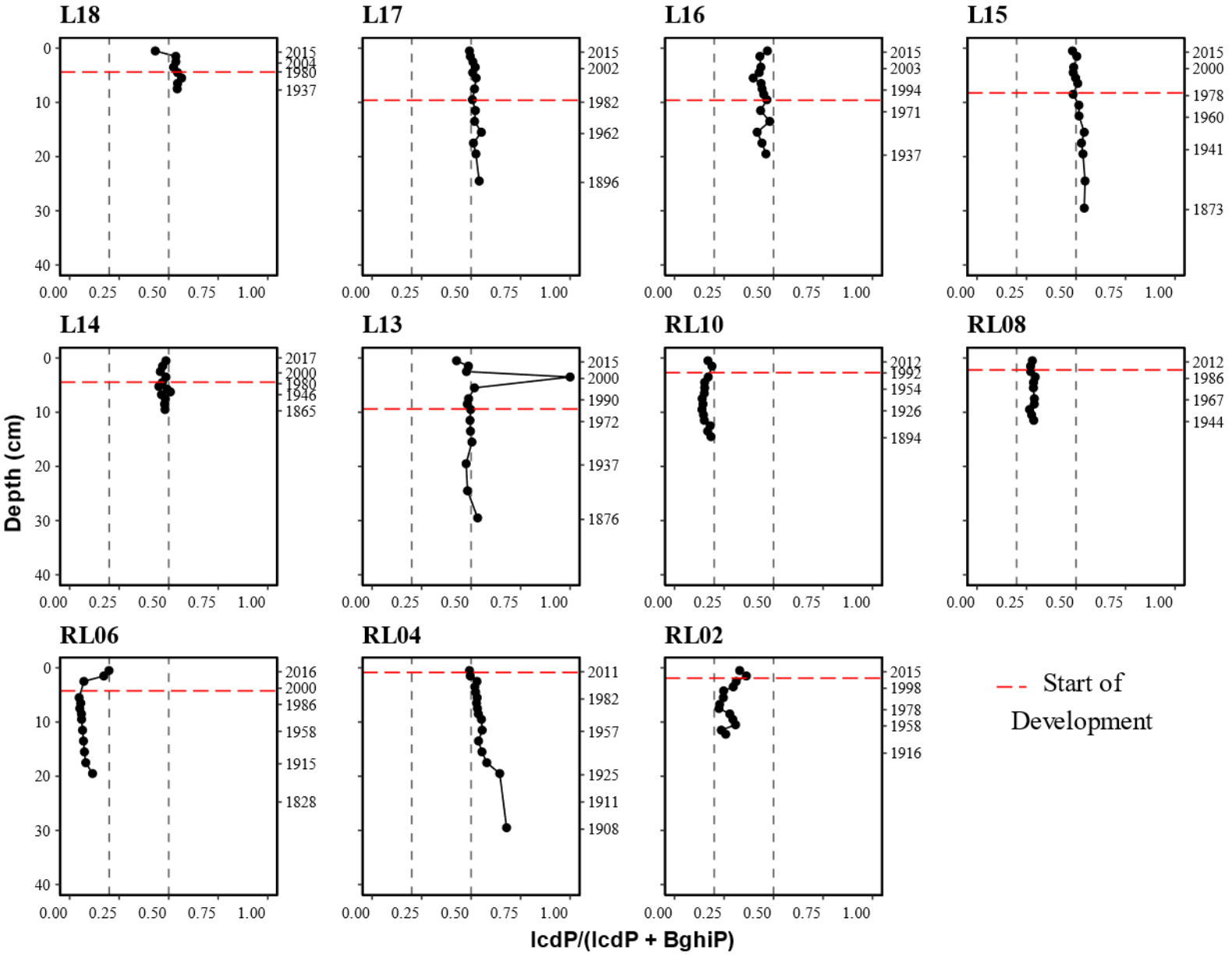

Figure S2- 4: Scatter plots of the IcdP/(IcdP+BghiP) PAC diagnostic ratio as a function of depth to test for dominant regional emission sources. The vertical dashed lines indicate diagnostic ratios of 0.2 and 0.5. A ratio of < 0.2 suggest a petrogenic source, a ratio of 0.2-0.5 suggest a petroleum combustion source and a ratio > 0.5 suggests a grass, wood and coal combustion source (Yunker et al., 2002; Tobiszewski et Namiesnik, 2012). The horizontal, red line corresponds to the year when oil sands operations began near each lake.

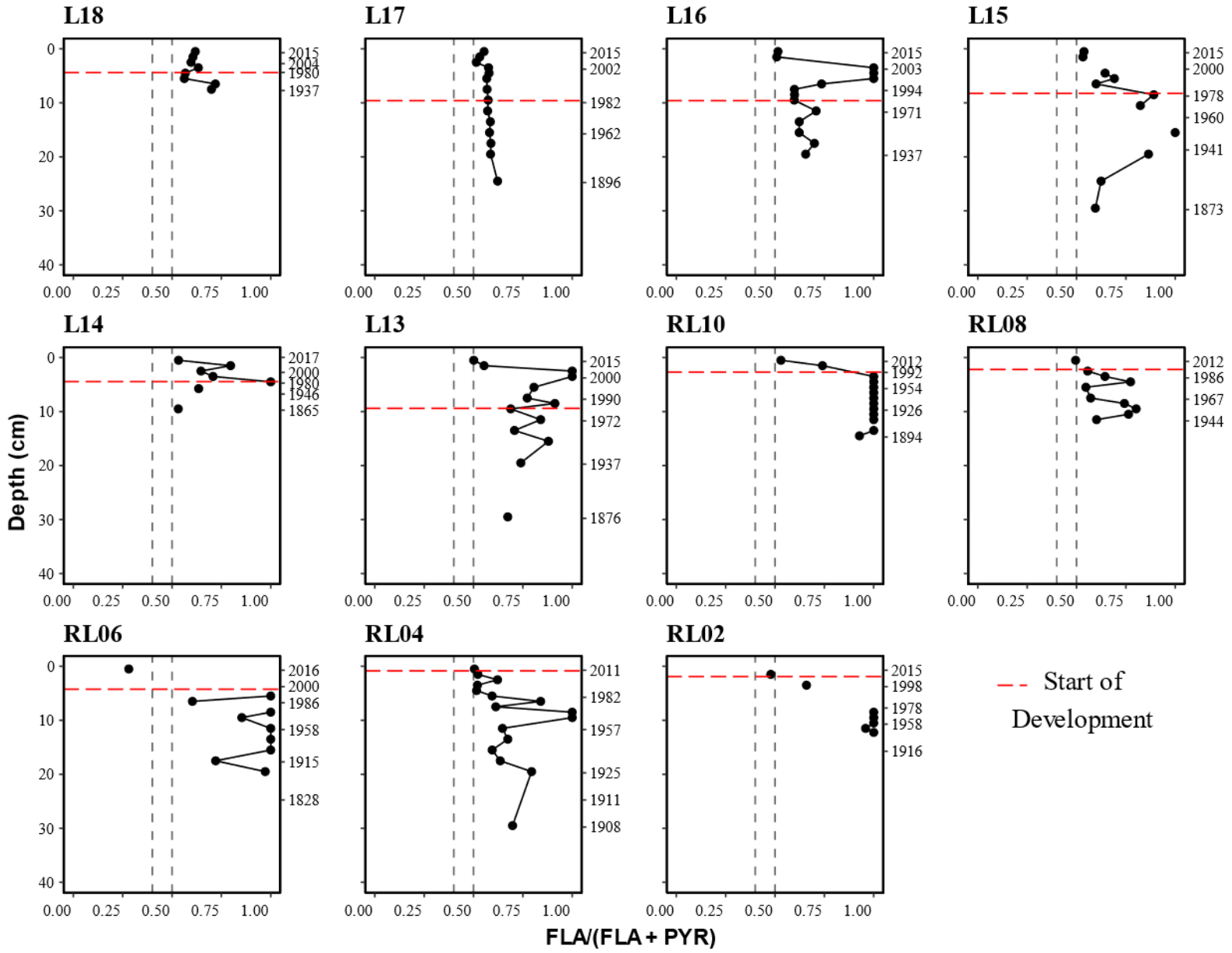

Figure S2- 5: Scatter plots of the FLA/(FLA+PYR) PAC diagnostic ratio as a function of depth to assess potential regional emission sources. The vertical dashed lines indicate diagnostic ratios of 0.4 and 0.5. A ratio of < 0.4 suggest a petrogenic source, ratios of 0.4-0.5 suggest fossil fuel combustion sources, and a ratio > 0.5 suggests a grass, wood or coal combustion source (De La Torre-Roche et al., 2009; Tobiszewski et Namiesnik, 2012). The horizontal, red line corresponds to the year when oil sands operations began near each lake.

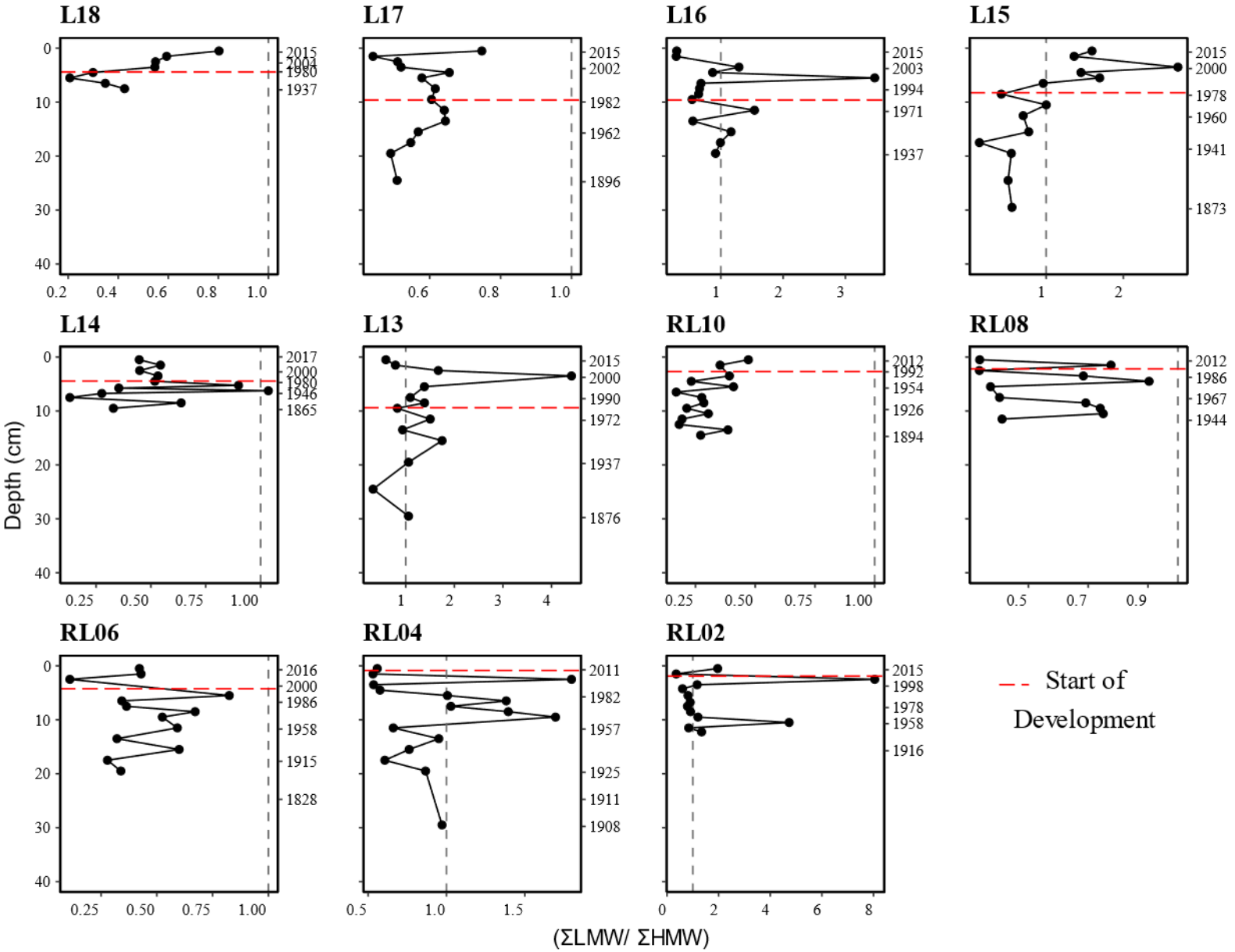

Figure S2- 6: Scatter plots of the ΣLMW/ΣHMW PAC concentrations as a function of depth to assess the transition between petrogenic and pyrogenic emission sources. ΣLMW compounds are the sum of two and three ring PACs, ΣHMW compounds are the sum of four and five ring PACs. The vertical dashed line indicates a ratio of 1. Datapoints < 1 suggest a pyrogenic source. Data points > 1 suggest petrogenic sources (Zhang et al., 2008; Tobiszewski et Namiesnik, 2012). The horizontal, red line corresponds to the year when oil sands operations began near each lake.

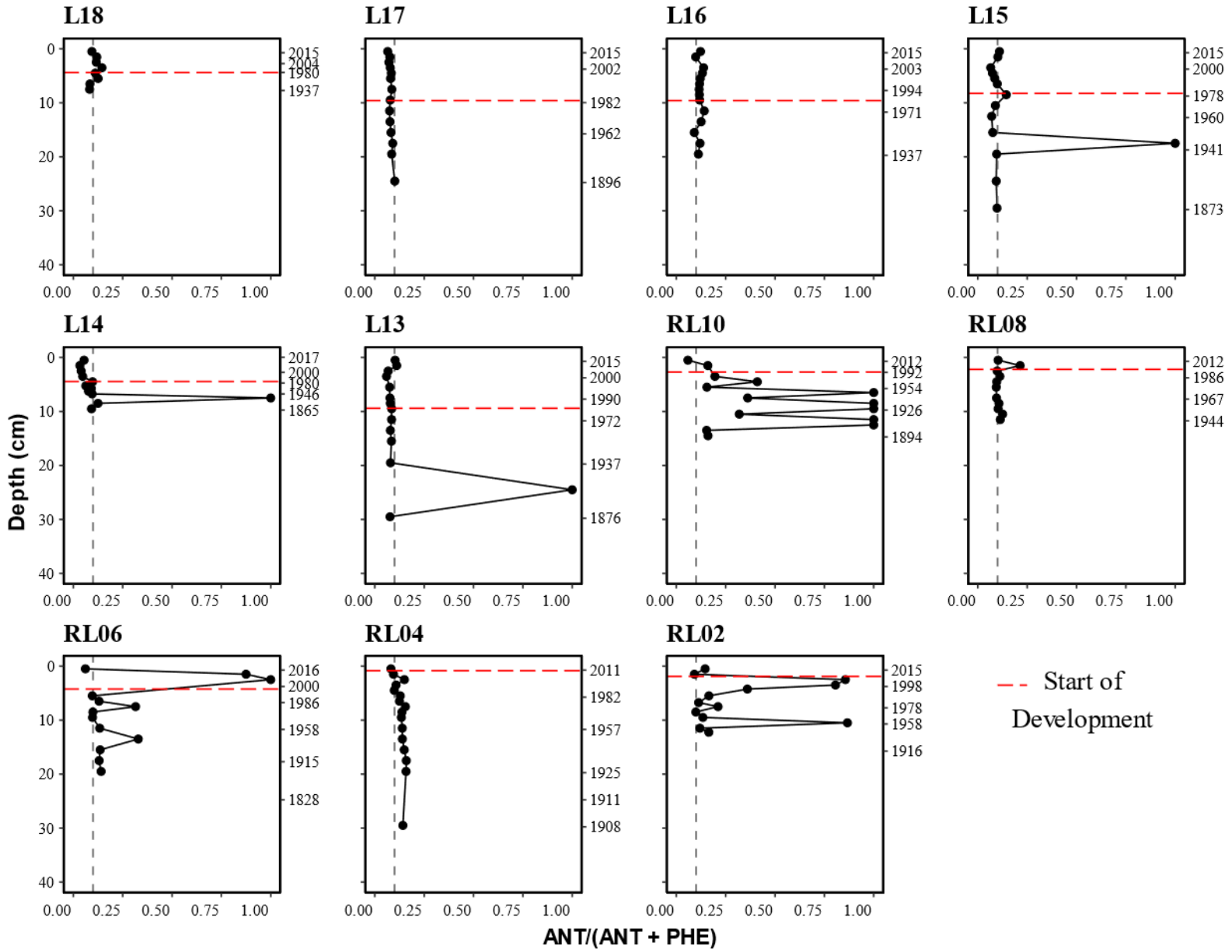

Figure S2- 7: : Scatter plots of the ANT/(ANT+PHE) PAC diagnostic ratio as a function of depth to assess the transition between petrogenic and pyrogenic emission sources. The vertical dashed line indicates a diagnostic ratio of 0.1. A ratio of < 0.1 suggest a petrogenic source whereas a ratio > 0.1 suggests a pyrogenic source (Pies et al., 2008; Tobiszewski et Namiesnik, 2012). The horizontal, red line corresponds to the year when oil sands operations began near each lake.

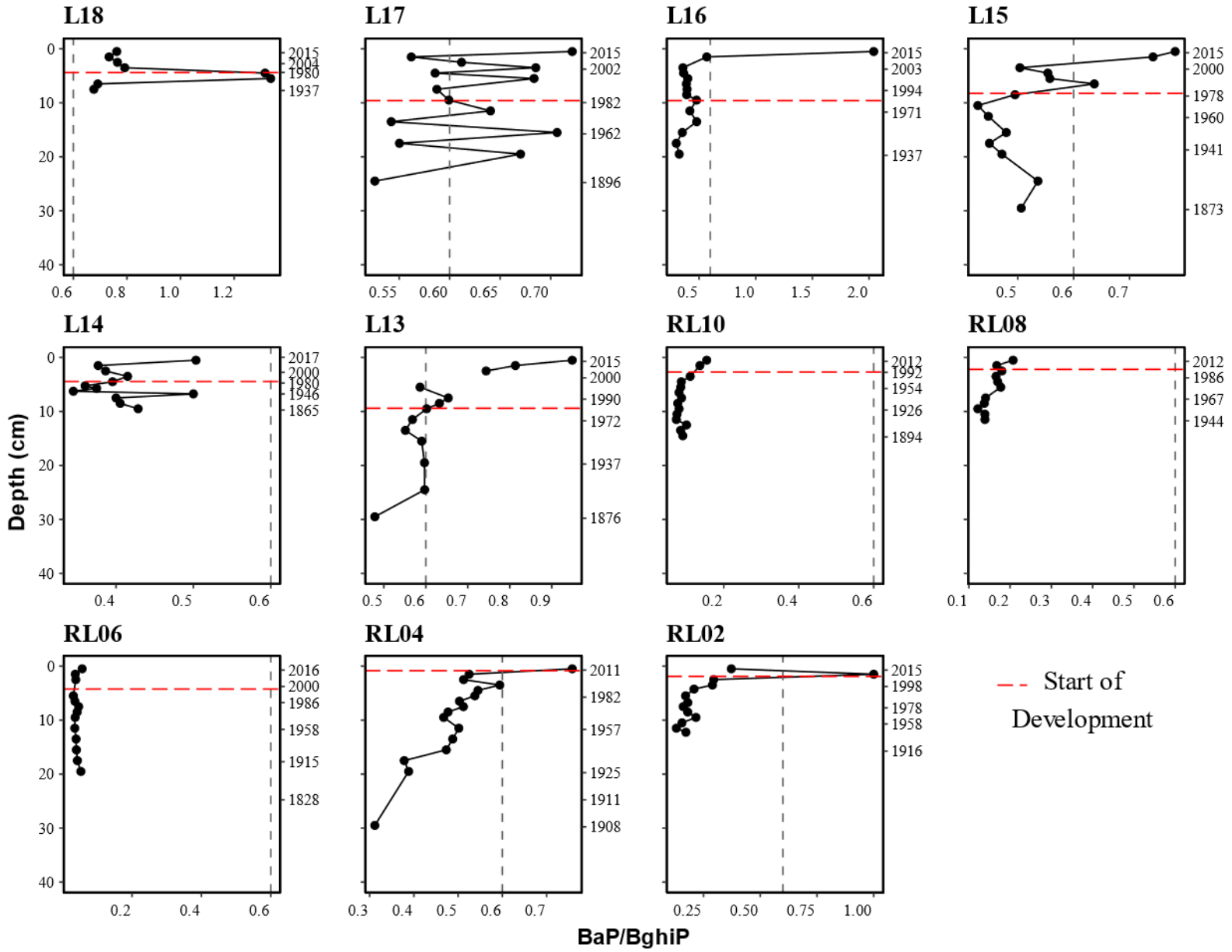

Figure S2- 8: Scatter plots of the BaP/BghiP PAC diagnostic ratio as a function of depth to test for potential traffic emission sources. The vertical dashed line indicates a diagnostic ratio of 0.6. A ratio of < 0.6 suggest non-traffic emission sources whereas a diagnostic ratio > 0.6 suggests a traffic emission source (Katsoyiannis et al., 2005; Tobiszewski et Namiesnik, 2012). The horizontal, red line corresponds to the year when oil sands operations began near each lake.

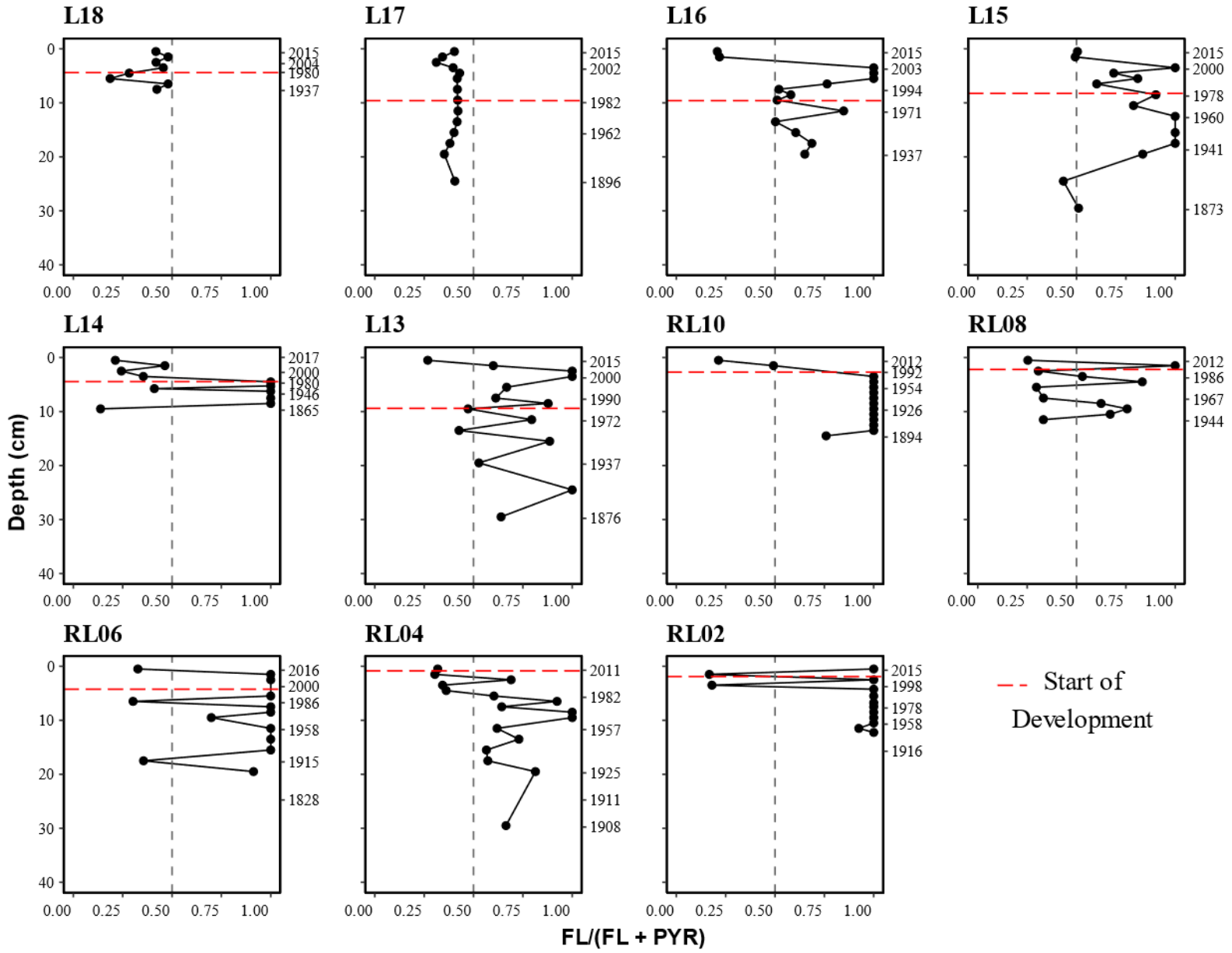

Figure S2- 9: Scatter plots of the FL/(FL+PYR) PAC diagnostic ratio as a function of depth to distinguish fuel emission sources. The vertical dashed line indicates a diagnostic ratio of 0.5. A ratio of < 0.5 suggest a petrol emission source whereas a ratio > 0.5 suggests a diesel emission source (Ravindra et al., 2008a; Tobiszewski et Namiesnik, 2012). The horizontal, red line corresponds to the year when oil sands operations began near each lake.

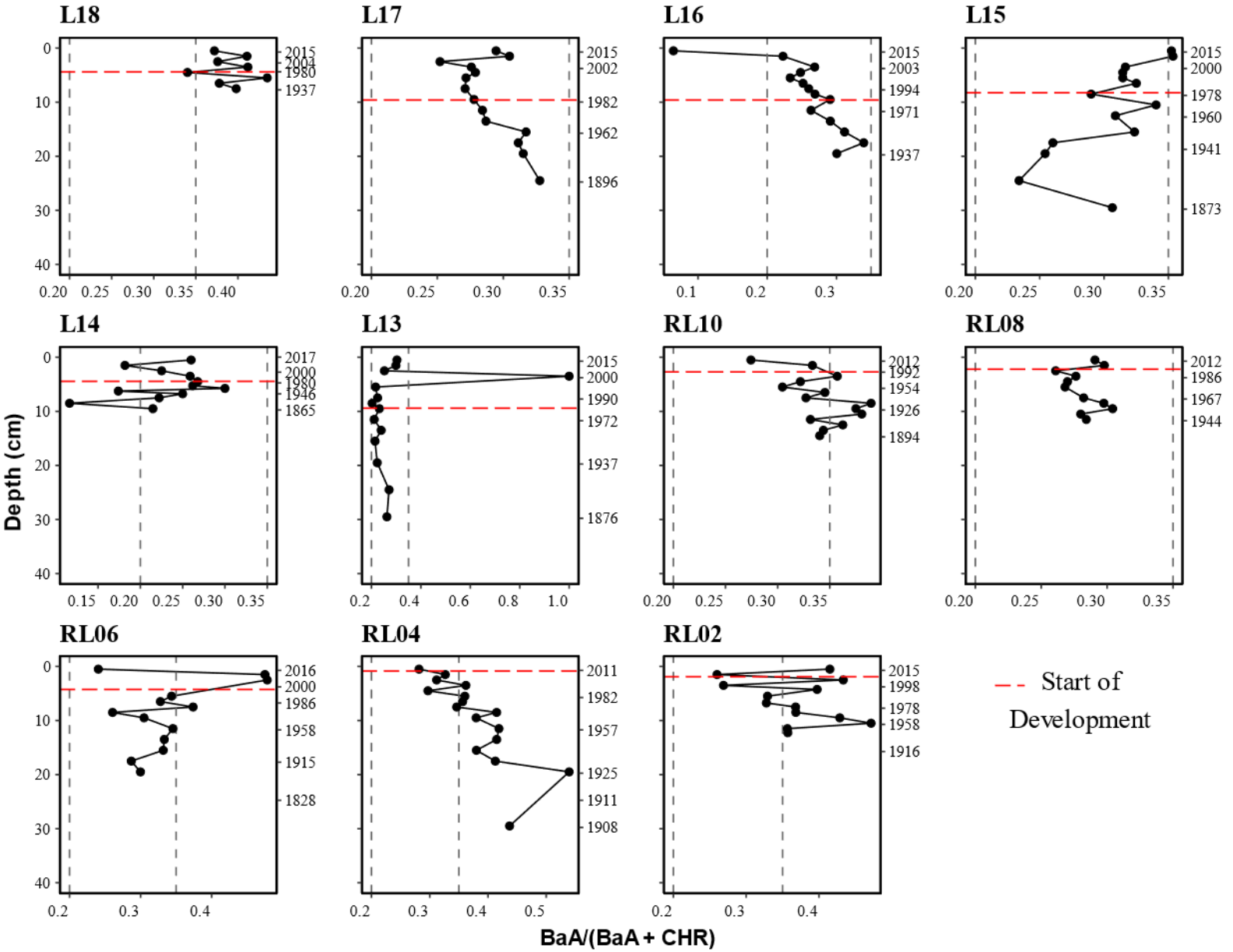

Figure S2- 10: Scatter plots of the BaA/(BaA+CHR) PAC diagnostic ratio as a function of depth to test for potential emission sources. The vertical dashed lines indicate diagnostic ratios of 0.2 and 0.35. A ratio of < 0.2 suggest a petrogenic source, a ratio of 0.2 -0.35 suggest a coal combustion source and a ratio > 0.35 suggests a vehicular emissions source (Yunker et al., 2002; Tobiszewski et Namiesnik, 2012). The horizontal, red line corresponds to the year when oil sands operations began near each lake. *CHR also included triphenylene.

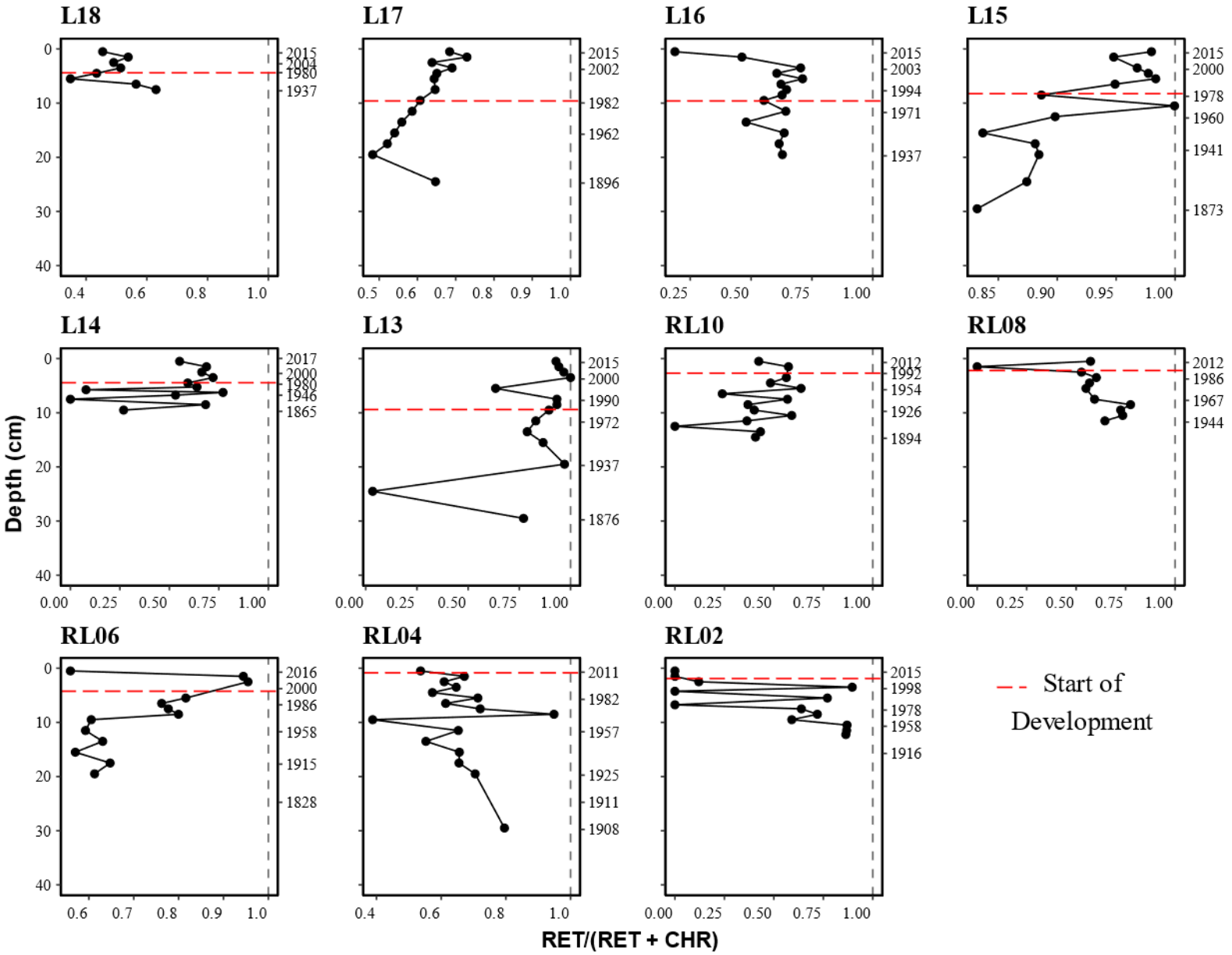

Figure S2- 11: Scatter plots of the RET/(RET+CHR) PAC diagnostic ratio as a function of depth to test for potential forest fire emission sources. The vertical dashed line indicates a diagnostic ratio of 1.0. A ratio of ~ 1.0 suggest a wood burning source (Yan et al., 2005; Tobiszewski et Namiesnik, 2012). The horizontal, red line corresponds to the year when oil sands operations began near each lake. *CHR also included triphenylene.

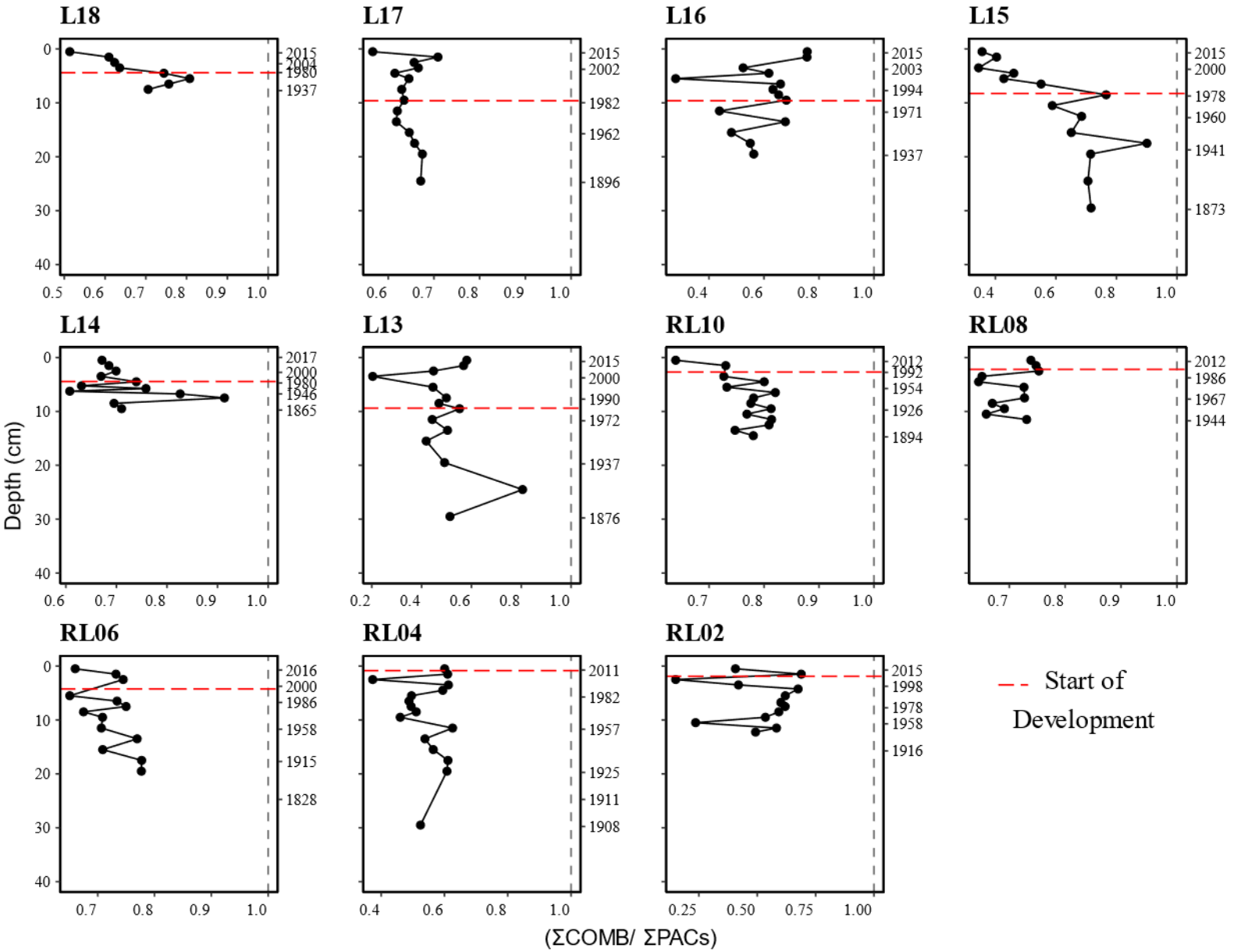

Figure S2- 12: Scatter plots of the ΣCOMB/ΣPACs PAC concentrations as a function of depth to test for potential combustion sources. ΣCOMB compounds consist of FLA, PYR, BaA, CHR, BkF, BbF, IcdP and BghiP. ΣPACs compounds are the sum of total non-alkylated PACs. The vertical dashed line indicates a ratio of 1. A ratio of ~1 suggest a combustion source (Ravindra et al., 2008a; Tobiszewski et Namiesnik, 2012). The horizontal, red line corresponds to the year when oil sands operations began near each lake.

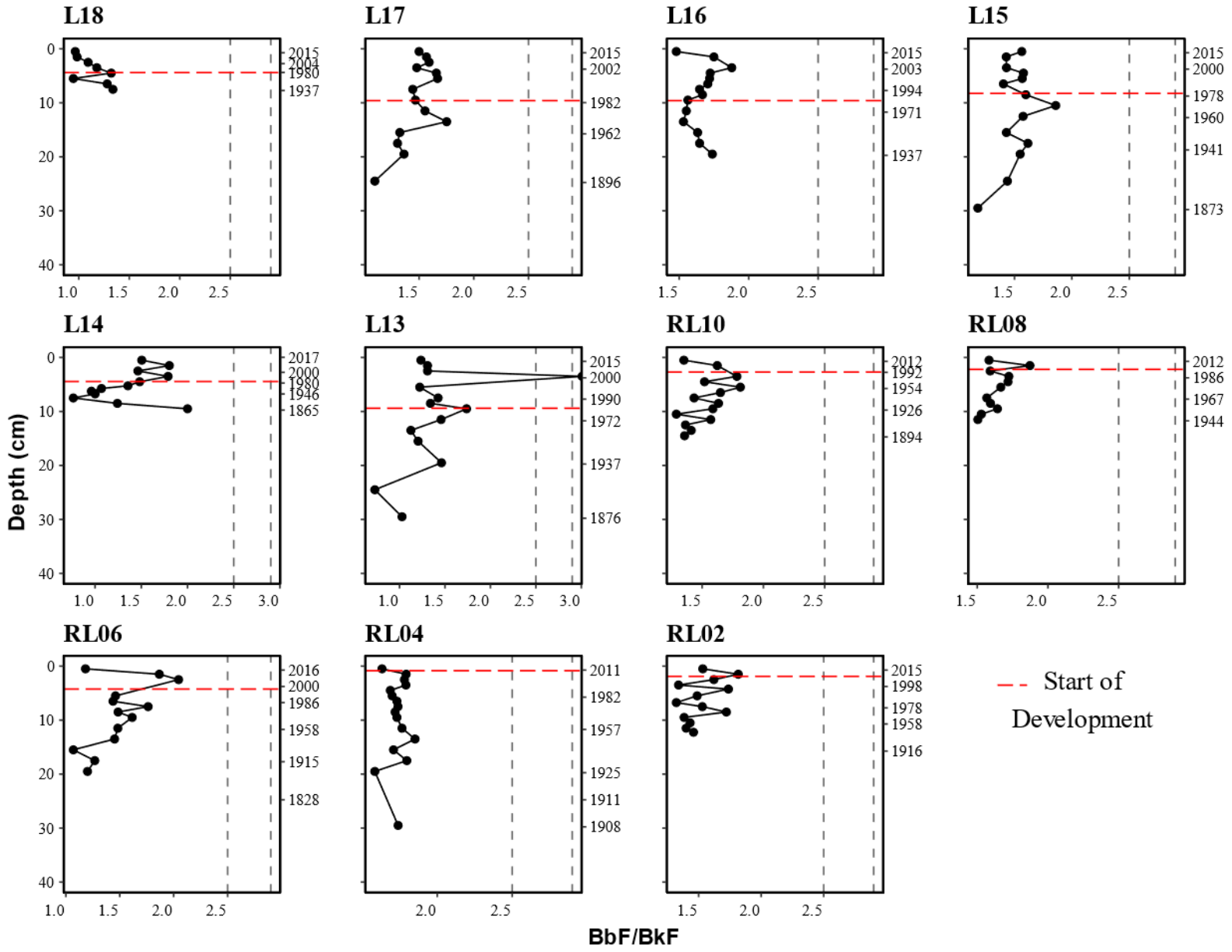

Figure S2- 13: Scatter plots of the BbF/BkF PAC diagnostic ratio as a function of depth to test for potential aluminum smelter emission sources. The vertical dashed lines indicate diagnostic ratios of 2.5 and 2.9. A ratio between 2.5 and 2.5 suggest aluminum smelter emission sources (Callen et al., 2011; Tobiszewski et Namiesnik, 2012). The horizontal, red line corresponds to the year when oil sands operations began near each lake.

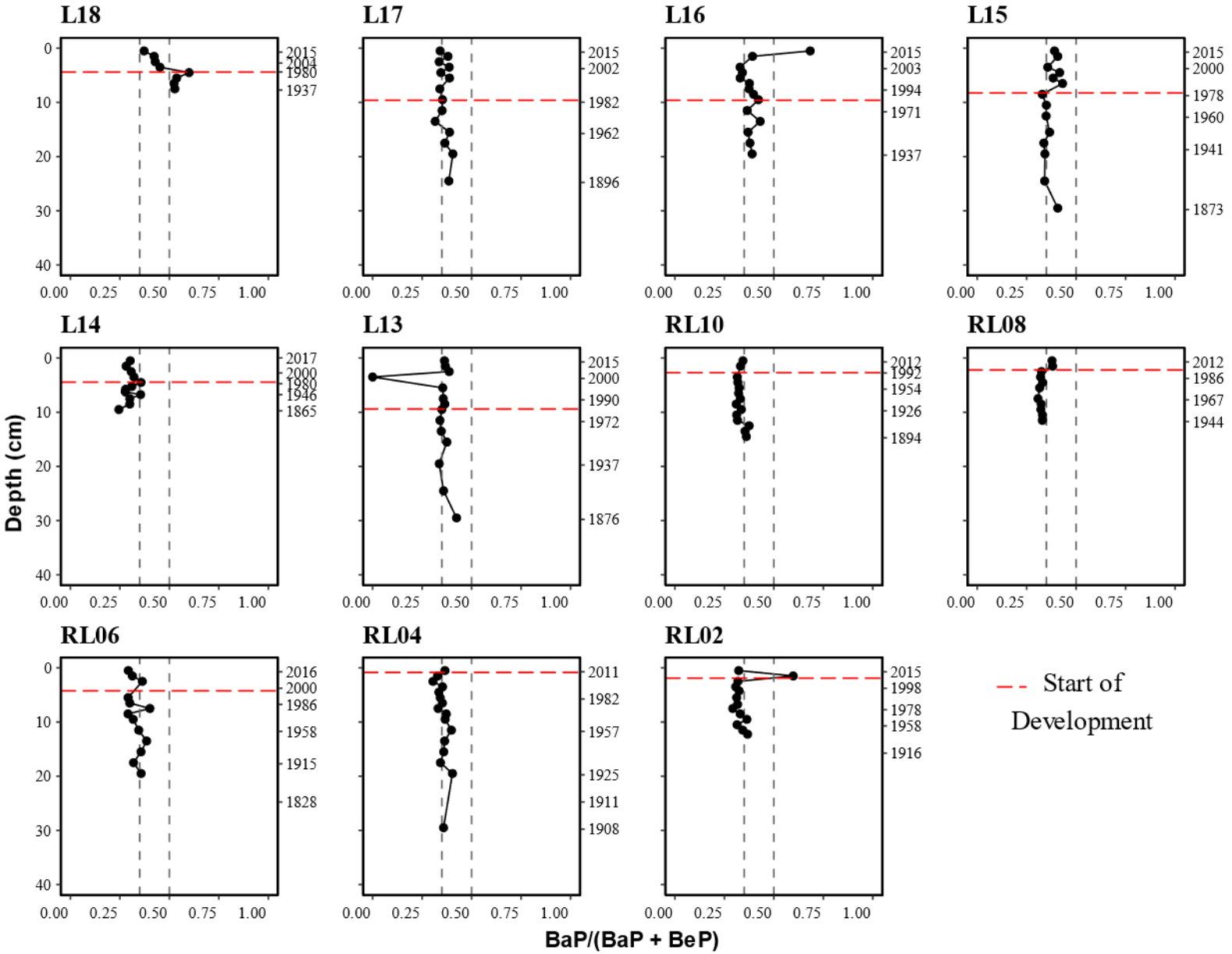

Figure S2- 14: Scatter plots of the BaP/(BaP+BeP) PAC diagnostic ratio as a function of depth to test for potential particle degradation. The vertical dashed lines indicate diagnostic ratios of 0.35 and 0.5. A ratio of ~ 0.5 suggest a fresh particle source whereas a diagnostic ratio < 0.5 suggests a photolysis emission source (Oliveira et al., 2011; Tobiszewski et Namiesnik, 2012). The horizontal, red line corresponds to the year when oil sands operations began near each lake.

Chapter 3. Using *n*-Alkanes and Biomarkers as Forensic Indicators of Petroleum Derived Contamination in Cold Lake, Alberta

Kirsten K. Smythe[1]; Colin A. Cooke[2,3]; Paul E. Drevnick[2]; Robert J. Cornett[1,5]; Jules M. Blais[1,4]

[1] Department of Earth & Environmental Sciences, University of Ottawa, Ottawa, Ontario

[2] Environment & Parks, Government of Alberta, Edmonton, Alberta

[3] Department of Earth and Atmospheric Science, University of Alberta Edmonton, Alberta

[4] Department of Biology, University of Ottawa, Ottawa, Ontario

[5] Deceased

Abstract

This study applies petroleum hydrocarbon (PHC) fingerprinting of *n*-alkanes and petroleum biomarkers (steranes, hopanes, terpanes) in lake sediments cores form the Cold Lake oil sands region to track temporal changes in chemical composition following the onset of thermal *in-situ* activity. We recorded statistically higher concentrations of *n*-alkanes and petroleum biomarkers in sediments deposited following the onset of oil sands activities (1980s - 2000s) in lakes surrounded by *in-situ* infrastructure.

n-alkanes exhibited odd-carbon number preferences over even-number carbon, indicating plant waxes and biogenic PHC sources dominated the composition of *n*-alkanes in this region. The carbon preference index, diagnostic ratios and principal component analyses established that C_{17} algal *n*-alkanes and C_{23}, C_{25}, C_{27} and C_{29} *n*-alkanes (indicative of higher plant matter and macrophytes) dominate the study lakes. The presence of short-chained, even-numbered *n*-alkanes from thermal degradation of biomass during combustion indicated inputs from forest fires, vehicle emissions and fossil fuel combustion sources in addition to biogenic sources.

Low abundances of steranes and the absence of $C_{33\text{-}35}$ hopanes suggest that biomarker origins were not bitumen derived. The depletion of steranes and longer chain hopanes recorded in lake sediments indicated that petrogenic hopenoids originated from the aerosol deposition of fossil fuel emissions such as traffic exhaust and natural gas combustion. These findings suggest that petroleum biomarker composition in lake sediments near Cold Lake is influenced increasingly by the operations of oil sands infrastructure, but not from a raw bitumen source. This study evaluated historical patterns of *n*-alkanes and petroleum biomarkers in radiometrically dated lake sediment cores, allowing for comparisons between open-pit mining regions and *in-situ* oil sands regions to be determined.

3.1 Introduction

The Canadian oil sands are the largest reserve of bitumen and the third-largest crude oil reserve in the world (CAPP, 2018b). The formation of the Alberta bituminous sands occurred during the Cretaceous period because of the petrogenesis of ancient sea deposits. As the sea retreated, the petroleum reserves migrated north, becoming trapped by Clearwater shales, and mixed with fluvial sands that were concurrently deposited (Droppo et al., 2019). Light hydrocarbons, such as paraffins and naphthalenes, were evaporated or metabolized by microbes, yielding heavy crude bitumen reserves dominated by large molecules such as asphaltenes and maltenes (saturates, aromatics, and resins) (Broughton, 2013; Conly et al., 2002).

Petroleum hydrocarbons (PHCs) encompass a broad range of aromatic and saturated compounds such as polycyclic aromatic hydrocarbons (PACs), natural alkanes (*n*-alkanes), terpanes, hopanes, steranes, asphaltenes, and resins (Yang et al., 2011). Depending on the conditions of petroleum formation, oil deposits exhibit unique compound distribution patterns that can be applied to determine PHC sources through chemical fingerprinting (Evans et al., 2016; Hall et al., 2012; Wang et al., 2016; Yang et al., 2011).

n-alkanes are chemical compounds consisting of homologous long-chain alcohols, aldehydes, esters, and hydrocarbons. Similar to PACs, *n*-alkanes originate from natural sources (plant waxes and soils) as well as anthropogenic sources (fossil fuel combustion) (Olajire et al., 2008). During bitumen formation, *n*-alkanes and light hydrocarbons are almost entirely depleted by evaporation, microbial degradation through porous media, or weathering, resulting in a distribution of *n*-alkanes that is both biological and non-biological in origin (Andreou and Rapsomanikis, 2009; Grice et al., 1968). *n*-alkanes can help distinguish different petroleum sources based on their proportion of odd-to-even numbered compounds. Plant-derived *n*-alkanes frequently have a distinct odd carbon number preference, whereas petroleum-derived *n*-alkanes exhibit a carbon indifference (Grice et al., 1968; Yang et al., 2011).

Chemical characterization is dependent on the distinct signature of the petroleum product. Petrogenic *n*-alkanes have signatures that are indicative of their origin and, therefore, can be used in environmental forensics to determine their originating source. Alberta oil sands are significantly biodegraded and exhibit large chromatographic regions of unresolved complex mixtures (UCM) from *n*-C_{10} to *n*-C_{40} (Yang et al., 2011). Typically, refined oils will contain a

substantial fraction of small chained *n*-alkanes ranging from n-C_9 to n-C_{36} (Yang et al., 2011). Higher viscosity crude oils, such as bitumen, contain less overall *n*-alkanes, ranging from n-C_{16} to n-C_{36} (Yang et al., 2011).

The carbon preference index (CPI) can facilitate the differentiation amongst biogenic and petrogenic *n-a*lkane origins. This CPI establishes the ratio of odd to even-numbered *n*-alkanes over a fixed range. Petrogenic hydrocarbon sources have a CPI index approaching 1, whereas biogenic hydrocarbon sources have higher CPI values ranging from 2–12 (Andreou and Rapsomanikis, 2009; Grice et al., 1968; Simoneit, 2005; Zhen Wang et al., 2009). In general, carbon numbers greater than n-C_{27} reflect a carbon signature derived from higher plant waxes and fungi, whereas lower carbon numbers (C_{16} & C_{17}) infer inputs from algae and bacteria. C_{20} & C_{21} *n*-alkanes are typical of petroleum origins, including diesel exhaust (Miyake et al., 2005; Olajire et al., 2008). A caveat to using *n*-alkanes for petroleum fingerprinting is that *n*-alkanes are subject to specific compositional and physical property changes and thus become unreliable tools for chemical fingerprinting as petroleum products weather (Wang et al., 2016).

Petroleum biomarkers are complex molecules derived from living organisms synthesized during petrogenesis (Brooks et al., 1988; Wang et al., 2016). Biomarker patterns remain unaffected despite the evaporation and emulsification, dispersion, dissolution, biodegradation and photooxidation of petroleum and, as such, are compared to their biological precursors for chemical fingerprinting (Jia et al., 2013; Stout and Wang, 2016). Terpanes, hopanes, and steranes are generated and preserved exclusively within petroleum deposits and have little or no structural change from their parent biochemicals, as they retain most of their original carbon skeleton, making them highly specific for source identification (Wang et al., 2016). Biodegradation of compound classes generally transitions from *n*-alkanes > acyclic isoprenoids > steranes > hopanes > terpanes, making biomarkers superior compounds for chemical fingerprinting than PACs or *n*-alkanes which have many sources in the environment (Brooks et al., 1988). Petroleum biomarkers have been used to determine origins of oil spills, types of source rocks, thermal maturity of petroleum reserves, depositional conditions of environmental contaminants, and patterns of contaminant deposition (Bieger et al., 1996; Jia et al., 2013; Liao et al., 2012; Wang et al., 2016, 2006; Yang et al., 2012; Yu et al., 2012; Yunker and Macdonald, 2003). Many crude oils exhibit a characteristic biomarker abundance of C_{29} & C_{30} αβ hopanes

and C_{23} & C_{24} terpanes with a sterane dominance of C_{27}, C_{28}, C_{29} S & R homologs. Biomarker concentrations typically decrease with greater thermal maturity of the host reserve; therefore, biomarker concentrations in light oils and condensates are deficient when compared to heavy oils such as bitumen (Stout and Wang, 2016; Wang et al., 2016).

PHC characterization and chemical fingerprinting have been applied within the northern Alberta oil sands region where bitumen outcrops introduce petroleum to the environment naturally (Roy, 2018; Salat, 2019; Wang et al., 2014). Alberta bitumen, Athabasca oil sands samples and Peace-Athabasca Delta samples have been analyzed to identify petroleum inputs and distinguish natural and anthropogenic petroleum sources in environmental matrices (Roy, 2018; Salat, 2019; Wang et al., 2014; Yang et al., 2011). Biomarker distributions in water, soil, lake sediment and tailings pond sediment samples are consistent with the typical features of bitumen in regions as far north as the Peace Athabasca Delta indicating bitumen from the Alberta oil sands deposits are present in these environments (Roy, 2018; Salat, 2019; Wang et al., 2014).

The Cold Lake region is isolated from bitumen processing facilities, tailings ponds and open-pit mining operations by more than 300 km. The Cold Lake bitumen deposit does not incise the surface and therefore has no known mechanism for natural bitumen introduction to the surrounding environment (Baturin-Pollock et al., 2010). The Cold Lake oil field relies on thermal *in-situ* oil sands extraction to access the deep bitumen reserves. High-temperature and high-pressure steam and solvent are injected into the bitumen reserves through cyclic steam stimulation drilling (CSS) and steam-assisted gravity drainage drilling (SAGD) to decrease the bitumen viscosity and separate it from the sand matrix for collection (AER, 2018c). Over-pressurization of the shale containment rock during these operations have resulted in 5 non-targeted flow-to-surface (FTS) events to occur since 2009 (AER, 2016). One such flow-to-surface event contaminated an unnamed water body (9-21, (Korosi et al., 2016a)), which was subsequently drained and dredged as a cleanup measure. A conservative estimate of 800 000 m^3 of bitumen spilled into the environment as a result of these five flow-to-surface events (AER, 2016).

The objective of this study is to determine whether *in-situ* oil sands operations have altered the PHC composition in the Cold Lake region, specifically *n*-alkanes and petroleum biomarkers. We quantified PHCs in radiometrically-dated lake sediment cores to determine

whether or not they increased following *in-situ* bitumen extraction or if evidence exists of non-reported flow-to-surface events. Principal component analyses, CPI analyses, and diagnostic ratios allow us to determine how PHC composition in lake sediments relates to petrogenic or biogenic sources.

3.2 Methodology

3.2.1 Study Area

This study examines lake sediment cores collected throughout the Cold Lake oil field of Central/North-Eastern Alberta, Canada. The Cold Lake oil field is the only oil sands region in Canada to rely exclusively on thermal *in-situ* oil extraction techniques to access the bitumen deposits 300 – 600 m below the surface (Imperial Oil Resources Limited, 2016). The Cold Lake region provides an ideal environment to quantify PHC inputs from *in-situ* activity as it is located ~300 km southeast from all major bitumen processing facilities, open-pit mines and tailings ponds (CAPP, 2019).

3.2.2 Study Sites and Core Collection

We cored lake basins at their depocenter using a Uwitec gravity corer (Mondsee, Austria) and sectioned them into 0.5-cm intervals with a modified Glew vertical extruder (Glew, 1988). Sediments were stored in pre-labelled Whirl-Pak® bags, frozen, and shipped to the University of Ottawa, where they were stored at -18^{o}C until analysis. The eleven lakes, cored in late August and early September of 2017, were selected based on lake size and proximity to oil sands developments (Table 3-1, Figure 3-1).

Table 3- 1: Summary of lake parameters. Lakes marked with a Y are within the Cold Lake Air Weapons Range (CLAWR), lakes marked with an N are off the CLAWR. Distance refers to the mean distance of each lake from *in-situ* oil wells to the southwest. Well density refers to the number of wells situated within a 7 km radius from the coring location.

Sample Coordinates	Lake ID	Lake Name	CLAWR	Area (m^2)	Distance (m)	Well Density (#)	Start of Oil Sands
55.0805, -110.5597	RL02		Y	147.4	1487	23	2007
55.0673, -110.5645	RL04		Y	794.3	1299	31	2007
54.9111, -110.6014	RL06		Y	44.86	4345	13	1998
54.8619, -110.5837	RL08		Y	144.7	2361	35	1998
54.8028, -110.3778	RL10		Y	43.10	2809	21	1998
54.7227, -110.6595	L13	Sinclair Lake	N	1888	3321	43	1980
54.7114, -110.3942	L14	May Lake	N	3117	4688	15	1980
54.6648, -110.5437	L15	Bourque Lake	N	9944	1625	>100	1980
54.6081, -110.4601	L16		N	252.0	916.5	>100	1980
54.5895, -110.4753	L17	McDougall Lake	N	505.6	1009	88	1980
54.6306, -110.2775	L18	Marie Lake	N	34 600	6584	5	1980

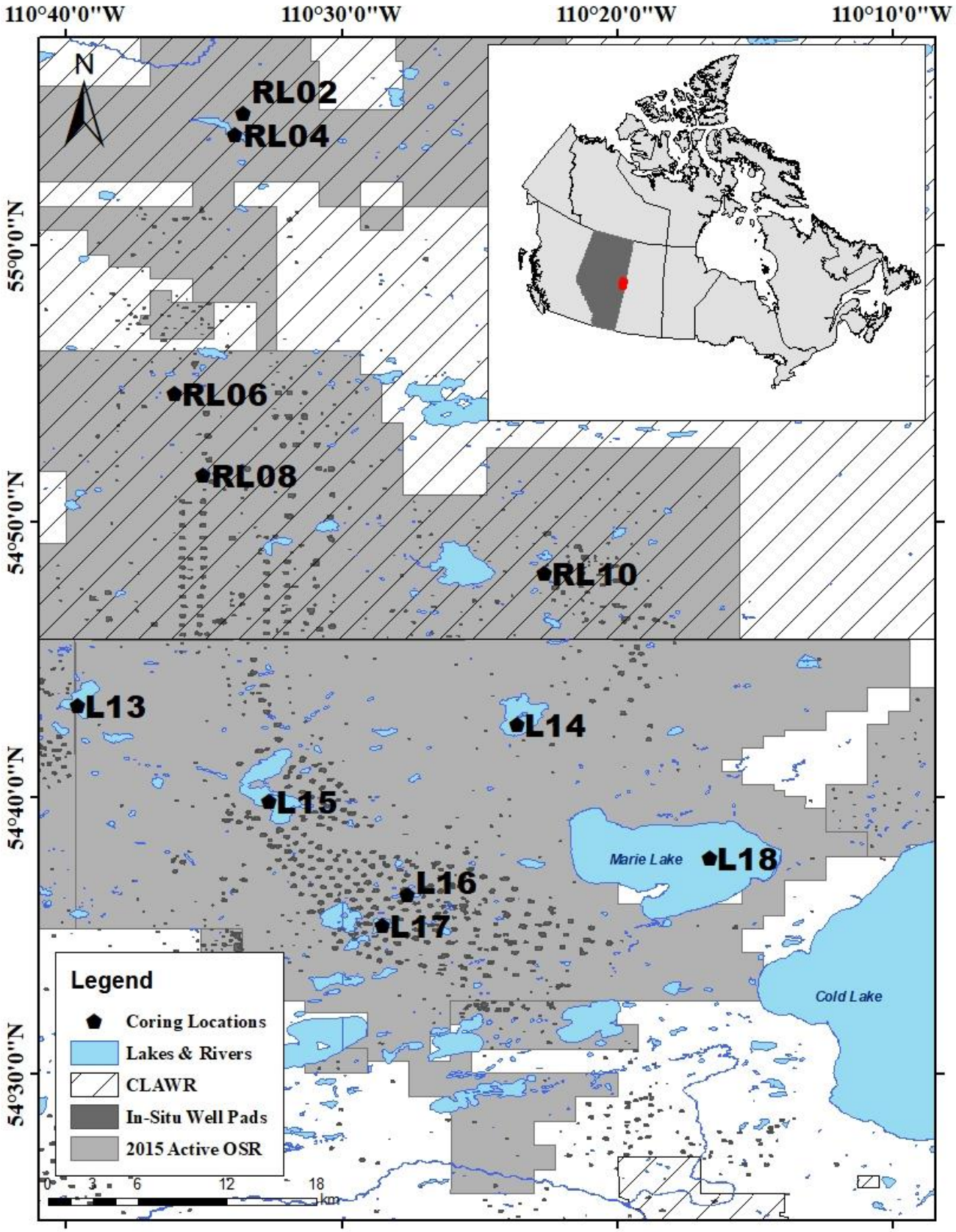

Figure 3- 1: Map of the 11 study lakes within the active oil sands region (OSR) of the Cold Lake Oil Field (AEP, 2019).*Not shown are *in-situ* well pads surrounding Lakes RL02 and RL04

3.2.3 Radiometric Dating

Using ScienTissimMe software (Barry's Bay, ON, Canada) and gamma spectrometry, we created age-depth profiles for each sediment core using a constant rate of supply (CRS) model from unsupported ^{210}Pb gamma activity, described by Appleby (2001). Briefly, we compacted 1–3 cm^3 of homogenized, freeze-dried sediment into Sarstedt polypropylene 8mL gamma tubes using an Eppendorf Centrifuge 5810 at 2000 rotations per minute (rpm) for 15 minutes. We recorded precise heights and weights for density and volume determinations. Tubes were sealed with a septum and 1 inch of clear Devcon® 2-Ton Epoxy # 14260 to prevent the loss of ^{222}Rn (Appleby et al., 1986). Following a 21-day equilibration period, an Ortec High Purity Germanium Gamma Spectrometer counted each sample for 23 hours (82800s) using MAESTRO version 6.08 software (Advanced Measurement Technology Inc. Oak Ridge, TN, USA). Unsupported ^{210}Pb activity profiles established sedimentation rates and sediment ages when corrected to ^{214}Pb and constant rate of supply (CRS) dating models (Appleby and Oldfield, 1978).

We measured ^{137}Cs activities from the 661.66 keV gamma spectroscopy peak as an independent chronostratigraphic marker to corroborate the CRS dates.^{137}Cs is a common isotope used in gamma spectroscopy as it was widely distributed as a result of above-ground nuclear weapons testing in the 1960s, producing a peak abundance in 1963 (Omelchenko et al., 2005; Taylor et al., 1988). Spectrometer efficiency calibrations using Certified Reference Materials (IAEA-312 & IAEA-385) from the International Atomic Energy Association (Vienna, Austria) were applied to corroborate the ^{210}Pb dates (Figure S2-1).

3.2.4 Elemental Analyses

Total organic carbon (TOC), nitrogen, hydrogen, and sulphur content (% CNS), were established at the Ján Veizer Stable Isotope Laboratory (University of Ottawa, Ottawa, Ontario, Canada) using a VarioEL cube elemental analyzer (Elementar Americas Inc., New York, NY, USA), described by Skierszkan et al. (2013). Machine detection efficiency was calibrated using standards of sulfanilamide and sulfanilic acid.

We selected four lakes for total mercury analyses based on their size and proximity to *in-situ* wells. 0.05 g of freeze-dried sediments were analyzed using an Sp-3D automatic mercury analyzer (Nippon Instrument Corporation, Singapore) and ran alongside Marine Sediment Certified Reference Material (MESS-3) and NIST-2704 Buffalo River Sediments from the National Research Council of Canada for instrument efficiency corrections. Every 10^{th} sample was analyzed in duplicate producing an average standard deviation of 1.05 ng Hg/g. All total mercury analyses were conducted through the University of Ottawa LANSET laboratories (Ottawa, Ontario, Canada). Summaries of all elemental analyses are in the supplementary information (Figure S2-2).

3.2.5 Petroleum Hydrocarbon Extraction and Analysis

Petroleum biomarkers and *n*-alkanes were extracted from homogenized lake sediments using the US EPA extraction procedure #3540C, adapted for Accelerated Solvent Extraction (ASE) as per the methodologies outlined in Chapter 2. Before ASE extraction, samples were spiked with an internal standard of n-tetracosane (D50, 98 %) (Cambridge Isotope Laboratories Inc. Tewksbury, MA, USA) and C_8-C_{40} *n*-alkanes in dichloromethane (DCM), purchased from Supelco (Bellefonte, PA, USA) and were used for *n*-alkane recovery determinations. National Institute of Standards and Technology (NIST), Standard Reference Material (SRM) #2233, biomarker standards of hopanes and steranes in 2,2,4 trimethylpentane (TMP), were obtained from Sigma-Aldrich (Oakville, ON, Canada). Target analytes for *n*-alkanes and petroleum biomarkers are summarized in the supplementary information (Tables S3-1 & S3-2).

The *n*-alkane and petroleum biomarker (F1 fraction) column cleanup used 22 mL of hexanes through a 6 g, 644 silica gel (Fisher S7441) column. The F1 fraction was collected in 1 mL of TMP and evaporated to 1 mL using a 0.4 bar nitrogen stream. A 10x dilution sample was then spiked with 10 µL of p-terphenyl (D_{14}, 98 %) internal standard and analyzed using gas chromatography coupled with mass spectrometry (GC-MS). We interpreted GC-MS chromatograms using MSD ChemStation Data Analysis F.01.03 Software (Agilent Technologies, Santa Clara, CA, USA). The mean recovery for the n-tetracosane (D50, 98 %) surrogate target compound ($\pm$ 1 standard deviation (STDEV)) was 60.2 $\pm$ 19.5 %.

3.2.6 Statistical Analyses

We executed all data transformations, statistical analyses, and visualizations in the RStudio statistical environment, version 3.6.1 (R Core Team, 2018). We generated all plots using the *ggplot2* and the *ggpubr* packages. Mapping and distance determinations were completed using ESRI's ArcGIS 10.6.1 (ESRI ArcGIS Desktop, 2018). CRS dating models allowed us to categorize sediments in each core based on their time of deposition (before or after the onset of *in-situ* oil sands development).

We calculated petroleum hydrocarbon diagnostic ratios for source determination and chemical characterization. The diagnostic ratios selected for these analyses were used to track historical changes in PHC sources and ascertain whether bituminous inputs are influenced in the Cold Lake region as a result of oil sands activity. The diagnostic ratios calculated in this chapter include:

- n-C_{14} / Phytane
- n-C_{17} / Pristane
- n-C_{18} / Phytane
- n-C_{23} / Phytane
- n-C_{29} / Phytane
- Pristane / Phytane
- C_{21} T / C_{22} T
- C_{21} T / C_{21+23} T
- C_{21} T / C_{23} T
- C_{23} T / C_{24} T
- C_{23} T / C_{30} αβ H
- C_{24} T / C_{30} αβ H
- C_{27} Ts / C_{27} Tm
- Σ C_{27-29} ααβ S / Σ C_{21-24} T
- C_{27} ααβ S / C_{29} ααβ S
- C_{29} αβ H / C_{30} αβ H
- C_{30} αβ H / ΣC_{31-35} (S+R) H
- C_{31} (S) H / C_{31} (R) H
- C_{31} (R) H / C_{29} αβ H
- C_{32} (R) H / C_{31}(R) H
- C_{33}(R) H / C_{32} (R) H
- C_{33} (S) H / C_{33} (R) H
- C_{31} (S) H / C_{31} (S+R) H
- C_{34} (S) H / C_{35} (S) H
- C_{34} (R) H / C_{35} (R) H
- ΣSteranes / ΣTerpanes
- Gammacerane /C_{30} αβ H

The carbon preference index (CPI), as determined by Wang et al. (2009), was calculated using equations 1 and 2 to identify petrogenic or biogenic *n*-alkane origins in the sediments and to track the change in CPI over time. This index compares the sum of odd-numbered *n*-alkanes to the sum of even-numbered *n*-alkanes in the range of C_8-C_{40}. Similarly, the CPI can be calculated based on equation 2, comparing the sum of the odd carbon number *n*-alkanes in the C_{23}-$_{34}$ range to the sum of the even-carbon-number C_{23}-$_{34}$ *n*-alkanes. Petrogenic hydrocarbons sources have a CPI approaching 1, whereas biogenic hydrocarbon sources have higher CPI, ranging from 2–12 (Andreou and Rapsomanikis, 2009; Grice et al., 1968; Simoneit, 2005; Zhen Wang et al., 2009).

$$CPI_{8\text{-}40} = \Sigma \text{ (odd-numbered } n\text{-alkanes)} / \Sigma \text{ (even-numbered } n\text{-alkanes)} \quad (1)$$

$$CPI_{23\text{-}34} = (C_{23} + C_{25} + C_{27} + C_{29} + C_{31} + C_{33}) / (C_{24} + C_{26} + C_{28} + C_{30} + C_{32} + C_{34}) \quad (2)$$

Principal component analyses (PCA) using relative abundances of *n*-alkanes and biomarkers assessed the transition in PHC composition through each core. Sediments were compared to a passively plotted Cold Lake Bitumen Sample, obtained from Environment and Climate Change Canada (Ottawa, Ontario, Canada). PCA biplots were created within the *factoextra* R package, using the function fviz_pca_biplot(). Passively plotted points were added to the PCA biplot using the *ggbiplot* and *devtools* R packages.

The change PHC burden in each lake following the onset of oil sands activity was tested using an ANOVA as per the method outlined in Chapter 2, modified from Cheney et al. (2020). Residuals of the analysis of variance (ANOVA) were tested using the R packages *Car*, *gvlma,* and *lmtest.* When the assumptions of a parametric test were not met, permutation tests assessed the validity of the model. In cases when permutation tests did not corroborate the findings of the ANOVA models, non-parametric tests were applied using the *lmperm* package.

3.3 Results and Discussion

3.3.1 Petroleum Biomarkers

Total biomarker concentrations fluctuated substantially throughout each lake sediment core. Variable sedimentation rates explain these fluctuations within each lake as petroleum biomarker accumulation rates remained relatively consistent (Figure 3-2) (Eickmeyer et al.,

2016). Total biomarker accumulation rates in Lakes L18, L17, L16, and RL02 all increased at the onset of oil sands development in their surrounding regions. Lake L13 is distinct from the other study lakes because it exhibited elevated total biomarker accumulation rates compared to the others, reaching a peak concentration of 582 µg m^{-2} yr^{-1} in 1994 before returning to ~178 µg m^{-2} yr^{-1} in the early 2000s. L13 borders two oil sands development regions. The area to the north of L13 began *in-situ* oil sands operations in the mid-1990s. To the south, *in-situ* activity started in the 1980s. The spike in L13 biomarkers appears to be associated with oil sands development in the northern region beginning in the mid-1990s. Total biomarker accumulation rates increase slightly in Lakes L15 and RL10 following the onset of oil sands operations. The accumulation rates of petroleum biomarkers in L18, L16, L15, L14, RL10, RL06, and RL02 are very low indicating that natural introductions of bitumen are unlikely. RL08 and RL10 are the lakes located closest to the historical FTS events that occurred in the Cold Lake region. Neither lake exhibits a spike in petroleum biomarkers between 2009 and 2013, indicating that petroleum from these flow-to-surface events did not contribute to petrogenic enrichment in these lakes.

We conducted an ANOVA to compare total biomarker accumulation rates in sediments deposited before and after oil sands operations began and observed statistically higher accumulation rates (p-value < 0.001) in L17, L16, L15, L14, RL10, RL06, and RL02 (Figure 3-3). Lakes L13 and RL04 also exhibited statistically significant changes (p-value < 0.05). RL08 and L18 did not change significantly following the onset of oil sands activity. These findings indicate that oil sands activity is likely contributing to the petroleum biomarker enrichment observed in these lakes. Note that petroleum biomarker concentrations in these lakes are consistently very low; therefore, increases that occurred post-development are driven more by an increase in non-petroleum biomarkers (Yang et al., 2011).

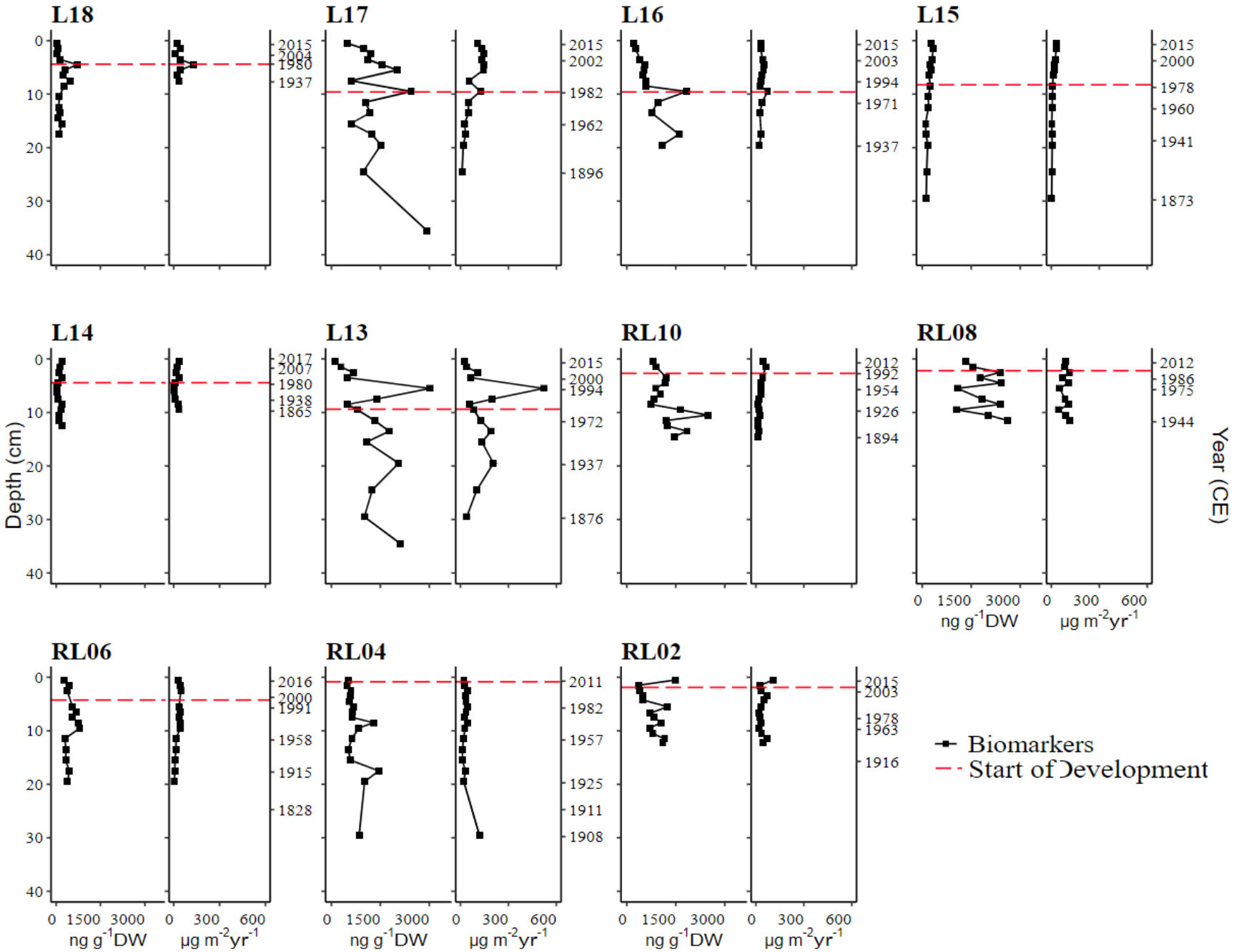

Figure 3- 2: Total petroleum biomarkers profiles as a function of depth. Scatter plots of the total concentration (ng g^{-1} DW) of the targeted petroleum biomarker compounds with respect to biomarker accumulation rate (ug m^2 yr^{-1}) down core. All plots have the same Y axis, representing depth downcore in centimeters. Left plots depict the total concentration of biomarkers corrected for dry weight. Plots to the right depict the rate of total biomarker flux. Dates were established using the CRS dating model. Biomarker flux was not calculated below the horizon of unsupported ^{210}Pb activity as it exceeded the limitations of the CRS dating model. The dashed red line corresponds to the year when oil sands operations began near each lake.

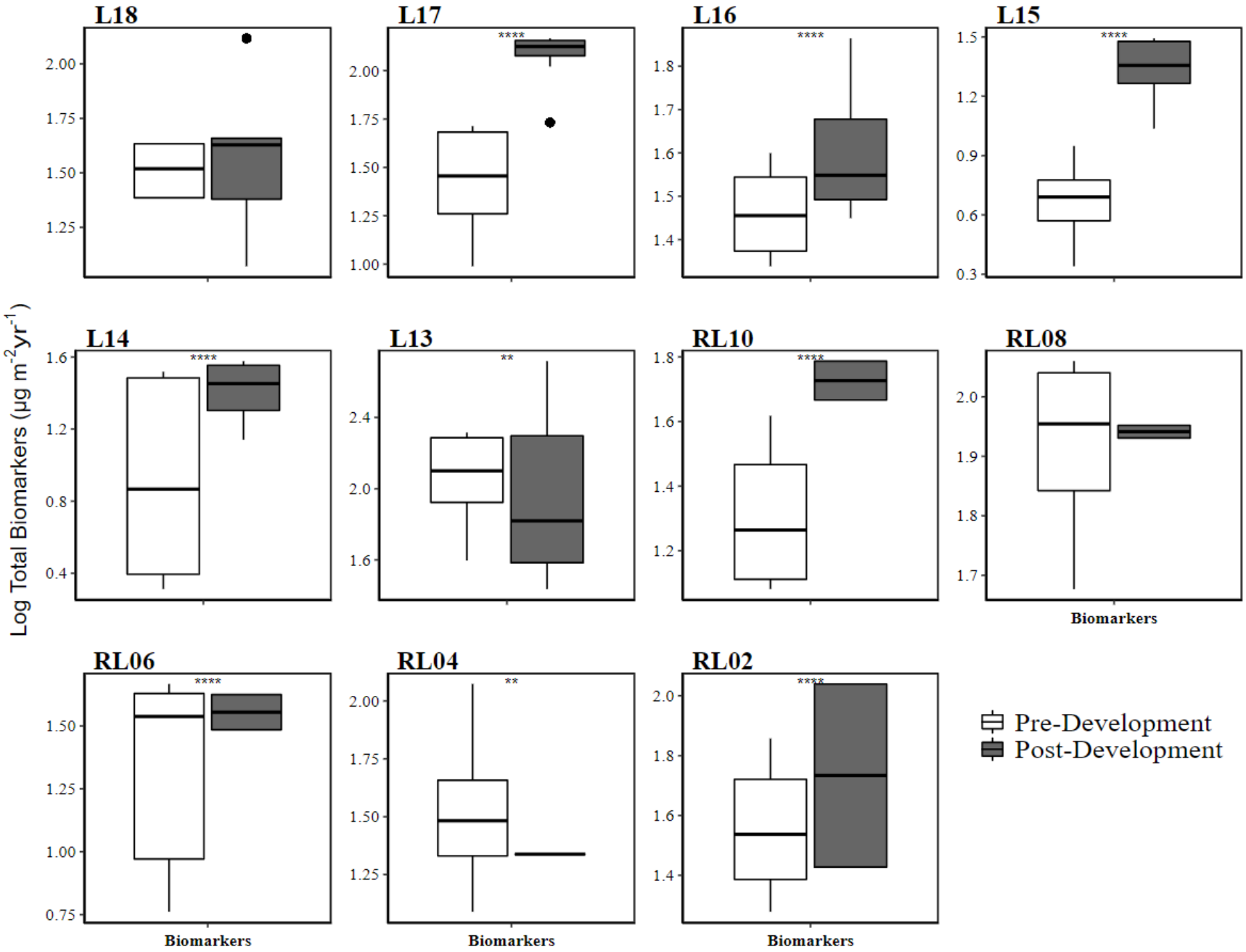

Figure 3- 3: Boxplots showing the change in log transformed total biomarker accumulation rates (log µg m^2 yr^{-1}) between sediments deposited before and after oil sands operations began. (p-value < 0.05 (**), p value < 0.001 (****)).

C_{27} terpanes, $C_{29\text{-}30}$ αβ hopanes, and $C_{31\text{-}33}$ R and S hopanes dominated the total petroleum biomarker abundances in all study lakes (Figure S3-1). Typically, crude oils exhibit a characteristic biomarker abundance of C_{29} & C_{30} αβ hopanes and C_{23} & C_{24} terpanes with a sterane dominance of $C_{27\text{-}29}$ ααα (Stout and Wang, 2016). The study lakes were mostly depleted of C_{33} (R) – C_{35} (R and S) hopanes as well as C_{21}-C_{27} terpanes. $C_{27\text{-}29}$ αββ steranes accounted for less than 5% of the relative biomarker abundance in the study lakes however were most abundant in lakes L18, L17, L16, L15, L14 and RL06. Terpanes and steranes are abundant in oils and extracts from source rocks; therefore, the low abundances present in our lake sediments indicate that bitumen deposits are not introducing petroleum biomarkers to these lake systems (Yu et al., 2012). We removed C_{32} (S) Hopanes from the suite of biomarkers examined in this study as they were unresolvable from co-extracted oleanane compounds (Wang et al., 2016).

Low abundances of steranes and the absence of $C_{33\text{-}35}$ hopanes suggest that biomarker origins are not bitumen derived. The elevated abundance of C_{27} terpanes, $C_{29\text{-}30}$ αβ hopanes, and $C_{31\text{-}33}$ R and S hopanes mimics that of the Cold Lake bitumen sample. The depletion of steranes and longer chain hopanes implies that these petrogenic hopenoids are likely from aerosol deposition from fossil fuel combustion emissions such as traffic exhaust / natural gas combustion (Rogge et al., 1993) and forest fires (Radzi Bin Abas et al., 2001). Biomarker distribution corroborates the findings from Chapter 2, suggesting that traffic emissions and natural gas combustion for steam generation are likely driving the PHC enrichment in regional lakes and not the introduction of raw bitumen.

Yang et al. (2011) identified biomarker diagnostic ratios in raw Alberta bitumen, diluted crude bitumen, upgraded heavy synthetic crude oil and in an Alberta sweet mixed blend. We applied the same diagnostic ratios to the lakes in this study and determined that they are not receiving inputs from bitumen (Figures S3-2 -S3-21). Since the start of oil sands developments in Cold Lake, we observed increasing diagnostic ratios in all lakes except L15 for C_{23} T /C_{30} αβ H, C_{24}T /C_{30} αβ H, C_{30} αβ H /∑$C_{31\text{-}35}$ H, C_{31}(S) /C_{31}(R), and ∑Steranes /∑Terpanes (Figures S3-6, S3-7, S3-10, S3-13, and S3-21). Although these increases coincided with the start of oil sands activity C_{21} T /C_{22} T ratios indicated that these transitions are likely a result of light oils as opposed to crude oil inputs (Figure S3-2) (Rogge et al., 1993). Similarly, we did not record

decreasing C31(R) H /C29 αβ H, and C33(R) H /C32(R) H ratios in the sediments that would indicate petroleum influences (Figures S3-14 and S3-16).

Diagnostic ratios of C_{31} (S) H /C_{31} (R) H, C_{32} (R) H /C_{31} (R) H, C_{33} (R) H /C_{32} (R) H, C_{33}(S) H /C_{33} (R) H, C_{34}(S) H /C_{35}(S) H, and C_{34}(R) H /C_{35}(R) H comparing S and R hopanes did not approach a ratio of one meaning that these lakes have inputs from unstable petroleum sources such as fuels. S/R ratios of 1 are indicative of a thermally mature and stable petroleum source such as bitumen (Dastillung and Albrecht, 1976). These findings indicate that petrogenic PHCs are not dominant in these lake systems and are more likely influenced by biomass and fossil fuel emissions (Figures S3-13, S3-15, S3-16, S3-17, S3-18, and S3-19) (Dastillung and Albrecht, 1976).

Downcore principal component analyses of petroleum biomarker abundances recorded the shift in the composition of the top 5 contributing compounds compared to a CLB sample (Figure 3-4). PCA axes 1 and 2 explain ~66.5 % of the variance in the data. Biomarker composition in modern sediments varied from the oldest recorded sediments, with C_{33} (S), C_{31} (S), and C_{32} (R) hopanes explaining the highest proportion of variation in the direction opposite modern sediments. $C_{21\text{-}23}$ terpanes explained a substantial portion of the variance in all lakes except L16, L15, RL08, RL04 and RL02, with the directionality shifting towards modern sediments. These findings indicate light oils such as natural gas and fuels increasing in abundance in lakes densely surrounded by oil sands activity. $C_{29\text{-}30}$ αβ hopanes and $C_{27\text{-}29}$ αββ steranes in Lakes L18, L16, L15, and RL08 point towards modern sediments indicating an increased influence of petroleum biomarkers that are commonly associated with crude oils (Stout and Wang, 2016). Throughout time, the lake profiles do not exhibit a distinct shift towards or away from the Cold Lake bitumen sample; however, Lakes L17, L14, and RL10, most closely resemble the composition of bitumen compared to the other study lakes. These findings indicate that petroleum biomarker composition in regional lake sediments is increasingly influenced by fossil fuel and combustion emission sources, suggesting that the implementation of oil sands infrastructure is contributing to PHC enrichment, but raw bitumen is not.

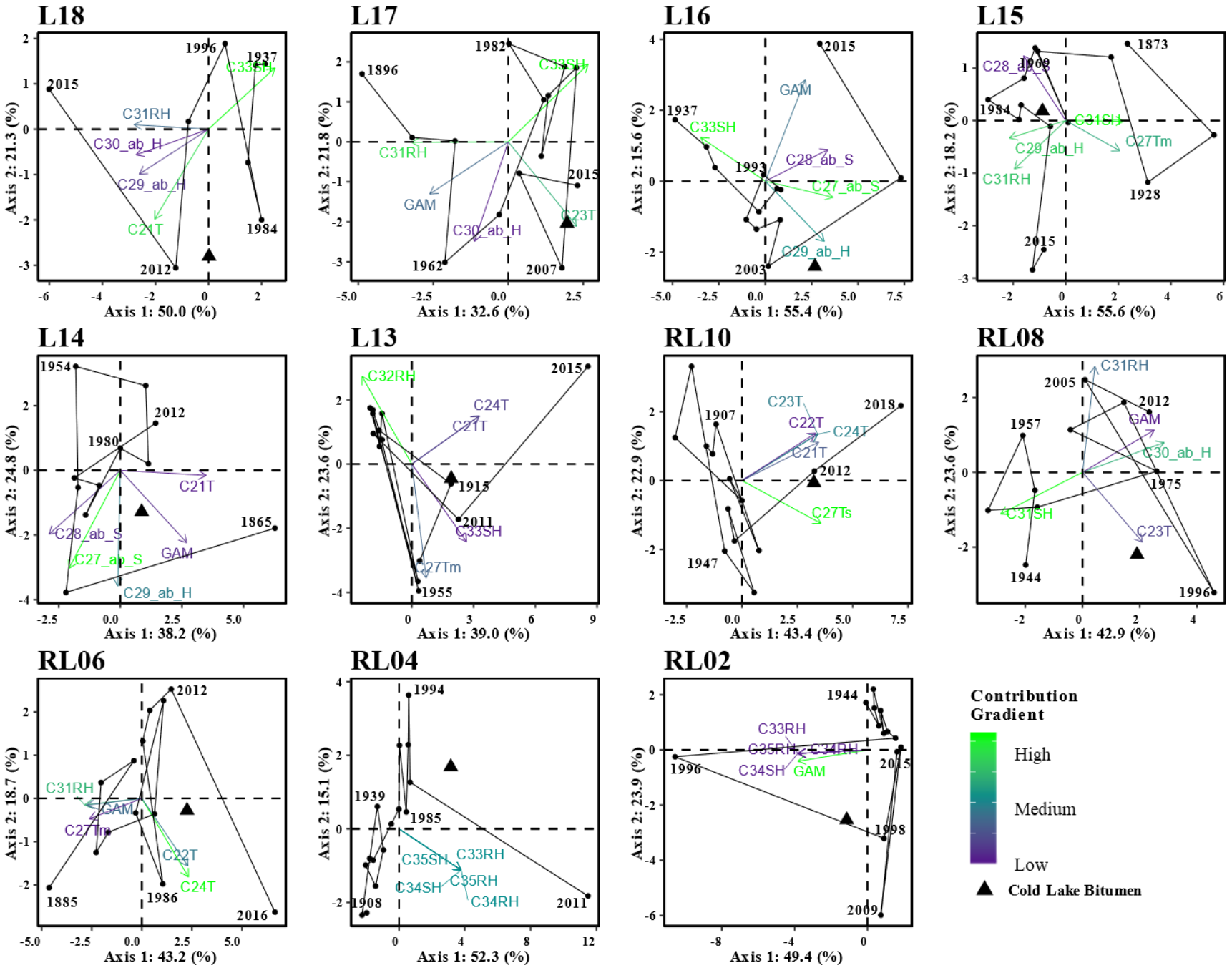

Figure 3- 4: Ordination biplots showing the changes in principal components along axes 1 & 2 scores throughout time for the relative abundance of petroleum biomarkers in lake sediment cores. Each lake profile depicts sample scores and the top 5 contributing biomarkers as the explanatory variables. Sediment intervals are connected in order of downcore chronologies (black sold line) with a Cold Lake bitumen sample (black triangle) plotted passively. The contribution gradient indicates the order of individual contribution to Axes 1:2 for each of the most abundant compounds.

3.3.2 n-Alkanes

Total *n*-alkane concentrations and accumulation rates in Lakes L15 and RL02 increased steadily at the onset of oil sands operations implying *in-situ* activities are driving these changes (Figure 3-5). We recorded a spike in L16 and L13 coinciding with oil sands development in the 1980s and 1990s; however, concentrations subsequently decreased, potentially a result of *n*-alkane enrichment from the implementation of the oil sands infrastructure that subsequently dropped once wells were constructed and operational.

We conducted an ANOVA to compare total *n*-alkane accumulation rates in sediments deposited before and after oil sands operations began and observed statistically higher accumulation rates (p-value < 0.001) in all lakes except RL04 which decreased in modern sediments (Figure 3-6). Oil sands operations around RL04 did not begin until 2007; therefore, too few data points are available to test the change in PHC composition since oil sands operations began near that lake. These trends suggest that in addition to abundant leaf waxes and plant residues commonly found in sediments, oil sands activity is a likely contributing to the *n*-alkanes composition in all lakes except RL04 (Ficken et al., 2000).

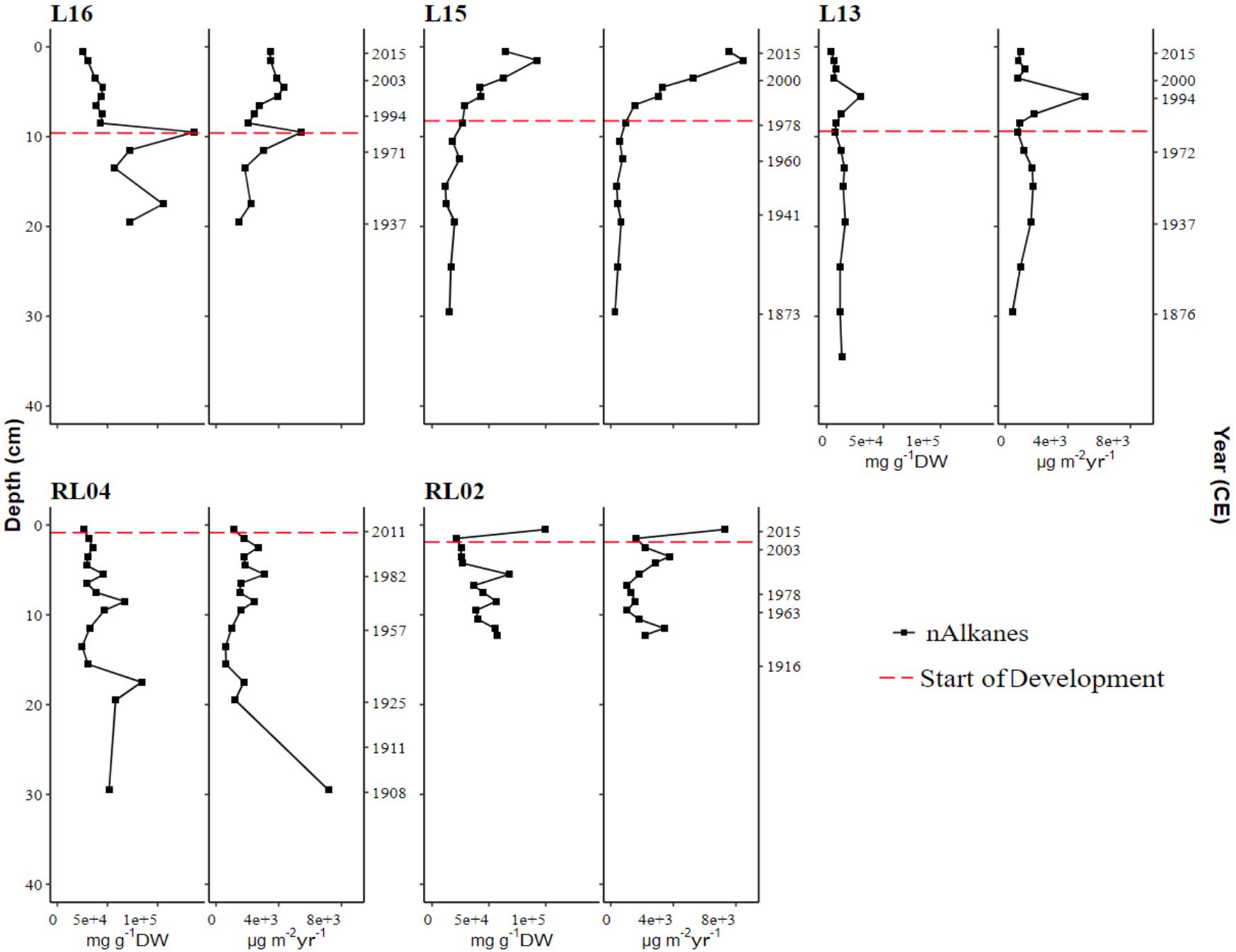

Figure 3- 5: Total *n*-alkane profiles as a function of depth. Scatter plots of the total concentration (mg g^{-1} DW) of the targeted *n*-alkanes with respect to sediment *n*-alkane flux (ug m^2 yr^{-1}) down core. All plots have the same Y axis, representing depth downcore in centimeters. Left plots for each lake depict the total concentration of *n*-alkanes corrected for dry weight. Plots to the right for each lake depict the accumulation rate of total *n*-alkanes (not calculated below the horizon of unsupported ^{210}Pb activity). The dashed red line corresponds to the year when oil sands operations began around each lake as determined by the CRS dating model.

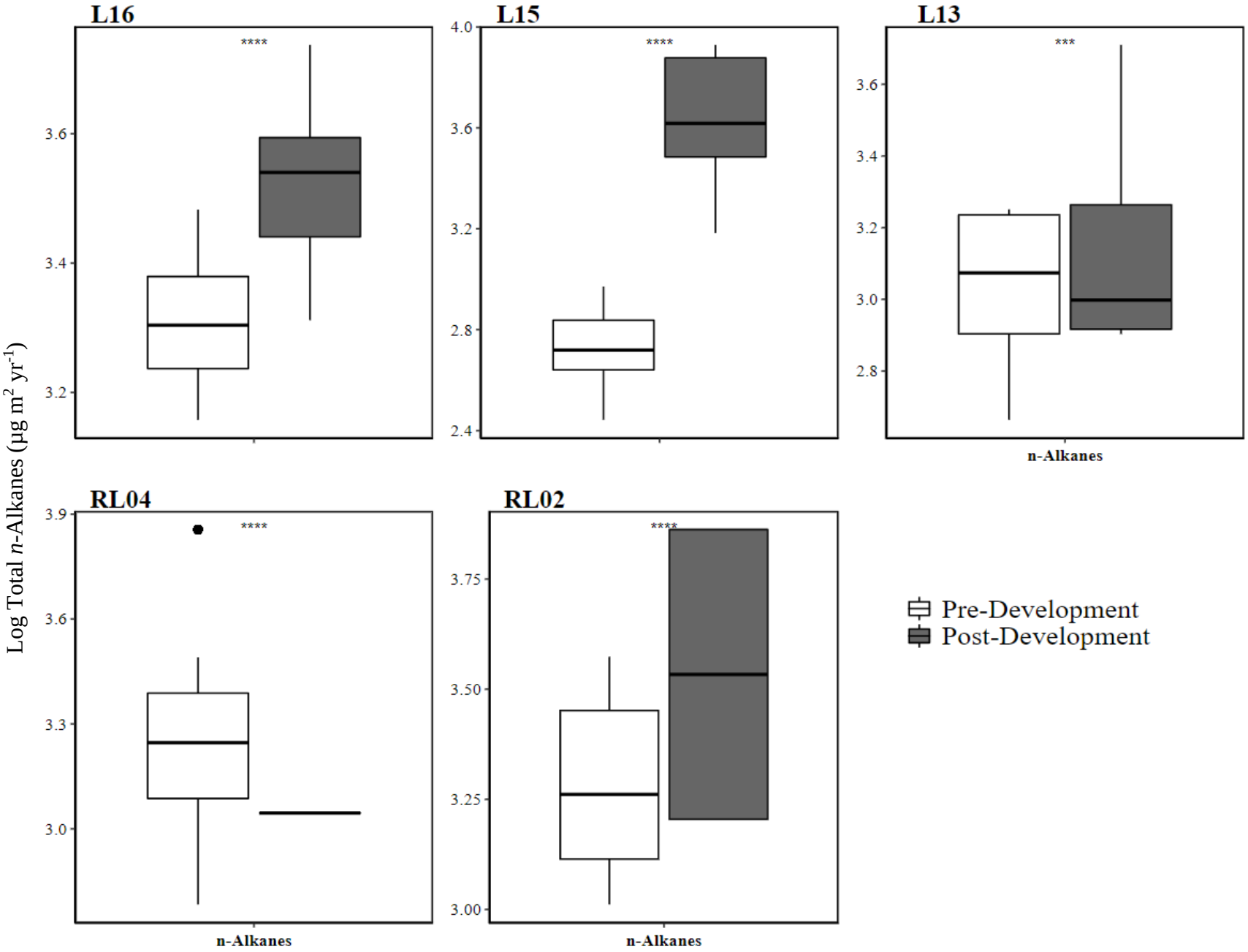

Figure 3- 6: Boxplots showing the change in log transformed total *n*-alkane accumulation rates (log µg m^2 yr^{-1}) between sediments deposited before and after oil sands operations began. (*p*-value < 0.05 (***), *p*-value < 0.001 (****)).

The carbon preference index indicated strong biogenic PHC origins when accounting for C_8-C_{40} and C_{23}-C_{34} *n*-alkanes (Figures 3-7 and S3-1). A CPI of ~1 shows a petrogenic *n*-alkane source whereas a CPI from 2-12 suggests biogenic origins, likely from aquatic and terrestrial plant biomass (Ahad et al., 2011; Zhendi Wang et al., 2009). RL04 exhibited the lowest CPI of 3.9 in 1950. The CPI in L16 peaked at 11 in 2003 and has since been decreasing in modern sediments to 5.1. Although *n*-alkane profiles in Figure 3-4 showed increasing concentrations and accumulation rates since the onset of oil sands activity in Lakes L15 and RL02, the CPI established that they were not from petroleum sources. The CPI in all lakes ranged from 3.9 to 11.4, indicating epicuticular leaf waxes as the dominant *n*-alkane source (Ahad et al., 2011).

C_8-C_{40} *n*-alkane distribution confirms biogenic origins as there is a strong odd-numbered carbon dominance in all sediment cores (Figure S3-22). The concentration of short-chained *n*-alkanes (C_{11} – C_{16}) in Lakes L16, L15, L13, RL04, and RL02 were near 0 whereas these are the dominant *n*-alkanes present in the CLB sample. Elevated C_{21} and C_{22} abundances characterize *n*-alkanes in petroleum sources. In all of the study lakes, we observed slight enrichment in C_{21} and phytane indicating an influence of diesel emissions (Miyake et al., 2005; Olajire et al., 2008). The spike in C_{17} recorded in all lakes is attributed to algae in the sediments, as C_{17} is a common algae biomarker (Fang et al., 2014; Ficken et al., 2000). C_{23}, C_{25}, C_{27} and C_{29} dominate the composition of *n*-alkanes in the study lakes in a bell-shaped distribution. This pattern of odd-numbered *n*-alkanes corroborated the findings of the CPI and suggested that higher plant matter and macrophytes are the dominant sources of *n*-alkanes to these lake basins (Fang et al., 2014). Similar distributions of C_{23} and C_{29} *n*-alkanes indicate both terrestrial and aquatic organic matter inputs (Ficken et al., 2000). Observations recorded during sample collection confirmed the presence of submerged aquatic macrophytes and terrestrial leaf litter in all 6 of the lake basins.

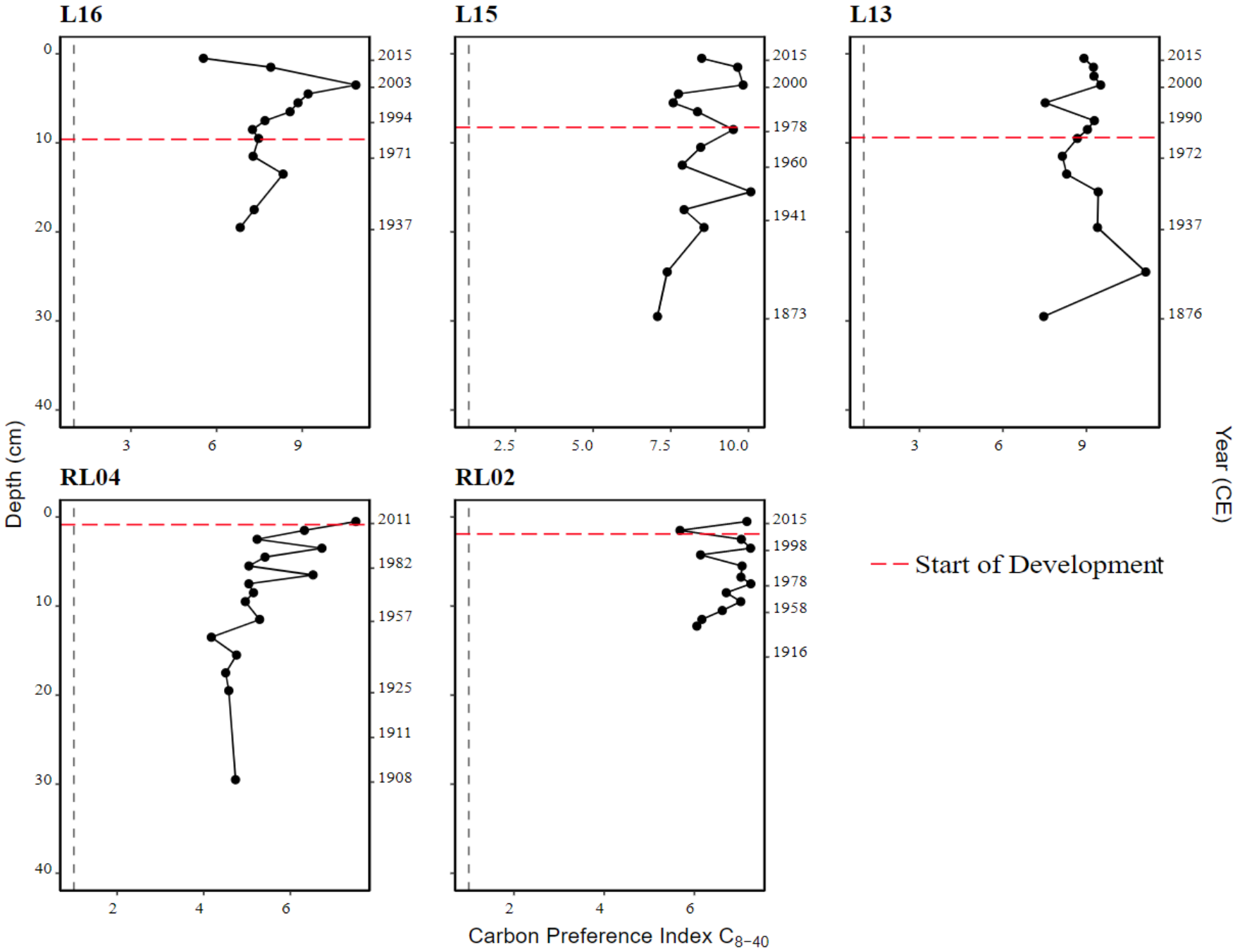

Figure 3- 7: Scatter plot profiles of the Carbon Preference Index (C_{8-40}) as a function of depth as per Wang et al. (1999). The vertical dashed line indicated a CPI of 1, at which point n-alkanes transition from petrogenic to biogenic in source. The dashed red line corresponds to the year when oil sands operations began near each lake.

Diagnostic ratios comparing heptadecane (C_{17}) to pristane commonly assess the relative contribution of petrogenic hydrocarbons in sediments (Ahad et al., 2011). C_{17} /pristane ratios ≤ 1 reflect petroleum contamination whereas ratios > 2 reflect significant contributions from algae. All 6 study lakes exhibited significantly elevated C_{17} /pristane ratios marking significant algal *n*-alkane influences (Figure S3-25) (Readman et al., 2002).

n-alkane principal component analyses using relative abundances explains 57.4% of the variance within axes 1 and 2 (Figure 3-8). Throughout the cores, the sediment *n*-alkane composition does not transition towards the Cold Lake bitumen, despite a distinct change in composition from the bottom to the top of the cores. Corroborating the findings of the CPI and diagnostic ratio analyses, the compounds explaining the highest proportion of variance in all lakes are the odd-numbered *n*-alkanes. These C_{25}-C_{31} *n*-alkanes are from epicuticular waxes in terrestrial plant debris. Lake L16 is unique as the C_{23}-C_{29} *n*-alkanes all point away from modern sediments and the Cold Lake bitumen sample. In late 1990s, the composition of L16 approaches that of the Cold Lake bitumen; however, distinctly transitions away in 2003. Modern sediments in all lakes do not resemble the composition of a Cold Lake bitumen sample and are transitioning to be less similar in composition. Algal biomass in lake L15 outweighs the contribution of terrestrial *n*-alkanes, likely due to L15 being the largest and deepest lake. Short chained, even-numbered *n*-alkanes are a result of thermal degradation of biomass during a fire, causing long-chain hydrocarbons to be reduced (Eckmeier and Wiesenberg, 2009). C_{16} *n*-alkanes explain the most variance in L15, directionally towards the top of the core, indicating forest fires are playing an increasing role in PHC deposition. These findings indicate that petrogenic inputs are not resulting in compositional changes in *n*-alkanes throughout time, potentially as a result of petroleum indicators having been degraded or diluted by the abundance of biogenic *n*-alkanes in the sediments (Stout and Wang, 2016).

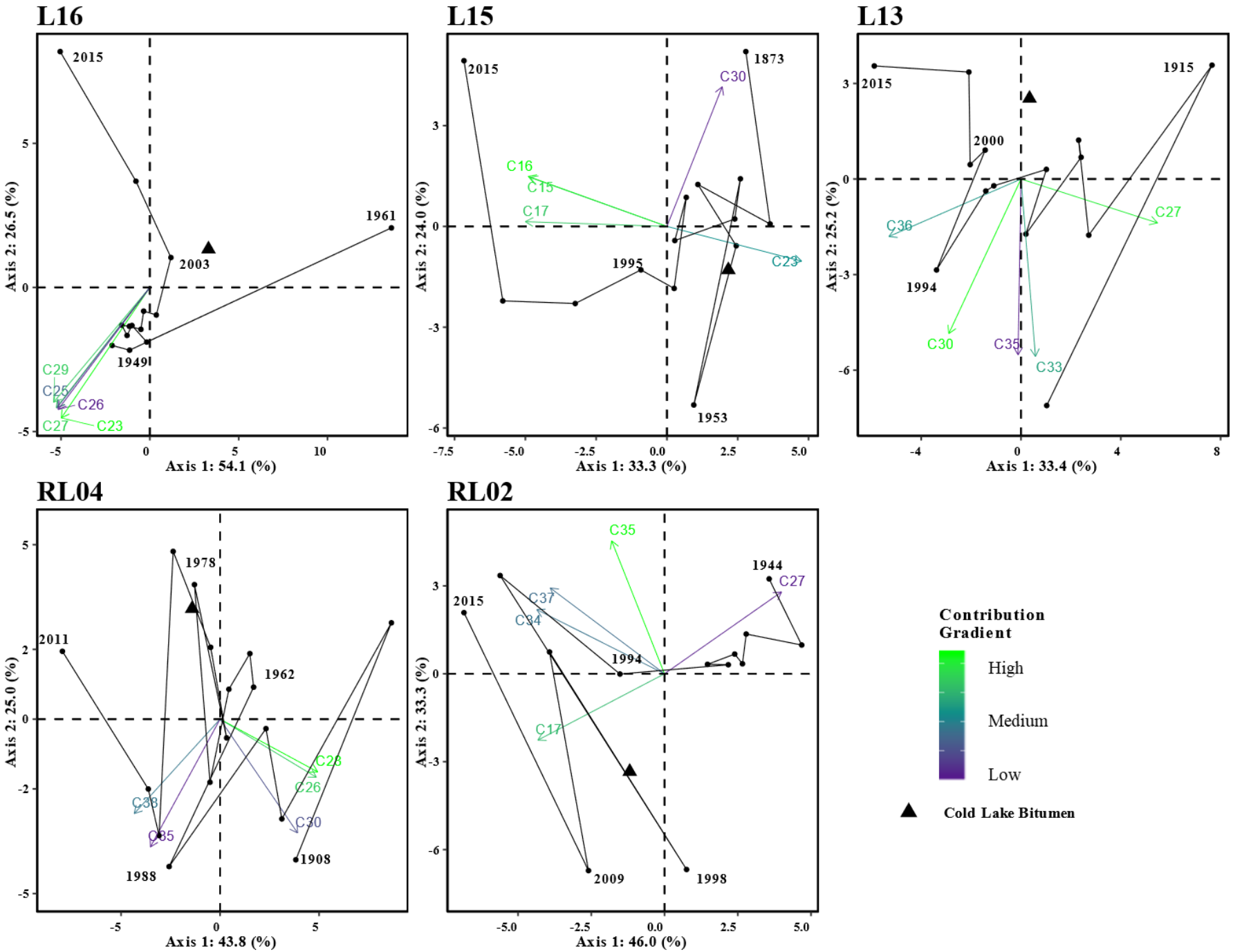

Figure 3- 8: Ordination biplots showing the changes in principal components along axes 1 & 2 scores throughout time for the relative abundance of *n*-alkanes in lake sediment cores. Each lake profile depicts sample scores and the top 5 contributing *n*-alkanes as the explanatory variables. Sediment intervals are connected in order of downcore chronologies (black sold line) with a Cold Lake bitumen sample (black triangle) plotted passively. The contribution gradient indicates the order of individual contribution to Axes 1:2 for each of the most abundant compounds.

3.4 Conclusions

This study is the first to analyze petroleum biomarkers and *n*-alkanes in the Cold Lake oil sands region. Total *n*-alkane and total biomarker profiles exhibited significant increases in PHC accumulation rates following the onset of oil sands activity, similar to that observed in polycyclic aromatic compound profiles. Diagnostic ratios, carbon preference indices, and principal component analyses allowed us to chemically fingerprint *n*-alkane and biomarker composition in lake sediments to determine PHC sources.

n-alkanes exhibited a strong odd-numbered carbon-chain preference, indicating strongly biogenic origins. The CPI and diagnostic ratios corroborated these findings, establishing that C_{17} algal *n*-alkanes and C_{23}, C_{25}, C_{27} and C_{29} *n*-alkanes indicate higher plant matter and macrophytes dominate these lake systems. Prevalence of short-chained, even-numbered *n*-alkanes from thermal degradation of biomass during combustion indicated inputs from forest fires, vehicle emissions and fossil fuel combustion.

Petroleum biomarkers are more reliable for chemical fingerprinting as they are resistant to weathering and chemical alteration. Low abundances of steranes and the absence of $C_{33\text{-}35}$ hopanes suggest that biomarker origins are not bitumen derived. The depletion of steranes and longer chained hopanes recorded in lake sediments implies that petrogenic hopenoids are from aerosol deposition from fossil fuel combustion emissions such as traffic exhaust / natural gas combustion. These findings indicate that petroleum biomarker composition in regional lake sediments is increasingly influenced by fossil fuel and combustion emission sources, suggesting that the implementation of oil sands infrastructure is contributing to PHC enrichment, but raw bitumen is not.

This study confirms that bitumen is confined to the deposits situated deep below the surface as we record no evidence to support natural bitumen introduced to the environment. As the Cold Lake region is susceptible to non-target bitumen seeps, it would be beneficial to use petroleum hydrocarbon fingerprinting to identify petroleum source origins in the event of future FTS events. Additionally, this method can be applied to future studies to observe whether unreported FTS events have impacted other lakes both in the Cold Lake oil sands region and in other *in-situ* areas.

Chapter 3: Supplementary Information

Table S3- 1: List of petroleum biomarkers analyzed in this study, including abbreviations used in the text and target ions for GC-MS.

Name	Code	Target Ion
Terpanes		
C_{21} terpane	C_{21} T	191
C_{22} terpane	C_{22} T	191
C_{23} terpane	C_{23} T	191
C_{24} terpane	C_{24} T	191
Hopanes		
C_{27} 18A-hopane II (Ts)	C_{27} Ts	191
C_{27} 17A-hopane (Tm)	C_{27}Tm	191
C_{29} αβ hopane	C_{29} αβ H	191
C_{30} αβ hopane	C_{30} αβ H	191
C_{31} (R) hopane	C_{31} (R) H	191
C_{31} (S) hopane	C_{31} (S) H	191
C_{32} (R) hopane	C_{32} (R) H	191
C_{32} (S) hopane	C_{32} (S) H	191
C_{33} (R) hopane	C_{33} (R) H	191
C_{33} (S) hopane	C_{33} (S) H	191
C_{34} (R) hopane	C_{34} (R) H	191
C_{34} (S) hopane	C_{34} (S) H	191
C_{35} (R) hopane	C_{35} (R) H	191
C_{35} (S) hopane	C_{35} (S) H	191
Gammacerane	GAM	191
Steranes		
C_{27} αββ sterane	C_{27} αββ S	218
C_{28} αββ sterane	C_{28} αββ S	218
C_{29} αββ sterane	C_{29} αββ S	218

Table S3- 2: List of *n*-alkanes analyzed in this study, including abbreviations used in the text and target ions for GC-MS

Name	Code	Target Ion
C_{11}	C_{11}	57.05
C_{12}	C_{12}	57.05
C_{13}	C_{13}	57.05
C_{14}	C_{14}	57.05
C_{15}	C_{15}	57.05
C_{16}	C_{16}	57.05
C_{17}	C_{17}	57.05
Pristane	Pristane	57.05
Phytane	Phytane	57.05
C_{19}	C_{19}	57.05
C_{20}	C_{20}	57.05
C_{21}	C_{21}	57.05
C_{22}	C_{22}	57.05
C_{23}	C_{23}	57.05
C_{24}	C_{24}	57.05
C_{25}	C_{25}	57.05
C_{26}	C_{26}	57.05
C_{27}	C_{27}	57.05
C_{28}	C_{28}	57.05
C_{29}	C_{29}	57.05
C_{30}	C_{30}	57.05
C_{31}	C_{31}	57.05
C_{32}	C_{32}	57.05
C_{33}	C_{33}	57.05
C_{34}	C_{34}	57.05
C_{35}	C_{35}	57.05
C_{36}	C_{36}	57.05
C_{37}	C_{37}	57.05
C_{38}	C_{38}	57.05
C_{39}	C_{39}	57.05
C_{40}	C_{40}	57.05

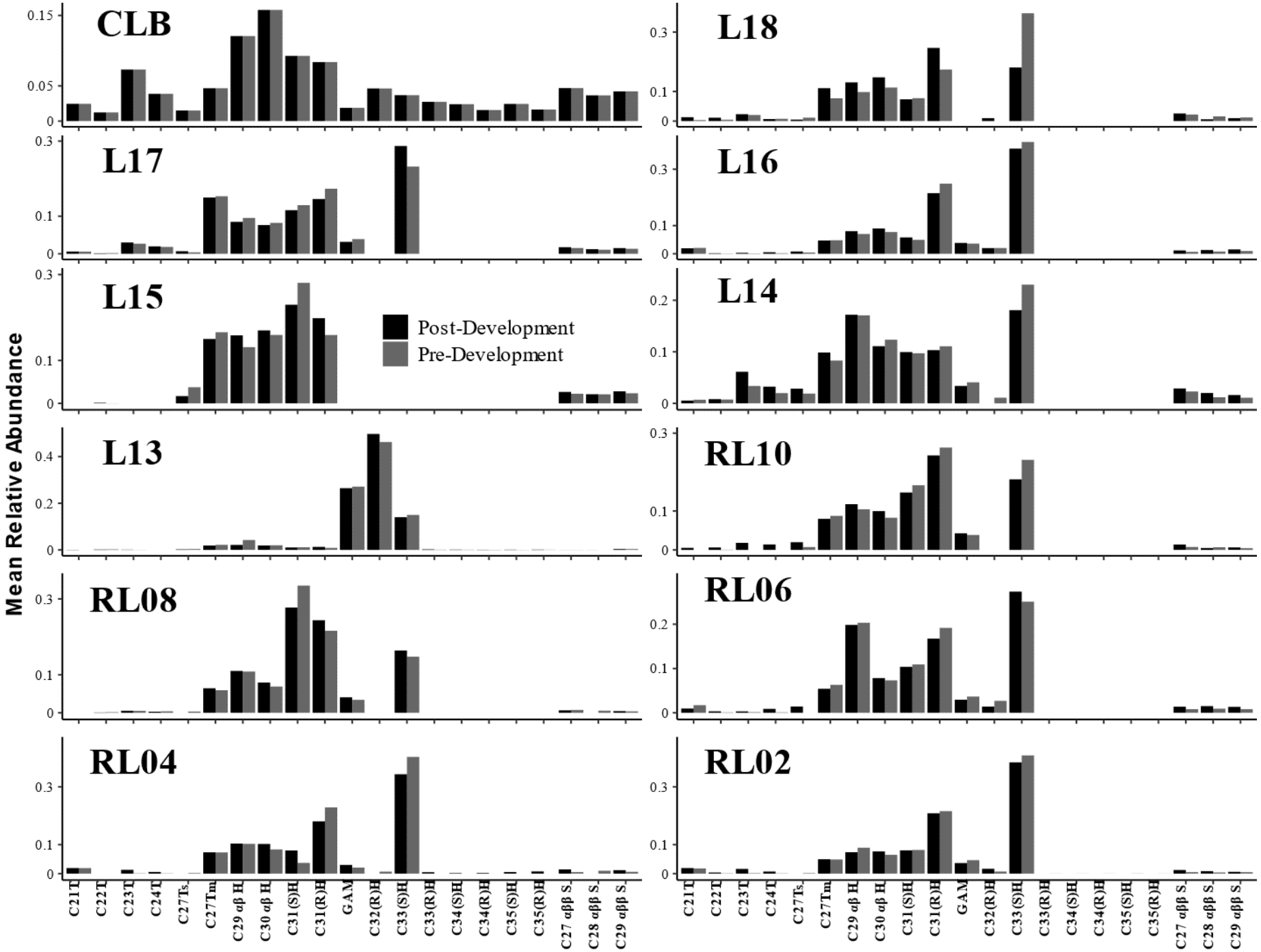

Figure S3- 1: Bar graphs of the mean relative abundance distribution of all petroleum biomarkers when compared to a Cold Lake bitumen sample (CLB). All mean biomarker abundances are categorized based on the time in which they were deposited Pre- (Grey) and Post- (Black) oil sands development. CLB sample is irrespective of pre/post conditions.

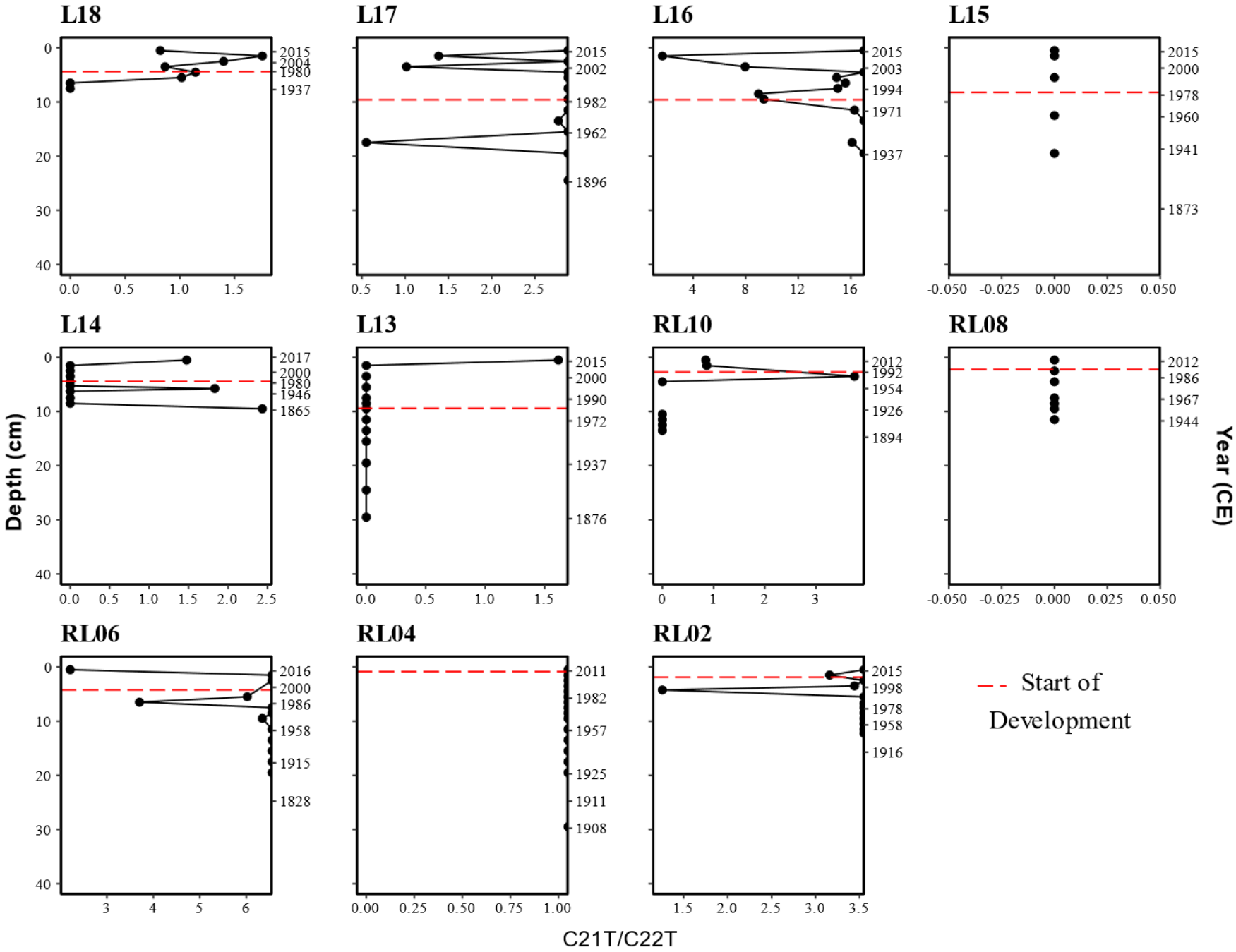

Figure S3- 2: Scatter plots of the C_{21} T / C_{22} T diagnostic ratio as a function of depth. The dashed red line corresponds to the year when oil sands developments began near each lake.

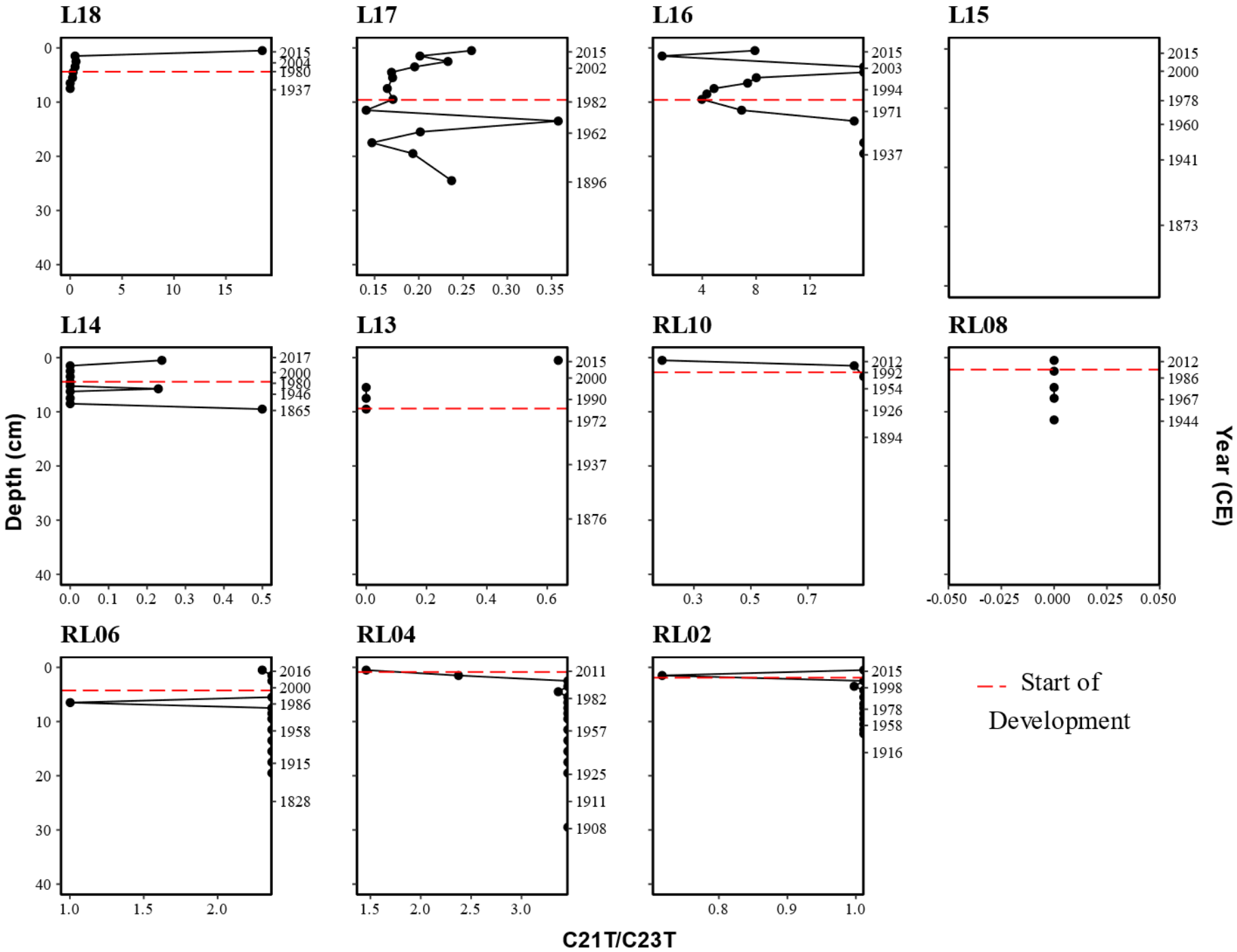

Figure S3- 3: Scatter plots of the C_{21} T / C_{23} T diagnostic ratio as a function of depth. The dashed red line corresponds to the year when oil sands developments began near each lake. Blank plots represent lakes where no C_{21} nor C_{23} terpanes were present.

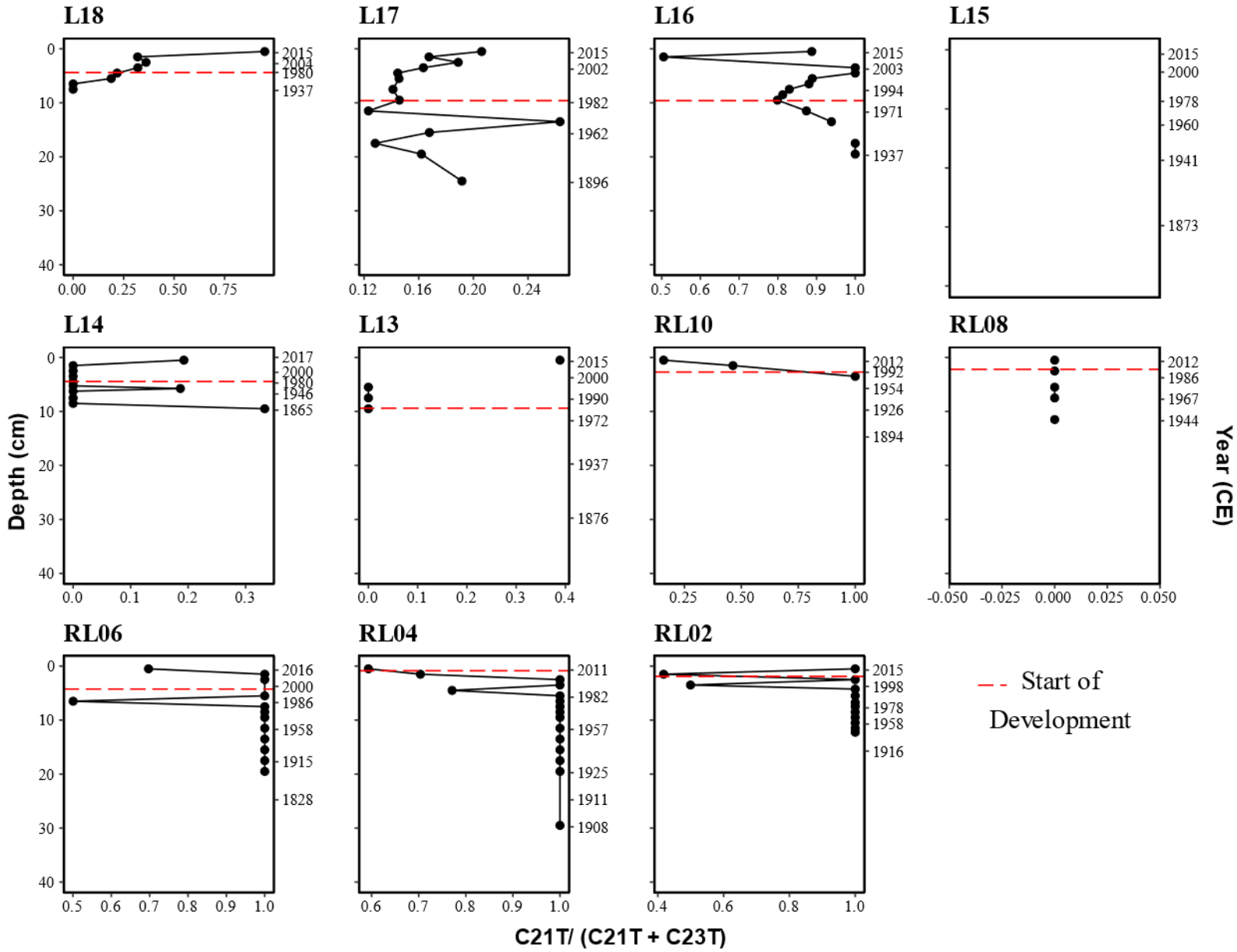

Figure S3- 4: Scatter plots of the C_{21} T / C_{21+23} T diagnostic ratio as a function of depth. The dashed red line corresponds to the year when oil sands developments began near each lake. Blank plots represent lakes where no C_{21} nor C_{23} terpanes were present.

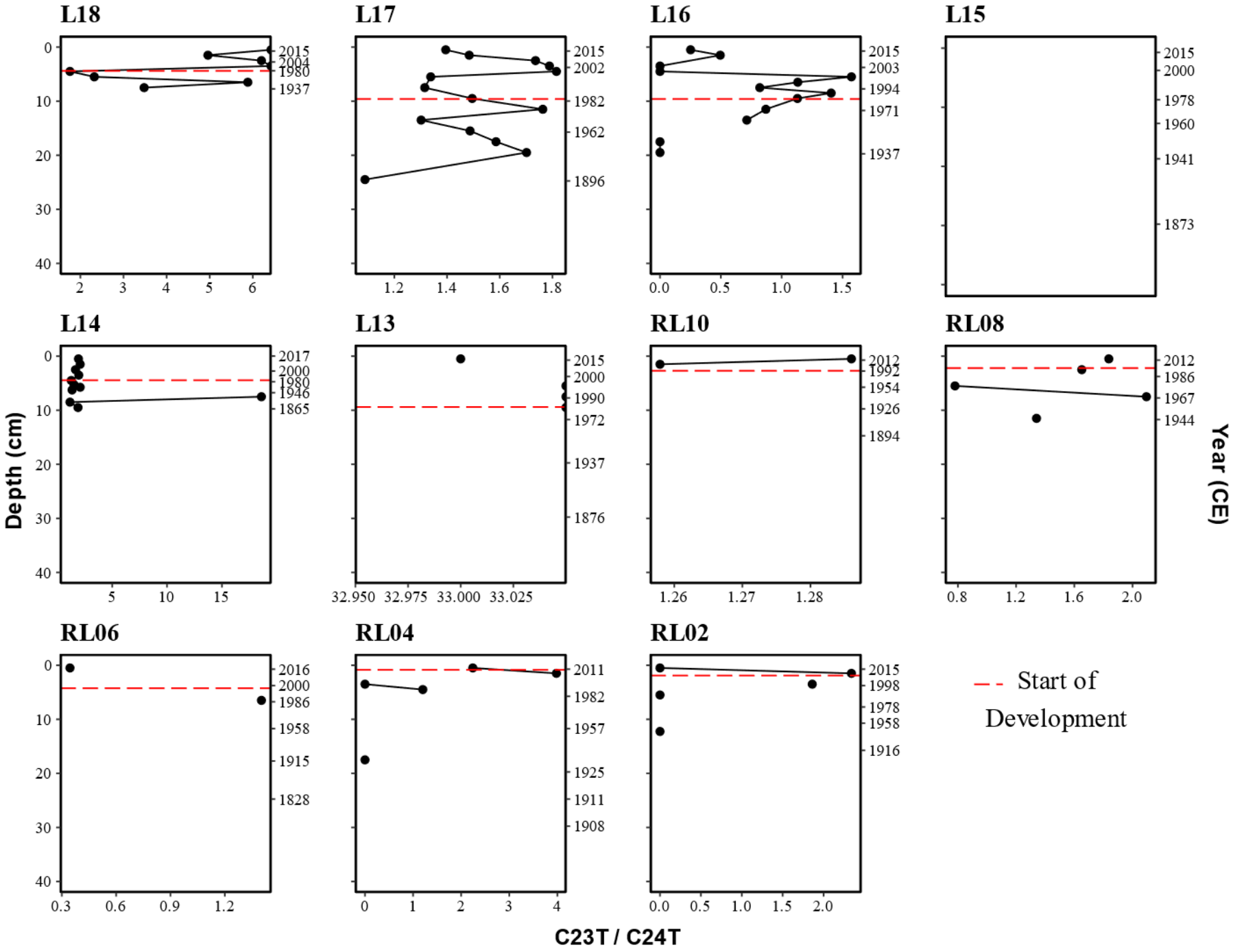

Figure S3- 5: Scatter plots of the C_{23} T / C_{24} T diagnostic ratio as a function of depth. Diagnostic ratios of 1.9 are indicative of an Alberta bitumen source (Yang et al., 2011). The dashed red line corresponds to the year when oil sands developments began near each lake. Blank plots represent lakes where no C_{23} nor C_{24} terpanes were present.

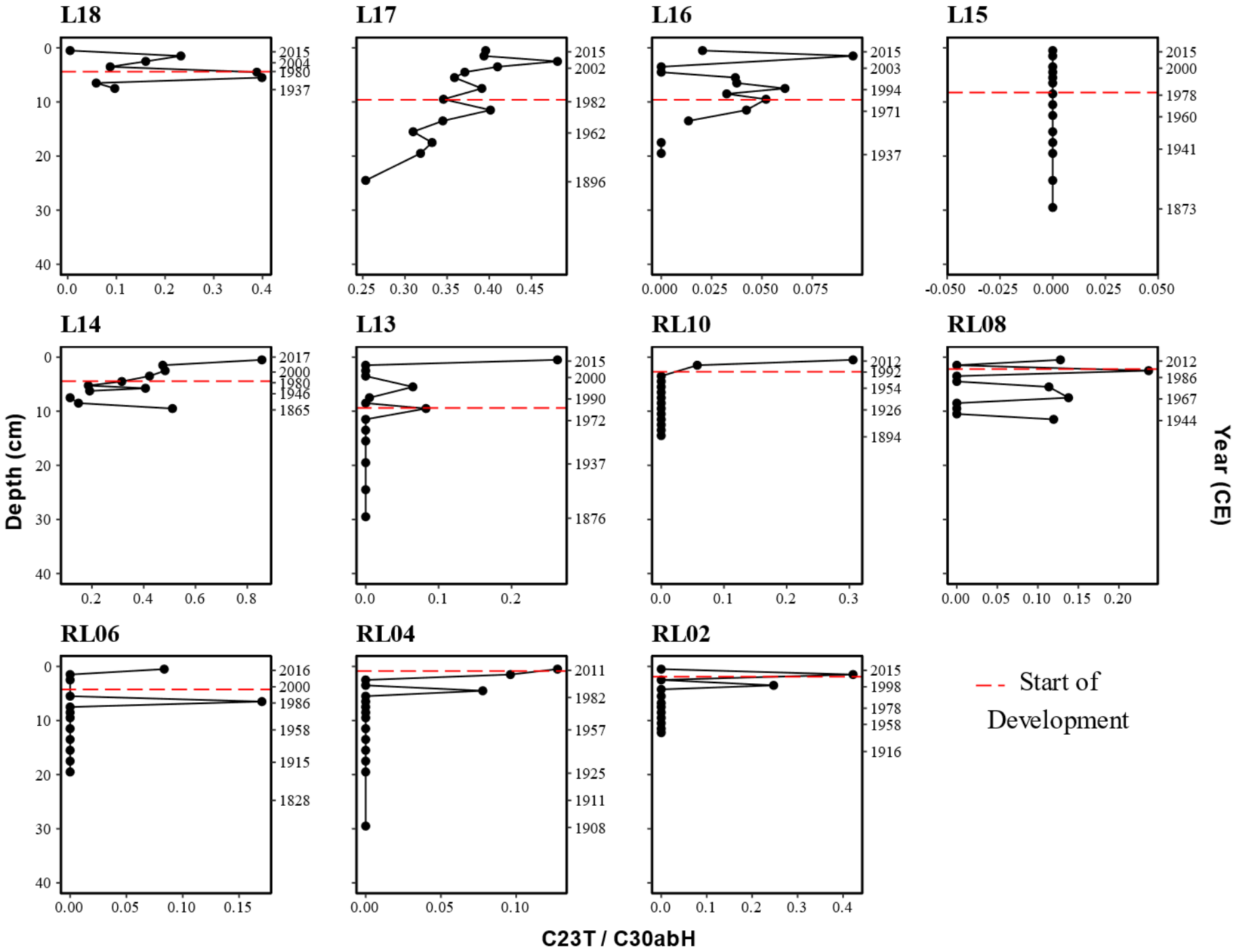

Figure S3- 6: Scatter plots of the C_{23} T / C_{30} αβ H T diagnostic ratio as a function of depth. Diagnostic ratios of 0.41 are indicative of an Alberta bitumen source (Yang et al., 2011). The dashed red line corresponds to the year when oil sands developments began near each lake.

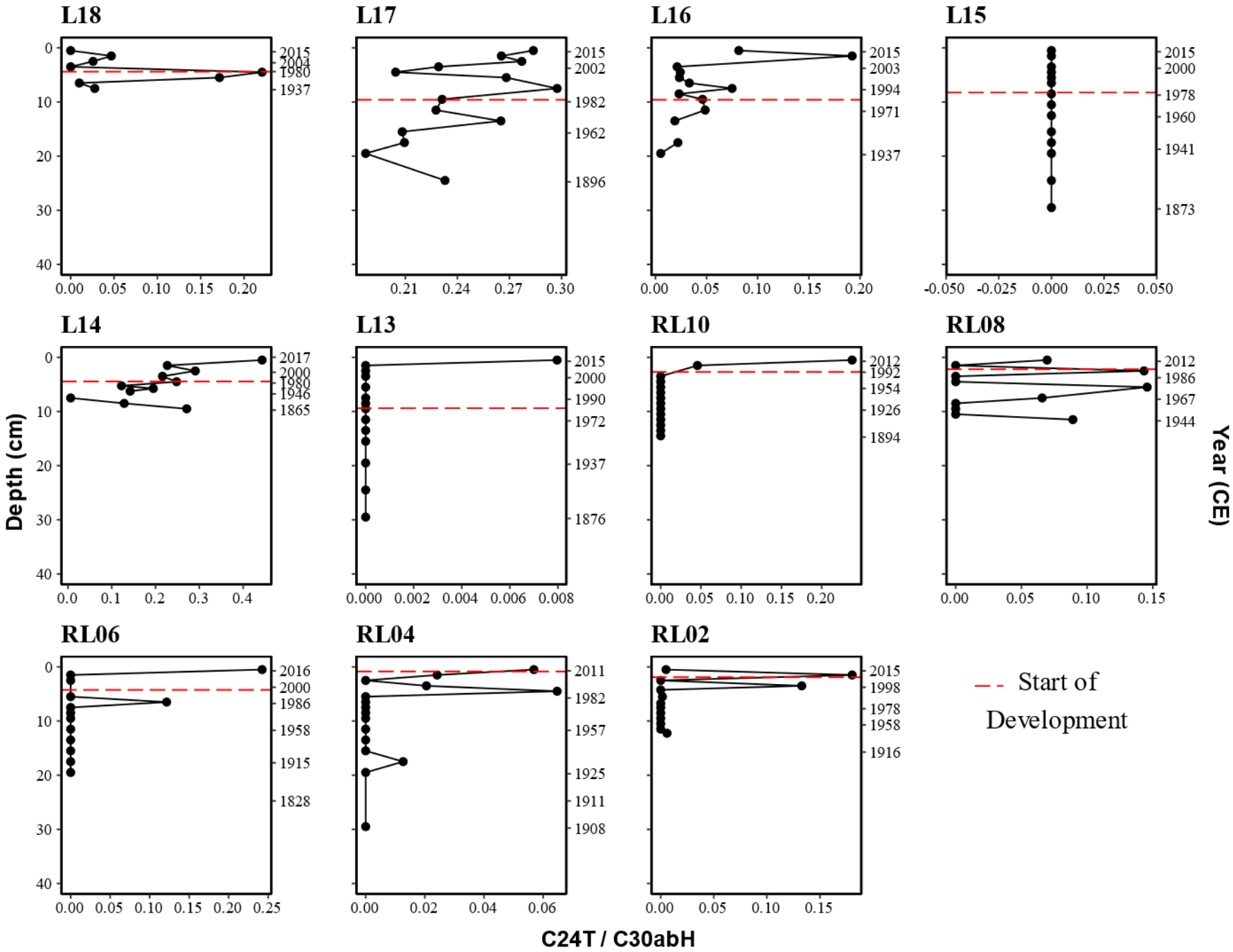

Figure S3- 7: Scatter plots of the C_{24} T / C_{30} αβ H T diagnostic ratio as a function of depth. Diagnostic ratios of 0.22 are indicative of an Alberta bitumen source (Yang et al., 2011). The dashed red line corresponds to the year when oil sands developments began near each lake.

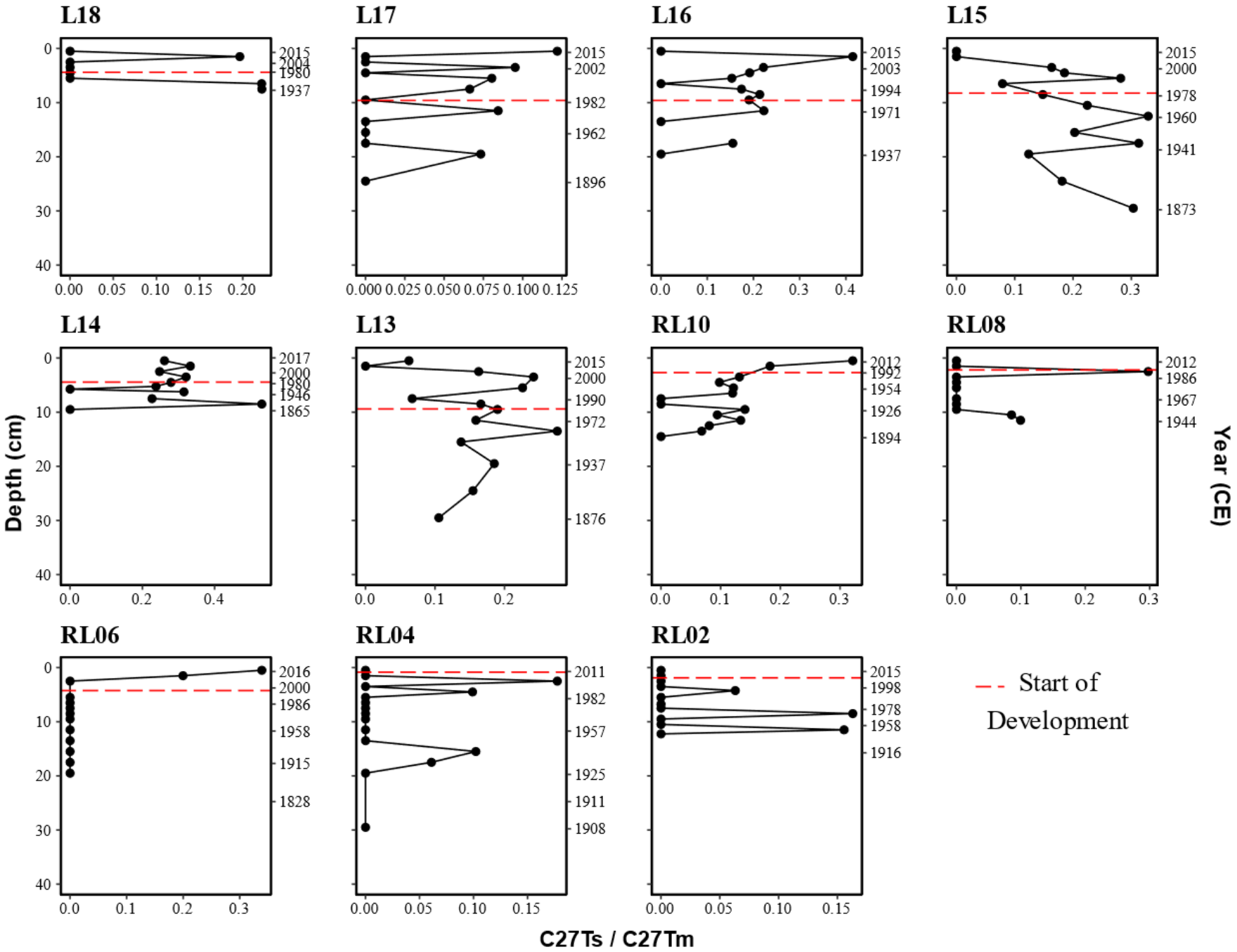

Figure S3- 8: Scatter plots of the C_{27} Ts / C_{27} Tm diagnostic ratio as a function of depth. Diagnostic ratios of 0.29 are indicative of an Alberta bitumen source (Yang et al., 2011). The dashed red line corresponds to the year when oil sands developments began near each lake**.**

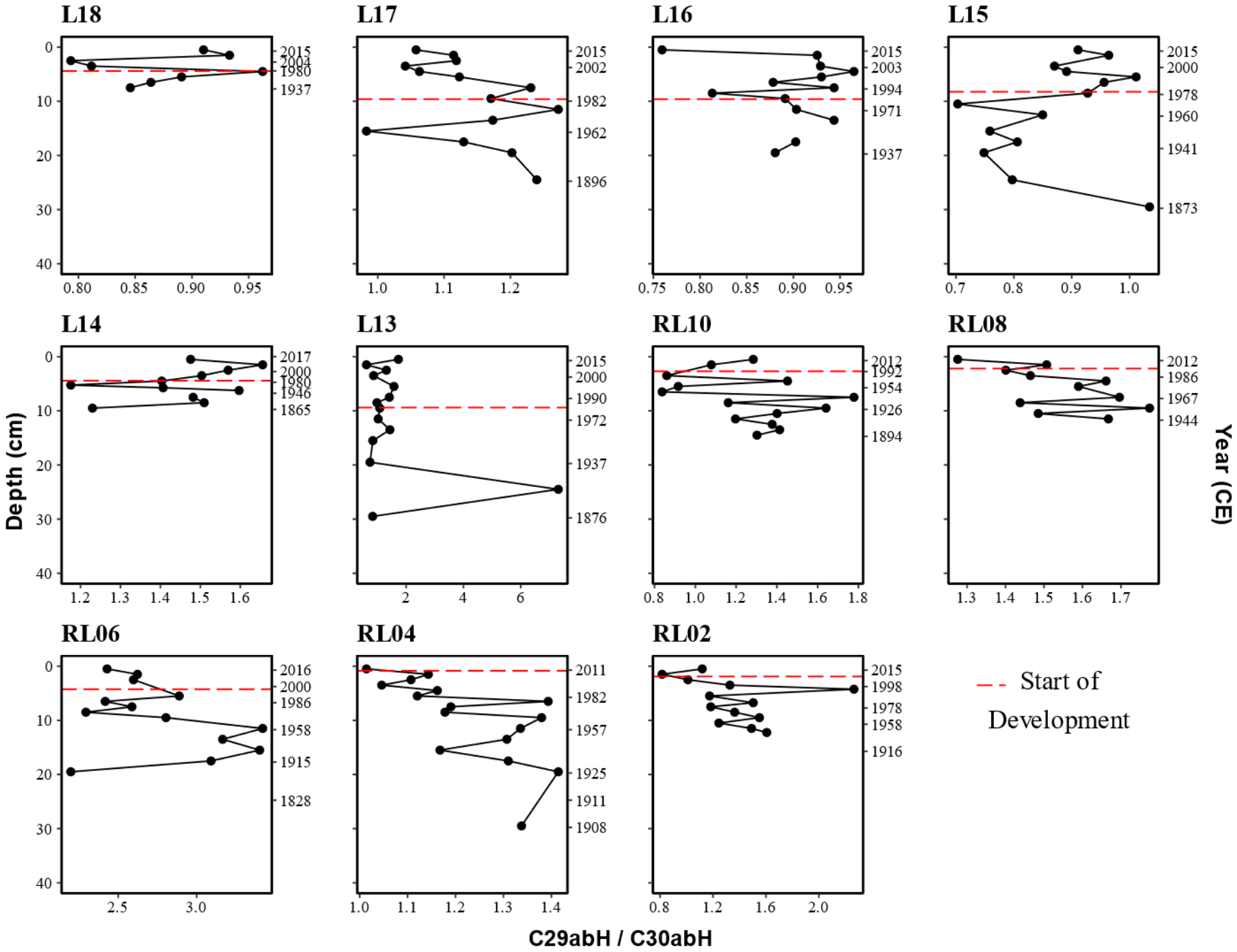

Figure S3- 9: Scatter plots of the C_{29} αβ H / C_{30} αβ H diagnostic ratio as a function of depth. Diagnostic ratios of 0.85 are indicative of an Alberta bitumen source (Yang et al., 2011). The dashed red line corresponds to the year when oil sands developments began near each lake.

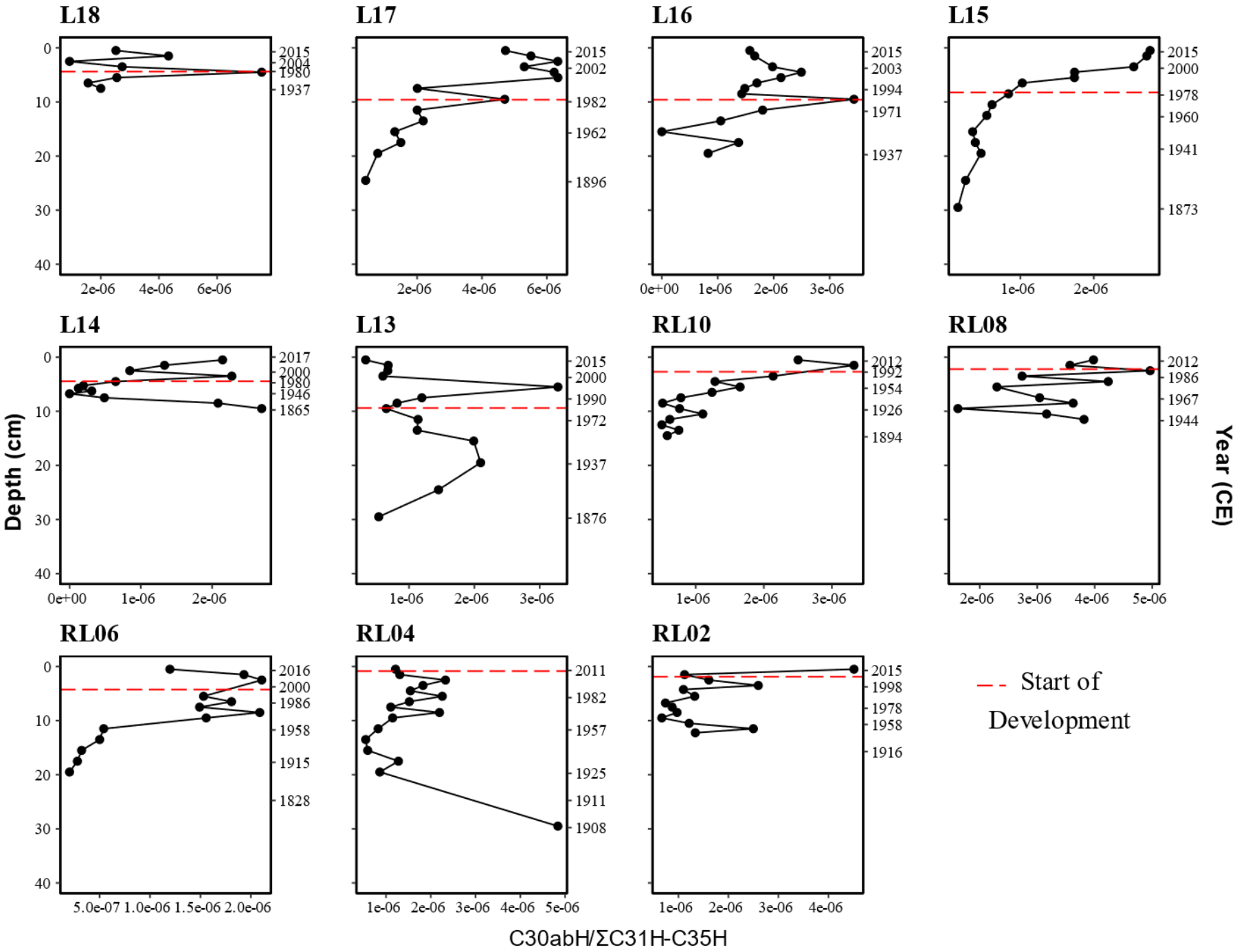

Figure S3- 10: Scatter plots of the C_{30} αβ H / $\Sigma C_{31\text{-}35}$ (S+R) H diagnostic ratio as a function of depth. Diagnostic ratios of 0.45 are indicative of an Alberta bitumen source (Yang et al., 2011). The dashed red line corresponds to the year when oil sands developments began near each lake.

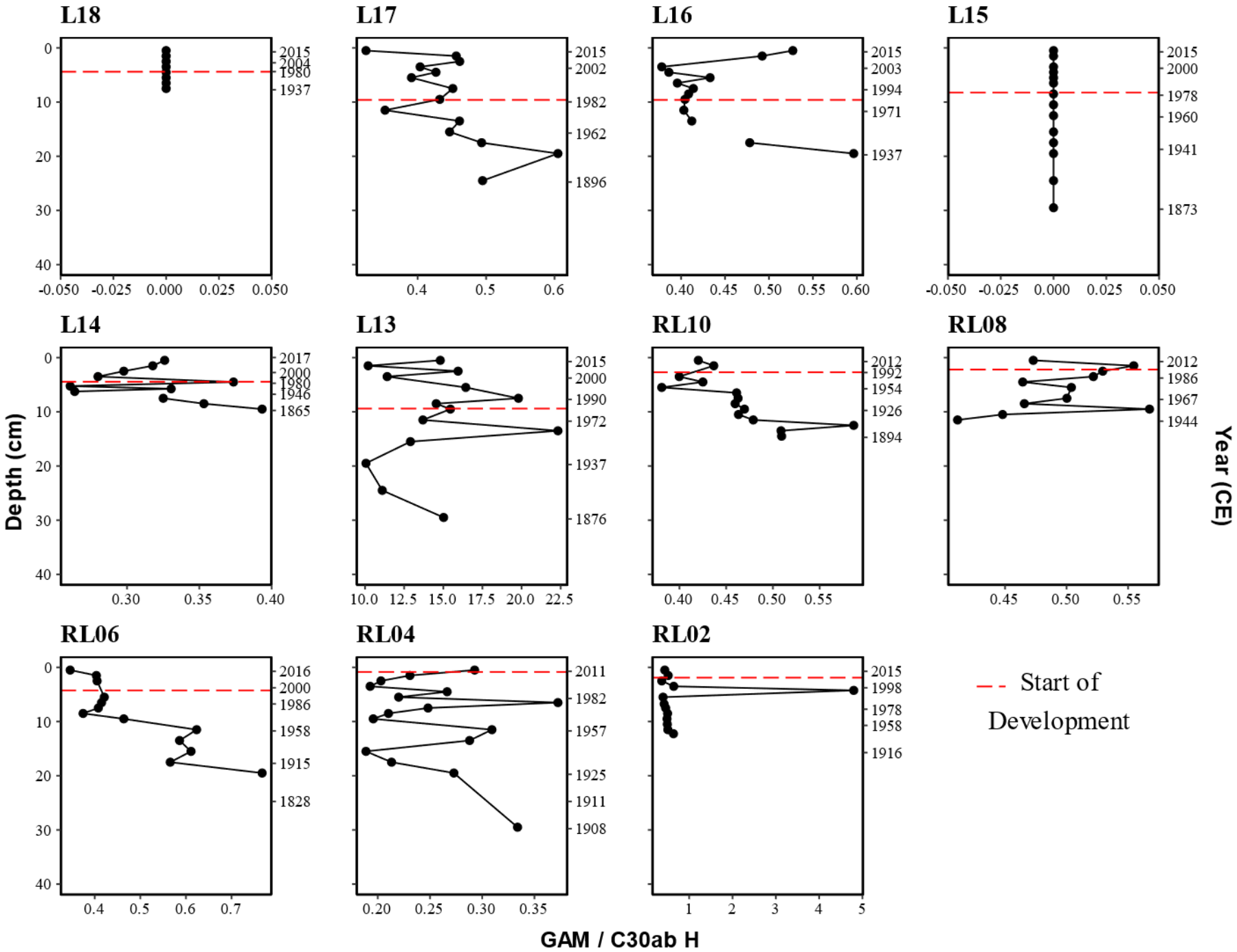

Figure S3- 11: Scatter plots of the Gammacerane /C_{30} αβ H diagnostic ratio as a function of depth. The dashed red line corresponds to the year when oil sands developments began near each lake.

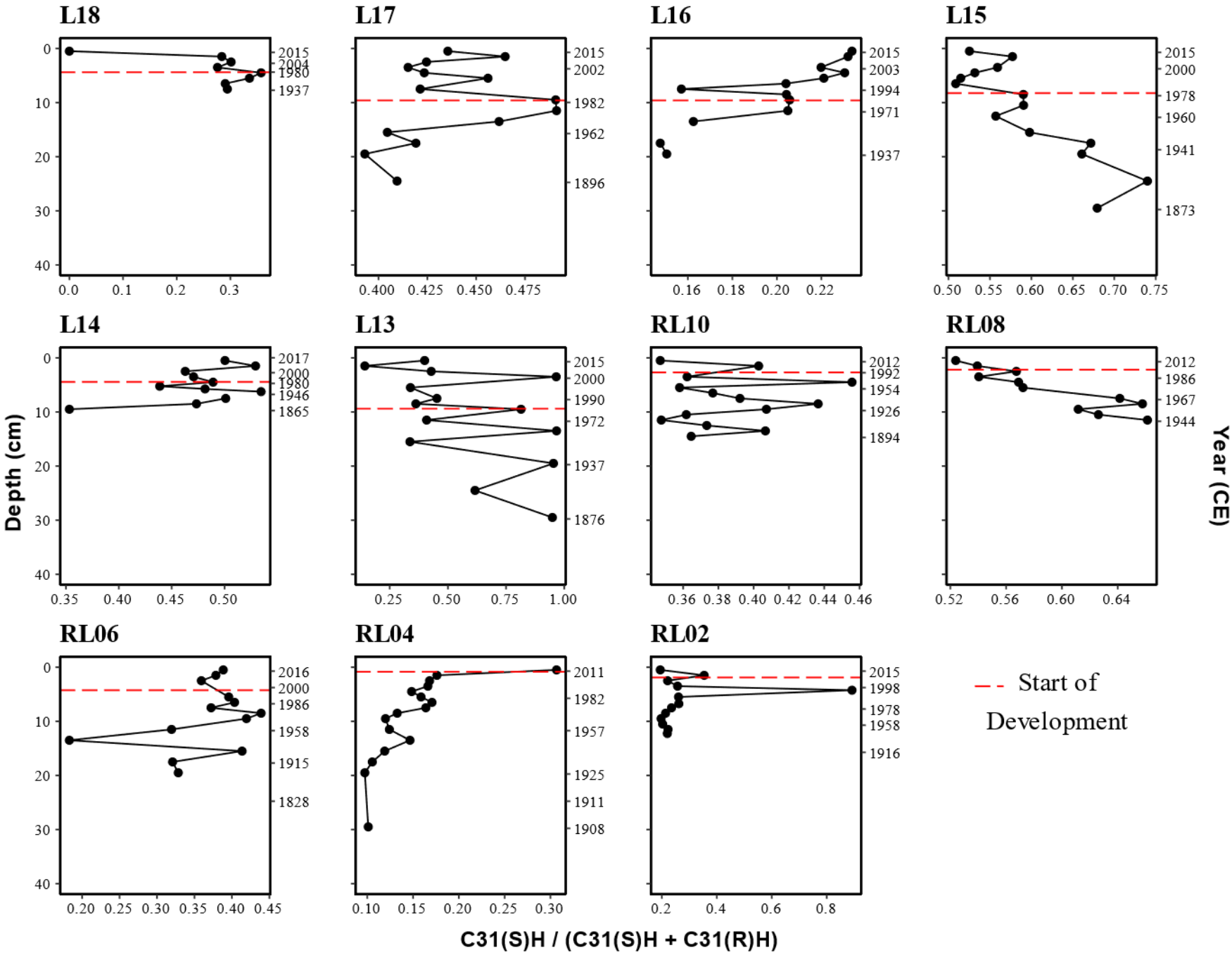

Figure S3- 12: Scatter plots of the C_{31} (S) H / C_{31} (S+R) H diagnostic ratio as a function of depth. The dashed red line corresponds to the year when oil sands developments began near each lake.

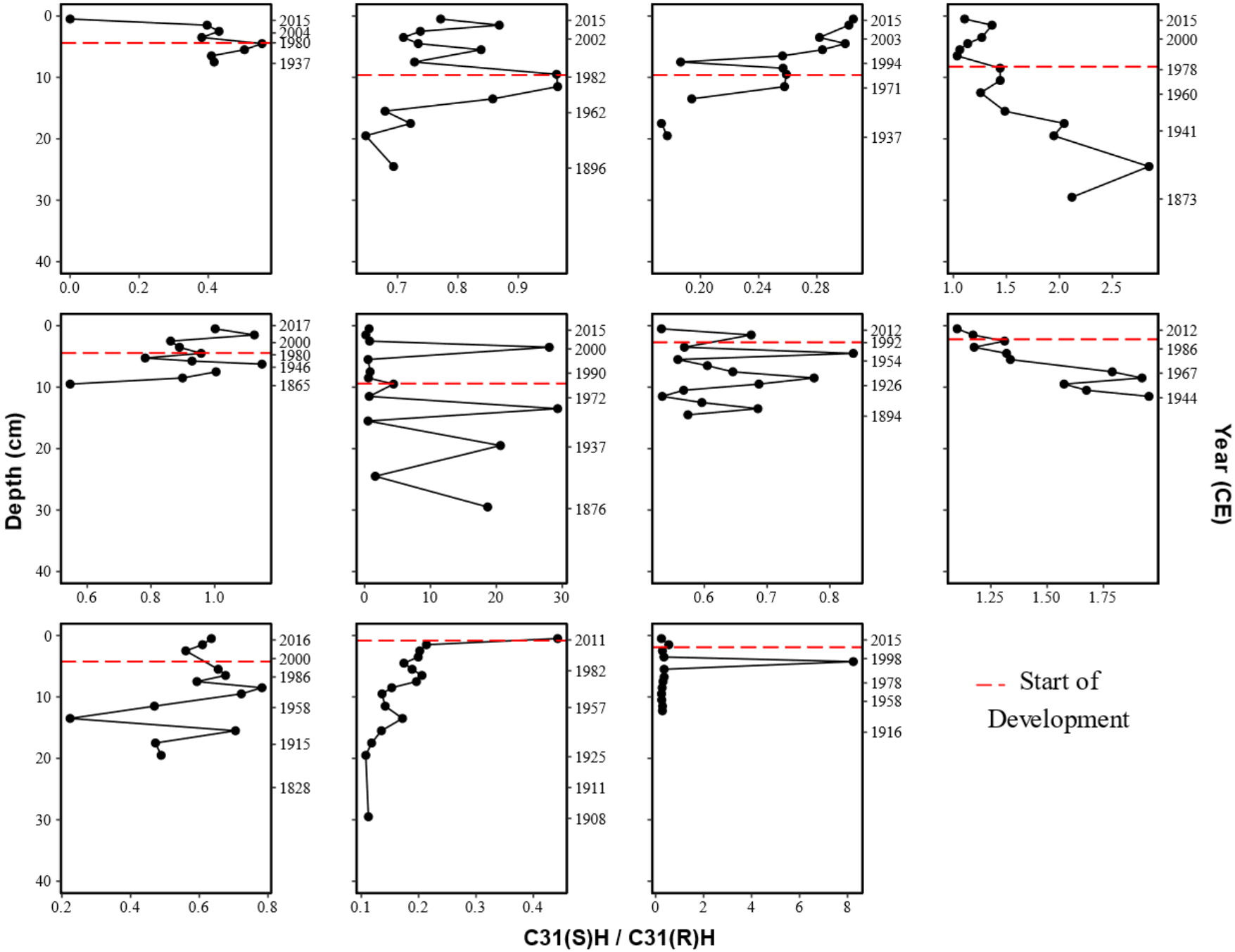

Figure S3- 13: Scatter plots of the C_{31} (S) H / C_{31} (R) H diagnostic ratio as a function of depth. Diagnostic ratios of 1.37 are indicative of an Alberta bitumen source (Yang et al., 2011). The dashed red line corresponds to the year when oil sands developments began near each lake.

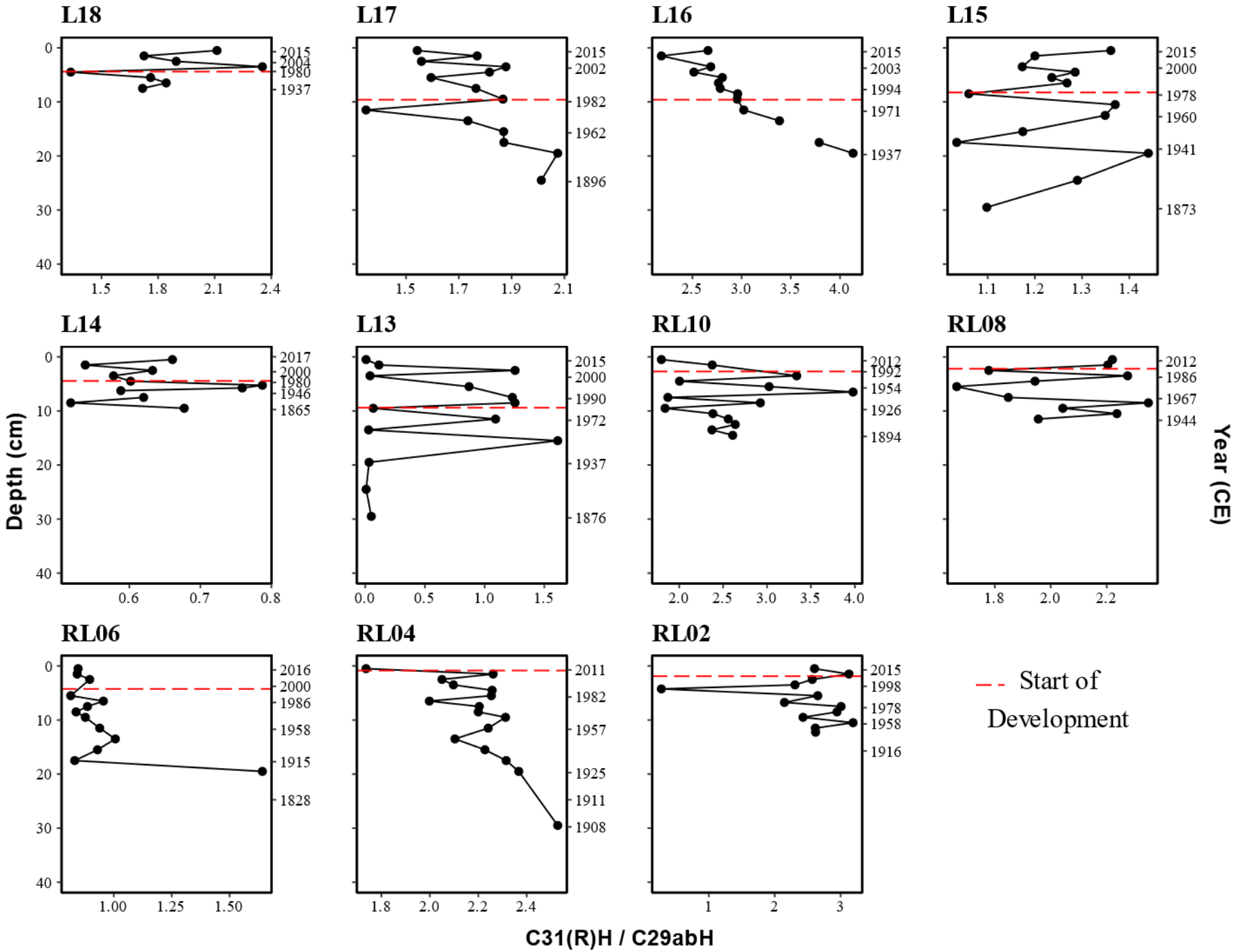

Figure S3- 14: Scatter plots of the C_{31} (R) H / C_{29} αβ H diagnostic ratio as a function of depth. The dashed red line corresponds to the year when oil sands developments began near each lake.

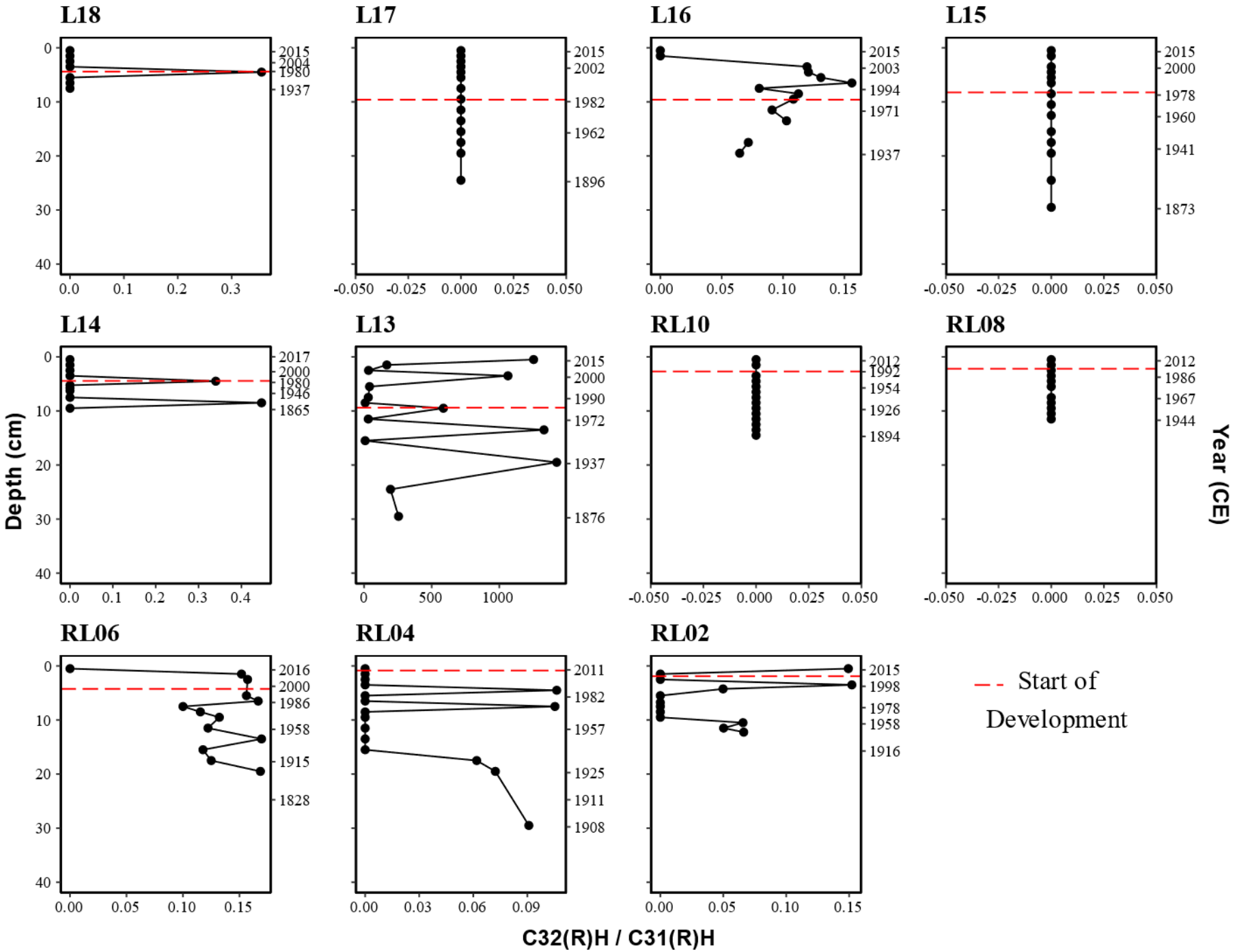

Figure S3- 15: Scatter plots of the C_{32} (R) H / C_{31}(R) H diagnostic ratio as a function of depth. The dashed red line corresponds to the year when oil sands developments began near each lake.

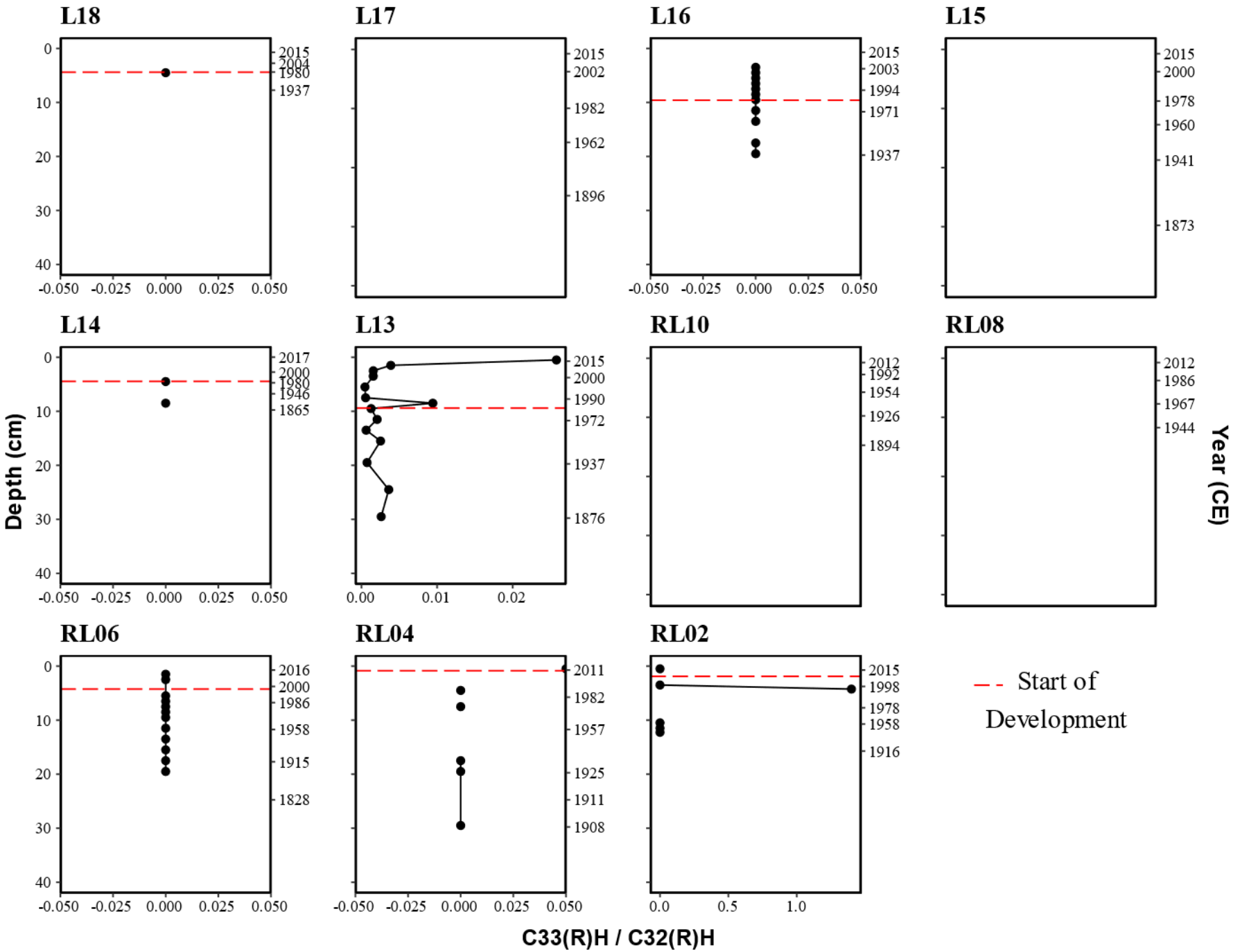

Figure S3- 16: Scatter plots of the C_{33} (R) H / C_{32} (R) H diagnostic ratio as a function of depth. The dashed red line corresponds to the year when oil sands developments began near each lake. Blank plots represent lakes where no C_{33} nor C_{32} (R) hopanes were present.

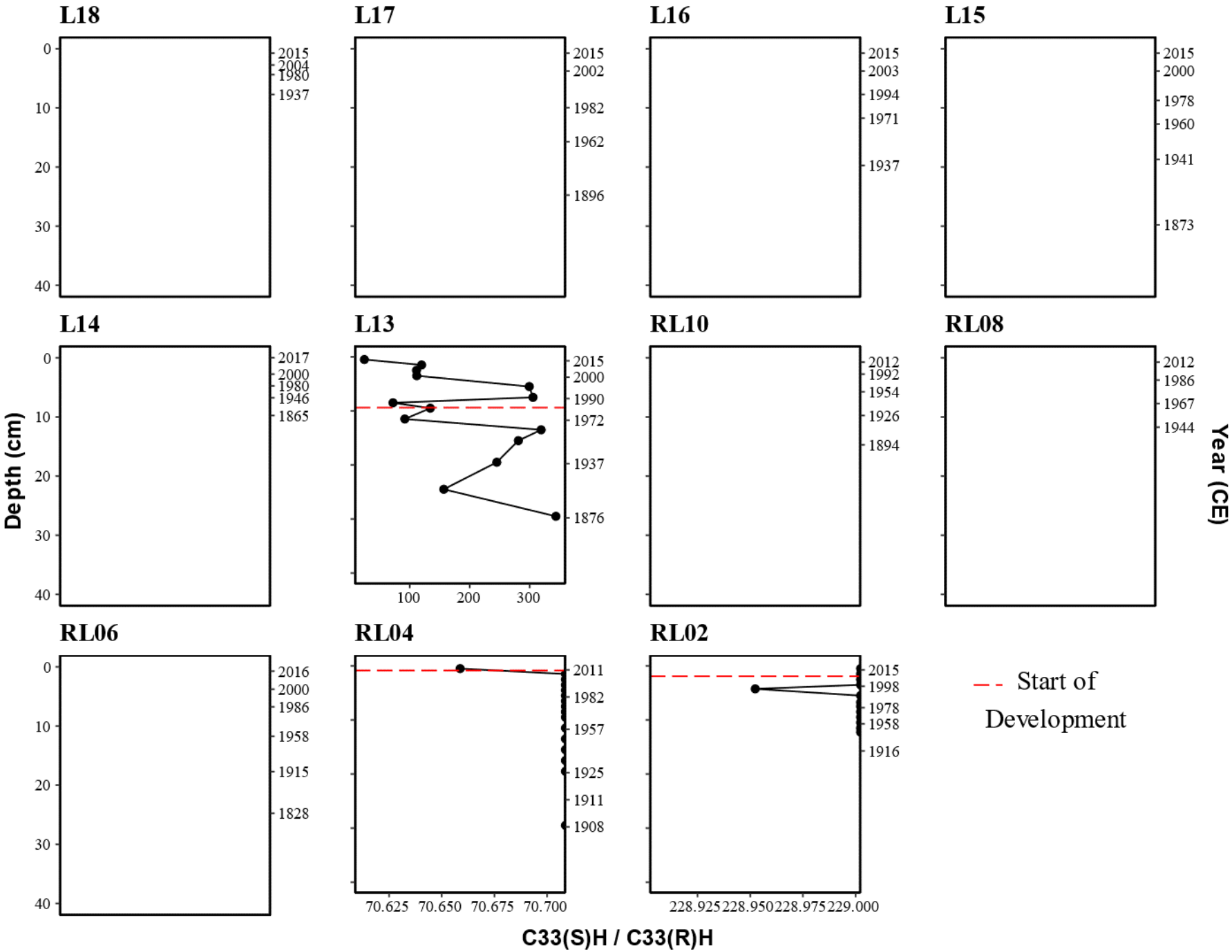

Figure S3- 17: Scatter plots of the C_{33} (S) H / C_{33} (R) H diagnostic ratio as a function of depth. The dashed red line corresponds to the year when oil sands developments began near each lake. Blank plots represent lakes where no C_{33} S nor R hopanes were present.

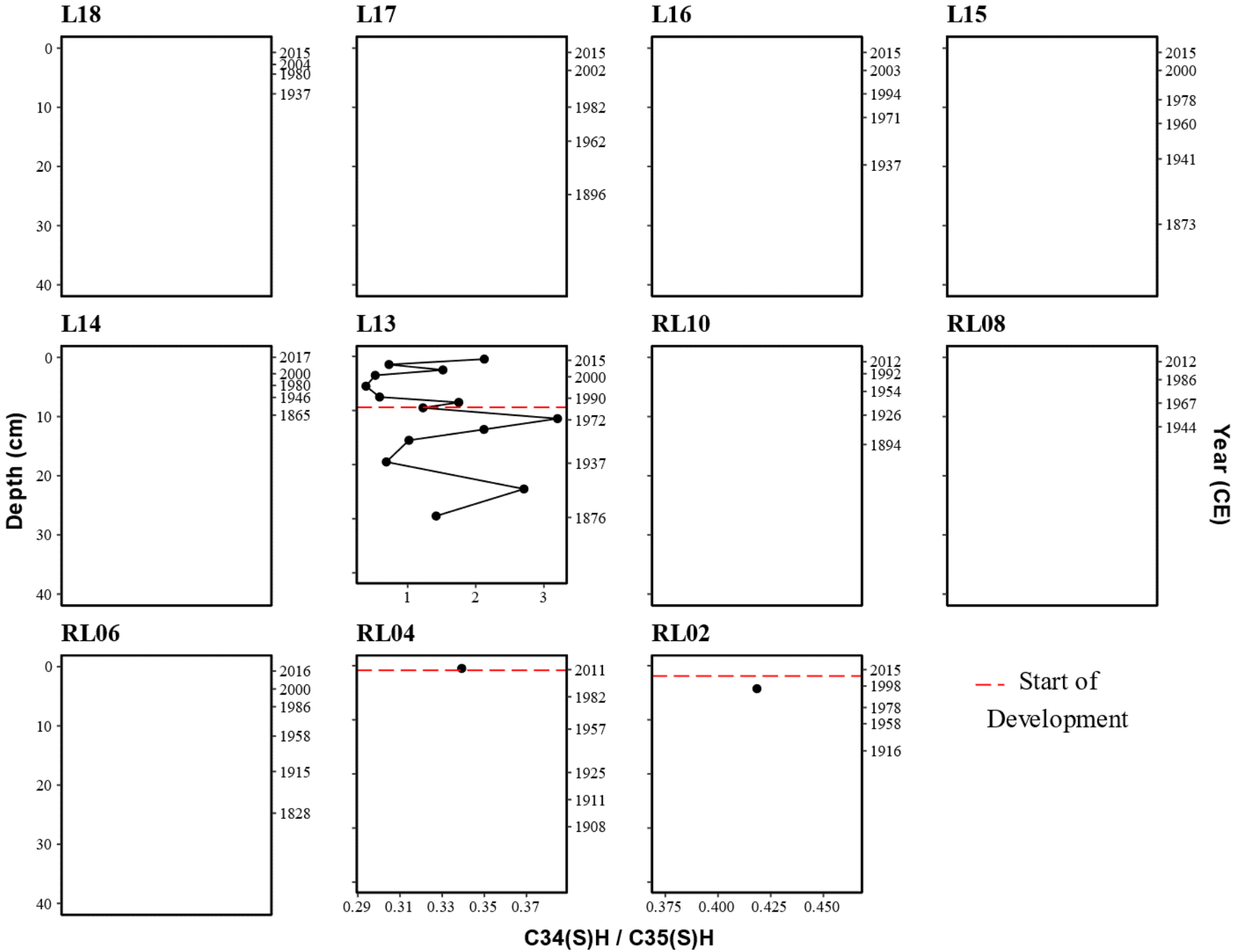

Figure S3- 18: Scatter plots of the C_{34} (S) H / C_{35} (S) H diagnostic ratio as a function of depth. Diagnostic ratios of 0.95 are indicative of an Alberta bitumen source (Yang et al., 2011). The dashed red line corresponds to the year when oil sands developments began near each lake. Blank plots represent lakes where no C_{34} nor C_{35} (S) hopanes were present.

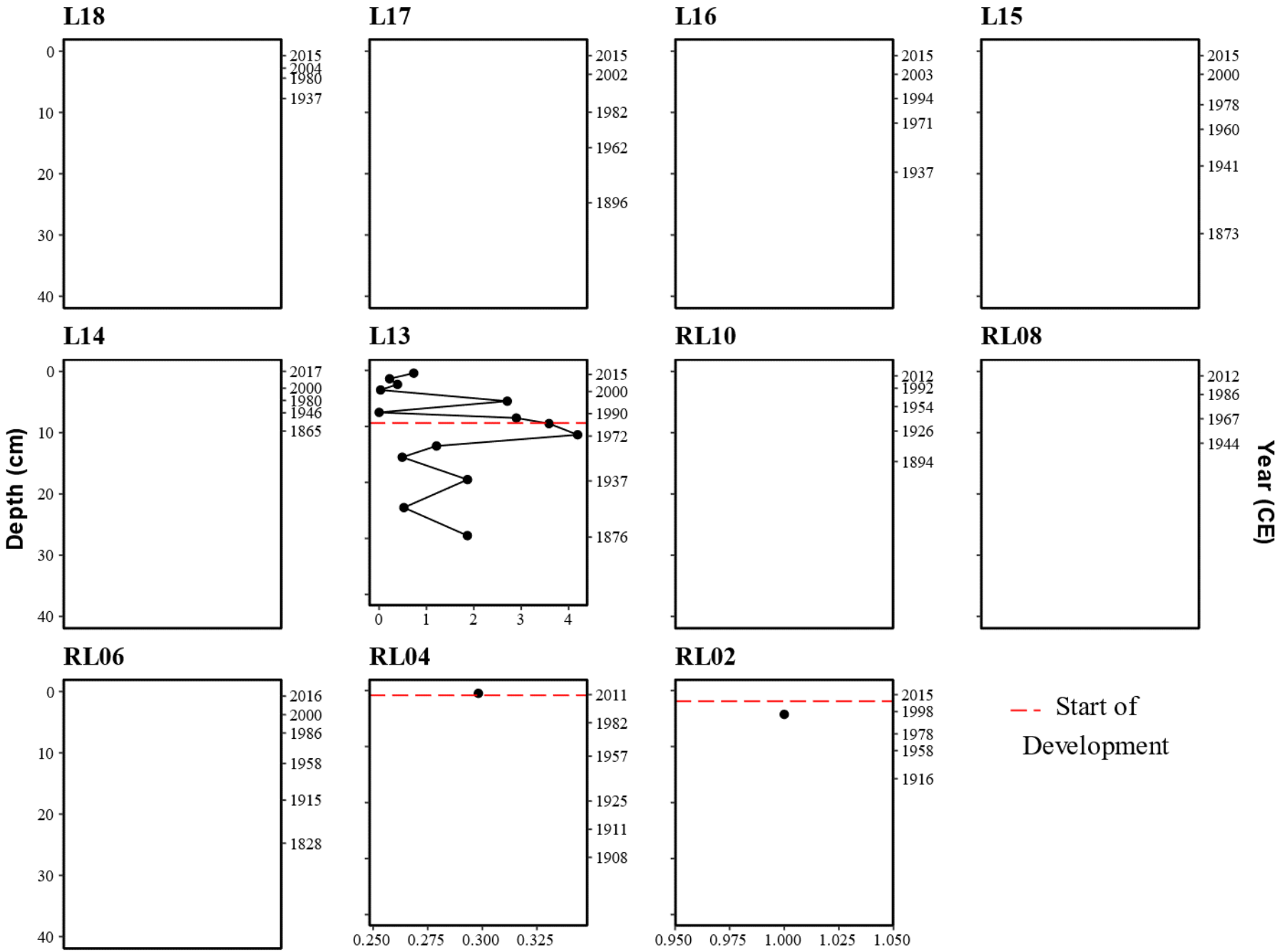

Figure S3- 19: Scatter plots of the C_{34} (R) H / C_{35} (R) H diagnostic ratio as a function of depth. Diagnostic ratios of 0.92 are indicative of an Alberta bitumen source (Yang et al., 2011). The dashed red line corresponds to the year when oil sands developments began near each lake. Blank plots represent lakes where no C_{34} nor C_{35} (R) hopanes were present.

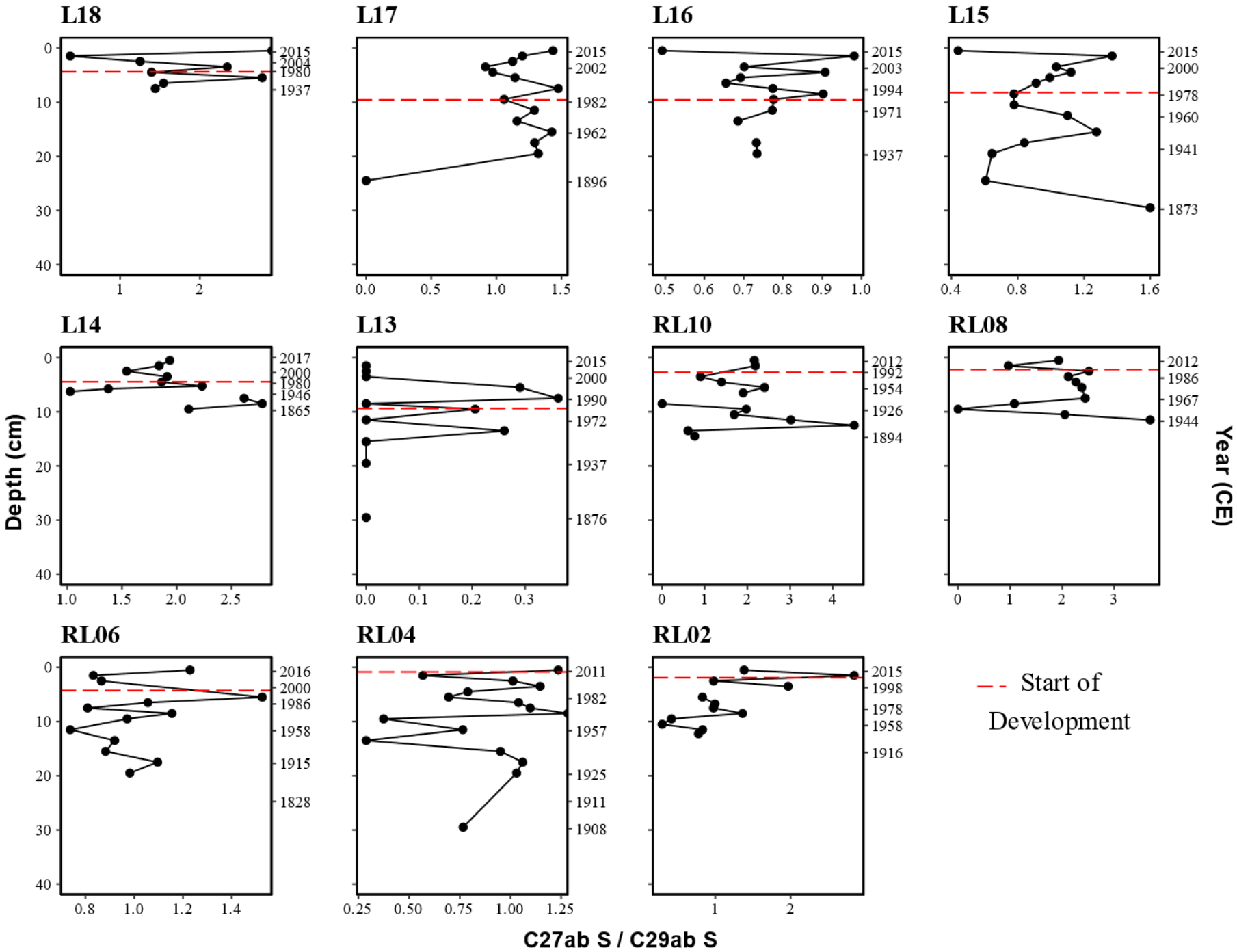

Figure S3- 20: Scatter plots of the C_{27} αββ S / C_{29} αββ S diagnostic ratio as a function of depth. Diagnostic ratios of 1.15 are indicative of a raw Alberta bitumen source. A ratio of 0.85-0.9 indicates an upgraded / refined bitumen origin (Yang et al., 2011). The dashed red line corresponds to the year when oil sands developments began near each lake.

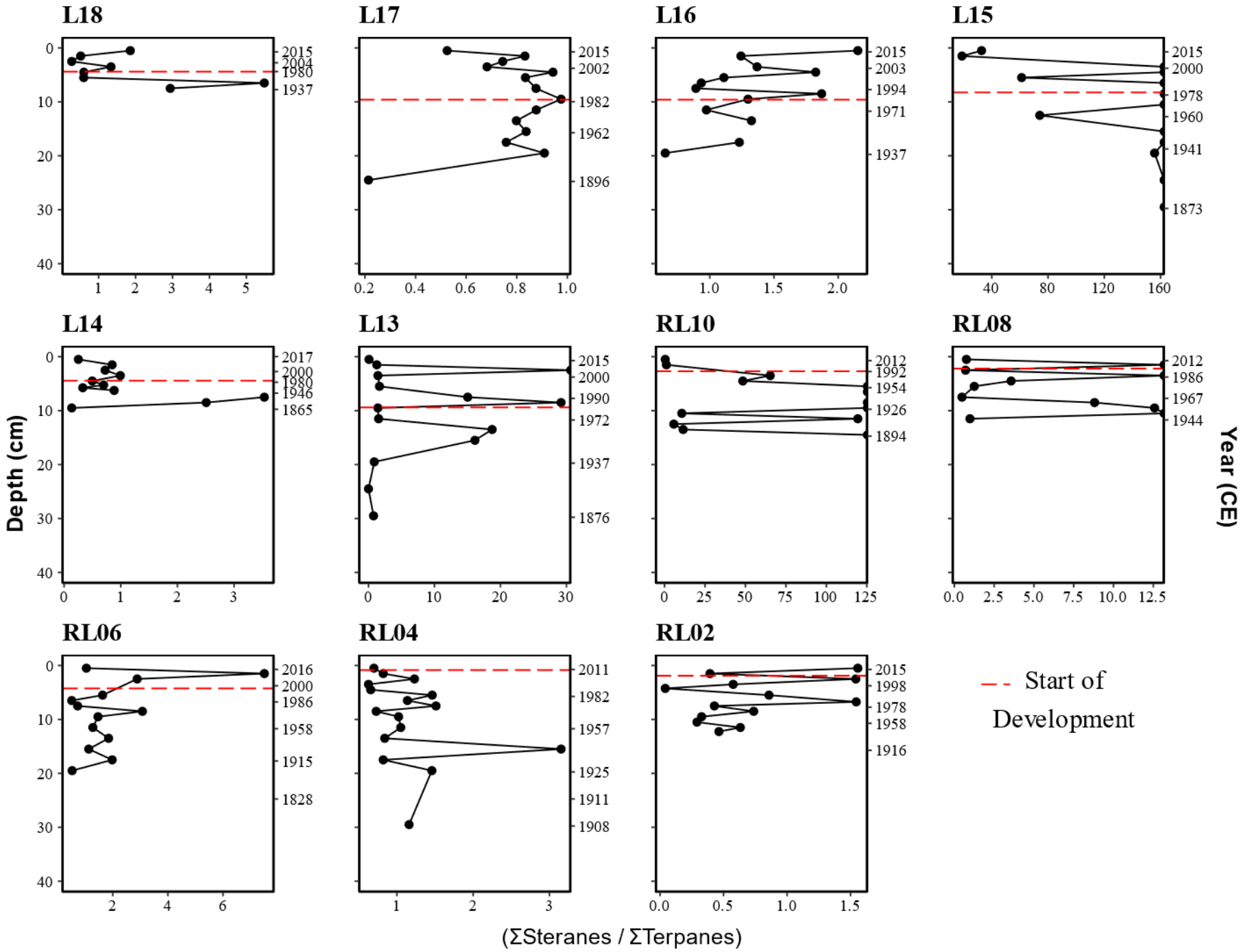

Figure S3- 21: Scatter plots of the ΣSteranes / ΣTerpanes diagnostic ratio as a function of depth. Diagnostic ratios of 0.12 are indicative of a raw Alberta bitumen source. A ratio of 0.35-0.55 indicates an upgraded / refined bitumen origin (Yang et al., 2011). The dashed red line corresponds to the year when oil sands developments began near each lake.

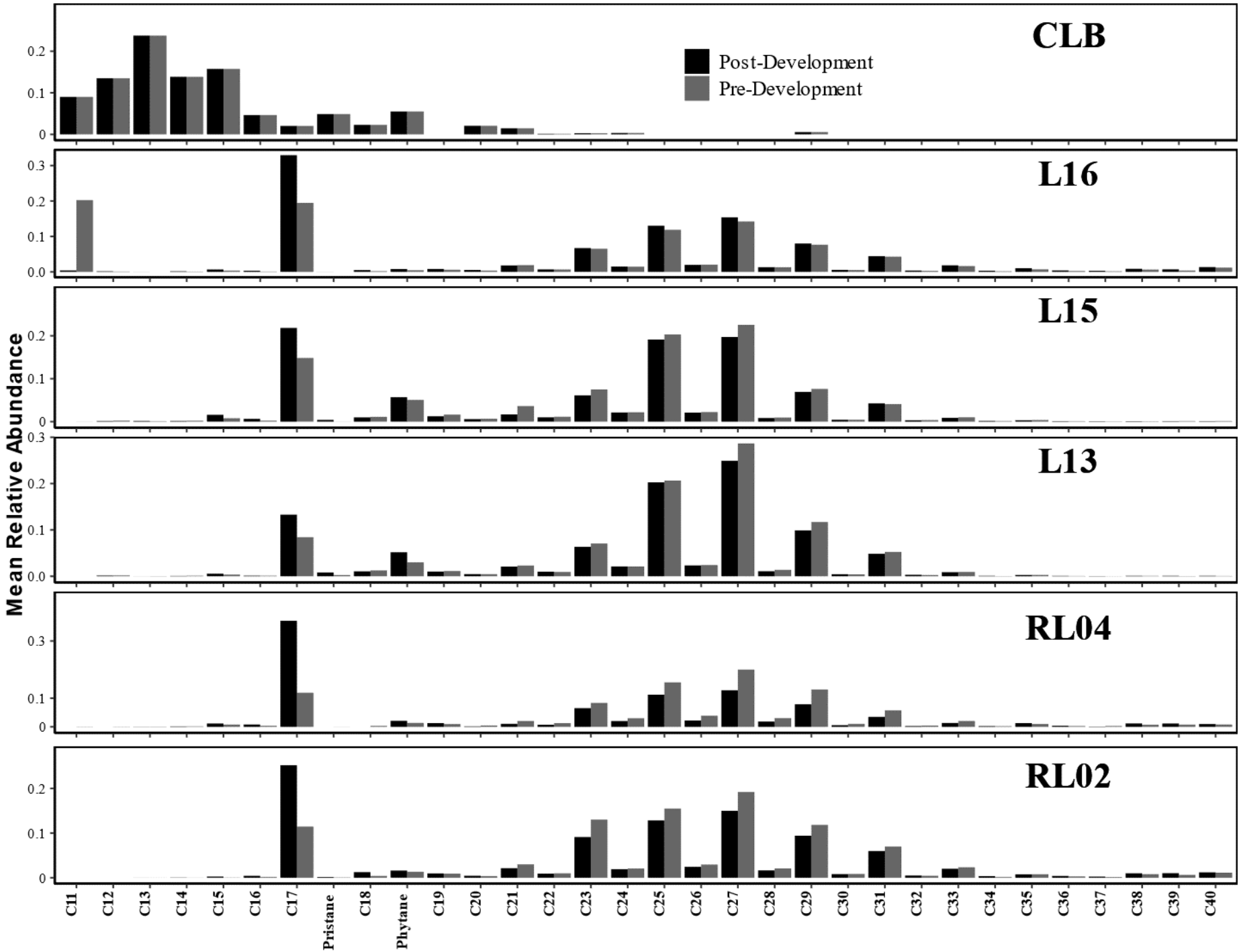

Figure S3- 22: Bar graphs of the mean relative abundance distribution of all n-alkanes when compared to a Cold Lake bitumen sample (CLB). All mean *n*-alkanes abundances are categorized based on the time in which they were deposited Pre- (Grey) and Post- (Black) oil sands development. CLB sample is irrespective of pre/post conditions.

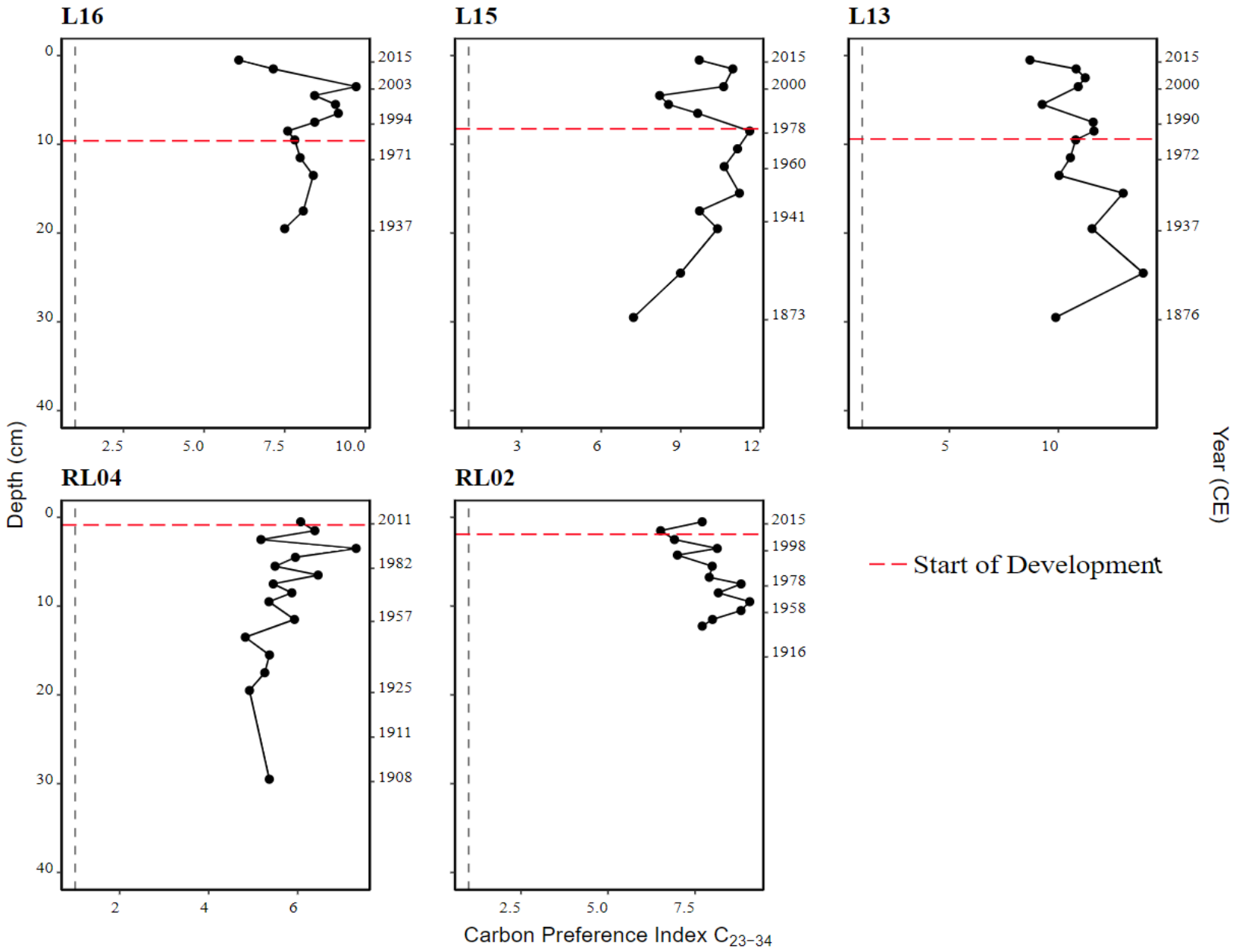

Figure S3- 23: Scatter plot profiles of the Carbon Preference Index (C_{23-34}) as a function of depth as per Wang et al. (2009). The vertical dashed line indicated a CPI of 1, at which point n-alkanes transition from petrogenic to biogenic in source. The dashed red line corresponds to the year when oil sands operations began near each lake.

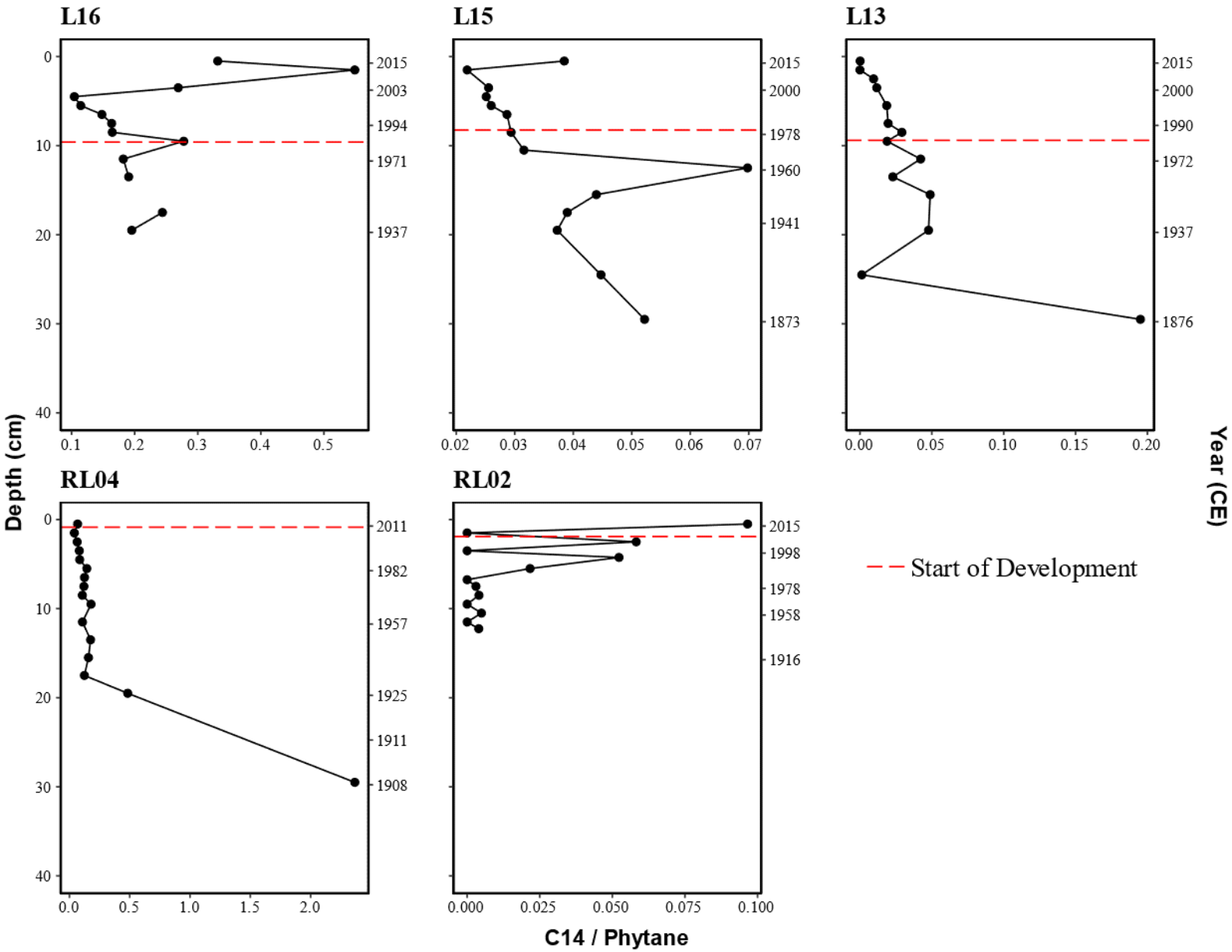

Figure S3- 24: Scatter plots of the C_{14} / Phytane diagnostic ratio as a function of depth. The dashed red line corresponds to the year when oil sands developments began near each lake.

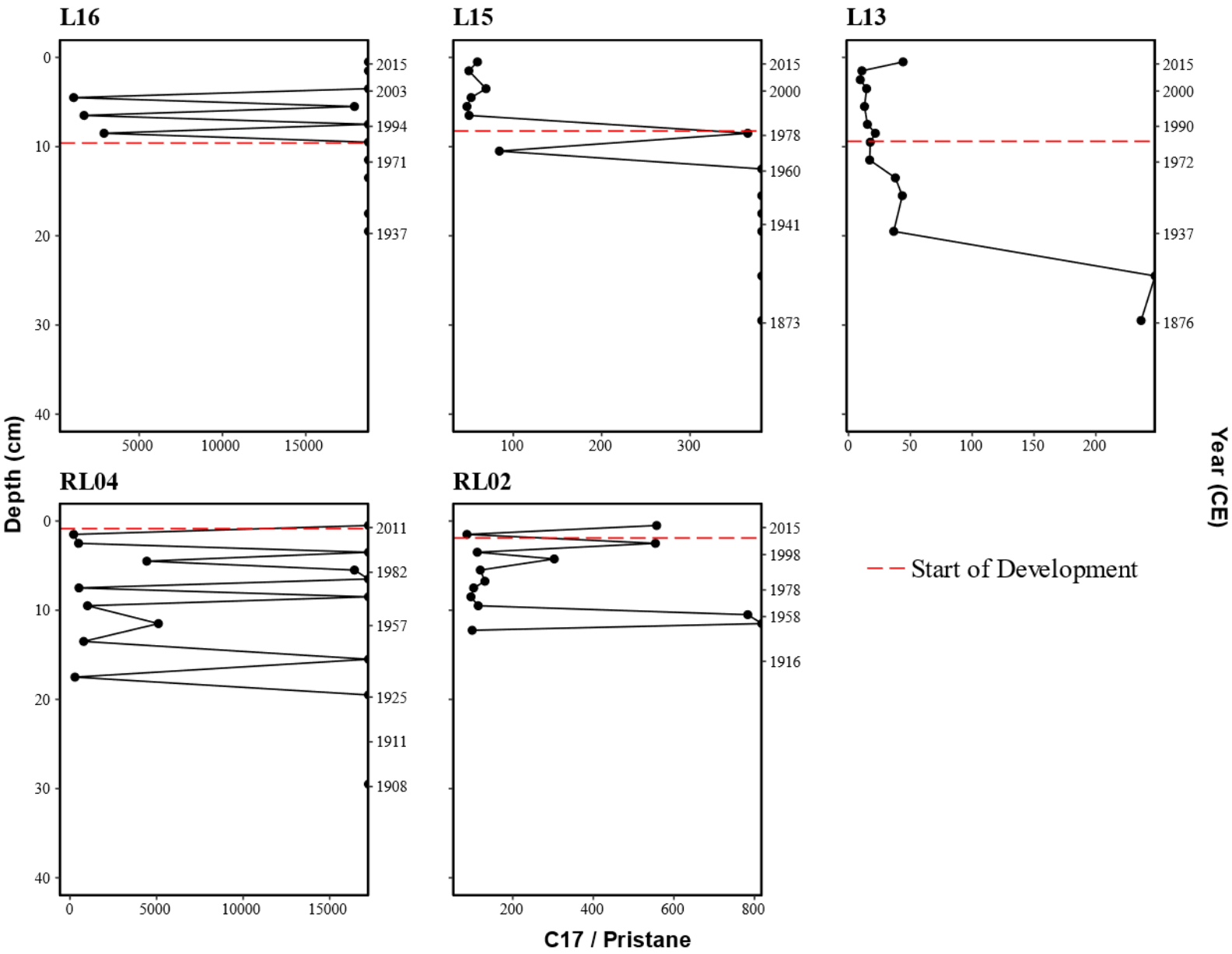

Figure S3- 25: Scatter plots of the C_{17} / Pristane diagnostic ratio as a function of depth. The dashed red line corresponds to the year when oil sands developments began near each lake.

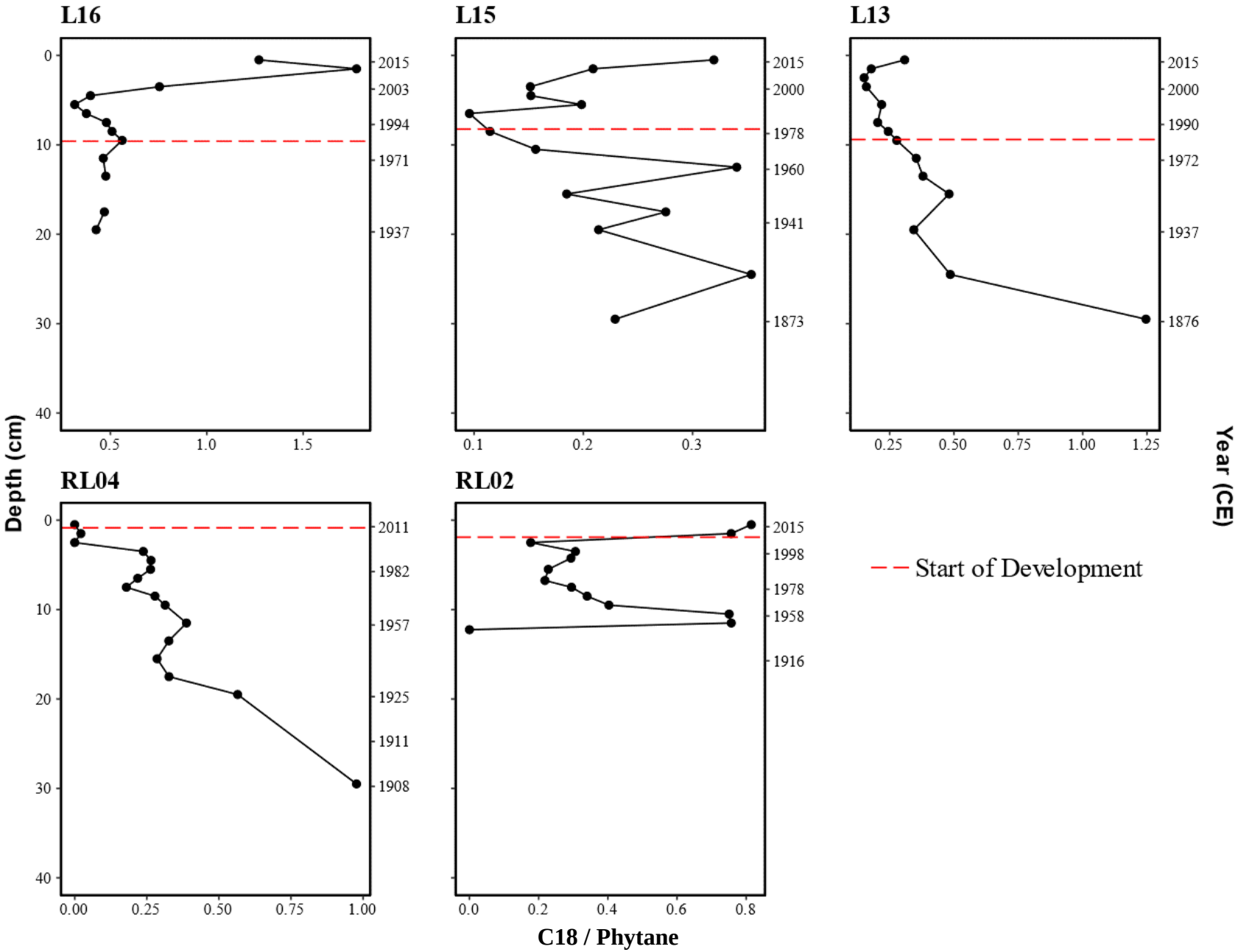

Figure S3- 26: Scatter plots of the C_{18} / Phytane diagnostic ratio as a function of depth. The dashed red line corresponds to the year when oil sands developments began near each lake

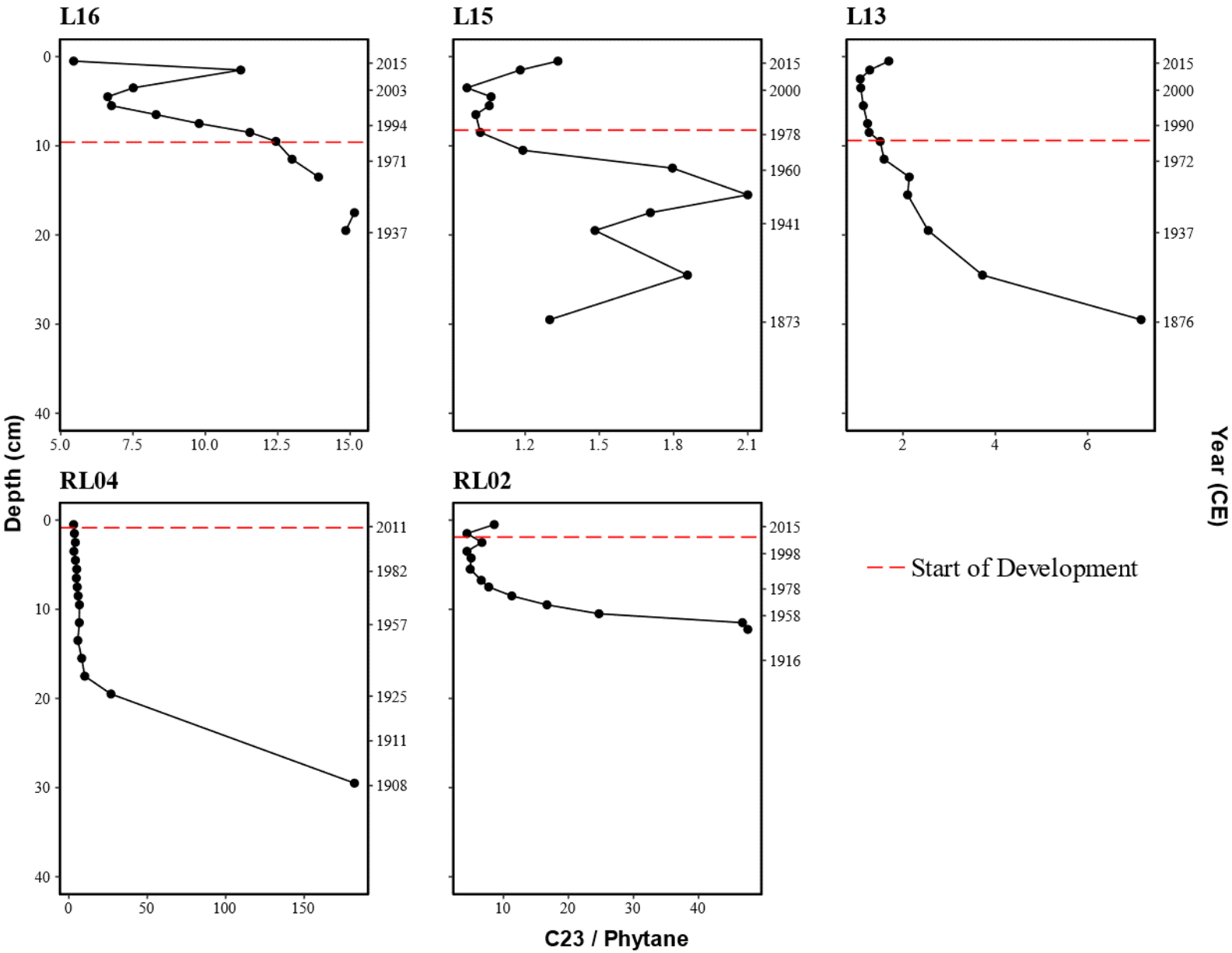

Figure S3- 27: Scatter plots of the C_{23} / Phytane diagnostic ratio as a function of depth. The dashed red line corresponds to the year when oil sands developments began near each lake.

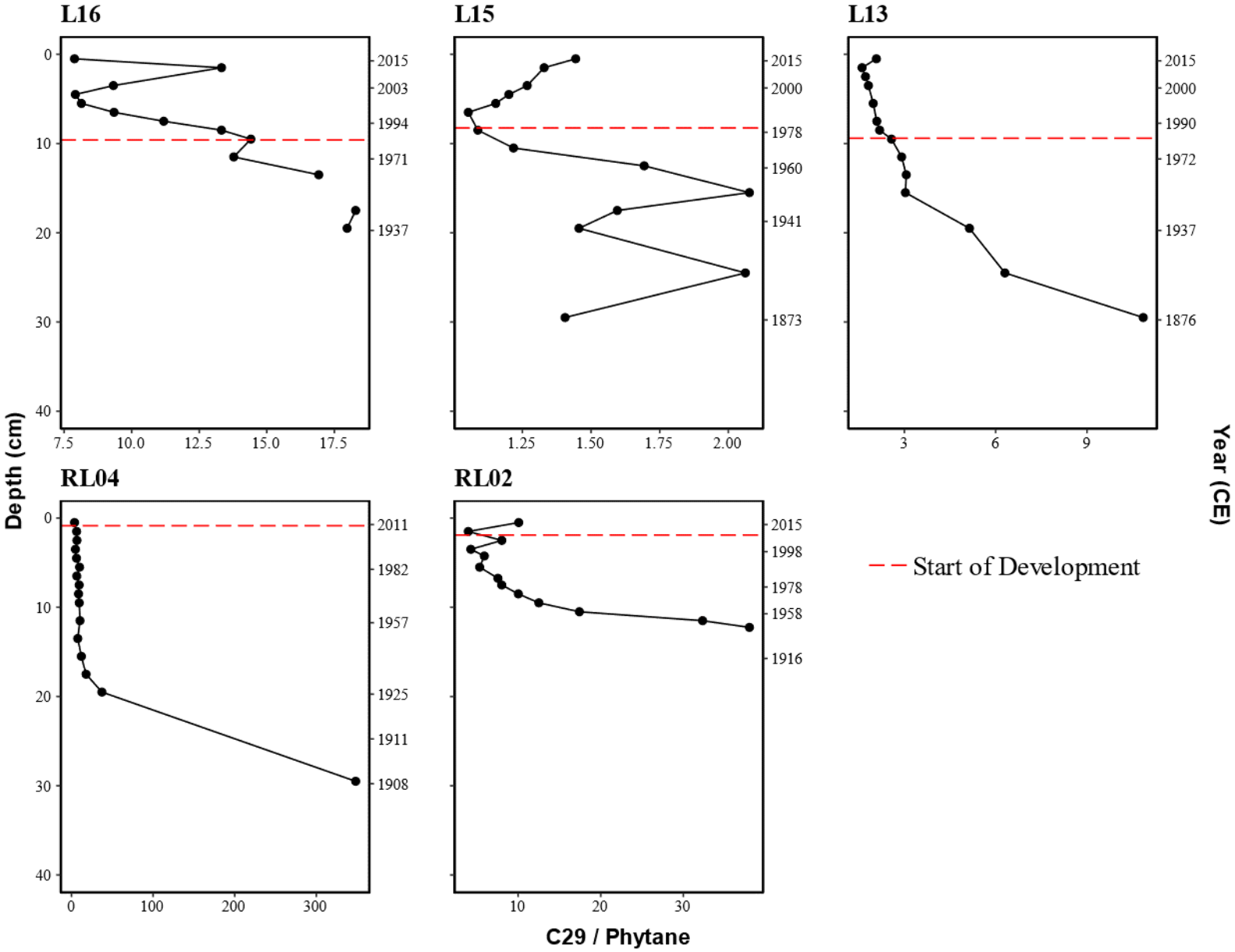

Figure S3- 28: Scatter plots of the C_{29} / Phytane diagnostic ratio as a function of depth. The dashed red line corresponds to the year when oil sands developments began near each lake.

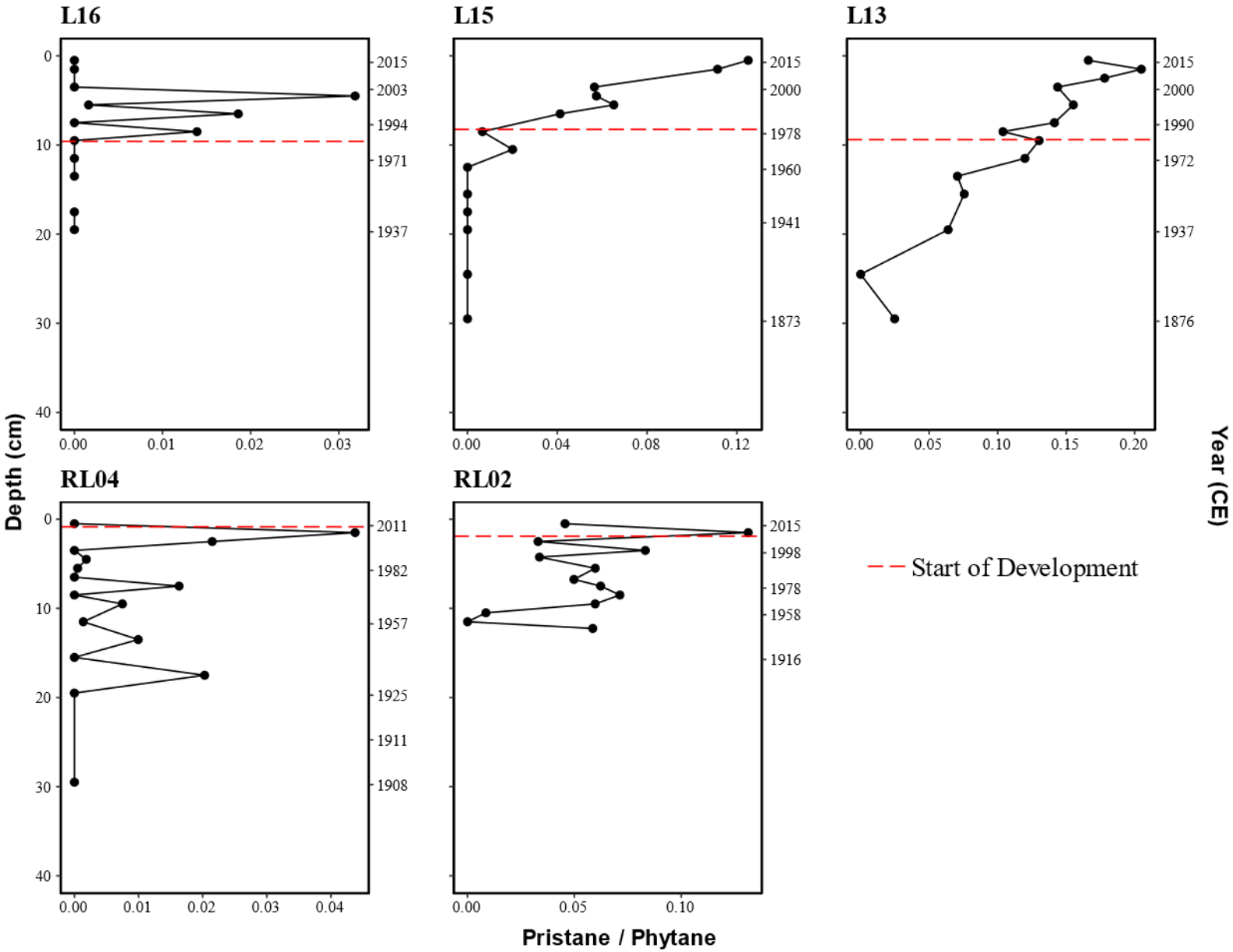

Figure S3- 29: Scatter plots of the Pristane / Phytane diagnostic ratio as a function of depth. The dashed red line corresponds to the year when oil sands developments began near each lake.

Chapter 4: General Conclusions

This thesis evaluated petroleum hydrocarbons (PHCs) in radiometrically dated lake sediment cores to track their distribution and to characterize their sources within the Cold Lake oil sands region. This study is the first to chemically fingerprint petroleum biomarkers and *n*-alkanes in the Cold Lake region. Additionally, this is the first study to establish a relationship between distance from *in-situ* oil sands operations and petroleum hydrocarbon enrichment in regional lakes.

We hypothesized that the expanding thermal *in-situ* oil sands operations in the Cold Lake region are leading to petroleum hydrocarbon contamination. Firstly, we predicted that PHCs in modern lake sediments would be elevated when compared to those deposited before the onset of oil sands activity. Secondly, we predicted that PHCs would be enriched in lakes closest to *in-situ* infrastructure, similar to the distribution observed in open-pit mining regions near upgraders, petcoke piles and open-pit mines. Lastly, we predicted that petroleum fingerprinting using a Cold Lake bitumen sample could characterize bituminous PHCs in regional lakes and facilitate source identification. We tested these hypotheses by measuring the concentration and composition of *n*-alkanes, petroleum biomarkers, alkylated PACs, and unsubstituted PACs in lake sediment cores collected through the Cold Lake oil field.

4.1 Chapter 2 Outcomes

Chapter 2 of this thesis aims to determine whether *in-situ* oil sands extraction contributes to PAC contamination in the environment. We used diagnostic ratios, pyrogenic indices, principal component analyses, and chemical fingerprinting techniques to track spatial and temporal variations in PAC deposition since oil sands activity began in the Cold Lake region. Our results indicate that *in-situ* oil sands activities have raised the concentration and deposition of PACs across the Cold Lake region, becoming more petrogenic in composition. Diagnostic ratios and pyrogenic indices demonstrated that PACs in modern sediments closely reflect a petroleum combustion source, most likely from diesel-fueled vehicular emissions and the combustion of natural gas used to generate steam for *in-situ* oil extraction. Expansions of oil sands operations within the Cold Lake oil field will likely increase the burden of petrogenic PACs in regional lakes to a point where alkylated species dominate over unsubstituted PACs.

Increases in alkylated PAC abundances would have significant environmental and human health implications as these PACs may be carcinogenic, mutagenic, and toxic.

Linear modelling demonstrated a statistically significant relationship between the distance from oil sands wells and PAC accumulation rates in surrounding lakes. This model can be used to prioritize sampling locations and target regions at risk of being enriched in PACs within *in-situ* oil sands. Kelly et al. (2009) established a gradient of PAC enrichment dependent on the proximity to open-pit mining regions. The characteristic bullseye pattern has influenced monitoring protocols and environmental remediation efforts throughout the Athabasca oil sands region.

The results from this chapter suggest that *in-situ* operations are a likely source of PAC contamination to lakes surrounded by *in-situ* activity; however, emissions are more likely originating from natural gas combustion for steam generation, and exhaust from vehicles more than from Cold Lake bitumen itself.

4.2 Chapter 3 Outcomes

Chapter 3 uses petroleum hydrocarbon (PHC) fingerprinting of *n*-alkanes and petroleum biomarkers (steranes, hopanes, terpanes) in lake sediment cores from the Cold Lake oil sands region to track temporal changes in chemical composition following the onset of thermal *in-situ* activity. This chapter aims to determine whether *in-situ* oil sands operations have altered the PHC composition in the Cold Lake region, specifically *n*-alkanes and petroleum biomarkers. We quantified PHCs in radiometrically-dated lake sediment cores to determine whether or not they increased following *in-situ* bitumen extraction or if evidence exists of non-reported flow-to-surface events. We applied principal component analyses, carbon preference index analyses, and diagnostic ratios to determine how PHC composition in lake sediments relates to petrogenic or biogenic sources. Our results indicated that total *n*-alkane and total biomarker profiles exhibited significant increases in PHC accumulation rates following the onset of oil sands activity, similar to that observed in polycyclic aromatic hydrocarbon profiles.

n-alkanes exhibited odd-carbon number preferences over even-number carbon, indicating plant waxes and biogenic PHC sources dominated the composition of *n*-alkanes in this

region. Chemical fingerprinting confirmed higher plant matter, and macrophytes dominated these lake systems. Prevalence of short-chained, even-numbered *n*-alkanes from thermal degradation of biomass during combustion indicated inputs from forest fires, vehicle emissions and fossil fuel combustion in addition to biogenic sources. Sterane, hopane and terpane profiles indicated aerosol deposition from fossil fuel combustion emissions such as traffic exhaust / natural gas combustion driving petroleum biomarker enrichment. The results from *n*-alkanes, petroleum biomarkers and PACs all indicate that PHC burden in Cold Lake lakes are influenced increasingly by fossil fuel and combustion emission sources, and not raw bitumen.

Chapter 3 confirmed that bitumen is not introduced into the environment naturally like the Athabasca oil sands region. As the Cold Lake region is susceptible to non-target bitumen seeps, it would be beneficial to use petroleum hydrocarbon fingerprinting to identify petroleum source origins in the event of future FTS events. Additionally, this method can be applied to future studies to observe whether unreported FTS events have impacted other lakes both in the Cold Lake oil sands region and in other *in-situ* areas.

4.3 Concluding Remarks

This thesis provided a robust analysis of historical PACs, *n-a*lkanes, and petroleum biomarkers within the Cold Lake region. All three suites of contaminants indicated that raw bitumen inputs are not driving compositional changes in PHCs, nor do they record occurrences of unreported flow-to-surface events. More likely, petrogenic PHCs have been introduced into these lakes anthropogenically as a result of fossil fuel combustion from vehicles and natural gas combustion corresponding with expanding *in-situ* oil sands operations.

Alberta Oil Sands research has focused strongly on open-pit mining and bitumen processing operations within the Athabasca Oil Sands Region. The results from this study confirm that *in-situ* oil sands activity is also leading to environmental contamination in the Cold Lake region in increasing proportions. As such, this method of oil sands extraction and the emissions associated with it should receive more attention from the scientific community. The Cold Lake oil sands area is 17 834 km^2, of which 7415 km^2 is dominated by agriculture (ABMI, 2019). The Cold Lake region also has the highest density of high-quality recreational lakes in Alberta (ABMI, 2016). The imperial oil expansion project has proposed to expand *in-situ*

developments in the southern Cold Lake region, therefore adding to the burden of PHCs. Should the proportion of PHCs continue to increase, there will be significant environmental and human health implications in this region. Therefore, ongoing monitoring and continual characterization of contaminants in this region are of great importance.

References:

ABMI, 2019. Alberta Biodiversity and Monitoring Institute 2018-2019 Annual Report. Edmonton, Alberta, Canada.

ABMI, 2016. The Status of Biodiversity in the Grassland and Parkland Regions of Alberta. Edmonton, Alberta, Canada.

AER, 2018a. Alberta Energy Regulator Annual Report 2017/2018. Edmonton, Alberta, Canada.

AER, 2018b. Control Effectiveness Assessment of Solvent Injection Processes. Calgary, Alberta, Canada.

AER, 2018c. Risk Assessment of Solvent Injection Processes. Calgary, Alberta, Canada.

AER, 2016. Root Cause and Regulatory Response Report - Canadian Natural Resources Ltd. Primrose Bitumen Emulsion Releases, 2013. Calgary, Alberta, Canada.

AER, 2015. 2014/2015 Alberta Energy Regulator Annual Report. Calgary, Alberta, Canada.

Ahad, J.M.E., Gammon, P.R., Gobeil, C., Jautzy, J., Krupa, S., Savard, M.M., Studabaker, W.B., 2014. Evaporative emissions from tailings ponds are not likely an important source of airborne PAHs in the Athabasca oil sands region. Proc. Natl. Acad. Sci. U. S. A. https://doi.org/10.1073/pnas.1403515111

Ahad, J.M.E., Ganeshram, R.S., Bryant, C.L., Cisneros-Dozal, L.M., Ascough, P.L., Fallick, A.E., Slater, G.F., 2011. Sources of n-alkanes in an urbanized estuary: Insights from molecular distributions and compound-specific stable and radiocarbon isotopes. Mar. Chem. 126, 239–249. https://doi.org/10.1016/j.marchem.2011.06.002

Ahad, J.M.E., Jautzy, J.J., Cumming, B.F., Das, B., Laird, K.R., Sanei, H., 2015. Sources of polycyclic aromatic hydrocarbons (PAHs) to northwestern Saskatchewan lakes east of the Athabasca oil sands. Org. Geochem. 80, 35–45. https://doi.org/10.1016/j.orggeochem.2015.01.001

Ahad, J.M.E., Pakdel, H., Savard, M.M., Calderhead, A.I., Gammon, P.R., Rivera, A., Peru, K.M., Headley, J. V., 2013. Characterization and quantification of mining-related "naphthenic acids" in groundwater near a major oil sands tailings pond. Environ. Sci. Technol. 47, 5023–5030. https://doi.org/10.1021/es3051313

Andersson, J.T., Achten, C., 2015. Time to Say Goodbye to the 16 EPA PAHs? Toward an Up-to-Date Use of PACs for Environmental Purposes. Polycycl. Aromat. Compd. 35, 330–354. https://doi.org/10.1080/10406638.2014.991042

Andreou, G., Rapsomanikis, S., 2009. Origins of n-alkanes, carbonyl compounds and molecular biomarkers in atmospheric fine and coarse particles of Athens, Greece. Sci. Total Environ. 407, 5750–5760. https://doi.org/10.1016/j.scitotenv.2009.07.019

Appleby, P.G., 2001. Chronostratigraphic Techniques in Recent Sediments, in: Last, W.M., Smol, J.P. (Eds.), Tracking Environmental Change Using Lake Sediments: Basin Analysis, Coring, and Chronological Techniques. Springer Netherlands, Dordrecht, pp. 171–203. https://doi.org/10.1007/0-306-47669-X_9

Appleby, P.G., Nolan, P.J., Gifford, D.W., Godfrey, M.J., Oldfield, F., Anderson, N.J., Battarbee, R.W., 1986. 210Pb dating by low background gamma counting. Hydrobiologia 143, 21–27. https://doi.org/10.1007/BF00026640

Appleby, P.G., Oldfield, F., 1978. The calculation of lead-210 dates assuming a constant rate of supply of

unsupported 210Pb to the sediment. Catena 5, 1–8. https://doi.org/10.1016/S0341-8162(78)80002-2

Arens, C.J., Arens, J.C., Hogan, N.S., Kavanagh, R.J., Berrue, F., Van Der Kraak, G.J., van den Heuvel, M.R., 2017. Population impacts in White Sucker (*Catostomus commersonii*) exposed to oil sands-derived contaminants in the Athabasca River. Environ. Toxicol. Chem. 9999, 1–10. https://doi.org/10.1002/etc.3735

Asif, M., Grice, K., Fazeelat, T., 2009. Assessment of petroleum biodegradation using stable hydrogen isotopes of individual saturated hydrocarbon and polycyclic aromatic hydrocarbon distributions in oils from the Upper Indus Basin, Pakistan. Org. Geochem. 40, 301–311. https://doi.org/10.1016/j.orggeochem.2008.12.007

Attanasi, E.D., Meyer, R.F., Trinnaman, J.., Clarke, A., 2007. 2007 Survey of Energy Resources. London.

Ayles, B.G., Dubé, M., Rosenberg, D., 2004. Oil Sands Regional Aquatic Monitoring Program (RAMP) Scientific Peer Review of the Five Year Report (1997-2001). Winnipeg.

Barfknecht, T.R., Hites, R.A., Cavaliers, E.L., Thilly, W.G., 1982. Human cell mutagenicity of polycyclic aromatic hydrocarbon components of diesel emissions, in: EPA Diesel Emissions Symposium. Raleigh, North Carolina, USA , pp. 277–294.

Bata, T., Parnell, J., Bowden, S., Boyce, A., 2016. Origin of heavy oil in cretaceous petroleum reservoirs. Bull. Can. Pet. Geol. 64, 106–118. https://doi.org/10.2113/gscpgbull.64.2.106

Baturin-Pollock, C., Sitek, N., Chan, D., Hurst, T., 2010. Geology and Resource Assessment of the Grand Rapids, Southern Cold Lake, Alberta, Canada 10288.

Beck, E.M., Smits, J.E.G., St Clair, C.C., 2015. Evidence of low toxicity of oil sands processaffected water to birds invites re-evaluation of avian protection strategies. Conserv. Physiol. 3, 1–16. https://doi.org/10.1093/conphys/cov038

Bell, M., Blais, J.M., 2019. "-Omics" workflow for paleolimnological and geological archives: A review. Sci. Total Environ. https://doi.org/10.1016/j.scitotenv.2019.03.477

Bell, M.A., Overy, D.P., Blais, J.M., 2020. A continental scale spatial investigation of lake sediment organic compositions using sedimentomics. Sci. Total Environ. 719. https://doi.org/10.1016/j.scitotenv.2020.137746

Bieger, T., Hellou, J., Abrajano, T.A., 1996. Petroleum biomarkers as tracers of lubricating oil contamination. Mar. Pollut. Bull. 32, 270–274. https://doi.org/10.1016/0025-326X(95)00151-C

Boyle, J., Chiverrell, R., Schillereff, D., 2015. Lacustrine Archives of Metals from Mining and Other Industrial Activities---A Geochemical Approach, in: Blais, J.M., Rosen, M.R., Smol, J.P. (Eds.), Environmental Contaminants: Using Natural Archives to Track Sources and Long-Term Trends of Pollution. Springer Netherlands, Dordrecht, pp. 121–159. https://doi.org/10.1007/978-94-017-9541-8_7

Brookes, P., 1977. Mutagenicity of Polycyclic Aromatic Hydrocarbons. Mutat. Res. 39, 257–284.

Brooks, P.W., Fowler, M.G., Macqueen, R.W., 1988. Biological marker and conventional organic geochemistry of oil sands/heavy oils, Western Canada basin. Org. Geochem. https://doi.org/10.1016/0146-6380(88)90144-1

Broughton, P.L., 2013. Devonian salt dissolution-collapse breccias flooring the Cretaceous Athabasca oil sands deposit and development of lower McMurray Formation sinkholes, northern Alberta Basin, Western Canada. Sediment. Geol. 283, 57–82. https://doi.org/10.1016/j.sedgeo.2012.11.004

Bytnerowicz, A., Hsu, Y.M., Percy, K., Legge, A., Fenn, M.E., Schilling, S., Frączek, W., Alexander, D., 2016. Ground-level air pollution changes during a boreal wildland mega-fire. Sci. Total Environ. 572, 755–769. https://doi.org/10.1016/j.scitotenv.2016.07.052

Camus, L., Birkely, S.R., Jones, M.B., B??rseth, J.F., Gr??svik, B.E., Gulliksen, B., L??nne, O.J., Regoli, F., Depledge, M.H., 2003. Biomarker responses and PAH uptake in Mya truncata following exposure to oil-contaminated sediment in an Arctic fjord (Svalbard). Sci. Total Environ. 308, 221–234. https://doi.org/10.1016/S0048-9697(02)00616-2

CAPP, 2019. 2019 Crude Oil Forecast, Markets and Transportation. Calgary, Alberta, Canada.

CAPP, 2018a. Oil and Natural Gas Priorities: Putting Canada on the World Stage - An Energy Platform for Canada. Edmonton, Alberta, Canada.

CAPP, 2018b. 2018 Economic Report Series: Canada's Role in the World's Future Energy Mix. Edmonton, Alberta, Canada.

CAPP, 2018c. 2018 Economic Report Series: A Global Vision for the Future of Canadian Oil and Natural Gas. Edmonton, Alberta, Canada.

CAPP, 2017. Crude Oil Extraction and Drilling Methods [WWW Document]. Can. Assoc. Pet. Prod. URL https://www.capp.ca/oil/extraction/ (accessed 3.3.20).

Carls, M.G., 2006. Nonparametric Identification of Petrogenic and Pyrogenic Hydrocarbons in Aquatic Ecosystems. Environ. Sci. Technol. 4233–4239. https://doi.org/10.1021/es052498g

Charry-Sanchez, J., Betancourt-Torcat, A., Ricardez-Sandoval, L., 2014. An optimization energy model for the upgrading processes of Canadian unconventional oil. Energy 68, 629–643. https://doi.org/10.1016/j.energy.2014.03.016

Chen, H., Teng, Y., Wang, J., 2012. Source apportionment of polycyclic aromatic hydrocarbons (PAHs) in surface sediments of the Rizhao coastal area (China) using diagnostic ratios and factor analysis with nonnegative constraints. Sci. Total Environ. 414, 293–300. https://doi.org/10.1016/J.SCITOTENV.2011.10.057

Cheney, C.L., Eccles, K., Kimpe, L.E., Thienpont, J.R., Korosi, J.B., Blais, J.M., 2020. Determining the effects of past gold mining using a sediment palaeotoxicity model. Sci. Total Environ. 718, 137308. https://doi.org/10.1016/j.scitotenv.2020.137308

Cheng, I., Wen, D., Zhang, L., Wu, Z., Qiu, X., Yang, F., Harner, T., 2018. Deposition Mapping of Polycyclic Aromatic Compounds in the Oil Sands Region of Alberta, Canada and Linkages to Ecosystem Impacts. Environ. Sci. Technol. 52, 12456–12464. https://doi.org/10.1021/acs.est.8b02486

Clair, T.A., Percy, K.E., 2015. Assessing Forest Health in the Athabasca Oil Sands Region Final Report, Wood Buffalo Environmental Association Technical Reports.

Colavecchia, M. V., Backus, S.M., Hodson, P. V., Parrott, J.L., 2004. Toxicity of oil sands to early life stages of fathead minnows (Pimephales promelas). Environ. Toxicol. Chem. 23, 1709–1718. https://doi.org/10.1897/03-412

Conly, F.M., Crosley, R.W., Headley, J. V, 2002. Characterizing sediment sources and natural hydrocarbon inputs in the lower Athabasca River, Canada. J. Environ. Eng. Sci. 1, 187–199. https://doi.org/10.1139/S02-013

Cooke, C.A., Kirk, J.L., Muir, D.C.G., Wiklund, J.A., Wang, X., Gleason, A., Evans, M.S., 2017. Spatial

and temporal patterns in trace element deposition to lakes in the Athabasca oil sands region (Alberta, Canada). Environ. Res. Lett. 12. https://doi.org/10.1088/1748-9326/aa9505

Crump, D., Williams, K.L., Chiu, S., Zhang, Y., Martin, J.W., 2017. Athabasca Oil Sands Petcoke Extract Elicits Biochemical and Transcriptomic Effects in Avian Hepatocytes. Environ. Sci. Technol. 51, 5783–5792. https://doi.org/10.1021/acs.est.7b00767

Dastillung, M., Albrecht, P., 1976. Molecular test for oil pollution in surface sediments. Mar. Pollut. Bull. 7, 13–15. https://doi.org/10.1016/0025-326X(76)90282-4

De La Torre-Roche, R.J., Lee, W.-Y., Campos-Díaz, S.I., 2009. Soil-borne polycyclic aromatic hydrocarbons in El Paso, Texas: Analysis of a potential problem in the United States/Mexico border region. J. Hazard. Mater. 163, 946–958. https://doi.org/10.1016/j.jhazmat.2008.07.089

Debenest, T., Turcotte, P., Gagné, F., Gagnon, C., Blaise, C., 2012. Ecotoxicological impacts of effluents generated by oil sands bitumen extraction and oil sands lixiviation on Pseudokirchneriella subcapitata. Aquat. Toxicol. 112–113, 83–91. https://doi.org/10.1016/j.aquatox.2012.01.021

Droppo, I.G., di Cenzo, P., Parrott, J., Power, J., 2019. The Alberta oil sands eroded bitumen/sediment transitional journey: Influence on sediment transport dynamics, PAH signatures and toxicological effect. Sci. Total Environ. 677. https://doi.org/10.1016/j.scitotenv.2019.04.313

Eckmeier, E., Wiesenberg, G.L.B., 2009. Short-chain n-alkanes (C16-20) in ancient soil are useful molecular markers for prehistoric biomass burning . J. Archaeol. Sci. 36, 1590–1596. https://doi.org/10.1016/j.jas.2009.03.021

Eickmeyer, D.C., Kimpe, L.E., Kokelj, S. V., Pisaric, M.F.J., Smol, J.P., Sanei, H., Thienpont, J.R., Blais, J.M., 2016. Interactions of polychlorinated biphenyls and organochlorine pesticides with sedimentary organic matter of retrogressive thaw slump-affected lakes in the tundra uplands adjacent to the Mackenzie Delta, NT, Canada. J. Geophys. Res. Biogeosciences 121, 411–421. https://doi.org/10.1002/2015JG003069

Evans, M., Davies, M., Janzen, K., Muir, D., Hazewinkel, R., Kirk, J., De Boer, D., 2016. PAH distributions in sediments in the oil sands monitoring area and western Lake Athabasca: Concentration, composition and diagnostic ratios. Environ. Pollut. 213, 671–687. https://doi.org/10.1016/j.envpol.2016.03.014

Evans, M.S., Talbot, A., 2012. Investigations of mercury concentrations in walleye and other fish in the Athabasca River ecosystem with increasing oil sands developments. J. Environ. Monit. 14, 1989–2003. https://doi.org/10.1039/C2EM30132F

Fang, J., Wu, F., Xiong, Y., Li, F., Du, X., An, D., Wang, L., 2014. Source characterization of sedimentary organic matter using molecular and stable carbon isotopic composition of n-alkanes and fatty acids in sediment core from Lake Dianchi, China. Sci. Total Environ. 410–421. https://doi.org/10.1016/j.scitotenv.2013.10.066

Ficken, K.J., Li, B., Swain, D.L., Eglinton, G., 2000. An n-alkane proxy for the sedimentary input of submerged/Floating freshwater aquatic macrophytes. Org. Geochem. 31, 745–749.

Frank, R.A., Roy, J.W., Bickerton, G., Rowland, S.J., Headley, J. V., Scarlett, A.G., West, C.E., Peru, K.M., Parrott, J.L., Conly, F.M., Hewitt, L.M., 2014. Profiling oil sands mixtures from industrial developments and natural groundwaters for source identification. Environ. Sci. Technol. 48, 2660–2670. https://doi.org/10.1021/es500131k

Galarneau, E., Hollebone, B.P., Yang, Z., Schuster, J., 2014. Preliminary measurement-based estimates of PAH emissions from oil sands tailings ponds. Atmos. Environ. 97, 332–335.

https://doi.org/10.1016/j.atmosenv.2014.08.038

Glew, J.R., 1988. A portable extruding device for close interval sectioning of unconsolidated core samples, Journal of Paleolimnology. Kluwer Academic Publishers.

Grice, R.E., Locksley, H.D., Scheinmann, F., 1968. Alkane Distribution as Biological Markers: Presence and Possible Origin of n-Alkanes in Guttiferae Heartwoods. Nature 218, 892–893. https://doi.org/10.1038/218892a0

Guéguen, C., Cuss, C.W., Cho, S., 2016. Snowpack deposition of trace elements in the Athabasca oil sands region, Canada. Chemosphere 153, 1–6. https://doi.org/10.1016/j.chemosphere.2016.03.020

Hall, R.I., Wolfe, B.B., Wiklund, J.A., Edwards, T.W.D., Farwell, A.J., Dixon, D.G., 2012. Has Alberta Oil Sands Development Altered Delivery of Polycyclic Aromatic Compounds to the Peace-Athabasca Delta? PLoS One 7. https://doi.org/10.1371/journal.pone.0046089

Head, I.M., Jones, D.M., Larter, S.R., 2003. Biological activity in the deep subsurface and the origin of heavy oil. Nature. https://doi.org/10.1038/nature02134

Headley, J. V, Akre, C., Conly, F.M., Peru, K.M., Dickson, L.C., 2001. Preliminary characterization and source assessment of PAHs in tributary sediments of the Athabasca River, Canada. Environ. Forensics 2, 335–345. https://doi.org/DOI: 10.1006/enfo.2001.0064

Hebert, C.E., Weseloh, D.V.C., Macmillan, S., Campbell, D., Nordstrom, W., 2011. Metals and polycyclic aromatic hydrocarbons in colonial waterbird eggs from Lake Athabasca and the Peace-Athabasca Delta, Canada. Environ. Toxicol. Chem. 30, 1178–1183. https://doi.org/10.1002/etc.489

Hein, F.J., 2017. Geology of bitumen and heavy oil: An overview. J. Pet. Sci. Eng. 154, 551–563. https://doi.org/10.1016/j.petrol.2016.11.025

Hein, F.J., Cotterill, D.K., 2006. The Athabasca oil sands - A regional geological perspective, Fort McMurray area, Alberta, Canada. Nat. Resour. Res. 15, 85–102. https://doi.org/10.1007/s11053-006-9015-4

Hein, F.J., Marsh, R.., 2008. Regional geologic framework, depositional models and resource estimates of the oil sands of Alberta, Canada, in: The World Heavy Oil Congress : Unconventional Oil Challenging Conventional Expectations. World Heavy Oil Congress, Edmonton.

Hostettler, F.D., Lorenson, T.D., Bekins, B.A., 2013. Petroleum Fingerprinting with Organic Markers. Environ. Forensics 14, 262–277. https://doi.org/10.1080/15275922.2013.843611

Hrudey, S.E., Xu, Z., 2010. Environmental and Health Impacts of Canada ' s Oil Sands Industry, The Royal Society of Canada Expert Pannel. Ottawa, Ontario, Canada. https://doi.org/10.1371/journal.pbio.1001247

Hsu, Y.M., Harner, T., Li, H., Fellin, P., 2015. PAH measurements in air in the Athabasca oil sands region. Environ. Sci. Technol. 49, 5584–5592. https://doi.org/10.1021/acs.est.5b00178

IEA, 2017. World Energy Outlook 2017 – Analysis - IEA, International Energy Agency.

Imperial Oil Resources Limited, 2016. Imperial Oil Resources Limited Cold Lake Expansion Project Volume 1-Project Description.

Irvine, G.M., Blais, J.M., Doyle, J.R., Kimpe, L.E., White, P.A., 2014. Cancer risk to First Nations' people from exposure to polycyclic aromatic hydrocarbons near in-situ bitumen extraction in Cold Lake, Alberta. Environ. Heal. 13. https://doi.org/10.1186/1476-069X-13-7

Jariyasopit, N., Harner, T., Wu, D., Williams, A., Halappanavar, S., Su, K., 2016. Mapping Indicators of Toxicity for Polycyclic Aromatic Compounds in the Atmosphere of the Athabasca Oil Sands Region. Environ. Sci. Technol. 50, 11282–11291. https://doi.org/10.1021/acs.est.6b02058

Jautzy, J., Ahad, J.M.E., Gobeil, C., Savard, M.M., 2013. Century-Long Source Apportionment of PAHs in Athabasca Oil Sands Region Lakes Using Diagnostic Ratios and Compound-Speci fi c Carbon Isotope Signatures. Environ. Sci. Technol. 47, 6155–6163. https://doi.org/10.1021/es400642e

Jautzy, J.J., Ahad, J.M.E., Gobeil, C., Smirnoff, A., Barst, B.D., Savard, M.M., 2015a. Isotopic Evidence for Oil Sands Petroleum Coke in the Peace-Athabasca Delta. Environ. Sci. Technol. 49, 12062–12070. https://doi.org/10.1021/acs.est.5b03232

Jautzy, J.J., Ahad, J.M.E., Hall, R.I., Wiklund, J.A., Wolfe, B.B., Gobeil, C., Savard, M.M., 2015b. Source Apportionment of Background PAHs in the Peace-Athabasca Delta (Alberta, Canada) Using Molecular Level Radiocarbon Analysis. Environ. Sci. Technol. 49, 9056–9063. https://doi.org/10.1021/acs.est.5b01490

Jia, W., Wang, Q., Peng, P., Xiao, Z., Li, B., 2013. Isotopic compositions and biomarkers in crude oils from the Tarim Basin: Oil maturity and oil mixing. Org. Geochem. https://doi.org/10.1016/j.orggeochem.2013.01.002

Jiang, C.D., Bennett, B., Larter, S.R., Adams, J.J., Snowdon, L.R., 2010. Viscosity and API gravity determination of solvent extracted heavy oil and bitumen. J. Can. Pet. Technol. 49, 20–27. https://doi.org/10.2118/139427-PA

Jiang, Q., Thornton, B., Houston, J.R., Spence, S., 2009. Review of Thermal Recovery Technologies for the Clearwater and Lower Grand Rapids Formations in the Cold Lake Area in Alberta. Pet. Soc. 16–18.

Katsoyiannis, A., Terzi, E., Cai, Q.-Y., 2007. On the use of PAH molecular diagnostic ratios in sewage sludge for the understanding of the PAH sources. Is this use appropriate? Chemosphere 69, 1337–1339. https://doi.org/10.1016/j.chemosphere.2007.05.084

Keith, L.H., 2014. The Source of U.S. EPA's Sixteen PAH Priority Pollutants. Polycycl. Aromat. Compd. 35, 147–160. https://doi.org/10.1080/10406638.2014.892886

Kelly, E.N., Schindler, D.W., Hodson, P. V, Short, J.W., Radmanovich, R., Nielsen, C.C., 2010. Oil sands development contributes elements toxic at low concentrations to the Athabasca River and its tributaries. Proc. Natl. Acad. Sci. U. S. A. 107, 16178–16183. https://doi.org/10.1073/pnas.1008754107

Kelly, E.N., Short, J.W., Schindler, D.W., Hodson, P. V., Ma, M., Kwan, A.K., Fortin, B.L., 2009. Oil sands development contributes polycyclic aromatic compounds to the Athabasca River and its tributaries. Proc. Natl. Acad. Sci. U. S. A. 106, 22346–51. https://doi.org/10.1073/pnas.0912050106

Kirk, J.L., Muir, D.C.G., Gleason, A., Wang, X., Lawson, G., Frank, R.A., Lehnherr, I., Wrona, F., 2014. Atmospheric deposition of mercury and methylmercury to landscapes and waterbodies of the athabasca oil sands region. Environ. Sci. Technol. 48, 7374–7383. https://doi.org/10.1021/es500986r

Klemt, W.H., Kay, M.L., Wiklund, J.A., Wolfe, B.B., Hall, R.I., 2020. Assessment of vanadium and nickel enrichment in Lower Athabasca River floodplain lake sediment within the Athabasca Oil Sands Region (Canada). Environ. Pollut. 265, 114920. https://doi.org/10.1016/j.envpol.2020.114920

Korosi, J.B., Cheng, W., Blais, J.M., 2015. Organic Pollutants in Sediment Core Archives, in: Blais, J.M., Rosen, M.R., Smol, J.P. (Eds.), Environmental Contaminants: Using Natural Archives to Track Sources and Long-Term Trends of Pollution. Springer Netherlands, Dordrecht, pp. 161–185.

https://doi.org/10.1007/978-94-017-9541-8_8

Korosi, J.B., Cooke, C.A., Eickmeyer, D.C., Kimpe, L.E., Blais, J.M., 2016a. In-situ bitumen extraction associated with increased petrogenic polycyclic aromatic compounds in lake sediments from the Cold Lake heavy oil fields (Alberta, Canada). Environ. Pollut. 218, 915–922. https://doi.org/10.1016/j.envpol.2016.08.032

Korosi, J.B., Eickmeyer, D.C., Chin, K.S., Palmer, M.J., Kimpe, L.E., Blais, J.M., 2016b. Examining spatial patterns in polycyclic aromatic compounds measured in stream macroinvertebrates near a small subarctic oil and gas operation. Environ. Monit. Assess. https://doi.org/10.1007/s10661-016-5175-9

Korosi, J.B., Irvine, G., Skierszkan, E.K., Doyle, J.R., Kimpe, L.E., Janvier, J., Blais, J.M., 2013. Localized enrichment of polycyclic aromatic hydrocarbons in soil, spruce needles, and lake sediments linked to in-situ bitumen extraction near Cold Lake, Alberta. Environ. Pollut. 182, 307–315. https://doi.org/10.1016/j.envpol.2013.07.012

Korosi, J.B., Thienpont, J.R., Smol, J.P., Blais, J.M., 2017. Paleo-ecotoxicology: What Can Lake Sediments Tell Us about Ecosystem Responses to Environmental Pollutants? Environ. Sci. Technol. acs.est.7b02375. https://doi.org/10.1021/acs.est.7b02375

Kurek, J., Kirk, J.L., Muir, D.C.G., Wang, X., Evans, M.S., Smol, J.P., 2013a. Legacy of a half century of Athabasca oil sands development recorded by lake ecosystems. Proc. Natl. Acad. Sci. U. S. A. 110, 1761–6. https://doi.org/10.1073/pnas.1217675110

Kurek, J., Kirk, J.L., Muir, D.C.G., Wang, X., Evans, M.S., Smol, J.P., 2013b. Legacy of a half century of Athabasca oil sands development recorded by lake ecosystems. Proc. Natl. Acad. Sci. U. S. A. 110, 1761–1766. https://doi.org/10.1073/pnas.1217675110

Landis, M.S., Studabaker, W.B., Pancras, J.P., Graney, J.R., White, E.M., Edgerton, E.S., 2019. Source apportionment of ambient fine and coarse particulate matter polycyclic aromatic hydrocarbons at the Bertha Ganter-Fort McKay community site in the Oil Sands Region of Alberta, Canada. Sci. Total Environ. 666, 540–558. https://doi.org/10.1016/j.scitotenv.2019.02.126

Lemieux, C.L., Long, A.S., Lambert, I.B., Lundstedt, S., Tysklind, M., White, P.A., 2015. Cancer risk assessment of polycyclic aromatic hydrocarbon contaminated soils determined using bioassay-derived levels of benzo[a]pyrene equivalents. Environ. Sci. Technol. 49, 1797–1805. https://doi.org/10.1021/es504466b

Lemieux, C.L., Long, A.S., Lambert, I.B., Lundstedt, S., Tysklind, M., White, P.A., 2014. In Vitro Mammalian Mutagenicity of Complex Polycyclic Aromatic Hydrocarbon Mixtures in Contaminated Soils. Environ. Sci. Technol. 49, 1787–1796. https://doi.org/10.1021/es504465f

Liao, Y., Fang, Y., Wu, L., Geng, A., Hsu, C.S., 2012. The characteristics of the biomarkers and δ 13C of n-alkanes released from thermally altered solid bitumens at various maturities by catalytic hydropyrolysis. Org. Geochem. https://doi.org/10.1016/j.orggeochem.2012.01.014

Lima, A.L.C., Eglinton, T.I., Reddy, C.M., 2003. High-resolution record of pyrogenic polycyclic aromatic hydrocarbon deposition during the 20th century. Environ. Sci. Technol. 37, 53–61. https://doi.org/10.1021/es025895p

Lin, Y., Ma, Y., Qiu, X., Li, R., Fang, Y., Wang, J., Zhu, Y., Hu, D., 2015. Sources, transformation, and health implications of PAHs and their nitrated, hydroxylated, and oxygenated derivatives in PM2.5 in Beijing. J. Geophys. Res. Atmos. 120, 7219–7228. https://doi.org/10.1002/2015JD023628

Manzano, C.A., Marvin, C., Muir, D., Harner, T., Martin, J., Zhang, Y., 2017. Heterocyclic Aromatics in

Petroleum Coke, Snow, Lake Sediments, and Air Samples from the Athabasca Oil Sands Region. Environ. Sci. Technol. 51, 5445–5453. https://doi.org/10.1021/acs.est.7b01345

Manzano, C.A., Muir, D., Kirk, J., Teixeira, C., Siu, M., Wang, X., Charland, J.P., Schindler, D., Kelly, E., 2016. Temporal variation in the deposition of polycyclic aromatic compounds in snow in the Athabasca Oil Sands area of Alberta. Environ. Monit. Assess. 188. https://doi.org/10.1007/s10661-016-5500-3

Masliyah, J., Zhou, Z.J., Xu, Z., Czarnecki, J., Hamza, H., 2004. Understanding Water-Based Bitumen Extraction from Athabasca Oil Sands. Can. J. Chem. Eng. 82, 628–654. https://doi.org/10.1002/cjce.5450820403

Meyer, R.F., Freeman, P.A., 2006. Siberian Platform: Geology and Natural Bitumen Resources. Reston, Virginia.

Miyake, T., Nakazawa, F., Kohno, M., Uetake, J., Suzuki, K., Kameds, T., Fujii, Y., Nakawo, M., Ohta, K., 2005. Concentrations, deposition rates and source variations of n-alkanes in Sofiyskiy Glacier, Russian Altai Mountains. Bull. Glaciol. Res. 81–87.

Moorhouse, J., Huot, M., Dyer, S., 2010. Drilling Deeper: The In Situ Oil Sands Report Card, The Pembina Institute. Drayton Valley, Alberta.

Mukhametshina, A., Hascakir, B., 2014. Bitumen extraction by expanding solvent-steam assisted gravity drainage (ES-SAGD) with asphaltene solvents and non-solvents, in: Society of Petroleum Engineers - SPE Heavy Oil Conference Canada 2014. Society of Petroleum Engineers, Calgary, pp. 178–193. https://doi.org/10.2118/170013-ms

Neff, J.M., Stout, S.A., Gunster, D.G., 2005. Ecological risk assessment of polycyclic aromatic hydrocarbons in sediments: identifying sources and ecological hazard. Integr. Environ. Assess. Manag. 1, 22–33. https://doi.org/10.1897/IEAM_2004a-016.1

Nimana, B., Canter, C., Kumar, A., 2015. Energy consumption and greenhouse gas emissions in the recovery and extraction of crude bitumen from Canada's oil sands. Appl. Energy 143, 189–199. https://doi.org/10.1016/j.apenergy.2015.01.024

Ohiozebau, E., Tendler, B., Codling, G., Kelly, E., Giesy, J.P., Jones, P.D., 2016. Potential health risks posed by polycyclic aromatic hydrocarbons in muscle tissues of fishes from the Athabasca and Slave Rivers, Canada. Environ. Geochem. Health 1–22. https://doi.org/10.1007/s10653-016-9815-3

Olajire, A.A., Olujobade, M., Olabemiwo, O., 2008. n-Alkane distributions in soil and water samples collected near Agbabu bitumen field of southwestern Nigeria. Int. J. Environ. Stud. 65, 769–779. https://doi.org/10.1080/00207230701862264

Omelchenko, A., Lockhart, L.W., Wilkinson, P., 2005. Study of the Depositional Characteristics of the Lake Sediments Across Canada with Pb-210 and Cs-137. Mod. Tools Methods Water Treat. Improv. Living Stand. 48. https://doi.org/https://doi.org/10.1007/1-4020-3116-5_2

OSMP, 2019. Oil Sands Monitoring Program: Annual Report for 2018-2019. Edmonton, Alberta, Canada.

OSMP, 2018. Oil Sands Monitoring Program Annual Report for 2017-2018. Edmonton, Alberta, Canada.

Parajulee, A., Wania, F., 2014. Evaluating officially reported polycyclic aromatic hydrocarbon emissions in the Athabasca oil sands region with a multimedia fate model. Proc. Natl. Acad. Sci. U. S. A. 111, 3344–3349. https://doi.org/10.1073/pnas.1319780111

Parrott, J.L., Raine, J.C., McMaster, M.E., Hewitt, L.M., 2019. Chronic toxicity of oil sands tailings pond

sediments to early life stages of fathead minnow (Pimephales promelas). Heliyon 5, e02509. https://doi.org/10.1016/j.heliyon.2019.e02509

Pies, C., Hoffmann, B., Petrowsky, J., Yang, Y., Ternes, T.A., Hofmann, T., 2008. Characterization and source identification of polycyclic aromatic hydrocarbons (PAHs) in river bank soils. Chemosphere 72, 1594–1601. https://doi.org/10.1016/j.chemosphere.2008.04.021

Radzi Bin Abas, M., Mohd Tahir, N., Omar, N.Y., Yousef MJOmar, N., Bin Abas, Mr., Aziz Ketuly, K., MohdTahir, N., 2001. Heavy molecular-weight organic compounds in the atmosphere: The hopanes. Malaysian J. Anal. Sci. 7, 203–208.

Ravindra, K., Sokhi, R., Rene´van Grieken, R., 2008. Atmospheric polycyclic aromatic hydrocarbons: Source attribution, emission factors and regulation. Atmos. Environ. 42, 2895–2921. https://doi.org/10.1016/j.atmosenv.2007.12.010

Readman, J.W., Fillmann, G., Tolosa, I., Bartocci, J., Villeneuve, J.-P., Catinni, C., Mee, L.D., 2002. Petroleum and PAH contamination of the Black Sea. Mar. Pollut. Bull. 48–62.

Rogge, W.F., Hildemann, L.M., Mazurek, M.A., Cass, G.R., Simoneit, B.R.T., 1993. Sources of Fine Organic Aerosol. 2. Noncatalyst and Catalyst-Equipped Automobiles and Heavy-Duty Diesel Trucks, Environ. Sci. Technoi.

Romaniuk, A., Rahmanifard, H., Hosseini, H., 2019. Canadian Crude Oil and Natural Gas Production, Supply Costs, economic Impacts and Emissions Outlook (2019-2039). Calgary, Alberta, Canada.

Rose, N.L., Turner, S.D., Yang, H., Yang, C., Hall, C., Harrad, S., 2018. Palaeotoxicity: Reconstructing the risk of multiple sedimentary pollutants to freshwater organisms. Environ. Geochem. Health 40, 1667–1682. https://doi.org/10.1007/s10653-018-0080-5

Ross, M.S., Pereira, A.D.S., Fennell, J., Davies, M., Johnson, J., Sliva, L., Martin, J.W., 2012. Quantitative and qualitative analysis of naphthenic acids in natural waters surrounding the canadian oil sands industry. Environ. Sci. Technol. 46. https://doi.org/10.1021/es303432u

Roy, J.W., Bickerton, G., Frank, R.A., Grapentine, L., Hewitt, L.M., 2016. Assessing Risks of Shallow Riparian Groundwater Quality Near an Oil Sands Tailings Pond. Groundwater 54, 545–558. https://doi.org/10.1111/gwat.12392

Roy, M.-C., 2018. Petrogenic Hydrocarbons in the Peace-Athabasca Delta and the Microbes that Degrade Them: Assessing Hydrocarbon Degradation Potential of Indigenous Microbial Communities. Master Sci. Thesis Thesis. University of Ottawa. https://doi.org/10.1017/CBO9781107415324.004

Salat, A., 2019. Tracking the History of Alberta Oil Sands Contaminants Using Lake Sediment Cores. Master Sci. Thesis. University of Ottawa. https://doi.org/10.1017/CBO9781107415324.004

Samsonov, S., Czarnogorska, M., 2014. Ground Deformation due to Steam Assisted Gravity Drainage and Cyclic Steam Stimulation Observed by RadarSat-2 in Alberta's Oil Sands, in: IEEE International Geoscience and Remote Sensing Symposium. IEEE, Quebec City, pp. 883–885. https://doi.org/10.1109/IGARSS.2014.6946566

Schiffer, S., Liber, K., 2017. Toxicity of aqueous vanadium to zooplankton and phytoplankton species of relevance to the athabasca oil sands region. Ecotoxicol. Environ. Saf. 137, 1–11. https://doi.org/10.1016/j.ecoenv.2016.10.040

Schindler, D.W., 2013. Water Quality Issues in the Oil Sands Region of the Lower Athabasca River, Alberta, in: Miall, A.D. (Ed.), Geoscience Canada. pp. 202–215. https://doi.org/dx.doi.org/10.12789/geocanj.2013.40.012

Schuster, J.K., Harner, T., Su, K., Mihele, C., Eng, A., 2015. First Results from the Oil Sands Passive Air Monitoring Network for Polycyclic Aromatic Compounds. Environ. Sci. Technol. 150209130312008. https://doi.org/10.1021/es505684e

Shahimin, M.M.F., Foght, J.M., Siddique, T., 2016. Preferential methanogenic biodegradation of short-chain n-alkanes by microbial communities from two different oil sands tailings ponds. Sci. Total Environ. https://doi.org/10.1016/j.scitotenv.2016.02.061

Shen, L., Schmidt, D.R., Dokht, R.H., Samsonov, S. V., Singhroy, V., Shipman, T., 2015. Geomechanical Modelling of Cyclic Steaming Induced Surface Deformation Heavy oil thermal EOR caprock integrity study View project Seismic structures of the Western Canada Sedimentary Basin View project. Soc. Pet. Eng. https://doi.org/10.2118/174415-MS

Simoneit, B.R.T., 2005. A review of current applications of mass spectrometry for biomarker/molecular tracer elucidations. Mass Spectrom. Rev. https://doi.org/10.1002/mas.20036

Skierszkan, E.K., Irvine, G., Doyle, J.R., Kimpe, L.E., Blais, J.M., 2013. Is there widespread metal contamination from in-situ bitumen extraction at Cold Lake, Alberta heavy oil field? Sci. Total Environ. 447, 337–344. https://doi.org/10.1016/j.scitotenv.2012.12.097

Stout, S.A., Wang, Z., 2016. Chemical Fingerprinting Methods and Factors Affecting Petroleum Fingerprints in the Environment, Second Edi. ed, Standard Handbook Oil Spill Environmental Forensics. Elsevier Inc. https://doi.org/10.1016/B978-0-12-809659-8.00003-6

Taylor, H.W., Svoboda, J., Henry, G.H.R., Wein, R.W., 1988. Post-Chernobyl 134Cs and 137Cs levels at some localities in northern Canada. Arctic 41, 293–296. https://doi.org/10.14430/arctic1735

Thienpont, J.R., Desjardins, C.M., Kimpe, L.E., Korosi, J.B., Kokelj, S. V, Palmer, M.J., Muir, D.C.G., Kirk, J.L., Smol, J.P., Blais, J.M., 2017. Comparative histories of polycyclic aromatic compound accumulation in lake sediments near petroleum operations in western Canada. Environ. Pollut. 231, 13–21. https://doi.org/10.1016/j.envpol.2017.07.064

Thienpont, J.R., Rühland, K.M., Pisaric, M.F.J., Kokelj, S. V., Kimpe, L.E., Blais, J.M., Smol, J.P., 2013. Biological responses to permafrost thaw slumping in Canadian Arctic lakes. Freshw. Biol. 58, 337–353. https://doi.org/10.1111/fwb.12061

Thorsen, W.A., Cope, W.G., Shea, D., 2004. Bioavailability of PAHs: Effects of Soot Carbon and PAH Source. Environ. Sci. Technol. 38, 2029–2037. https://doi.org/10.1021/es0306056

Timoney, K., Lee, P., 2014. CNRL ' s Persistent 2013 Bitumen Releases near Cold Lake , Alberta : Facts , Unanswered Questions , and Implications.

Timoney, K.P., Lee, P., 2011. Polycyclic Aromatic Hydrocarbons Increase in Athabasca River Delta Sediment: Temporal Trends and Environmental Correlates. Environ. Sci. Technol 45, 4278–4284. https://doi.org/10.1021/es104375d

Timoney, K.P., Lee, P., 2009. Does the Alberta Tar Sands Industry Pollute? The Scientific Evidence. Open Conserv. Biol. J. 3, 65–81. https://doi.org/10.2174/1874839200903010065

Tobiszewski, M., Namieśnik, J., 2012. PAH diagnostic ratios for the identification of pollution emission sources. Environ. Pollut. 162, 110–119. https://doi.org/10.1016/J.ENVPOL.2011.10.025

Van Wilgenburg, S.L., Hobson, K.A., Bayne, E.M., Koper, N., 2013. Estimation de la perte de nids d'oiseaux attribuable à l'exploration et à l'exploitation pétrolière et gazière dans le bassin sédimentaire de l'Ouest Canadien. Avian Conserv. Ecol. 8. https://doi.org/10.5751/ACE-00585-080209

Vila-Escalé, M., Vegas-Vilarrúbia, T., Prat, N., 2007. Release of polycyclic aromatic compounds into a Mediterranean creek (Catalonia, NE Spain) after a forest fire. Water Res. 41, 2171–2179. https://doi.org/10.1016/j.watres.2006.07.029

Wang, C., Chen, B., Zhang, B., He, S., Zhao, M., 2013. Fingerprint and weathering characteristics of crude oils after Dalian oil spill, China. Mar. Pollut. Bull. https://doi.org/10.1016/j.marpolbul.2013.03.034

Wang, Zhen, Chen, J., Yang, P., Tian, F., Qiao, X., Bian, H., Ge, L., 2009. Distribution of PAHs in pine (Pinus thunbergii) needles and soils correlates with their gas-particle partitioning. Environ. Sci. Technol. 43, 1336–1341. https://doi.org/10.1021/es802067e

Wang, Z., Fingas, M., Shu, Y.., Sigouin, L., Landriault, M., Lambert, P., 1999. Quantitative Characterization of PAHs in Burn Residue and Soot Samples and Differentiation of Pyrogenic PAHs from Petrogenic PAHs-The 1994 Mobile Burn Study. Environ. Sci. Technol. 3100–3109. https://doi.org/10.1021/es990031y

Wang, Z., Stout, S.A., Fingas, M., 2006. Forensic Fingerprinting of Biomarkers for Oil Spill Characterization and Source Identification. Environ. Forensics 7, 105–146. https://doi.org/10.1080/15275920600667104

Wang, Zhendi, Yang, C., Kelly-Hooper, F., Hollebone, B.P., Peng, X., Brown, C.E., Landriault, M., Sun, J., Yang, Z., 2009. Forensic differentiation of biogenic organic compounds from petroleum hydrocarbons in biogenic and petrogenic compounds cross-contaminated soils and sediments. J. Chromatogr. A 1216, 1174–1191. https://doi.org/10.1016/j.chroma.2008.12.036

Wang, Z., Yang, C., Parrott, J.L.L., Frank, R.A.A., Yang, Z., Brown, C.E.E., Hollebone, B.P.P., Landriault, M., Fieldhouse, B., Liu, Y., Zhang, G., Hewitt, L.M.M., 2014. Forensic source differentiation of petrogenic, pyrogenic, and biogenic hydrocarbons in Canadian oil sands environmental samples. J. Hazard. Mater. 271, 166–177. https://doi.org/10.1016/j.jhazmat.2014.02.021

Wang, Z., Yang, C., Yang, Z., Brown, C.E., Hollebone, B.P., Stout, S.A., 2016. Petroleum biomarker fingerprinting for oil spill characterization and source identification, in: Standard Handbook Oil Spill Environmental Forensics. Elsevier Inc., pp. 131–254. https://doi.org/10.1016/b978-0-12-803832-1.00004-0

Wilson, M.F., Kriz, J.F., 1984. Upgrading of middle distillate fractions of a syncrude from Athabasca oil sands. Fuel 63, 190–196. https://doi.org/10.1016/0016-2361(84)90035-8

Wong, R.C.K., Barr, W.E., Kry, P.R., 1992. Stress-strain response of Cold Lake oil sands. Can. Geotech. J. 30, 220–235.

WRI, 2018. WRI Annual Report 2018-19 | World Resources Institute.

Xu, G., 2018. Atmospheric Benzo[a]pyrene and vanadium evidence for the presence of petroleum coke dust in the Athabasca Oil Sands Region, Alberta, Canada. J. Clean. Prod. 171, 592–599. https://doi.org/10.1016/j.jclepro.2017.10.038

Yang, C., Wang, Z., Yang, Z., Hollebone, B., Brown, C.E., Landriault, M., Fieldhouse, B., 2011. Chemical Fingerprints of Alberta Oil Sands and Related Petroleum Products. Environ. Forensics 12, 173–188. https://doi.org/10.1080/15275922.2011.574312

Yang, C., Wang, Z.D., Hollebone, B., Brown, C.E., Landriault, M., Fieldhouse, B., Yang, Z.Y., 2012. Application of Light Petroleum Biomarkers for Forensic Characterization and Source Identification of Spilled Light Refined Oils. Environ. Forensics 13, 298–311.

https://doi.org/10.1080/15275922.2012.730114

Yeh, S., Jordaan, S.M., Brandt, A.R., Turetsky, M.R., Spatari, S., Keith, D.W., 2010. Land Use Greenhouse Gas Emissions from Conventional Oil Production and Oil Sands. Environ. Sci. Technol. 44, 8766–8772. https://doi.org/10.1021/es1013278

Yim, U.H., Ha, S.Y., An, J.G., Won, J.H., Han, G.M., Hong, S.H., Kim, M., Jung, J.H., Shim, W.J., 2011. Fingerprint and weathering characteristics of stranded oils after the Hebei Spirit oil spill. J. Hazard. Mater. https://doi.org/10.1016/j.jhazmat.2011.09.055

Young, R.F., Michel, L.M., Fedorak, P.M., 2011. Distribution of naphthenic acids in tissues of laboratory-exposed fish and in wild fishes from near the Athabasca oil sands in Alberta, Canada. Ecotoxicol. Environ. Saf. 74, 889–896. https://doi.org/10.1016/j.ecoenv.2010.12.009

Yu, S., Pan, C., Wang, J., Jin, X., Jiang, L., Liu, D., Lü, X., Qin, J., Qian, Y., Ding, Y., Chen, H., 2012. Correlation of crude oils and oil components from reservoirs and source rocks using carbon isotopic compositions of individual n-alkanes in the tazhong and tabei uplift of the tarim basin, China. Org. Geochem. https://doi.org/10.1016/j.orggeochem.2012.09.002

Yunker, M.B., Macdonald, R.W., 2003. Petroleum biomarker sources in suspended particulate matter and sediments from the Fraser River Basin and Strait of Georgia, Canada. Org. Geochem. 34, 1525–1541. https://doi.org/10.1016/S0146-6380(03)00157-8

Yunker, M.B., Macdonald, R.W., Vingarzan, R., Mitchell, R.H., Goyette, D., Sylvestre, S., 2002. PAHs in the Fraser River basin: a critical appraisal of PAH ratios as indicators of PAH source and composition. Org. Geochem. 33, 489–515. https://doi.org/10.1016/S0146-6380(02)00002-5

Zhang, W., Zhang, S., Wan, C., Yue, D., Ye, Y., Wang, X., 2008. Source diagnostics of polycyclic aromatic hydrocarbons in urban road runoff, dust, rain and canopy throughfall. Environ. Pollut. 153, 594–601. https://doi.org/10.1016/j.envpol.2007.09.004

Zhang, Y., Shotyk, W., Zaccone, C., Noernberg, T., Pelletier, R., Bicalho, B., Froese, D.G., Davies, L., Martin, J.W., 2016. Airborne Petcoke Dust is a Major Source of Polycyclic Aromatic Hydrocarbons in the Athabasca Oil Sands Region. Environ. Sci. Technol. 50, 1711–1720. https://doi.org/10.1021/acs.est.5b05092

Zhou, S., Huang, H., Liu, Y., 2008. Biodegradation and Origin of Oil Sands in the Western Canada Sedimentary Basin. J. Pet. Sci. 5, 87–94. https://doi.org/10.1007/s12182-008-0015-3